Modulation of plant chemistry by rhizosphere bacteria

Jeon, J.

Modulation of plant chemistry by rhizosphere bacteria

Je-Seung Jeon

Je-Seung Jeon
Modulation of plant chemistry by rhizosphere bacteria
The research described in this thesis was performed at the Department of Microbial Ecology of the Netherlands Institute of Ecology, NIOO-KNAW, Wageningen, The Netherlands; Je-Seung Jeon was supported by the Korean government scholarship program (2015-2017, National institute for international education: NIIED)

Design of the cover and layout: Je-Seung Jeon
Printed by GVO drukkers & vormgevers B.V. ||www.gvo.nl
ISBN: 978-94-6332-640-7

Modulation of plant chemistry by rhizosphere bacteria

Proefschrift

ter verkrijging van
de graad van Doctor aan de Universiteit Leiden,
op gezag van Rector Magnificus prof.mr. C.J.J.M. Stolker,
volgens besluit van het College voor Promoties
te verdedigen op donderdag 7 juli 2020
klokke 15.00 uur

door

Je-Seung Jeon
geboren te Pyeongchang-gun, Republiek Korea
in 1984

Thesis committee

Promotor:

Prof. Dr. Jos M. Raaijmakers

Professor of Microbial Ecology, Leiden University
Head of the Microbial Ecology department, Netherlands Institute of Ecology (NIOO-KNAW), Wageningen

Co-promoter:

Dr. Desalegn W. Etalo

Researcher and a project leader in the Microbial Ecology department, Netherlands Institute of Ecology (NIOO-KNAW), Wageningen

Other members:

Prof. Dr. Gilles van Wezel (chair)	Leiden University
Prof. Dr. Remko Offringa (secretary)	Leiden University
Assoc. Prof. Dr. Salma Balazadeh	Leiden University
Assoc. Prof. Dr. Young Hae Choi	Leiden University
Prof. Dr. Harro Bouwmeester	University of Amsterdam
Prof. Dr. Robert Hall	Wageningen University & Research

This research was conducted under the auspices of Leiden Graduate School and the Graduate School of Experimental Plant Sciences (EPS)

Table of Contents

Chapter 1

General introduction and thesis outline

General introduction

Plants produce a large number of primary and secondary metabolites with diverse functions. While primary metabolites are fundamental to growth and reproduction, secondary metabolites contribute to adaptation of plants to environmental change (Bourgaud *et al.*, 2001) and play a critical role in plant defense against herbivory and pathogen attack (Bennett & Wallsgrove, 1994; Rattan, 2010; Boulogne *et al.*, 2012). Over the past 70 years, natural product chemistry has led to the identification of more than 100,000 secondary metabolites (Wink, 2010). Many of these metabolites exhibit a vast array of pharmaceutical activities either as metabolite itself or as a scaffold for the synthesis of derivatives with enhanced or other bio-activities (Bourgaud *et al.*, 2001; Hartmann, 2007). Recent studies have shown that microorganisms colonizing plant surfaces (phyllosphere, rhizosphere) and internal plant tissue (endosphere) can induce changes in the plant metabolome, leading to alterations in the biosynthesis of known plant metabolites or of yet unknown plant metabolites (Scherling *et al.*, 2009; van de Mortel *et al.*, 2012; Huang *et al.*, 2014; Ryffel *et al.*, 2016). Hence, microbe-plant interactions have been proposed as a novel, generic means to boost the production of nutritionally and/or pharmaceutically valuable plant metabolites and to discover new plant metabolites and their corresponding biosynthetic genes and pathways. My thesis focuses on microbe-mediated modulation of plant chemistry and identification of bacterial traits involved in the induction of these plant metabolome changes. Specific emphasis is given to root-associated beneficial bacteria also referred to as Plant Growth-Promoting Rhizobacteria (PGPR).

The rhizosphere, the narrow zone (± 1-2 mm) surrounding and influenced by plant roots, is rich in small- and large-molecular weight compounds that serve as a carbon source for microbial growth (Bais *et al.*, 2006). In return, the rhizosphere microbiome provides a first

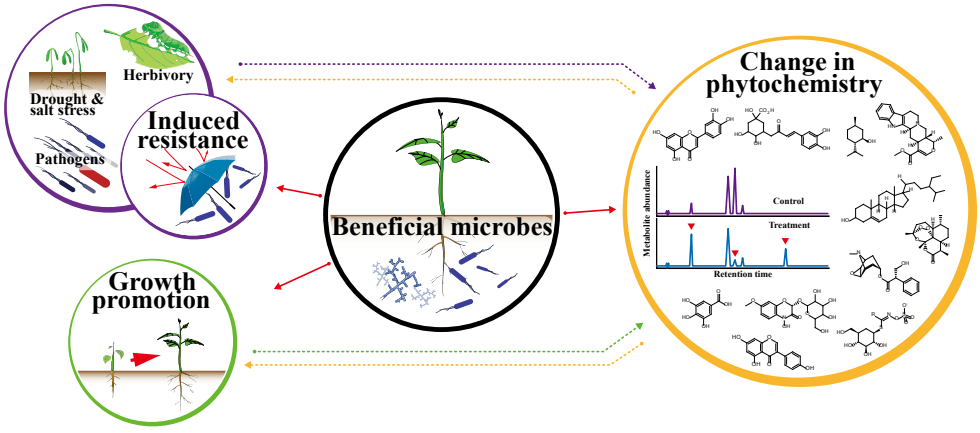

Fig 1. Direct and indirect mechanisms by which beneficial root-associated microorganisms can impact on plant growth and on plant tolerance to biotic and abiotic stress factors.

line of defense against infections by root pathogens (Raaijmakers & Mazzola, 2016) as well as other life-support functions for the plant including nutrient acquisition and growth promotion (Van Loon, 2007; Bhattacharyya & Jha, 2012), induction of systemic resistance against above-ground pathogens and herbivorous insects (Raupach *et al.*, 1996; Van Wees *et al.*, 1999; Ryu *et al.*, 2004; Haas & Défago, 2005), and enhanced plant tolerance to abiotic stress (e.g. salinity, drought) (Dimkpa *et al.*, 2009; Yang *et al.*, 2009). Several microbial traits and mechanisms involved in these interactions have been identified (Han *et al.*, 2006; Nam *et al.*, 2006; Kim *et al.*, 2007; Sumayo *et al.*, 2013; Cheng *et al.*, 2017), but how microorganisms alter plant chemistry and if/how these phytochemical changes affect plant growth and health are not well understood (**Fig 1**).

Plant growth-promoting rhizobacteria

Since Kloepper and colleagues termed plant growth promoting rhizobacteria (PGPR) for the first time in their experiment on radish in the 1970s (Kloepper, 1978), a large number of rhizobacterial genera including root endophytic bacteria have been described for their plant growth-promoting properties; these genera include, among others, *Agrobacterium*, *Arthrobacter*, *Azotobacter*, *Azospirillum*, *Bacillus*, *Burkholderia*, *Caulobacter*, *Chromobacterium*, *Erwinia*, *Flavobacterium*, *Micrococcus*, *Pseudomonas* and *Serratia* (Lodewyckx *et al.*, 2002; Gray & Smith, 2005; Bhattacharyya & Jha, 2012). Based on the underlying mechanisms of plant growth promotion, PGPRs are generally categorized into **biofertilizers**, **phytostimulators** and **biopesticides** (Lugtenberg & Kamilova, 2009; Bhattacharyya & Jha, 2012).

Biofertilizers refer to rhizobacteria that increase the availability and uptake of micro- and macronutrients such as iron, phosphate and nitrogen. Iron is an essential element that functions as a cofactor for many metabolic pathways including respiration and photosynthesis (Brittenham, 1994; Miller *et al.*, 1995). In soil, however, iron exists as Fe^{3+} which is unavailable to plants and microorganisms. Hence, iron is the third most limiting nutrient for the plant (Zhang *et al.*, 2009). Siderophores, high affinity iron chelators, are produced by several rhizobacterial genera (Kloepper, JW *et al.*, 1980; Sharma & Johri, 2003; Rajkumar *et al.*, 2010; Radzki *et al.*, 2013) and have been implicated in plant growth promotion via Fe-siderophore complex (Sharma & Johri, 2003). The possible mechanism implies that the microbial siderophores-Fe complex is taken up by the plant or do a ligand exchange with phytosiderophores (Masalha *et al.*, 2000; Vansuyt *et al.*, 2007; Ahmed & Holmström, 2014). Next to iron, also phosphate can be made available to the plant by microbes, albeit via other mechanisms. In addition to the 'classic' phosphorus acquisition via symbiosis with arbuscular mycorrhizal fungi, another wide-spread mechanism involves mineralization of inorganic phosphorus through acidification by organic acids produced by rhizobacteria (Rodríguez & Fraga, 1999). The hydroxyl and carboxyl groups of organic acids chelate the cation of phosphate converting the mineral phosphate into soluble forms (Kpomblekou-a

& Tabatabai, 1994). A number of reports investigated the impact of phosphate-solubilizing bacteria on plant growth promotion in various crops (Han & Lee, 2006; Zhao *et al.*, 2014; Kudoyarova *et al.*, 2017; Manzoor *et al.*, 2017). The conclusive role of P-solubilization in growth promotion is not evident in several of these studies. For example, De Freitas *et al.* (1997) reported that induced growth of canola by phosphate-solubilizing rhizobacteria was not via P-uptake but some other yet unknown mechanisms. A third essential element for plant growth is nitrogen. Apart from nitrogen fixation by symbiotic rhizobia, N_2 can also be fixed into ammonia by free-living rhizobacteria. Several studies have demonstrated that N_2-fixing *Azospirillum* can significantly increase crop yield (Baldani *et al.*, 1983; Rodrigues *et al.*, 2008), a phenotype that is also associated with an increased number of root hairs and lateral roots, thereby enhancing uptake of minerals and water (Okon *et al.*, 1998; Bashan *et al.*, 2004).

Phytostimulators are rhizobacteria that directly affect plant growth via the production of phytohormones such as indole-3-acetic acid (IAA), gibberellins, cytokinins, and abscisic acid (Lugtenberg & Kamilova, 2009; Cassán *et al.*, 2014). Several PGPR genera including *Rhizobium*, *Bradyrhizobium*, and *Azospirillum* can produce IAA via the indole-3-pyruvic acid (IPyA) pathway (Burdman *et al.*, 2000)) that utilizes tryptophan released by roots as the precursor. Other PGPRs such as *Azospirillum brasilense* can also produce IAA via tryptophan-independent pathways although the underlying mechanism(s) is yet not fully resolved (Jha & Saraf, 2015; Goswami *et al.*, 2016). Also other plant hormones such as giberellins, cytokinin, and abscisic acid, produced by various PGPR genera such as *Azospirillum* (Cassán *et al.*, 2014), *Bacillus* (Gutiérrez-Mañero *et al.*, 2001; Joo *et al.*, 2005) and *Pseudomonas* (García de Salamone *et al.*, 2001) can impact on plant growth and development. Another well-studied mechanism of hormone-mediated plant growth promotion by PGPRs is via 1-aminocyclopropane-1-carboxylate (ACC) deaminase, an enzyme that degrades ACC, a precursor of the plant hormone ethylene, into ammonia and α-ketobutyrate (John, 1991). ACC deaminase producing bacteria were shown not only to affect plant growth but also to provide protection against abiotic stresses such as drought, salinity, flooding, temperature, ultraviolet radiations, or heavy metals (Honma & Shimomura, 1978; Glick, 2014; Etesami *et al.*, 2015; Goswami *et al.*, 2016).

Over the past decade, substantial interest has emerged on the role of microbial volatile organic compounds (mVOCs) in plant growth promotion and induced systemic resistance (Schmidt *et al.*, 2015). mVOCs are small molecules (< 300 mw) that are highly diffusible through the air-filled spaces in the soil matrix and thereby can interact with plants and other organisms from a distance (Hiltpold & Turlings, 2008; Schulz-Bohm *et al.*, 2018; Sharifi & Ryu, 2018). Ryu *et al.* (2003; 2004) first reported 2,3-butanediol produced by *Bacillus subtilis* as an inducer of growth and systemic resistance (ISR) in Arabidopsis. Since then, various other bacterial species such as *Arthrobacter* (Velázquez-Becerra *et al.*, 2011), *Microbacterium* (Cordovez *et al.*, 2018), *Pseudomonas* (Park *et al.*, 2015; Jishma *et al.*, 2017; Rojas-Solís *et al.*, 2018),

and *Stenotrophomonas* (Rojas-Solís *et al.*, 2018) have been investigated mVOCs-mediated effects on growth and health of various plant species such as Arabidopsis, lettuce, moss, tobacco, and tomato. The classes of bioactive mVOCs include alkenes, alcohols, ketones, terpenes, benzonoids, and pyrazines (Schmidt *et al.*, 2015; Sharifi & Ryu, 2018). The study by Meldau *et al*. (2013) further showed that dimethyldisulfide (DMDS)-producing *Bacillus* sp. B55, when grown in minimal medium containing ^{35}S-labeled Na_2SO_4 as the sole S source, leads to incorporation of ^{35}S into plant proteins, suggesting that sulfurous mVOCs can feed directly into the plant's sulfur metabolism. Similarly, Arabidopsis exposed to mVOCs from *Bacillus amyloliquefaciens* (GB03) showed enhanced sulfur accumulation when traced with radioactive sulfate ($^{35}SO4^{-2}$). Subsequent microarray data analysis further indicated that mVOCs of strain GB03 induced transcription of genes responsible for sulfur assimilation and for aliphatic, indolic glucosinolate biosynthesis further evidenced by increases of 33 and 70% of the total glucosinolate content in shoots and root, respectively (Aziz *et al.*, 2016). In addition, treated plants exhibited a significant protection from herbivory by the insect *Spodoptera exigua*.

Biopesticides refer to PGPRs that suppress disease-causing agents (e.g. fungi, bacteria, nematodes) directly via specific metabolites such as antibiotics, hydrolytic enzymes, and mVOC such as hydrogen cyanide (HCN), or indirectly via induced systemic resistance (Vessey, 2003; Pieterse *et al.*, 2014). Over the last four decades, a large number of bacterial genera, including *Agrobacterium*, *Arthrobacter*, *Azotobacter*, *Bacillus*, *Burkholderia*, *Collimonas*, *Pantoea*, *Pseudomonas*, *Serratia*, *Stenotrophomonas*, and *Streptomyces* have been identified as biopesticides (Raaijmakers *et al.*, 2009; Raaijmakers & Mazzola, 2012). *Pseudomonas* and *Bacillus* are the most broadly studied genera as agronomic biocontrol agents. Despite similarities in their effects on plant growth and health, there is a large diversity of functional traits among the numerous species within these genera, with unique or shared gene clusters encoding bioactive compounds such as 2,4-diacetylphloroglucinol (2,4-DAPG), pyrrolnitrin, pyoluteorin, phenazines, 2,5-dialkylresorcinol, quinolones, rhamnolipids, and various lipopeptides (LPs) (Raaijmakers & Weller, 1998; Raaijmakers *et al.*, 2006; Gross & Loper, 2009; Raaijmakers *et al.*, 2010). LPs operate largely via membrane disruption leading to lysis of infectious propagules (e.g. zoospores) of plant pathogens (de Souza *et al.*, 2003) or trophozoites of the bacterivorous amoeba-flagellates (Mazzola *et al.*, 2009). Similarly, 2,4-DAPG produced by *Pseudomonas* spp. also exhibits broad-spectrum antimicrobial activities but, at high concentrations can also be phytotoxic (Raaijmakers & Weller, 1998; Haas & Défago, 2005; Weller *et al.*, 2007; Kwak *et al.*, 2012; Schlatter *et al.*, 2017). Similar to *Pseudomonas*, also *Bacillus* species harbor a large diversity of biosynthetic gene clusters for lipopeptides and polyketides such as surfactins, fengycins, iturins, macrolactin, difficidin, and oxidifficidin (Chen, X *et al.*, 2009; Raaijmakers *et al.*, 2010). These metabolites are active against a wide range of plant pathogenic fungi (Chen, X-H *et al.*, 2009; Yuan *et al.*, 2012) such as *Fusarium graminearum*, *Botrytis cinerea*, *Podosphaera fusca*, *Colletotrichum demiatium*, *Penicillium roqueforti*, *Aspergillus flavus*, and *Rhizoctonia solani* (Moyne *et al.*,

2001; Hiradate *et al.*, 2002; Yu *et al.*, 2002; Chitarra *et al.*, 2003; Toure *et al.*, 2004; Romero *et al.*, 2007; Wang *et al.*, 2007).

Several of these PGPRs and some of the bioactive compounds can also provide indirect plant protection by priming disease or pest resistance responses in a systemic manner. Such defense system is classified into two forms referred to as systemic acquired resistance (SAR) and induced systemic resistance (ISR). The onset of SAR is initiated when the surface-localized pattern-recognition receptors (PRRs) of the plant recognize conserved pathogen-associated molecular patterns (PAMPs) such as flagellin of avirulent or necrotrophic pathogens (Boller & Felix, 2009; Campos-Soriano *et al.*, 2012; Macho & Zipfel, 2015; Couto & Zipfel, 2016). This then increases the level of signaling molecules such as salicylic acid (SA) that in turn upregulate the expression of the antimicrobial pathogenesis-related (PR) genes, fortifying the plant against subsequent infection (Durrant & Dong, 2004; Fu & Dong, 2013). ISR is mediated by PGPR primarily through jasmonic acid (JA) and ethylene (ET), although some PGPRs can also induce resistance via the SA pathway (De Meyer & Höfte, 1997; van de Mortel *et al.*, 2012). Among the ISR-inducing genera, *Pseudomonas* and *Bacillus* are again the most well studied to date. ISR-inducing determinants of *Pseudomonas* and *Bacillus* identified to date include siderophores, SA, lipopolysaccharides (LPS), antibiotics (Meziane *et al.*, 2005; Bakker *et al.*, 2007), and also mVOCs such as 2,3-butanediol (Ryu *et al.*, 2004).

Recent studies in our lab led to the identification of other genes and traits of *Pseudomonas fluorescens* strain SS101 (*Pf* SS101) involved in ISR and growth promotion (Cheng *et al.*, 2017). Following a screening of a genome-wide random mutant library, we identified 21 mutants out of 7,488 that was compromised in their ability to promote Arabidopsis growth and to induce systemic resistance against the bacterial leaf pathogen *Pseudomonas syringae* pv. tomato (Pst). Subsequent analysis of root colonization, site-directed mutagenesis and genetic complementation revealed the involvement of phosphogluconate dehydratase gene *edd*, the response regulator gene *colR* and the adenylsulfate reductase gene *cysH* in growth promotion and ISR by *Pf* SS101. Further comparative plant transcriptome analysis indicated that sulfur metabolism of *Pf* SS101 influenced sulfur assimilation, auxin biosynthesis and transport, steroid biosynthesis and carbohydrate metabolism in Arabidopsis (Cheng *et al.*, 2017). These results were in line with results of a non-targeted metabolomics approach that showed that *Pf* SS101 differently regulated 50 metabolites in Arabidopsis (van de Mortel *et al.*, 2012). Genome-wide transcriptomics and screening with seven Arabidopsis mutants disrupted in *myb51, cyp79B2cyp79B3, cyp81F2, pen2, cyp71A12, cyp71A13,* or *myb28myb29* revealed that camalexin and indolic glucosinolates, sulfur containing metabolites, may contribute to the induced resistance response against *Pst* and the herbivorous insect *Spodoptera exigua* (van de Mortel *et al.*, 2012).

Modulation of plant metabolism by PGPRs

While growth promotion and induced resistance by PGPRs have drawn the attention for approximately 40 years (Kloepper, 1978), relatively few studies have addressed how PGPRs modulate plant metabolism. Nevertheless, the number of studies on PGPR-mediated effects on plant secondary metabolism shows an increasing trend (**Fig 2**), exemplifying its potential for the coming decade. The increasing interest is due in part to the overwhelming attention in research for plant microbiome assembly and functioning (Cordovez *et al.*, 2019) as well as the observation that PGPRs represent a novel and promising platform for boosting or redirecting the production of high value natural products (HVNPs) in plants. Compared to conventional breeding and plant genetic engineering, steering HVNPs via PGPRs has a few distinct advantages. Such merits include simplicity and generality of application, and attested safety to environmental issue in using bacteria as biological elicitors in farmland (Tabassum *et al.*, 2017). In addition, endless yet undiscovered rhizospheric and endophytic microbial candidates make this tool a future-directed platform.

Studies on PGPR-mediated phytochemical changes have covered a broad range of plant species from Arabidopsis as a model to medicinal plants and agricultural/horticultural crops. The majority of these studies focus on economically important plant species belonging to the Lamiaceae, Fabaceae and Asteraceae. On the PGPR-side, again *Pseudomonas* and

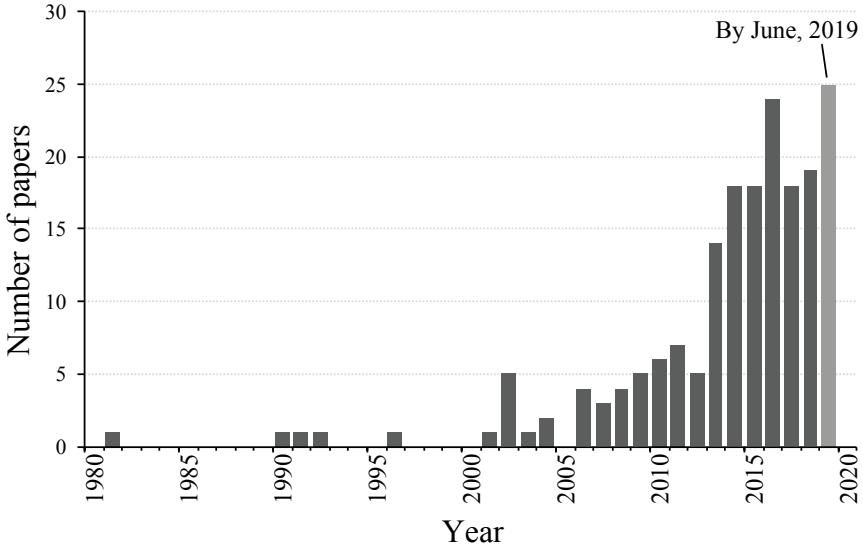

Fig 2. Number of articles available online (up to June 2019) that focus on "modulation of phytochemicals by beneficial bacteria". In the search for these articles we used the keyword combinations of "bacteria, beneficial rhizobacteria, PGPR, plant chemistry, plant secondary metabolite, plant metabolomics /metabolites, plant chemistry alteration/change, metabolite accumulation, HPLC, LC-MS/MS".

Bacillus were the most extensively studied rhizobacteria but also other genera are being tested for their effects on the plant metabolome (Etalo *et al.*, 2018). The overall objective in this research field is to investigate if PGPRs can increase the level of medicinal compounds in herbs and plant species. One of the best examples to date is the boost of artemisinin, the antimalarial bioactive chemical, in *Artemisia annua* by endophytic *Pseudonocardia* sp. via upregulation of the artemisinin biosynthesis genes *cyp71av1* and *cpr* (Li *et al.*, 2012). Similarly, an endophyte consortium, consisting of *Acinetobacter* and *Marmoricola* spp. induced the biosynthesis of benzylisoquinoline alkaloids (BIAs), bringing about a substantial increase of morphine production in *Papaver somniferum* (Ray *et al.*, 2019). Another recent study investigated the impact of various endophytic bacteria in *Panax ginseng* on the levels of ginsenosides, which are antitumor bioactive glycosylated triterpenes (Ji *et al.*, 2019).

Next to these medicinal plant compounds, PGPRs can also induce metabolome changes that affect (a)biotic stress tolerance. For instance, soybean (*Glycine max*) treated with *Stenotrophomonas maltophilia* N5.18 accumulated more isoflavonoids, phytoestrogen (Algar *et al.*, 2014). This study further demonstrated that another PGPR *Curtobacterium* sp. strain M84 also induced isoflavonoids levels in soybean after infestations by the bacterial leaf pathogen *Xanthomonas axonopodis* pv. *glycines*, suggesting a potential correlation between isoflavonoids accumulation and systemic resistance. In the same manner, *Bacillus velezensis* YC7010 significantly induced tricin, a flavonone glycoside, as well as contents of lignin and cellulose in rice (*Oryza sativa*), thereby triggering defense mechanism against the brown planthopper *Nilaparvata lugens* (Rashid *et al.*, 2018). Similarly, treatment of cotton with consortia of PGPR (9 *Bacillus* spp.) resulted in significant expression of (+)-δ-cadinene synthase gene family, gossypol accumulation and anti-herbivory against *Spodoptera exigua* (Zebelo *et al.*, 2016).

Notwithstanding the growing efforts to investigate PGPR-plant interactions, the bacterial traits involved in rhizobacteria-mediated plant metabolome changes remain largely unknown. Recently, the production of phenylacetic acid (PAA) by *Bacillus fortis* IAGS162 ameliorated *Fusarium* wilt disease in tomato (Akram *et al.*, 2016). Exposure of PAA to the media supporting tomato seedling growth led to changes in defense-related pathways together with up-regulation of various phenylpropanoid precursors. For *Pseudomonas aeruginosa* PM12, methoxybenzene methanol (HMB) was identified as a bacterial determinant that triggered systemic resistance in tomato against *Fusarium* wilt disease. An additional chemical analysis by GC-MS revealed the impact of HMB on primary and secondary metabolism, signaling and defense pathways in tomato (Fatima & Anjum, 2017). Moreover, several other studies revealed that mVOCs from various PGPR strains also impact on primary metabolism (Wenke *et al.*, 2019), flavonoid biosynthesis (Zhang *et al.*, 2007), or sulfur metabolism (Aziz *et al.*, 2016) but a comprehensive analysis of the specific mVOCs that trigger these responses and the signal transduction pathways leading to these plant metabolome changes has not been conducted yet for most of these PGPRs.

Table 1. Examples of PGP R strains and traits associated with changes in the plant metabolome

PGPR strain	PGPR trait	Plant	plant metabolome changes	Reference
Bacillus fortis IAGS162	phenylacetic acid (PAA)	Tomato	induction of shikimate and phenylpropanoid pathways	(Akram *et al.*, 2016)
Pseudomonas aeruginosa PM12	methoxybenzene methanol (HMB)	Tomato	increase of sugars, organic acids, polyamines, amino acids and salicylic acid	(Fatima & Anjum, 2017)
Bacillus amyloliquefaciens GB03	Sulfurous volatiles, dimethyldisulfide (DMDS)	Arabidopsis	increase of aliphatic and indolic glucosinolates	(Aziz *et al.*, 2016)
Pseudomonas fluorescens SS101	Sulfur metabolism (*cysH* gene)	Arabidopsis, Broccoli	increase of IAA, camalexin, hydroxycinnamates, and aliphatic glucosinolates in Arabidopsis; increase of flavonoids, hydroxycinnamates, indolic glucosinolates in Broccoli	(van de Mortel *et al.*, 2012; Cheng *et al.*, 2017), Chapter **5**

Thesis outline

Numerous beneficial rhizobacteria (PGPRs) can promote plant growth and trigger systemic resistance, thereby enhancing crop yield and improving plant quality traits. The recent technological developments in LC/GC hyphenated mass spectrometry have opened opportunities to study PGPR-mediated changes in phytochemistry as a novel platform that can be integrated in microbiome-mediated plant breeding. To date, however, the underlying mechanisms, bacterial traits and specificity in plant metabolome responses to single PGPRs or consortia of PGPRs, also referred to as synthetic communities (syncoms), remain largely elusive. Hence, the **overall aim of my thesis** is to study PGPR-induced changes in the metabolome of different plant species and to identify the bacterial traits involved in the induction of these plant metabolome changes. In **Chapter 2**, I provide an up-to-date overview of the existing literature on microbe-mediated effects on the plant metabolome. It provides an overview of phytochemical changes triggered by soil and plant-associated bacteria in diverse plant species, ranging from Arabidopsis as a model plant to crop, herbal, and medicinal plant species. Furthermore, this chapter also proposes a novel concept termed "Microbial-Gene Positioning System (m-GPS)" as a comprehensive tool to investigate the underlying mechanisms and genes associated with microbe-mediated modulation of plant chemistry.

To investigate the specificity of plant metabolome changes induced by rhizobacteria, I conducted a so-called 'blind date' experiment in **Chapter 3**, combining three strains of distinct rhizobacterial genera (*Pseudomonas*, *Microbacterium*, *Paraburkholderia*) and three different plant species, representing the model plant Arabidopsis, the medicinal plant Artemisia, and the crop plant Broccoli. Bacterial and host-specific effects were investigated via untargeted plant metabolomics, aided by root and shoot phenotyping and bacterial root colonization. Also the association between altered plant metabolism and plant growth is investigated based on the resource allocation theory and pathway analysis evidenced by chemical analyses. In **Chapter 4**, I looked into the diversity of phytochemical changes upon exposure of two Broccoli cultivars to different *Paraburkholderia* species. In this chapter, I not only looked into changes in plant secondary metabolism but also into changes in primary metabolism induced by these rhizobacterial species. In the following two experimental **Chapters 5** and **6**, I focus on the identification of bacterial traits and genes associated with the changes observed in plant phenotypes and metabolome described in **Chapters 3** and **4**. More specifically, for *Pseudomonas fluorescens* SS101, I investigated if *cysH*, a gene involved in sulfur metabolism, is associated with growth promotion and ISR, and if these phenotypic changes in two Brassica plant species (Arabidopsis and Broccoli) can be explained by the observed metabolome changes. In **Chapter 6**, I conducted a genome-wide transcriptome analysis on *Paraburkholderia graminis* (*Pbg*) colonizing the roots of Broccoli to identify potential gene candidates and pathways associated with the phenotypic and metabolic changes induced in two Broccoli cultivars.

Final **Chapter 7** integrates the findings of this thesis and addresses the potential use of rhizobacteria for sustainable agriculture and as a novel technological platform for the production of pharmaceutical products such as HVNPs.

Chapter 2

Modulation of plant chemistry by beneficial root microbiota

Desalegn W. Etalo, Je-Seung Jeon, Jos M. Raaijmakers

DWE and J-SJ are shared first author

Nat. Prod. Rep., 2018,35, 398-409

https://doi.org/10.1039/C7NP00057J

Abstract

Plants are colonized by an astounding number of microorganisms that can reach cell densities much greater than the number of plant cells. Various plant-associated microorganisms can have profound beneficial effects on plant growth, development, physiology and tolerance to (a)biotic stress. In return, plants release metabolites into their direct surroundings, thereby feeding the microbial community and influencing their composition, gene expression and the production of secondary metabolites. Similarly, microbes living on and in plant tissue may induce known and yet unknown biosynthetic pathways in plants leading to diverse alterations in the plant metabolome. Here, we provide an overview of the impact of beneficial microbiota on plant chemistry, with an emphasis on bacteria living on or inside root tissues. We will also provide new perspectives on deciphering the yet untapped potential of microbe-mediated alteration of plant chemistry as an alternative platform to discover new pathways, genes and enzymes involved the biosynthesis of high value natural plant products.

Keywords: microbe-plant interactions; beneficial rhizobacteria; phytochemistry; natural products

Introduction

Plant metabolites are estimated to be more than 100,000 at present (Wink, 2010) and new analogues are still being discovered in a rapid pace. Many plant-derived compounds exhibit a diverse array of biological activities including protection against herbivores and pathogenic microorganisms. Furthermore, plant metabolites are a major source of pharmaceuticals, either as the active ingredient of a crude plant extract or as a scaffold for chemical synthesis and structural modifications(Cragg & Newman, 2013; Bauer & Brönstrup, 2014). Recent studies have shown that specific microorganisms colonizing plant surfaces (phyllosphere, rhizosphere) and internal plant tissue (endosphere) can induce changes in the plant metabolome, leading to alterations in the biosynthesis of known plant metabolites or to the induction of yet unknown metabolites (Scherling *et al.*, 2009; van de Mortel *et al.*, 2012; Huang *et al.*, 2014; Ryffel *et al.*, 2016). Hence, microbe-plant interactions may provide a novel and more generic means to boost the production of agriculturally and/or pharmaceutically interesting plant metabolites and to discover structurally new plant metabolites and their corresponding biosynthetic genes and pathways.

For centuries, reductionist approaches gave primary importance to the interplay between the plant, abiotic conditions (light, water, CO_2) and physico-chemical characteristics of the soil. Over the past decade, Next Generation Sequencing (NGS) technologies have demonstrated that plants are colonized by an astounding number of taxonomically diverse (micro)organisms that can reach cell densities much greater than the number of plant cells. Several members of this plant-associated microbial community can influence plant growth, development and health(Mendes *et al.*, 2013; Panke-Buisse *et al.*, 2015). Consistent with the terminology used for microorganisms colonizing the human body, the collective communities of plant-associated microorganisms, their genomes and interactions are referred to as the plant microbiome (Mendes *et al.*, 2013). Plants attract and feed their microbiome by the exudation of photosynthetically fixed carbon into their direct surroundings, i.e., spermosphere, phyllosphere, rhizosphere and endosphere (Haichar *et al.*, 2008; Rudrappa *et al.*, 2008; Shidore *et al.*, 2012; Reinhold-Hurek *et al.*, 2015). The rhizosphere, the narrow zone (± 1-2 mm) surrounding and influenced by plant roots, is rich in small- and large-molecular weight compounds that serve as a carbon source for microbial growth (Bais *et al.*, 2006). In return, the rhizosphere microbiome provides a first line of defense against infections by root pathogens (Raaijmakers & Mazzola, 2016) as well as other life-support functions for the plant including nutrient acquisition and growth promotion (Van Loon, 2007; Bhattacharyya & Jha, 2012), induction of systemic resistance against above-ground pathogens and herbivorous insects (Raupach *et al.*, 1996; Van Wees *et al.*, 1999; Ryu *et al.*, 2004; Haas & Défago, 2005), and enhanced plant tolerance to abiotic stress (e.g. salinity, drought) (Dimkpa *et al.*, 2009; Yang *et al.*, 2009). Several microbial traits and mechanisms involved in these interactions have been identified (Han *et al.*, 2006; Nam *et al.*, 2006; Kim *et al.*, 2007; Sumayo *et al.*, 2013), but how microorganisms alter plant chemistry and if/how these

phytochemical changes affect plant growth, development and health are not well understood yet (**Fig 1**). Here, we provide an up-to-date overview of studies on microbe-mediated modulation of plant chemistry, with specific emphasis on endophytic and rhizosphere bacteria. The impact of other (micro)organisms, including plant pathogenic fungi, arbuscular mycorrhizal fungi, symbiotic nitrogen-fixing bacteria and parasitic weeds, on plant chemistry is not reviewed here; we refer the reader to other relevant literature (Bouwmeester *et al.*, 2003; Hahlbrock *et al.*, 2003; Furuhashi *et al.*, 2012; Okmen *et al.*, 2013; Schweiger *et al.*, 2014; Brusamarello-Santos *et al.*, 2017). In specific cases, we will address the putative mechanisms involved in the molecular interplay between beneficial bacteria and plants. Finally, we propose a conceptual framework for the potential use of plant-microbe interactions to elucidate and engineer plant metabolic pathways.

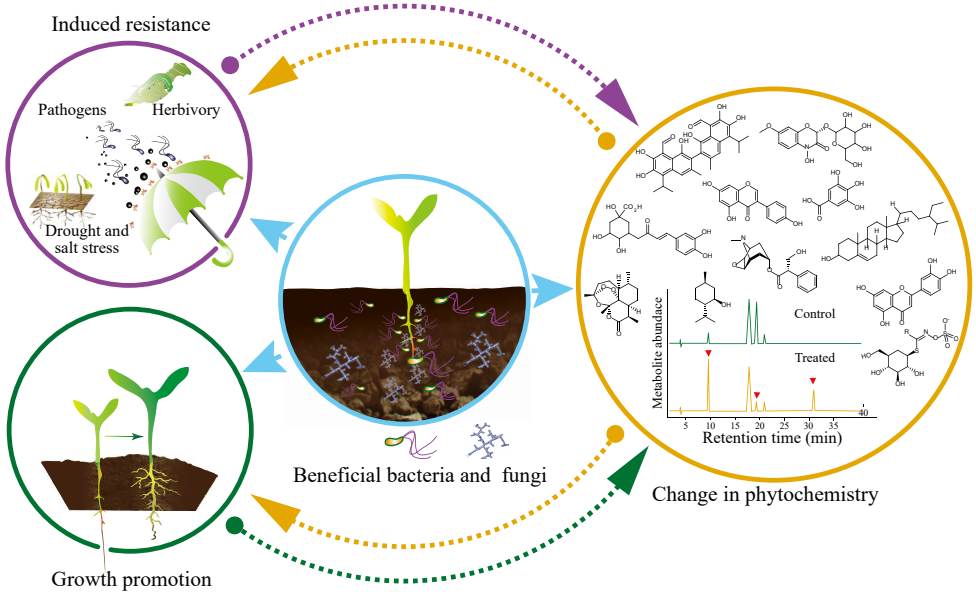

Fig 1. Influences of beneficial microbes on plant growth, health and chemistry. Beneficial microbes can enhance biomass, alter root system architecture, prime the plant defense against pathogens and phytophagous insects, enhance tolerance to drought and salt stress and alter phytochemistry. Phytochemical changes include induction, repression or biosynthesis of new metabolites in treated plants. Plants can also influence the composition and activity of root-associated beneficial microbes through their exudates. These beneficial microbes reside in the rhizosphere and endosphere of the host plant. The causal relationships between changes in phytochemistry, growth promotion and induced resistance (dotted arrows) are not well understood.

Modulations of plant chemistry by endophytes and beneficial root microbes

Endophytes are microbes that colonize living, internal tissues of plants without causing any immediate, overt negative effects on plant performance (Hardoim *et al.*, 2015). Although the number of studies on plant-endophyte interactions is increasing rapidly, the number of plant as well as microbial species investigated to date only represent the tip of the iceberg. With approximately 300,000 higher plants and their endophytic microbiomes, there is an enormous metabolic potential yet to be discovered. To date, effects of endophytes on the plant metabolome are more frequently studied and reported for fungi than for bacteria (Zhilin *et al.*, 2007; Huang *et al.*, 2008; Staniek *et al.*, 2008; Shukla *et al.*, 2014).

Endophytic fungi

Endophytic fungi are an important source of therapeutically active compounds. Some of the well-known examples include amongst others the tetracyclic diterpenoid anticancer drug paclitaxel from *Taxomyces andreanae* (Stierle *et al.*, 1993), the potent anticancer, antiviral, antioxidant, antibacterial and anti-rheumatic agent podophyllotoxin from *Sinopodophyllum hexandrum* (Yang *et al.*, 2003), the cognitive enhancer lycopodium alkaloid huperzine-A from *Shiraia* sp. (Zhu *et al.*, 2010), the antimicrobial agent enfumafungin from *Hormonema* sp. (Schwartz *et al.*, 2000), the lactone cholesterol-lowering agent lovastatin from *Aspergillus luchuensis* (El-Gendy *et al.*, 2016), a nonpeptidal antidiabetic agent from *Pseudomassaria* sp. (Zhang *et al.*, 1999) and the diterpene pyrones immunosuppressive agents subglutinol A and B from *Fusarium subglutinans* (Lee *et al.*, 1995). Furthermore, in plants, endophytic fungi are effective as biocontrol agents of plant diseases, insect pests and nematodes (Rowan, 1993; Ostlind *et al.*, 1997; Daisy *et al.*, 2002; Schwarz *et al.*, 2004; Tanaka *et al.*, 2005; Wicklow *et al.*, 2005; Li *et al.*, 2008; Wang *et al.*, 2013; Gupta *et al.*, 2016; Kim *et al.*, 2016; Schouten, 2016; Singh *et al.*, 2016). For more comprehensive information on bioactive metabolites from endophytic fungi we recommend the reader to excellent reviews of Newman and Cragg (Newman & Cragg, 2015).

In addition to having the biosynthesis machinery for the above mentioned bioactive metabolites, endophytic fungi are also know to play an important role in boosting metabolite biosynthesis of their host. Inoculation of endophyte-free *Catharanthus roseus* plants with the fungi *Curvularia* sp. and *Choanephora infundibulifera* enhanced the level of vindoline, a terpenoid indole alkaloid (TIA), in the leaves by 403% and 229%, respectively. Real-time PCR further showed that structural and regulatory genes involved in the TIA biosynthesis pathways were significantly upregulated in endophyte-inoculated plants when compared to endophyte-free plants (Pandey, Shiv S. *et al.*, 2016). Polysaccharide fraction from *Trichoderma atroviride*, an endopyte isolated from *Salvia miltiorrhiza,* significantly boosted the biosynthesis of tanshionones in hairy root cultures and also induced transcription of genes involved in tanshinone biosynthesis (Ming *et al.*, 2013). Also comparative metabolomics and

transcriptomics of ryegrass infected with *Epichloe festucae* and non-infected plants revealed that the endophyte caused 'reprogramming' of the host's metabolism, favoring secondary metabolism at the expense of primary metabolism. Particularly, flavonoids and anthocyanins showed significant accumulation in plants infected with the endophyte (Dupont *et al.*, 2015).

Endophytic and rhizosphere bacteria

Similar to endophytic fungi, endophytic and rhizospheric bacteria isolates are capable of producing a large number of bioactive metabolites and detailed reviews on this topic are provided by, among others, Gunatilaka (2006) and Singh *et al.* (2017). Several studies have shown profound effects of bacterial endophytes on their host's primary and secondary metabolism. For example, comparative primary metabolome analysis of poplar plants that were inoculated with *Paenibacillus* sp. showed significant increases in the levels of asparagine, urea and threitol, whereas a number of intermediates such as organic acids (malate, succinate, fumarate, citrate), amino acids (phenylalanine, 2-ketoglutatate, oxo-proline) and the sugar phosphate (fructose-6-phosphate) were reduced in the inoculated plants (Scherling *et al.*, 2009). Secondary metabolite profiling of grapevine treated with the endophytic bacterium *Enterobacter ludwigii* showed a significant increase in the level of vanillic acid and a decrease in the concentration catechin, esculin, arbutin, astringin, pallidol, ampellopsin, D-quadrangularin and isohopeaphenol. In roots and stems, also changes in the levels of epicatechin, procyanidin 1, taxifolin and the sum of quercetin-3- glucoside and quercetin-3-galactoside were detected (Lopez-Fernandez *et al.*, 2016).

Other studies on bacteria-mediated changes in phytochemistry reported to date involve the model plant species *Arabidopsis thaliana,* medicinal plants, food crops, ornamentals and trees/shrubs. Crop and medicinal plants categories, each encompassing 25 and 16 plant species, respectively, were the major hosts used in the reviewed articles. Among the reviewed articles, a total of 53 plant species belonging to 28 families were used to investigate bacteria-mediated phytochemical alterations. Lamiaceae, representing the herb plant that encopasses 8 plant species, was the most widely used plant family, followed by Fabaceae (7) and Asteraceae (5).

When investigating bacteria-mediated alteration in phytochemistry, seudomonadales and Bacillales were the most widely used bacterial orders (on 16 plant families each), followed by Actinomycetales (on 9 plant families) (**Fig 2**). More detailed information pertinent to phytochemical alterations induced by rhizobacteria is summarized in **Supplementary Tables S1 and S2**. Furthermore, the chemical structures of several plant metabolites whose biosynthesis is altered by endophytic and rhizospheric bacteria are shown in **Fig 3**. The overall aim of the studies with medicinal plants was to investigate if rhizosphere or endophytic bacteria can affect the level of a specific medicinal compound(s). For example, endophytic actinobacterium *Pseudonocardia* sp. isolated from *Artemisia annua* induced artemisinin (an antimalarial agent) production in *Artemisia* by upregulating the expression

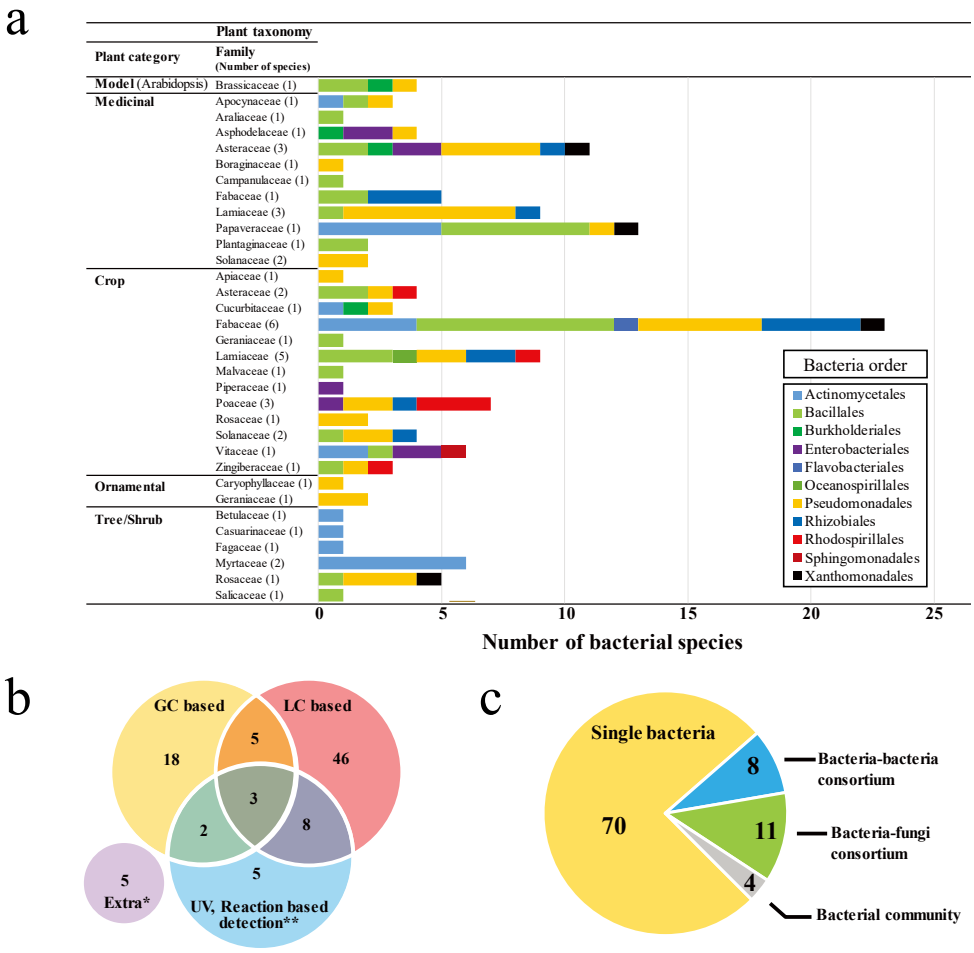

Fig 2. Plant families and bacterial orders described in the reviewed articles addressing microbe-mediated changes in phytochemistry. (**a**) taxonomy of the plants is indicated at family level along the Y-axis with the number of plant species belonging to the respective families indicated between brackets. Plant species are divided into five categories: model plant, medicinal plant, crop plant, ornamental plant and trees/shrubs. Similarly, the bacteria used in these studies are indicated at order level by colored bars and the number of bacterial species belonging to a given order is indicated along the X-axis. Details regarding the plants and bacterial species indicated in this graph are provided in the **Supplementary Tables S1 and S2**. (**b**) Analytical tools used to investigate changes in phytochemistry in response to beneficial microbes. The numbers in the Venn diagram correspond to the number of reviewed articles that used the indicated analytical tools to analyze microbe-mediated changes in phytochemistry. (**c**) Methods of application of beneficial microbes in studies involving microbe-mediated changes in phytochemistry. The numbers in the pie chart correspond to the number of reviewed articles that used one of the indicated application methods. *includes TLC and NMR, **involves reaction-based colorimetric/spectrophotometric quantitative analysis of specific groups of compounds such as total flavonoids, total phenolics, total proanthocyanidin, alkaloids and tannins.

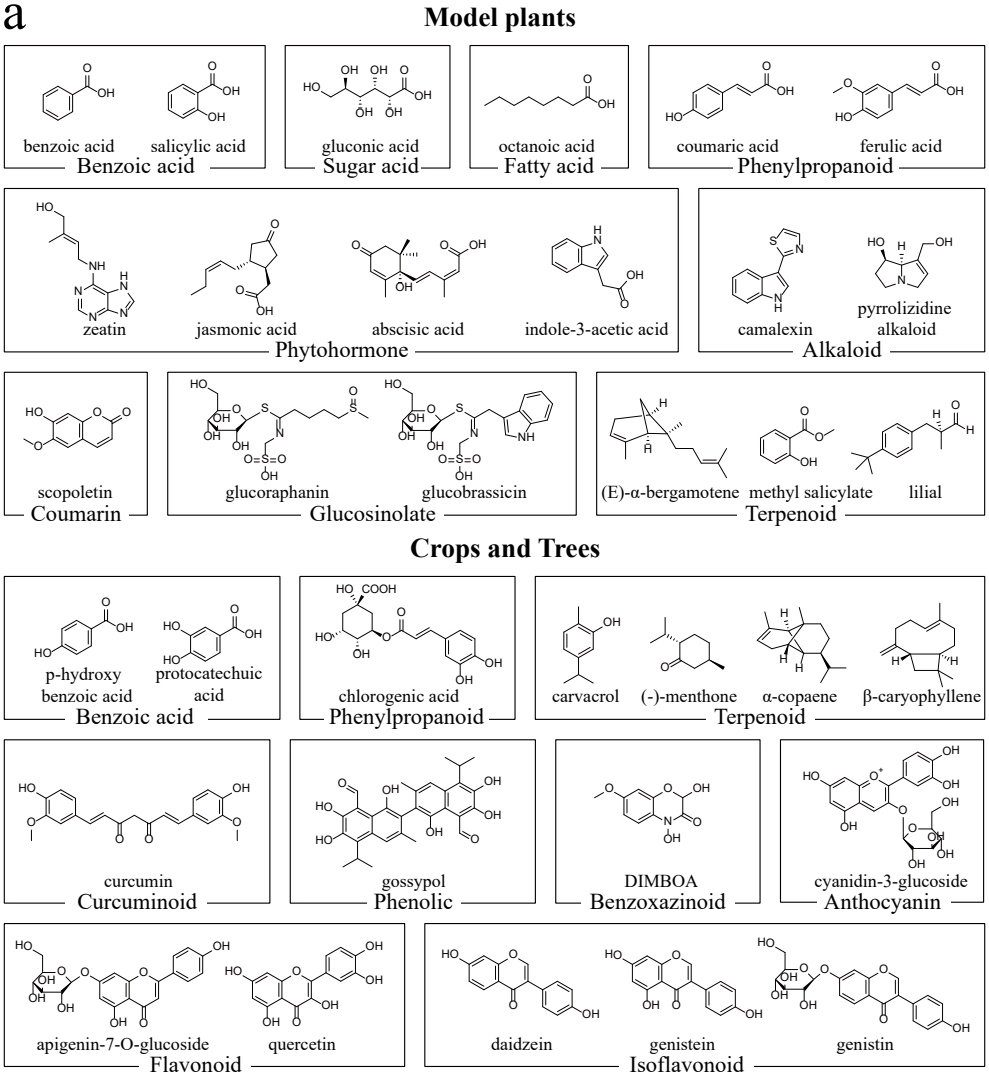

Fig 3. Chemical structures of representative plant metabolites that were changed by beneficial bacteria treatment. Detailed information on these list of metabolites is included in Supplementary **Table S1**.

of cytochrome P450 monooxygenase and cytochrome P450 oxidoreductase genes involved in artemisinin biosynthesis (Li *et al.*, 2012). Similarly, endophytic bacteria *Staphylococcus sciuri* and *Micrococcus* sp. boosted the production of therapeutically useful terpenoid indole alkaloids in *Catharanthus roseus,* including vindoline, serpentine and ajmalicine (Tiwari *et al.*, 2013). γ- Terpinene, cis-sabinene hydrate and thymol showed a significant increase when *Origanum majorana* plants were inoculated with three growth-promoting bacteria

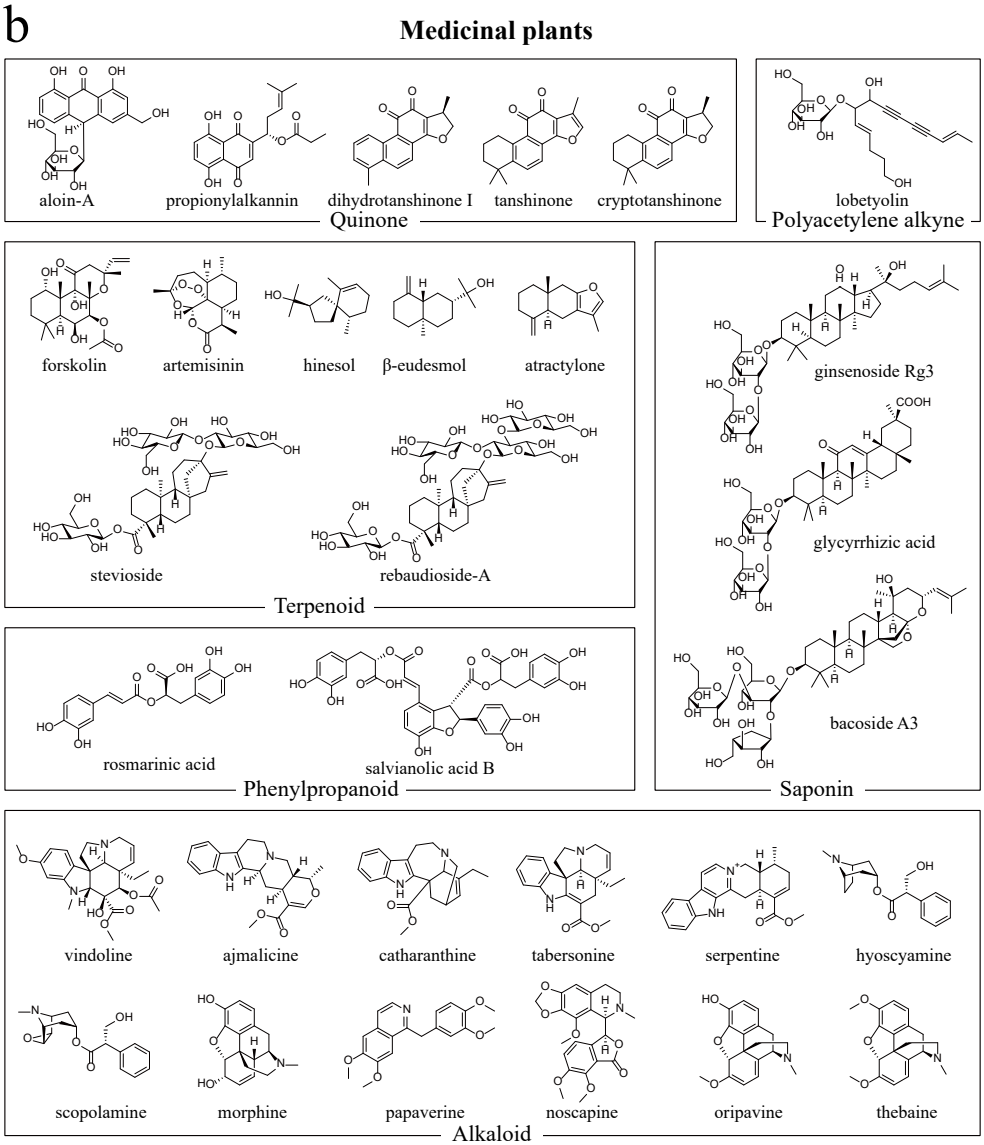

Fig 3. (Continued)

Pseudomonas fluorescens, *Bacillus subtilis* and *Azospirillum brasilense*. Inoculation of plants with *A. brasilense* only resulted in significant accumulation of carvacrol, a monoterpenoid and the major constituent of Oregano essential oils (Banchio *et al.*, 2010). Combined foliar and irrigation application of *Paenibacillus polymyxa,* an endophytic bacteria isolated from ginseng plant leaves, resulted in increased ginsenoside concentration in 1-4 year old ginseng plants by 37%, 45%, 68% and 80%, respectively (Gao *et al.*, 2015). In addition to boosting metabolite

biosynthesis of their host, root-associated bacteria are able to transform plant metabolites into different derivatives. For example, Giudice *et al.* (2015) showed the presence of root-associated bacteria in parenchymatous essential oil-producing cells. These bacteria were able to metabolize essential oil and as a consequence release large number of compounds, some of which were absent or present in very low amounts in the raw oil. Interestingly, axenic Vetiver plantlets produces *in vitro* only trace amounts of oils with strikingly different composition compared with the oils from *in vivo* Vetiver plantlets suggesting that root-associated bacteria contribute to the Vetiver oil composition. Some of the isolated root-associated bacteria were indeed able to induce the expression of the plant tepene synthase gene (Del Giudice *et al.*, 2008). Another interesting example is the conversion of the major ginsenoiside Rb1 to the potent antitumor compound ginsenoside Rg3 by *Burkholderia* sp. isolated from ginseng roots. Collectively, these studies demonstrated that endophytic bacteria can not only boost the levels of specific bioactive metabolites in their host but may also transform biologically less active forms of metabolites into active derivatives (Fu *et al.*, 2017). Other groundbreaking studies revealed that specific metabolites such as the known anti-tumor agent maytansine, a benzoansamacrolide, that was assumed to be of plant origin was actually synthesized by the endophytic bacterial community residing in the root cortex of *Putterlickia verrucosa* and *P. retrospinosa* plants (Kusari *et al.*, 2014).

Phytochemical changes and their impact on plant growth and health

In the coming sections, we will highlight several studies where plant growth promotion and plant protection against pests and diseases were investigated in relation to microbe-mediated changes in plant chemistry. Growth promotion and induced systemic resistance (ISR) are two of the most well-studied plant phenotypic responses to rhizosphere and endophytic bacteria (**Fig 1**). Similarly, a number of reports have shown global changes in the plant metabolome in response to inoculation with plant growth-promoting rhizobacteria (PGPR) (Dardanelli *et al.*, 2010; Walker *et al.*, 2011; Walker *et al.*, 2012; Algar *et al.*, 2013). Yet, the causal relationships between plant metabolome changes, plant growth promotion and/or protection (direct, indirect) conferred by these PGPRs are not well understood. In the following sections, the relationship between microbiome-mediated metabolome change and plant growth and health for model plants and crops will be discussed.

Model plants

Our earlier work showed that rhizobacterium *Pseudomonas fluorescens* strain SS101 promoted growth of *A. thaliana* and induced systemic resistance (ISR) to the bacterial leaf pathogen *Pseudomonas syringae* pv *tomato* (*Pst*) and the herbivore insect *Spodoptera exigua* (van de Mortel *et al.*, 2012). The ISR response correlated with increased levels of camalexin and glucosinolates, in particular the indole glucosinolates for insect resistance (van de

Mortel *et al.*, 2012). Mutant lines of *A. thaliana* defective in glucosinolate biosynthesis were compromised in resistance to both *Pst* and *S. exigua* (van de Mortel *et al.*, 2012), indicating an important role of these plant metabolites in the ISR response. Similar to beneficial bacteria, root colonization of *A. thaliana* by the beneficial fungus *Trichoderma asperelloides* T203 substantially altered the plant's primary metabolism with increased levels of amino acids and polyamines that are closely linked to plant growth and that act as a precursor for the biosynthesis of important defense-related secondary metabolites (Brotman *et al.*, 2012).

Even without direct physical contact with their host, beneficial rhizobacteria can influence plant metabolism, growth and health through the production of volatile organic compounds (VOCs). *Bacillus* sp B55, a rhizobacterium naturally associated with *Nicotiana attenuata* roots, produces sulfur-containing VOCs, in particular dimethyl disulfide (DMDS), which promoted plant growth. When strain B55 was grown in minimal medum containing ^{35}S-labeled Na_2SO_4 as the sole S source, plants absorbed and incorporated ^{35}S into their proteins, suggesting that provision of reduced sulfur to the plant is a possible mechanisms underlying growth promotion (Meldau *et al.*, 2013). Similarly, Arabidopsis exposed to VOCs from *Bacillus amyloliquefaciens* (GB03) showed enhanced sulfur accumulation when traced with radioactive sulfate ($^{35}SO4^{-2}$). Interestingly, microarray data analysis further indicated that several sulfate reduction genes and transcripts encoding genes for the majority of aliphatic glucosinolates and some genes involved in the indole-glucosinolate pathway were induced by the bacterial treatment. Furthermore, treated plants exhibited a significant increase in cysteine, the precursor for methionine that acts as the main substrate for aliphatic glucosinolate biosynthesis. Interestingly, glucosinolate analysis of plants exposed to BG03 VOCs showed 33 and 70% increases in the total glucosinolate content in shoots and roots, respectively, compared to the untreated control (Aziz *et al.*, 2016). Furthermore, treated plants showed significant reduction in herbivory by the insect *Spodoptera exigua*.

Crop plants

Similar to model plants, microbe-mediated changes in phytochemistry of crop plants appear to correlate with biomass enhancement and resistance against pathogens. For example, Betelvine plants treated with *Serratia marcescens* NBRI1213 showed a significant increase in biomass and retarded infection by *Phytophthora nicotianae*, an oomycete plant pathogen with broad host range. Plants treated with *S. marcescens* showed significant accumulation of gallic acid, ferulic acid, chlorogenic acid and caffeic acid (Lavania *et al.*, 2006), phenolic acids that exhibit antifungal and anti-oomycetes activities (Sarma & Singh, 2003; Widmer & Laurent, 2006; Ockels *et al.*, 2007; Nguyen *et al.*, 2013; Li *et al.*, 2017). Similarly, chickpea treated with *Pseudomonas fluorescens* (pfs3) accumulated similar potent antifungal phenolics and the level of these metabolites coincided with seedlings survival when challenged with the fungal root pathogen *Sclerotium rolfsii* (Sarma *et al.*, 2002). Moreover, rice plants treated with *Azospirullum* sp. B510 showed enhanced resistance against the rice blast fungus

Magnaporthe oryzae and the bacterial pathogen *Xanthomonas oryzae* (Yasuda *et al.*, 2009). Interestingly, *Azospirullum* sp. B510 induced p-coumaric and ferulic acid, which are major constituents of rice phenolics (Chamam *et al.*, 2013).

Similar to what is described above for model plants, rhizobacteria-mediated changes in phytochemistry in crop plants also may have an adverse effect on phytophagous insect performance. Treatment of cotton with consortia of rhizobacteria (composed of 9 *Bacillus* spp.) resulted in accumulation of gossypol and reduced herbivory by *Spodoptera exigua* via reduced the pupation and higher larval mortality. Transcriptional analysis further revealed that the rhizobacteria significantly upregulated the expression of the (+)-δ-cadinene synthase gene family involved in the biosynthesis of gossypol (Zebelo *et al.*, 2016). Collectively, these and other examples for model, medicinal, crop plants as well as trees/shrubs (**Supplementary Table S1**), signify the magnitude of changes that can be brought about by root-associated bacteria on the plant transcriptome and metabolome and how these changes can impact plant growth, development and health. Understanding the bacterial determinants involved in the alteration of the plant metabolome will shed more light on the fundamental mechanisms underlying of the activation of specific metabolic networks and their importance for the fitness to the host plant in managed or natural ecosystems.

Microbial traits and molecular mechanisms

Most of the studies reviewed here on rhizobacteria-mediated changes in phytochemistry did not provide direct evidence or insght into the underlying molecular mechanisms. Various bacterial determinants have been identified for their role in biological nitrogen fixation (Dixon & Kahn, 2004), production and regulation of phytohormones and analogues (Cassán *et al.*, 2014), siderophore production (Neilands, 1995) and phosphate solubilization (Rodríguez & Fraga, 1999). Our recent work involving site-directed mutagenesis and genetic complementation of *Pseudomonas fluorescens* strain *Pf* SS101 pointed to three genes, i.e. phosphogluconate dehydrates gene (*edd*), the response regulator gene *coIR* and the adenylsulfate reductase gene (*cysH*), involved in plant growth promotion and ISR. Also various other bacterial traits have been identified for their role in plant growth promotion and ISR, including lipopolysaccharides (Leeman *et al.*, 1995), salicylic acid (De Meyer & Höfte, 1997), siderophores (Sayyed *et al.*, 2013), 2-aminobenzoic acid (Yang *et al.*, 2011), cyclic lipopeptides (Ongena *et al.*, 2007), exopolysaccharides (Uma Sankari J. *et al*, 2011), cell wall degrading enzymes (Kobayashi *et al.*, 2002), flagella (Meziane *et al.*, 2005), 2,4-diacetylphloroglucinol (Weller *et al.*, 2004), 2,3-butanediol (Ryu *et al.*, 2004), and N-alkylated benzylamine (Ongena, M. *et al.*, 2005). To date, however, bacterial determinants involved in the alteration of the plant metabolome remain largely elusive. Recently, phenylacetic acid (PAA) produced by beneficial bacteria *Bacillus fortis* IAGS162 was shown to be a determinant of ISR against Fusarium wilt disease in tomato. Plants exposed to PAA and challenged with the fungal pathogen *F. oxysporum* f.sp. *lycopersici* showed extensive changes in their primary metabolism. Particularly, the shikimate

and phenylpropanoid pathways (l-phenylalanine, cinnamic acid, benzoic acid, caffeic acid, and salicyclic acid) were upregulated (Akram *et al.*, 2016). Similarly, 3-hydroxy-5-methoxy benzene methanol (HMB), isolated from extracellular metabolites of *Pseudomonas aeruginosa* PM12, was shown to have significant impact on the plant metabolome and to be a potent determinant of ISR. Tomato plants treated with HMB showed enhanced levels of sugars (fructose, glucose, sucrose), phosphorylated sugars (fructose-6- phosphate, glucose-6-phosphate, myo-inositol-phosphate), organic acids (α-ketoglutarate, malate, oxaloacetate, citrate, succinate), polyamines (picolinic acid, pipecolic acid, putrescine, spermidine), amino acids (phenylalanine, arginine, glutamine and proline) and salicylic acid. The levels of glycerol-3-phosphate, fumarate, cis- aconitate, leucine, tyrosine and threonine were reduced in plants treated with HMB when compared to untreated control plants (Fatima & Anjum, 2017). As indicated above, beneficial rhizobacteria can also influence the host metabolome via VOCs, that may influence the expression of various plant genes including those involved in flavonoid (Zhang *et al.*, 2007) or sulfur metabolism (Meldau *et al.*, 2013; Aziz *et al.*, 2016).

Microbial-Gene Positioning System (m-GPS)

The above-mentioned examples highlight the paramount importance of plant-associated microbes in shaping the metabolome landscape of their host. Microbe-mediated alteration or reprograming of the plant metabolome is dependent on the combination of plant species/cultivar and microbial species. For example, when two rice cultivars (Cigaron and Nipponbare) were inoculated with *Azospirillum lipoferum*, *the* impact on the root metabolome was greater for Cigaron. More specifically, treated Cigaron cultivars exhibited a reduction in the level of a number of flavonoids and an increase in the level of hydroxycinnamic acid derivatives and alkylresorcinol (Chamam *et al.*, 2013). In another study, treatment of these two rice cultivars with either *A. lipoferum* 4B (rhizospheric) or *Azospirillum sp*. B510 (endophytic) resulted in *Azospirillum* strain x cultivar specific changes in the metabolome. Strain 4B (rhizospheric bacteria isolated from Cigalon) induced major changes in secondary metabolism only in Cigalon roots, while strain B510 (endospheric bacteria isolated from Nipponbare) induced metabolic changes in shoots and roots of both rice cultivars (Chamam *et al.*, 2013). Whether these differences are truly strain specific or more related to their lifestyle, i.e. rhizosphere versus endosphere, remains to be resolved. Also treatment of seeds of two maize cultivars (PR37Y15 and DK315) with three beneficial bacteria *A. brasilense* CFN-535, *A lipoferum* CRT1 and *A. brasilense* UAP-154, revealed major *Azospirillum* strain-cultivar specific qualitative and quantitative changes in secondary metabolism, primarily benzoxazinoids (Walker *et al.*, 2011). Based on these observations, we postulate that microbes, due to their long standing co-evolutionary relationship with their host, serve as specialized engineers of the plant's primary and secondary metabolism. We predict that such specific alteration of the plant metabolome when interrogated by integration of different approaches involving transcriptomics, proteomics and metabolomics, can reveal new genes, enzymes, pathways

and metabolic networks in plants associated with growth, development and tolerance to (a) biotic stresses (**Fig 4**). In this context, microbe-plant interactions may serve as a valuable tool to predict and identify rate limiting/critical steps in plant metabolic pathways. To further frame the more fundamental concept behind this approach, we propose the term "microbial-Gene Positioning System (m-GPS)", which involves identification of metabolic pathways that are perturbed by the microbial treatment followed by mapping of the changes in the expression of genes and the activity of enzymes belonging to the corresponding metabolic pathways. Based on these analyses, pragmatic decisions can be made to pick the most influential gene(s) that is/are targeted by the beneficial microbes to impact the flux of a given metabolite(s). The role of these candidate genes can be validated using mutant lines or reverse genetics tools. If indeed these genes show an influential role in the biosynthesis of high value natural plant products (HVNPs), they can be used in conventional breeding or synthetic biology programs for trait improvement. Screening for allelic variants/orthologues of the candidate genes across plant species may further help to identify an elite allelic variant and the associated sequence information can be used for protein engineering intended to create ultra-enzymes in biotechnology and synthetic biology programs (**Fig 4a**). Similarly, bacterial traits involved in the modulation of the plant metabolome can be explored as an innovative strategy to improve the collective genome of the rhizosphere microbiome. Once prominent bacterial traits are identified, further screening of allelic variants/orthologues can be performed across several rhizobacterial species and strains of a given species. Using such strategy, best performing allelic variant(s) of bacterial traits in altering the plant metabolome can be used to enhance the content of HVNPs in plants (**Fig 4b**). The current targeted genome editing techniques such as the CRISPR/Cas system (Selle & Barrangou, 2015) will have a profound contribution to our quest to understand signal perception and downstream signalling and to ultimately engineer bacterial traits to impact plant chemistry.

Concluding remarks and future perspective

In this review, we provided an overview of microbe-mediated changes in plant chemistry and other plant phenotypes (enhanced growth, ISR). Establishing a causal relationship requires comprehensive understanding of the metabolic pathways involved in plant growth and defense, and of the microbial traits and mechanisms underlying the alteration of plant phenotypic and metabolic traits. Unravelling the chemical interplay between microbial metabolites, enzymes and elicitors and how these affect plant signal perception, signal transduction and the downstream metabolic networks requires systems-based approaches to connect host- and microbial traits with the observed changes in the metabolome, biomass and resistance to biotic stresses. The number of publications in the area of bacteria-mediated phytochemical alterations is increasing due to exciting developments in next generation sequencing and state-of-the-art LC/GC hyphenated mass spectrometry technologies **(Fig 2b)**. Future studies that focus on the beneficial microbe-mediated plant metabolome reprograming

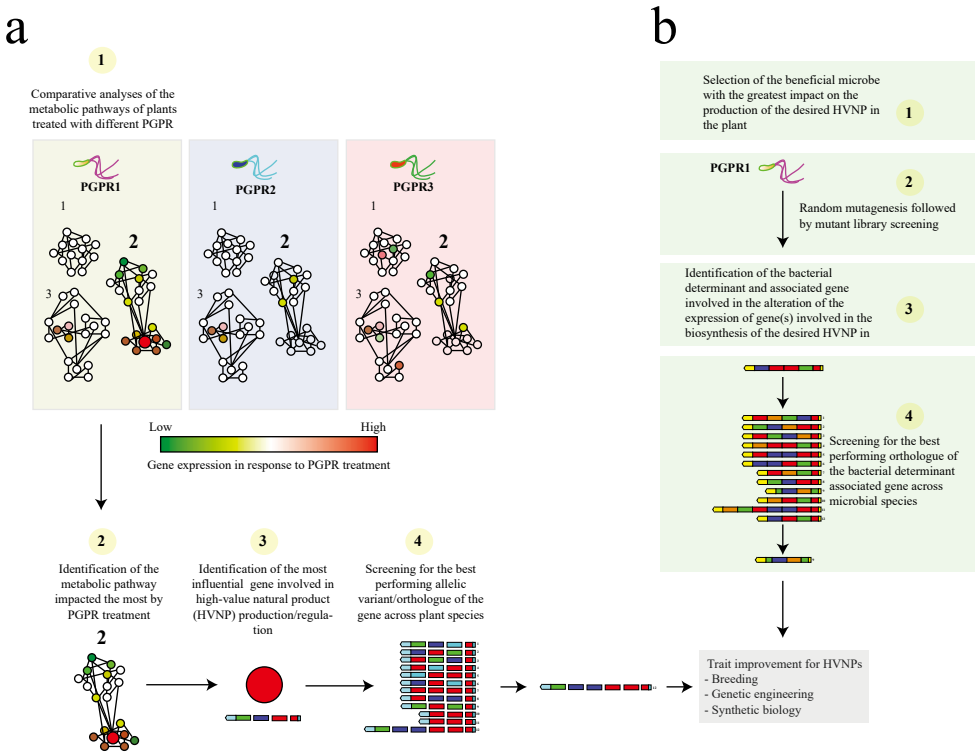

Fig 4. Illustration of the microbial Gene Positioning System (mGPS), a conceptual framework that proposes to use beneficial microbe-mediated alteration of plant metabolic pathways as a means to identify influential genes involved in the biosynthesis and regulation of High Value Natural Products (HVNPs). (**a**) The first strategy initially involves comparing the influence of different beneficial microbes on the plant metabolic pathways involved in the production of HVNPs (1), after which follows the identification of the metabolic pathway that is impacted the most by the treatment of beneficial microbes (2). Subsequently, the most influential gene in the biosynthetic pathway of HVNPs is identified (3); following this step, the performance of allelic variants/orthologues of the identified gene from different plant species is evaluated and the best performing allelic variant/orthologous gene is then used for improvement of HVNPs production in plants (4). (**b**) A second potential strategy to improve the production of HVNPs in plants is to screen a number of beneficial microbes for their impact on the production of targeted compounds (1). The best performing microbe is then subjected to random mutagenesis (2) to identify the microbial determinant involved in the alteration of HVNPs (3). Then, orthologous genes of the microbial determinant are evaluated for their ability to elicit maximum production of the targeted HVNPs (4).

will expand our horizon beyond the use of microbes as a biocontrol agent or as plant growth promotor only. Endophytes are receiving particular attention in this research field as they are assumed to have a more intimate association with their host plant than microorganisms that live in the 'spheres' (rhizosphere, phyllosphere). Interestingly, metabolites detected in crude extracts from plants could originate from the plant, the endophyte (Kusari *et al.*, 2014), from the combined effort of both (Kusari *et al.*, 2011; Heinig *et al.*, 2013), from modification

of the plant metabolites by endophytes (Tian *et al.*, 2014; Fu *et al.*, 2017), or even from modification of endophyte metabolites by the host plant (Strobel & Hess, 1997). Moreover, endosymbiotic bacteria residing inside the fungal hyphae (Hoffman & Arnold, 2010) as well as endophyte-endophyte interactions may even increase the complexity of the overall 'plant' metabolome. These examples underscore how the genetics and chemistry between plants and their microbiomes (i.e. the holobiont (Rohwer *et al.*, 2002; Rosenberg & Zilber-Rosenberg, 2016)) are intertwined to each other. Although most studies to date have focused on the impact of one microbial strain on the plant metabolome (**Fig 2c**), future studies that interrogate the relationships between the microbiome composition, its functions and plant metabolome dynamics will greatly help to understand the ecological significance of microbe-mediated alteration of the plant metabolome.

Supplementary materials

Table S1. Overview of studies on alterations in the chemistry of model, medicinal, crop and ornamental plant species induced by beneficial bacteria

Table S2. Overview of different bacterial genera studied for their impact on the chemistry of different plant species

Above supplementary tables are available at: https://doi.org/10.1039/C7NP00057J

Chapter 3

The metabolic signature of rhizobacteria-induced growth promotion in different plant species

Je-Seung Jeon, Natalia Carreno-Quintero, Ric De Vos,
Jos M. Raaijmakers and Desalegn W. Etalo

Manuscript under revision for publication

Abstract

Various rhizobacteria promote plant growth and trigger systemic resistance against leaf pathogens and phytophagous insects. To date, however, the underlying chemistry and metabolic signatures of these rhizobacteria-induced plant phenotypes are less understood. To identify core metabolic pathways that are targeted by growth-promoting rhizobacteria, we used combinations of three plant species and three rhizobacterial species and interrogated the plant shoot chemistry by untargeted metabolomics. Our results showed that a substantial part (50-64%) of the metabolites detected in host shoot tissue was differentially regulated by the rhizobacteria. Among others, the phenylpropanoid pathway was targeted by the rhizobacteria in each of the plant species. Differential regulation of the various branches of the phenylpropanoid pathways showed an association with either plant growth promotion or growth reduction. Overall, suppression of flavonoid biosynthesis was associated with growth promotion, while growth reduction showed elevated levels of flavonoids. Our study also showed that a number of pharmaceutically and nutritionally important metabolites in the plant shoot were significantly increased by rhizobacterial root treatment, providing new avenues to use rhizobacteria to tilt plant metabolism towards the biosynthesis of valuable natural plant products.

Keywords: beneficial rhizobacteria; plant metabolomics; bacteria-plant interactions; phenylpropanoids; flavonoids, metabolic alterations

Introduction

The rhizosphere, the narrow zone (± 1-2 mm) surrounding and influenced by plant roots, harbors a plethora of soil-borne microorganisms that can have deleterious or beneficial effects on plant growth and health (Raaijmakers *et al.*, 2009; Mendes *et al.*, 2013). Amongst the best-studied beneficial rhizosphere microbes are the Plant Growth-Promoting Rhizobacteria (PGPR). Their beneficial association is thought to be ancient and presumably has been shaped by co-evolutionary processes in the long-term interactions with their host plants (Lambers *et al.*, 2009). PGPR can enhance plant growth through direct and indirect mechanisms (Lugtenberg & Kamilova, 2009). The direct mechanisms involve facilitation of nutrient acquisition and modulation of phytohormones, whereas indirect effects involve reducing the inhibitory effects of biotic stress factors through parasitism, antibiosis, competition and the induction of systemic resistance (L. C. van Loon *et al.*, 1998; De Vleesschauwer & Höfte, 2009; Lugtenberg & Kamilova, 2009; Van der Ent *et al.*, 2009; Pineda *et al.*, 2010; Stringlis, I. A. *et al.*, 2018).

PGPR can also have profound effects on the physiology and metabolism of their host plants, not only by enhancing the production of known secondary metabolites but also by inducing the biosynthesis of yet-unknown compounds (van de Mortel *et al.*, 2012). The plant secondary metabolites affected by PGPR reported to date include, among others, polyphenols, flavonoids and glucosinolates but also primary metabolites such as carbohydrates and amino acids (Etalo *et al.*, 2018). So far, only a few studies have provided insights into the association between rhizobacteria-induced biochemical changes and plant growth and defense (Walker *et al.*, 2011; van de Mortel *et al.*, 2012; Weston *et al.*, 2012; Etalo *et al.*, 2018; Hu *et al.*, 2018; Stringlis, Ioannis A *et al.*, 2018).

PGPR can prime plant defense against pathogens and insect herbivores and at the same time promote plant growth. This is in contrast to the widely accepted concept of the trade-off between plant defense and plant fitness in general and plant growth in particular. Understanding the underlying growth- and defense-associated plant metabolic networks and unraveling their interactions is essential to understand and optimize rhizobacteria-mediated growth promotion and ISR. Although some reports indicated rhizobacteria-mediated changes in specific metabolites classes (Mishra *et al.*, 2006; Walker *et al.*, 2011; Chamam *et al.*, 2013), their overarching effects on the global metabolome of plants and in particular on core metabolite pathways that are co-occurring with growth promotion across plant species are not well understood. More specifically, PGPR-mediated re-routing of the plant's metabolism could give insight into the metabolic interplay between plant defense and growth. Furthermore, it is highly instrumental to understand the organization of metabolite routes, which consequently contribute to the engineering of the plant metabolism by tilting a particular pathway towards a desired target. Recently, PGPR-induced metabolic changes have attracted the interests of researchers for the development of new strategies to enhance the production of high value plant compounds (HVPC) (Etalo *et al.*, 2018).

Here, we studied the impact of three strains of different rhizobacterial genera on the phenotype and shoot metabolome of three plant species: *Arabidopsis thaliana* (model plant), *Brassica olearacea* var. italica (crop) and *Artemisia annua* (medicinal plant). Our primary interest was to identify core metabolic pathways that are targeted by rhizobacteria in different plant species and investigated their regulation under effective and ineffective rhizobacteria-plant partnerships that lead to plant growth promotion or growth reduction, respectively. A combination of *in vitro* bioassays and untargeted metabolomics was used to examine common and specific plant responses triggered by these different rhizobacterial strains. Our results show that inoculation of the plant root system with each of these rhizobacteria induced substantial changes in the shoot metabolome in a species-specific manner. Both growth-promoting and growth-reducing plant-rhizobacteria combinations revealed that the phenylpropanoid pathway is central to the plant metabolome response and that differential regulation of different branches of this pathway showed an association with positive and negative effects of the rhizobacteria on plant growth.

Materials and Methods

Plant material and growth

For *in vitro* experiment, seeds of *Arabidopsis thaliana* Columbia (Col-0) and *Artemisia annua* (kindly provided by Artemisia F1seed, Department of Biology, University of York, England) were surface sterilized as previously described (van de Mortel *et al.*, 2012). Seeds of *Brassica olearacea* var. italica, cultivar Coronado (kindly provided by Bejo Seeds, Warmenhuizen, the Netherlands) were surface sterilized for 30 min in 1% (v/v) sodium hypochlorite and 0.1 % (v/v) Tween 20 and then washed three times with ample sterile distilled water. After sterilization, seeds were pre-germinated on wet filter paper in plastic petri dishes and placed at 4 °C in the dark for 2 to 4 days. After the emergence of the radicle, seeds were sown on half-strength Murashige and Skoog (MS) medium containing 2.5% (w/v) sucrose and plant agar 12%. The plates were then transferred to a climate chamber at 21 °C /21 °C day/night; 180 µmol light $m^{-2}s^{-1}$, 16h light/8h dark cycle and 70% relative humidity. After 7 days for *A. thaliana* and *A. annua* and 3 days for *B. oleracea,* 2 µl of a washed bacterial cell suspension (OD_{600} = 1.0) was inoculated onto the root tips of the seedlings. After inoculation, plants were grown in the same growth chamber until harvest.

Bacterial strains and culture conditions

The rhizobacterial species *Paraburkholderia graminis* (*Pbg*) (Carrión *et al.*, 2018) and *Microbacterium* (MB) (Cordovez *et al.*, 2018) used in this study were originally isolated from the rhizosphere of sugar beet *Beta vulgaris*. *Pseudomonas fluorescens* (*Pf* SS101) was isolated from wheat rhizosphere (de Souza *et al.*, 2003). *Pf* SS101 was cultured in King's medium B (KB), while MB was cultured in Tryptone Soy broth (TSB) medium and *Pbg*

in Luria Bertani (LB) medium (Lennox, Carl Roth) at 25 °C for 16h. Bacterial cells were collected by centrifugation, washed three times with 10 mM $MgSO_{4,}$ and resuspended in 10 mM $MgSO_4$ to a final density of ~10^9 cells/ml (OD_{600} = 1.0).

Plant phenotyping

Fresh biomass of plant shoots was determined every two days until 11 days post inoculation (dpi) for Arabidopsis and Broccoli and 14 dpi for Artemisia. For each plant species, four independent biological replicates were used with 10 seedlings of Arabidopsis, 8 of Artemisia and 5 of Broccoli per biological replicate. Prior to root dry mass measurements, roots were carefully detached from the MS-agar and washed with sterile distilled water to remove agar. Thereafter, root dry biomass was determined (Ostonen *et al.*, 2007). Student's *t*-Test and two-way ANOVA were used to determine statistically significant ($P < 0.05$) differences between treatments.

Rhizobacteria colonization

Bacterial root colonization was determined at 11 dpi for Arabidopsis and Broccoli and at 14 dpi for Artemisia. Roots were collected in sterile glassware and their weight was determined. Root samples were vortexed for 60 s in 10 mM $MgSO_4$, sonicated for 60 s, and vortexed once more for 15 s. After serial dilution, 50 µl of the suspensions were plated onto PSA (*Pf* SS101 and *Pbg*) and TSA (MB) containing 100 µg ml^{-1} delvocid (DSM). After 3 days incubation at 25 °C, the number of colonies were determined for each of the replicates. Bacterial colonization was expressed as colony-forming units (cfu) per gram of root fresh weight.

Plant metabolite analysis

Sample collection and extraction

Shoots were harvested at 11 dpi for Arabidopsis (N=10) and Broccoli (N=5) seedlings, and at 14 dpi for Artemisia (N=8). For each plant species x rhizobacteria combination, 4 biological replicates comprising the aforementioned number of plants were used. Briefly, shoots were snap frozen in liquid nitrogen and ground to a fine powder under continuous cooling and kept at -80 °C until further use. For extraction of semipolar metabolites, 300 µL of 99.89% methanol containing 0.13% (v/v) formic acid was added to 100 mg powdered plant material in 2 ml round bottom Eppendorf tubes, and sonicated for 15 min followed by centrifugation for 15 min at 20,000 X*g*. The supernatants were transferred to a 96-well plate (AcroPrepTM, 350 µL, 0.45µm, PALL) and vacuum filtrated into a 96-deep-well autosampler plate (Waters) using a Genesis Workstation (Tecan Systems).

Metabolite analysis

An UltiMate 3000 U-HPLC system (Dionex) was used to create a 45 minutes linear gradient of 5-35% (v/v) acetonitrile in 0.1% (v/v) formic acid (FA) in water at a flow rate of 0.19 ml min^{-1}. 5 µl of each extract was injected and compounds were separated on a Luna C18 column (2.0 x 150 mm, 3µm; Phenomenex) maintained at 40 °C (De Vos *et al.*, 2007). The detection of compounds eluting from the column was performed with a Q-Exactive Plus Orbitrap FTMS mass spectrometer (Thermo Scientific). Full scan MS data were generated with electrospray in switching positive/negative ionization mode at a mass resolution of 35,000 (FWHM at m/z 200) in a range of m/z 95-1350. Subsequent MS/MS experiments for identification of selected metabolites were performed with separate positive or negative electrospray ionization at a normalized collision energy of 27 and a mass resolution of 17,500. The ionization voltage was optimized at 3.5 kV for positive mode and 2.5 kV for negative mode; capillary temperature was set at 250 °C; the auxiliary gas heater temperature was set to 220 °C; sheath gas, auxiliary gas and the sweep gas flow were optimized at 36, 10 and 1 arbitrary units, respectively. Automatic gain control was set a 3^{e6} and the injection time at 100 ms. External mass calibration with formic acid clusters was performed in both positive and negative ionization modes before each sample series.

LCMS data processing and analysis

Mass peak picking and alignment were performed using Metalign software (Lommen, 2009). Mass features in the resulting peak list were considered as a real signal if they are detected with an intensity of more than 3 times the noise value and in 3 out of the 4 biological replicates of at least one treatment. Mass features originating from the same metabolites were subsequently reconstituted based on their similar retention window and their intensity correlation across all measured samples, using MSClust software (Tikunov *et al.*, 2012). This resulted in the relative intensity of 725 putative metabolites in Arabidopsis, 868 in Artemisia and 1908 in broccoli, in which the metabolite abundance was represented by the Measured Ion Count (MIC), i.e the sum of the corrected intensity values of all mass features ions within the corresponding cluster. ANOVA and a threshold of at least a 2-fold change were applied to pinpoint compounds that were significantly different between rhizobacteria-treated and control samples. Log transformation and scaling of the data was performed in GeneMaths XT 1.6 (www.applied-maths.com). Transformed and scaled values were used for hierarchical cluster analysis using Pearson's correlation coefficient and Unweighted Pair Group Method with Arithmetic Mean (UPGMA).

Annotation of differential metabolites was performed after manually identifying the putative molecular ions within the clustered masses. In-house database was used to annotate metabolites detected in Arabidopsis and Broccoli by considering the observed accurate masses and retention times of the molecular ions. Secondly, if selected compounds were not

yet present in this experimentally obtained database, detected masses were matched with compound libraries, including Metabolomics Japan (www.metabolomics.jp), the Dictionary of Natural Products (http://dnp.chemnetbase.com), KNApSAcK (http://kanaya.naist.jp/KNApSAcK), and Metlin (http:// metlin.scripps.edu/) using a maximum mass deviation of 5 ppm. To annotate metabolites detected in Artemisia, we used the online Magma (Ridder *et al.*, 2013) in combination with the above-mentioned publicly available databases.

Statistical analysis

The relative changes in shoot biomass, root biomass in the combinations of the three plants and three rhizobacterial strains was analyzed with R Studio (Version 3.5.2). First, the normality and homogeneity of variance of the data was assessed and when the two assumptions are not met, the data was transformed using Box-Cox transformation using the package MASS. Differences were tested by two-way analysis of variance (ANOVA). A Tukey-HSD test was used to separate group mean values when the ANOVA was significant at $p < 0.05$. The ANOVA table is shown in Supplementary Material, **Table S1**. Differences between rhizobacterial treatments and non-treated control on raw phenotype parameters were compared by Student's *t*-Test.

Results

Plant growth promotion is bacteria and plant species-specific

To assess the magnitude of the changes in growth of Arabidopsis (a model plant), Artemisia (a medicinal plant) and Broccoli (a crop) upon rhizobacterial treatment (**Fig 1**), we used the percent change in fresh biomass of root and shoot relative to the non-treated, germ-free control plants. Two-way ANOVA showed that the impact of the three rhizobacteria on plant growth was highly dependent on the interacting partners (Supplementary Material, **Table S1**).

Effective partnerships

Root tip inoculation with *Pf* SS101 resulted in a significant increase in shoot biomass in both Arabidopsis and Artemisia (63.1% ± 4.7 and 38.7% ± 6.3, respectively) (**Fig 1a2**). Similarly, root tip inoculation with *Pbg* resulted in significant increases in shoot biomass of both Artemisia and Broccoli (470.4% ± 21.3 and 54.1% ± 11.9, respectively). Considering the relative increase in shoot biomass, *Pbg*-Artemisia was the most striking partnership with a biomass increase of almost 5-fold relative to the untreated control plants. Likewise, the effect of the rhizobacterial strains on root biomass was highly species-specific. *Pbg* resulted in significant increases in root biomass in both Artemisia and Broccoli (773.9% (± 28.2) and 258.8% (± 50.1), respectively) (**Fig 1b2**). To assess the temporal changes in plant growth, the time-dependent changes in plant biomass of the respective bacteria-plant combinations

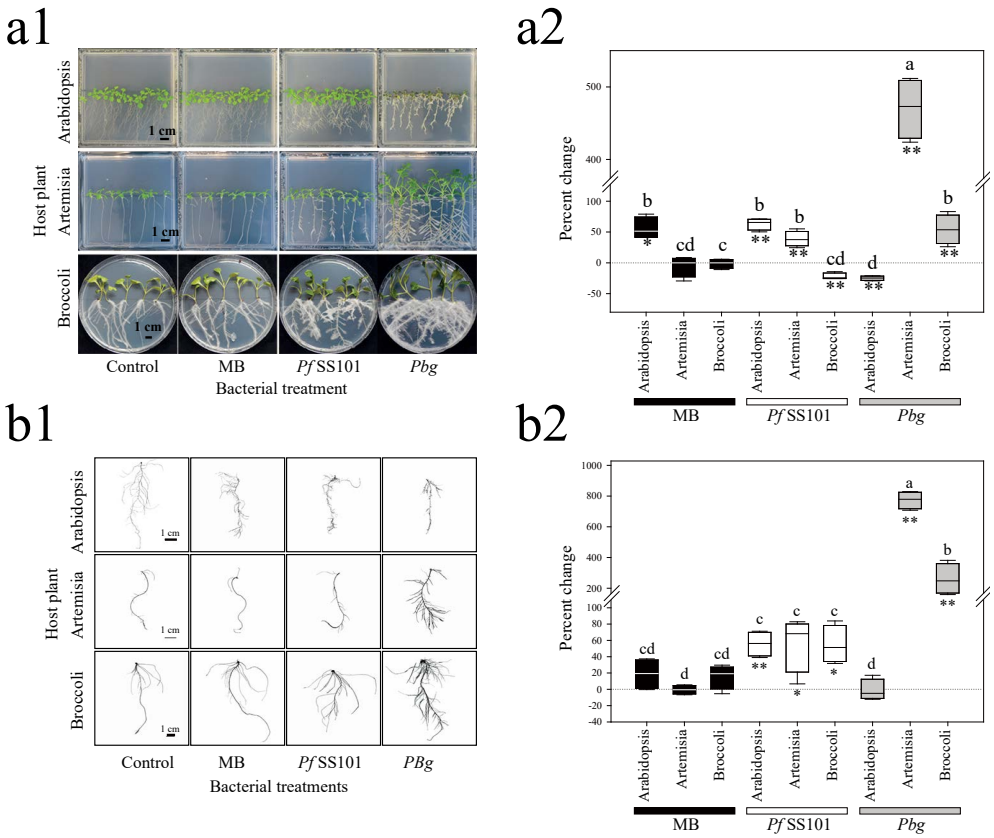

Fig 1. Phenotypic changes in response to rhizobacteria inoculation. Photographs of MS agar plates with Arabidopsis, Artemisia and Broccoli seedlings at 11/14/11 dpi, respectively (**a1**). Percent change in shoot fresh biomass (**a2**). Root morphology changes in response to rhizobacteria inoculation (**b1**). Percent change in root fresh biomass (**b2**). *Pf* SS101: *Pseudomonas fluorescens* SS101, MB: Microbacterium sp, Pbg: Paraburkholderia graminis. Asterisks denote statistical differences (two tailed Student's t test): * $P < 0.05$; ** $P < 0.01$. Means of percent changes with a different letter are significantly different based on Two way ANOVA (Tukey, $P < 0.05$).

were used as a measure (**Fig 2**). The best-performing combinations were characterized by an early and sustained growth promotion. For example, the combination *Pbg*-Artemisia showed a significant increase in shoot fresh biomass as early as 5 dpi, while growth promotion in the combination *Pf* SS101-Artemisia was only apparent after 13 dpi (**Fig 2c**). *Pbg*-Broccoli showed a significant and sustained plant growth promotion at 7 dpi compared to the control plants (**Fig 2b**). In Arabidopsis, only *Pf* SS101 induced a significant increase in shoot biomass (**Fig 2a**).

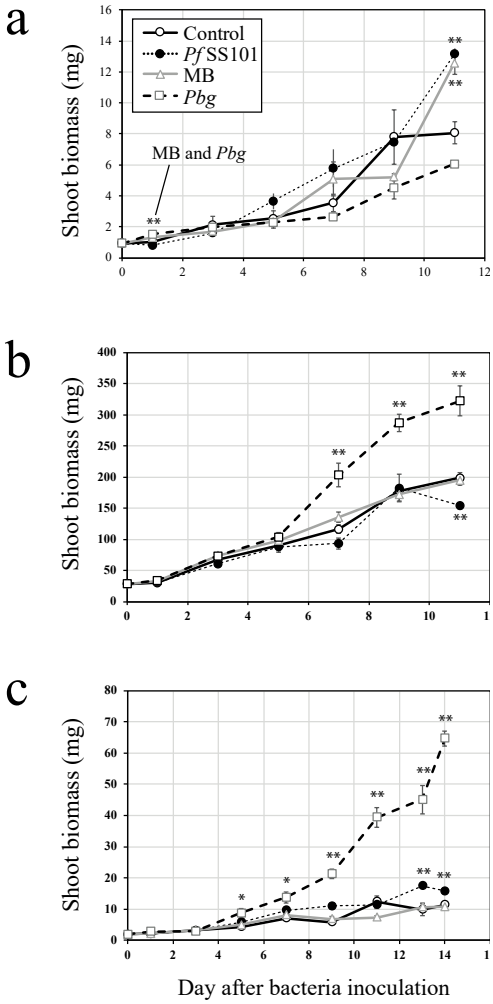

Fig 2. Temporal dynamics of growth of Arabidopsis **(a)**, Broccoli **(b)** and Artemisia **(c)** after inoculation with three distinct rhizobacterial strains. *Pf* SS101: *Pseudomonas fluorescens* SS101, MB: *Microbacterium* sp., : *Paraburkholderia graminis*. Error bars represent the standard error of the mean. Asterisks denote statistically significant differences (two tailed Student's t test): * $P < 0.05$; ** $P < 0.01$

Ineffective partnerships

Root tip inoculation of *Pf* SS101 resulted in a significant reduction (-22% ± 2.6) of the shoot biomass in Broccoli. Similarly, inoculation of Arabidopsis with *Pbg* significantly reduced the shoot biomass (-24.9% ± 1.8). Root tip inoculation of both Artemisia and Broccoli with MB had no significant impact on both shoot and root biomass (**Fig 1a2**).

Relationship between growth promotion and root colonization

In the gnotobiotic assays described here, root colonization was assessed when plants were 11 days old. Root colonization by *Pf* SS101 was considerable for Arabidopsis, Broccoli and Artemisia with populations ranging from $1.5 \pm 0.1 \times 10^5$ to $9.4 \pm 0.7 \times 10^7$ CFU·mg^{-1} root fresh weight. In contrast, MB colonization of roots varied greatly between different plant species: MB established population densities on Arabidopsis roots of $7.5 \pm 0.5 \times 10^6$ CFU·mg^{-1}, whereas on Artemisia roots MB densities were below the detection limit (2.3 CFU mg^{-1}). *Pbg* colonized roots of all three plant species at relatively high densities ranging from $8.1 \pm 0.3 \times 10^7$ to $1.0 \pm 0.1 \times 10^9$ CFU·mg^{-1} (Supplementary Material, **Table S2**). To determine correlations, if any, between the rhizosphere population densities and specific plant phenotypes (i.e. biomass), we plotted the rhizobacterial densities against various plant parameters (Supplementary Material, **Fig S2**). Colonization of the root at higher density showed a positive, negative or no association with the shoot and root biomass depending on the host-rhizobacteria combination. For example, *Pbg* showed higher population densities, compared to *Pf* SS101 and MB, on the root of Arabidopsis and Artemisia.

In Arabidopsis, high population densities of *Pbg* were associated with a significant reduction in shoot biomass while in Artemisia it resulted in substantial enhancement of the shoot biomass. In Broccoli, all three rhizobacterial strains showed a similar level of root colonization: *Pbg* showed significant increase in shoot biomass while *Pf* SS101 resulted in significant reduction in shoot biomass and MB showed no significant growth promotion. Hence, there was no clear overall correlation between root colonization and shoot biomass (Supplementary Material, **Fig S2a**). The lack of an overall association between root colonization and shoot biomass was also found for the root biomass (Supplementary Material, **Fig S2b**).

Global and specific rhizobacteria-induced changes in the plant shoot metabolome

LC-MS-based non-targeted metabolite profiling was used to investigate the global and specific effects of each of the three rhizobacterial strains on the occurrence and relative abundance of semi-polar secondary metabolites of Arabidopsis, Artemisia and Broccoli. Particular emphasis was given to investigate the metabolic alterations that differentiate effective from ineffective plant-rhizobacteria partnerships. An overview of metabolites that were significantly increased or reduced revealed that root inoculation with *Pbg* exerted the largest alteration of the shoot metabolome of Artemisia and Arabidopsis, combinations that represent the most effective and infective partnerships, respectively. Furthermore, most of the differential metabolites were unique for plants inoculated with *Pbg*, i.e they were below the detection limit in control plants. In Broccoli, the ineffective partnership with *Pf* SS101 accounted for the largest share of the 'upregulated' metabolites, whereas its effective partnership with *Pbg* accounted for the largest share of 'down-regulated' metabolites (**Fig 4a**). ANOVA with correction for multiple testing (Benjamini and Hochberg), principal component analysis (PCA) and hierarchical cluster analysis (HCA) were performed to investigate and visualize metabolite clusters that were significantly altered ($p < 0.05$, fold change > 2) in a rhizobacteria-plant specific manner (**Fig 3**). Below, we will discuss the most significant changes for each of the three plant species induced by the respective rhizobacterial strains.

Arabidopsis

Inoculation of Arabidopsis roots with each of the three rhizobacteria resulted in significant changes in the shoot metabolome. From the total of 725 metabolites that were detected in both positive and negative ionization mode, 465 (64%) metabolites were significantly different between at least two treatments. In the PCA, the first three principal components explained 89% of the total variance (**Fig 3a**). The first principal component (PC1), representing 56% of the total variance, was associated with metabolites that were highly induced (**Fig 3b** clusters **5**; 291 metabolites and **6**; 10 metabolites) or reduced in the ineffective partnership between *Pbg* and Arabidopsis (clusters **3**; 82 metabolites and **4**; 33 metabolites). *Pbg*-induced metabolites in cluster **5** primarily encompassed flavonoid glycosides including anthocyanins (cyanidin rutinoside, delphinidin rutinoside), tryptophan and its derivatives such as IAA, defense

or stress-associated metabolites such as salicylic acid, dihydroxybenzoic acid glucosides, scopolin and camalexin. The second principal component (PC2) explained 21% of the total variance and corresponded to metabolites that were increased (**Fig 3a and b**, clusters **2**; 18 metabolites and **6**; 9 metabolites) or decreased (cluster **7**; 10 metabolites) in the effective partnership of Arabidopsis with *Pf* SS101 and MB. Among the identified metabolites, the long-chain aliphatic glucosinolate glucohirsutin (8-(methylsulfinyl)octyl glucosinolate) was significantly increased in Arabidopsis shoot after inoculation with *Pf* SS101 or MB. From the same group of glucosinolates, 8-(methylthio) octyl glucosinolate was significantly increased after inoculation with *Pf* SS101 (Supplementary Material, **Table S4**). The third principal component (PC3) explained 12% of the total variation and was represented by metabolites that accumulated only after inoculation with either *Pf* SS101 or MB (**Fig 3a,** cluster **1**; 8 metabolites and cluster **9**; 7 metabolites, respectively). A fatty acyl glycoside demonstrated *Pf* SS101-specific accumulation while fumaric acid displayed MB-specific increases.

Broccoli

Similar to Arabidopsis, inoculation of Broccoli roots with each of the three rhizobacterial strains resulted in substantial alteration of the shoot metabolome. From the total of 1908 metabolites that were detected in either positive or negative ionization modes, 933 (49%) were significantly different between at least two treatments. For this set of metabolites, HCA revealed 8 distinct metabolite clusters of the host metabolome. Similar to Arabidopsis, PCA showed that the metabolome of Broccoli seedlings inoculated with different rhizobacteria is clearly different from the control and from each other. The first three PCs explained 84% of the total variance (**Fig 3c**). PC1, representing 47% of the total variance, was associated with metabolites that discriminate both the control and MB samples from the *Pbg* and *Pf* SS101 samples. These metabolites were either highly increased or highly decreased in plants inoculated by *Pbg* or *Pf* SS101 (**Fig 3d** decreased cluster **3** and induced clusters **6** and **7**) that represents effective and ineffective partnership with the host, respectively. The anticancer indole glucosinolate glucobrassicin also showed a significant increase in plants inoculated with *Pbg* and *Pf* SS101. PC2 explained 22% of the total variance and corresponded to metabolites that were either specifically altered in the *Pbg* or *Pf* SS101 treatments (**Fig 3d** induced (clusters **8** (*Pf* SS101) and **9** (*Pbg*)) or reduced by *Pbg* inoculation (cluster **4**)). Metabolites that were specifically induced in the ineffective partnership between *Pf* SS101 and the host were dominated by flavonoids such as kaempferol, quercetin glycosides and glucosinolates including glucoibervirin, neoglucobrassicin and 4-methoxyglucobrassicin. Furthermore, a number of hydroxycinnamates with or without conjugation with quinic acid, including chlorogenic acid (caffeoyl-quinic acid), coumaroyl quinic acid, sinapic acid and ferulic acid, were predominant in this metabolite cluster (cluster **7**). PC3 explained 15% of the total variation and corresponded to MB-induced metabolites represented in cluster **1** and induced metabolites by all three rhizobacteria in cluster **2**. Hexose 1-phosphate in cluster **1** showed a MB-specific increase. Meanwhile, some of the putatively annotated metabolites in

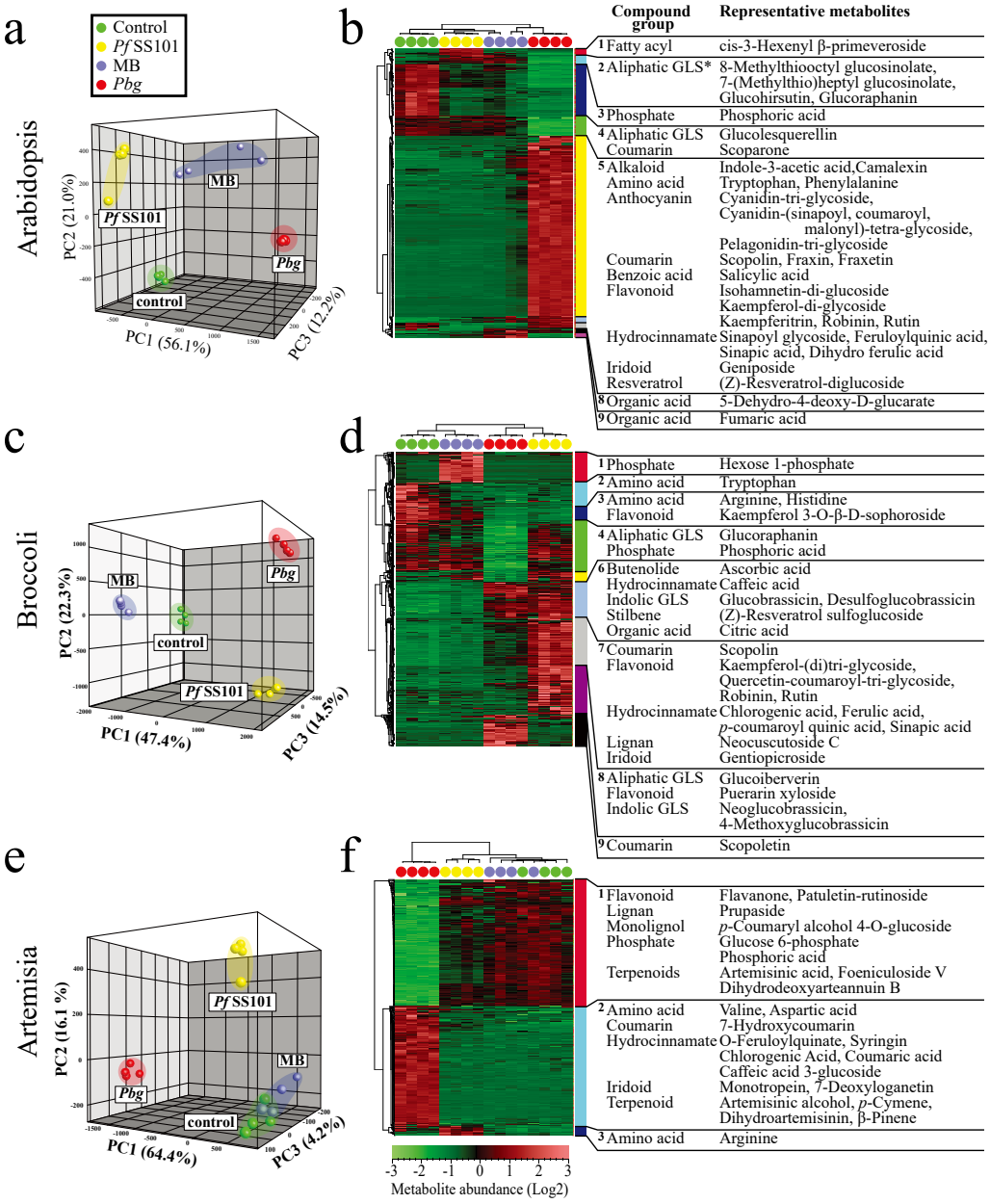

Fig 3. Rhizobacteria-mediated changes in the shoot metabolome. Shown are PCA and HCA results based on differentially regulated semi-polar metabolites in the shoot of Arabidopsis (**a** and **b**), Broccoli (**c** and **d**) and Artemisia (**e** and **f**) after root inoculation with three different rhizobacteria (*Pf* SS101: *Pseudomonas fluorescens* SS101, MB: *Microbacterium* sp. and *Pbg*: *Paraburkholderia graminis*). * GLS=glucosinolate, ** d=derivative. In the HCA, metabolite clusters are indicated by different colors and when none of the metabolites in a given cluster was annotated, the cluster number is omitted (clusters 6 and 7 in (b) and cluster 5 in (d)).

cluster **2** including tryptophan, a precursor of indole glucosinolates was reduced by all three rhizobacterial treatments.

Artemisia

From the total of 868 metabolites that were detected in the Artemisia shoot samples, 451 (52%) metabolites were significantly different between at least two rhizobacteria treatments. Unlike that of Arabidopsis and Broccoli, HCA revealed only few distinct metabolite clusters in Artemisia in response to the rhizobacteria (**Fig 3f**). In the PCA, the first two PCs explained 80% of the total variance (**Fig 3e**). The first principal component explained more than 64% of the total variance and corresponds to metabolites that were either reduced or enhanced during the most effective partnership of the host with *Pbg* (**Fig 3f** cluster **1 (**reduced metabolites) and cluster **2** (induced metabolites)). Flavanones, flavonol glycosides, coumarins, benzoic acid derivatives, acylated polyamine, catechin, fatty acyl glycosides of mono- and disaccharides, dipeptide and terpene glycosides showed significant reductions upon *Pbg* inoculation. Various other metabolites belonging to the compound classes hydroxycinnamoyl quinic acids and derivatives, organic acids, mono and diterpenoids, and iridoids showed a significant increase after root inoculation with *Pbg*. Treatment of Artemisia with *Pbg* resulted in significant reduction in artemisinic acid while the relative levels of both dihydroartemisinin and artemisinic alcohol significantly increased. PC2 explained 16% of the total variance and corresponded to induced metabolites (cluster **3**) in response to *Pf* SS101 inoculation. Putative metabolite identification revealed that the amino acid arginine, fatty acyl glycoside blumenol glycoside and phenylpropanoid glycoside derivatives were induced in a *Pf* SS101-specific manner.

Comparative analysis of rhizobacteria-induced plant shoot metabolome changes

The metabolome changes induced by the different rhizobacteria in the shoots of Arabidopsis and Broccoli were subjected to a comparative analysis as both plant species belong to the Brassicaceae family. Although total glucosinolate levels in shoots of both Brassica species were commonly upregulated by *Pf* SS101, glucosinolate subcategories were altered in a rhizobacteria-specific manner. For instance in Arabidopsis, the effective partnership with *Pf* SS101 enhanced the relative levels of aliphatic long-chain glucosinolates such as glucohirsutin and 8-methylthiooctyl glucosinolate, whereas the infective partnership between *Pf* SS101 and Broccoli led to an increase in the levels of indolic glucosinolates (i.e. glucobrassicin, desulfoglucobrassicin, 4-methoxyglucobrassicin and neoglucobrassicin) and short-chain aliphatic glucosinolates such as glucoibervirin. In contrast to the effective *Pf* SS101-Arabidopsis partnership, the ineffective *Pbg*-Arabidopsis partnership caused a drastic reduction of all detected aliphatic glucosinolates, (i.e. glucohirsutin (8-methylsulfinyloctyl glucosinolate), glucolesquerellin (6-methylthiohexyl glucosinolate), 7-methylthioheptyl glucosinolate and 8-methylthiooctyl glucosinolate. In Broccoli, both its ineffective partnership

with *Pf* SS101 and its effective partnership with *Pbg* caused significant increases of the indolic glucosinolate glucobrassicin. Meanwhile, the effective MB-Arabidopsis partnership led to upregulation of glucohirsutin while this rhizobacterial strain barely influenced the level of glucosinolates in Broccoli (Supplementary Material, **Table S5**). Flavonoids, on the other hand, were shown to respond in a more rhizobacteria-specific manner. In Arabidopsis, flavonoids were predominantly enhanced by both *Pbg* and MB treatments while in Broccoli

a

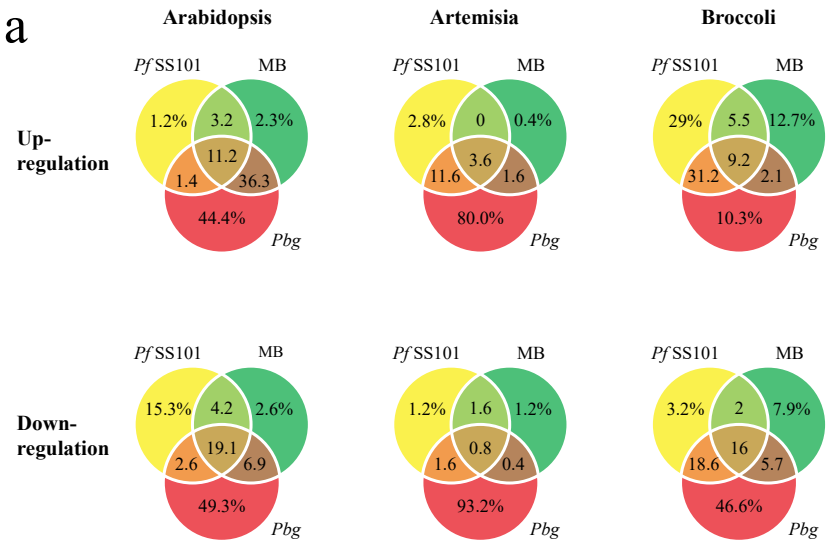

b

Plant	Rhizobacteria	Increased metabolites			Decreased metabolites		
		Total	Ionization		Total	Ionization	
			+	-		+	-
Arabidopsis	***Pf* SS101**	59	38	21	75	45	33
	MB	184	105	79	62	36	26
	Pbg	324	183	141	147	85	62
Artemisia	***Pf* SS101**	45	24	21	13	8	5
	MB	14	11	3	10	8	2
	Pbg	243	134	109	245	130	115
Broccoli	***Pf* SS101**	585	303	282	201	120	81
	MB	230	143	87	160	85	75
	Pbg	411	203	208	439	235	204

Fig 4. Rhizobacteria-mediated global changes in the shoot metabolome of the three different plant species. The Venn diagrams display the distribution of unique and shared differentially regulated metabolites in shoots of Arabidopsis, Artemisia and Broccoli **(a)**. Presented values are the sum of differentially regulated metabolites detected in either positive or negative ionization modes. Total number of metabolites increased and decreased in abundance based in either positive or negative ionization mode are presented in **(b)**. Further details are provided in Supplementary Table 2. *Pf* SS101: *Pseudomonas fluorescens* SS101, MB: *Microbacterium* sp., *Pbg*: *Paraburkholderia graminis*.

Pf SS101 elevated the level of many flavonoids (Supplementary Material, **Table S5**). Combination of Arabidopsis with *Pbg* and MB, and Broccoli with *Pf* SS101 represent ineffective partnerships. In conclusion, comparative metabolomics of the two Brassicaceae plant species suggests that regulation of particular biosynthetic pathways is rhizobacteria specific and host species dependent. Alteration to a particular branch of phenylpropanoid pathway showed co-occurrence with growth promotion (effective partnership) or growth reduction (ineffective partnership) in cross-species plant-rhizobacteria combination. Most interestingly, metabolite identification led to a list of natural products that are presumed to exert health promoting or pharmaceutically important effects during both effective and ineffective partnership between plants and rhizobacteria. The list of various metabolites that are presumed to have specific functions are summarized in Supplementary **Table S7**.

Discussion

Over the past decades, several studies indicated that beneficial rhizobacteria promote plant growth, induce systemic resistance against pathogens and phytophagous insects and can alter plant secondary metabolism (Van Peer *et al.*, 1991; Walker *et al.*, 2011; van de Mortel *et al.*, 2012; Etalo *et al.*, 2018; Hu *et al.*, 2018; Stringlis, Ioannis A *et al.*, 2018). Our results confirm and extend the importance of rhizobacteria in plant growth promotion (Barriuso *et al.*, 2008; van de Mortel *et al.*, 2012; Castanheira *et al.*, 2016; Cordovez *et al.*, 2018) and provide a unique insight into the global metabolome changes and specific plant metabolic signatures of effective and ineffective partnerships between rhizobacteria and their host plant. Effectiveness refers in this study to an interaction that resulted in growth promotion. Of the three tested rhizobacterial genera, none of the strains showed growth-promoting effects for all three different plant species indicating specificity in rhizobacteria-plant interactions. For example, *Pbg* established an effective partnership with Artemisia and Broccoli whereas interaction with Arabidopsis was deleterious given the significant reduction in biomass and the accumulation of stress-related dark-purple anthocyanins in the leaves (**Fig 1a1**). Even when there is effective partnership between rhizobacteria and the host, the extent of growth promotion can significantly differ as shown by the partnership of *Pbg* with Artemisia and Broccoli. The temporal analyses of the rhizobacteria-host interactions also demonstrated that establishment of effective partnership was characterized by early and sustained induction of growth promotion as was typically the case for the *Pbg* interaction with Artemisia and Broccoli (**Fig 2**). The differential growth response of the three plant species to *Pbg* inoculation exemplifies the need for finding the right partnership between rhizobacteria and host plant. The establishment of high population densities of PGPR on root is claimed to be associated with plant growth promotion. This may explain the lack of phenotypic responses of Artemisia to MB inoculation. However, our results also indicated that high rhizosphere population densities of the introduced strains can be associated with either growth promotion or growth reduction as was seen for the combination of *Pbg* with Artemisia (growth promotion) and *Pbg*

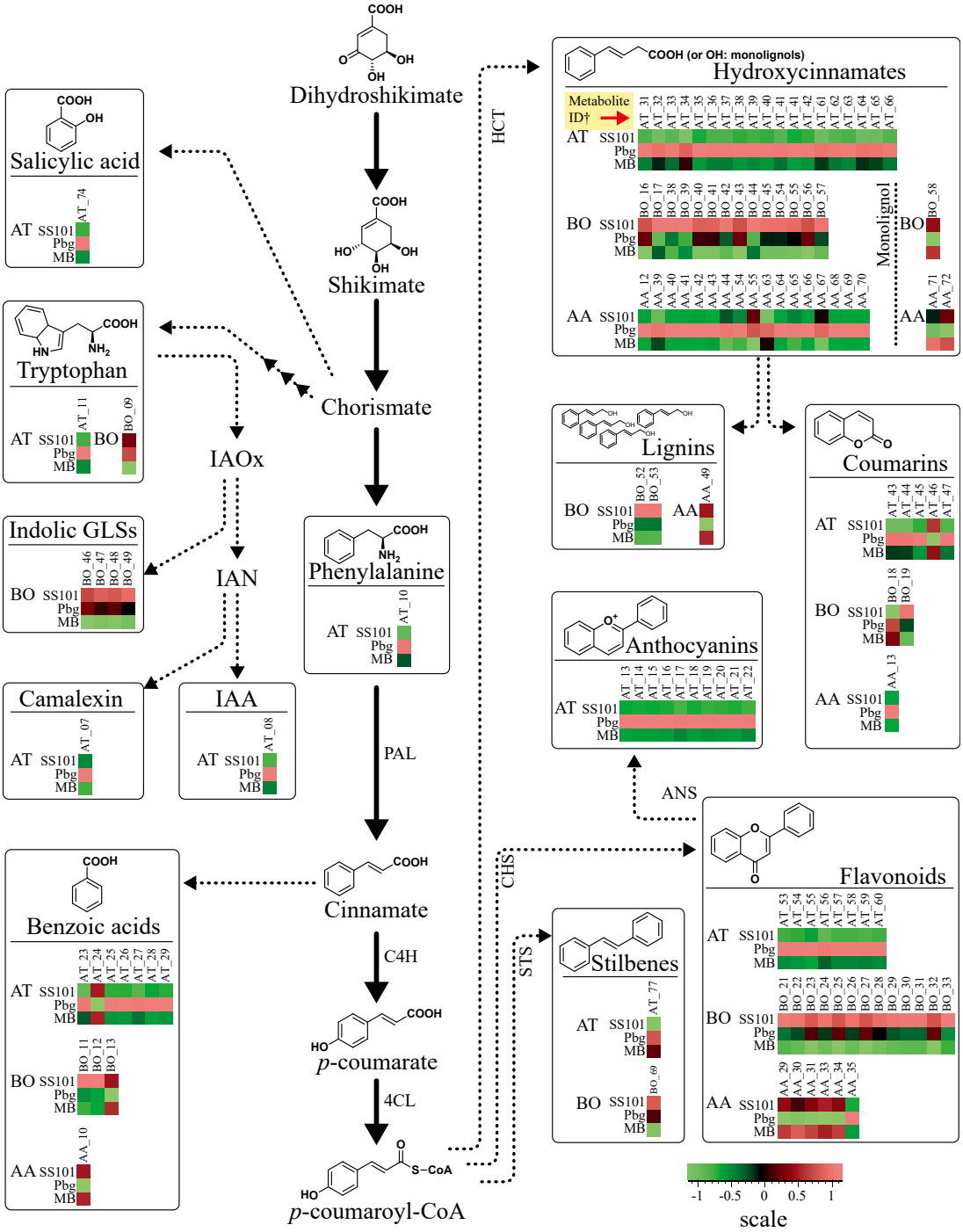
Dihydroshikimate
Shikimate
Chorismate
Salicylic acid
Tryptophan
IAOx
IAN
Indolic GLSs
Camalexin
IAA
Phenylalanine
PAL
Cinnamate
C4H
p-coumarate
4CL
p-coumaroyl-CoA
Benzoic acids
HCT
CHS
STS
ANS
Hydroxycinnamates
COOH (or OH: monolignols)
Metabolite ID†
Monolignol
Lignins
Coumarins
Anthocyanins
Flavonoids
Stilbenes
AT SS101 Pbg MB
BO SS101 Pbg MB
AA SS101 Pbg MB
-1 -0.5 0 0.5 1
scale

Fig 5.

with Arabidopsis (growth reduction) (Supplementary Material, **Fig S2a2** and **a1**, respectively).

Generally, rhizobacteria-mediated alteration of the plant metabolome can arise from effective or ineffective partnerships. The ineffective partnership between *Pbg* and Arabidopsis is characterized by the depletion of long- and short-chain aliphatic glucosinolates and massive accumulation of metabolites from the phenylpropanoid pathway including anthocyanin and other flavonoid glycosides (**Fig 3b**, Supplementary Material, **Table S4 and Fig 5**). The accumulation of stress/defense-related metabolites such as anthocyanin and other flavonoid glycosides, camalexin, β-d-glucopyranosyl indole-3-carboxylic acid and salicylic acid (**Fig 5**) suggest that *Pbg* is perceived by Arabidopsis as a biotic stressor (Hagemeier *et al.*, 2001; Oh *et al.*, 2014; Ali *et al.*, 2018). Similarly, the ineffective partnership between Broccoli and *Pf* SS101 resulted in a significant accumulation of flavonoids (**Fig 3d**, Supplementary Material, **Table S5**). Furthermore, there was a significant increase in the level of glucobrassicin and its derivatives such as neoglucobrassicin, desulfoglucobrassicin, and 4-methoxyglucobrassicin. Interestingly, 4-methoxyglucobrassicin was reported to be a signal molecule involved in plant defense against bacteria and fungi (Bednarek *et al.*, 2009; Clay *et al.*, 2009). This suggests that Broccoli perceived *Pf* SS101 as a foe or that *Pf* SS101 induced resistance against fungal/bacterial infections. In conclusion, the above two examples suggest an association between ineffective partnerships and accumulation of flavonoids in the host shoot tissues.

The metabolome profile of Arabidopsis inoculated with *Pbg* (an ineffective partnership) appears similar to that of the hydroxycinnamoyl transferase (HCT)-deficient Arabidopsis reported by (Besseau *et al.*, 2007). HTC and chalcone synthase (CHS) are key regulators of the phenylpropanoid pathway and influence the channeling of the key precursor *P*-coumaroyl CoA either to flavonoids or to monolignols and sinapoylmalate (**Fig 5**). Similar to the ineffective partnerships of *Pbg*-Arabidopsis or *Pf* SS101-Broccoli, HTC-mutants displayed high accumulation of flavonoids (Besseau *et al.*, 2007). Accumulation of flavonoid glycosides in Arabidopsis may affect auxin transport (Besseau *et al.*, 2007), distribution and turnover (Kuhn *et al.*, 2016), thereby affecting plant growth. Besseau *et al.* (2007) further showed that suppression of flavonoid production via CHS silencing, restored auxin transport and normal development of HCT-deficient plants. Another interesting *Pbg*-

◀◀◀ **Fig 5.** Rhizobacteria-mediated alteration of the phenylpropanoid pathway in three different plant species (*Arabidopsis thaliana* (AT), *Brassica oleracea* (BO) and *Artemisia annua* (AA)). The metabolites corresponding to the different branches of the phenylpropanoid pathway are indicated by the metabolite ID corresponding to each species and their level of accumulation is indicated by the scaled fold change corresponding to the green and red boxes for each of the metabolites. Fold change of metabolite abundance was calculated by dividing the average abundance of a metabolite in rhizobacteria treated plants to untreated control plants. For detailed information on the identity of the individual metabolites, consult the supplementary excel tables S4-S6. IAOx (indole-3-acetaldoxime), IAN (indole-3-acetonitrile), PAL (Phenylalanine ammonia-lyase), C4H (Cinnamate 4-hydroxylase), 4CL (4-coumarate-CoA ligase), CHS (Chalcone synthase), HCT (hydroxycinnamoyl-CoA shikimate/quinate hydroxycinnamoyl transferase) and STS (stilbene synthase).

induced chemotype in Arabidopsis is the accumulation of metabolites derived from the indole pathways such as IAA and camalexin. Indole-3-acetaldoxime (IAOx) plays important roles in plant development and defense response as a branching point for biosynthesis of indole glucosinolate, IAA and camalexin (Bak *et al.*, 2001). When compared to control plants, *Pbg*-treated Arabidopsis showed no significant change in the level of indole glucosinolates. However, both IAA and camalexin showed marked increases suggesting that *Pbg* inoculation leads to channeling of IAOx towards IAA and camalexin biosynthesis. Interestingly, the ineffective partnership between *Pf* SS101 and Broccoli was characterized by the accumulation of indolic glucosinolates while IAA and camalexin were not detected in the samples. Collectively, these results suggest that different rhizobacteria can influence the channeling of precursors towards specific branches of metabolic pathways involved in growth, development and/or stress tolerance in plant species-rhizobacteria specific manner. Of all rhizobacteria-plant combinations, the *Pbg*-Artemisia combination can be considered as the most effective partnership in terms of growth promotion. When compared to the control plants or plants treated with the other two rhizobacteria, the effective partnership between *Pbg* and Artemisia was hallmarked by a substantial alteration of the host metabolome (**Fig 3f** and **Fig 5**). This 'rewiring' of the Artemisia metabolome primarily involved accumulation of hydroxycinnamates and suppression of other phenolic compounds such as flavonoids and benzoic acid derivatives (**Fig 5**). *p*-Coumaroyl CoA is the central metabolite and branch-point in phenylpropanoid biosynthesis in plants. The channeling of this important precursor towards various branches of the phenylpropanoid pathway is mainly influenced by the enzymes hydroxycinnamoyl CoA:shikimate/quinatehydroxycinnamoyltransferase (HCT) and chalcone synthase (CHS) (**Fig 5**). Our results showed that one of the distinctive metabolic signatures between effective and ineffective partnerships is the differential regulation of the flavonoid pathway that is ubiquitously present in plant species. Under effective partnership, it is either suppressed or showed slight change in accumulation. Whereas, under ineffective partnership it showed high accumulation in the plant shoot (**Fig 5**). Considering our results and other reports on the negative role of flavonoids on auxin transport, auxin distribution and turnover (Jacobs & Rubery, 1988; Murphy *et al.*, 2000; Brown *et al.*, 2001; Besseau *et al.*, 2007; Kuhn *et al.*, 2011; Buer *et al.*, 2013; Kuhn *et al.*, 2016), suppression or tight regulation of flavonoids by rhizobacteria could be employed as a potential strategy to promote plant growth.

Our result clearly indicated that different rhizobacteria alter the host metabolome either in effective or ineffective partnerships. Both kinds of partnership can be employed to boost nutritionally and/or pharmaceutically important high value natural plant compounds (HVPC). For example, flavonoid glycosides induced in the ineffective partnership between *Pbg* and Arabidopsis are considered as vital phytochemicals in diets and are of great general interest due to their diverse bioactivities. Similarly, glucosinolates in Brassica species, hydroxycinnamic acid derivatives and dihydroartemisinin in Artemisia are potentially health-beneficial metabolites. In effective partnerships, the increase in these compounds is

even more pronounced when we consider the relative increase in the host biomass due to rhizobacteria inoculation. A typical example for this is the *Pbg*-Artemisia combination that resulted in five-fold increase in host biomass and up to three-fold increase per unit fresh tissue biomass in both artemisinic alcohol and dihydroartemisinin. The application of rhizobacteria to plant roots to boost economically or pharmaceutically interesting metabolites may be considered as a simple and generic approach. Moreover, breeding towards plant traits that promote the recruitment of effective rhizobacteria that induce health-promoting compounds could be considered as an alternative strategy. Understanding the underlying molecular mechanisms and traits by which beneficial rhizobacteria alter the host chemistry will be needed to optimize this microbe-mediated plant engineering strategy. This approach, referred to as "microbe Gene Positioning System (mGPS)" (Etalo et al., 2018), can be integrated with other approaches such as synthetic biology, gene-editing technologies and even with conventional breeding strategies to enhance HVPC production in crops and medicinal plants. Hence, efforts to engineer pharmaceutically and nutritionally important plant products should consider both the plant and its microbiome members as part of the puzzle.

Acknowledgements

Artemisia F1seed and Broccoli seeds were kindly provided by Department of Biology, University of York, York, UK and Bejo seed company (Trambaan1, 1749 CZ Warmenhuizen, The Netherlands), respectively. We are grateful to Bert Schipper and Henriëtte Vaneekelen for their help with LC-MS analysis and pre-processing of metabolomics data.

Supplementary materials

Table S1. Analysis of variance ANOVA (type II) of shoot and root biomass changes in three plants species inoculated with phylogenetically distinct rhizobacterial genera.

Sample	Factor	Sum Sq	Df	F value		Pr(>F)	
Shoot fresh biomass relative change	Plant species	2598.8	2	127.17		1.81E-14	***
	Bacterial species	2048.2	2	100.23		3.20E-13	***
	Plant species : Bacterial species	7500.8	4	183.53	<	2.2E -16	***
	Residuals	275.9	27				
Root fresh biomass relative change	Plant species	481.95	2	43.507		3.59E-09	***
	Bacterial species	1061.18	2	95.795		5.48E-13	***
	Plant species : Bacterial specie	1322.42	4	59.689		5.14E-13	***
	Residuals	149.55	27				
Root dry weight relative change	Plant species	894.3	2	30.101		1.338E-07	***
	Bacterial species	6860.2	2	230.893	<	2.2E-16	***
	Plant species : Bacterial species	4183.9	4	70.408		6.925E-14	***
	Residuals	401.1	27				

Significance codes: *** 0, ** 0.001, * 0.01.

Table S2. Population density of three rhizobacterial genera colonizing root of Arabidopsis (11 dpi), Artemisia (14 dpi) and Broccoli (11 dpi). *Pf* SS101: *Pseudomonas fluorescens* SS101, MB: *Microbacterium* sp., *Pbg*: *Paraburkholderia graminis*.

Plant species	*Pf* SS101	MB	*Pbg*
Arabidopsis thaliana	$9.9 \pm 0.5 \times 10^5$	$7.5 \pm 0.5 \times 10^6$	$1.2 \pm 0.1 \times 10^8$ CFU/mg*
Artemisia annua	$1.5 \pm 0.1 \times 10^5$	n.d.	$1.0 \pm 0.1 \times 10^9$ CFU/mg
Brassica oleracea	$9.4 \pm 0.7 \times 10^7$	$4.6 \pm 0.7 \times 10^7$	$8.1 \pm 0.3 \times 10^7$ CFU/mg

CFU: Colony forming unit
n.d.: not detected
*Values represent the average of 3 replicates ± SE

Table S3. Number of differentially regulated plant secondary metabolites in the shoots of Arabidopsis, Artemisia, and Broccoli after treatments of the roots with three rhizobacteria generas. *Pf* SS101: *Pseudomonas fluorescens* SS101, MB: *Microbacterium* sp., *Pbg*: *Paraburkholderia graminis*

Plant	Bacteria	Number of metabolites					
		Increased metabolites			Increased metabolites		
		Total	Ionization mode		Total	Ionization mode	
			+	-		+	-
Arabidopsis	*Pf* SS101 total	59	38	21	78	45	33
	MB_total	184	105	79	62	36	26
	Pbg total	324	183	141	147	85	62
	Pf SS101 only	4	2	2	29	17	12
	MB_only	8	5	3	5	4	1
	Pbg only	154	86	68	93	57	36
	Common in *Pf* SS101 and MB	50	32	18	44	26	18
	Common in *Pf* SS101 and *Pbg*	44	29	15	41	22	19
	Common in MB and *Pbg*	165	93	72	49	26	23
	Common in *Pf* SS101, MB, and *Pbg*	39	25	14	36	20	16
Artemisia	*Pf* SS101 total	45	24	21	13	8	5
	MB total	14	11	3	10	8	2
	Pbg total	243	134	109	245	130	115
	Pf SS101 only	7	4	3	3	2	1
	MB only	1	1	0	3	3	0
	Pbg only	201	111	90	238	128	110
	Common in *Pf* SS101 and MB	9	7	2	6	5	1
	Common in *Pf* SS101 and *Pbg*	38	20	18	6	2	4
	Common in MB and *Pbg*	13	10	3	3	1	2
	Common in *Pf* SS101, MB, and *Pbg*	9	7	2	2	1	1
Broccoli	*Pf* SS101 total	585	303	282	201	120	81
	MB total	230	143	87	160	85	75
	Pbg total	411	203	208	439	235	204
	Pf SS101 only	227	122	105	16	12	4
	MB only	99	66	33	40	12	28
	Pbg only	80	41	39	235	114	121
	Common in *Pf* SS101 and MB	115	70	45	91	56	35
	Common in *Pf* SS101 and *Pbg*	315	155	160	175	104	71
	Common in MB and *Pbg*	88	51	37	110	69	41
	Common in *Pf* SS101, MB, and *Pbg*	72	44	28	81	52	29

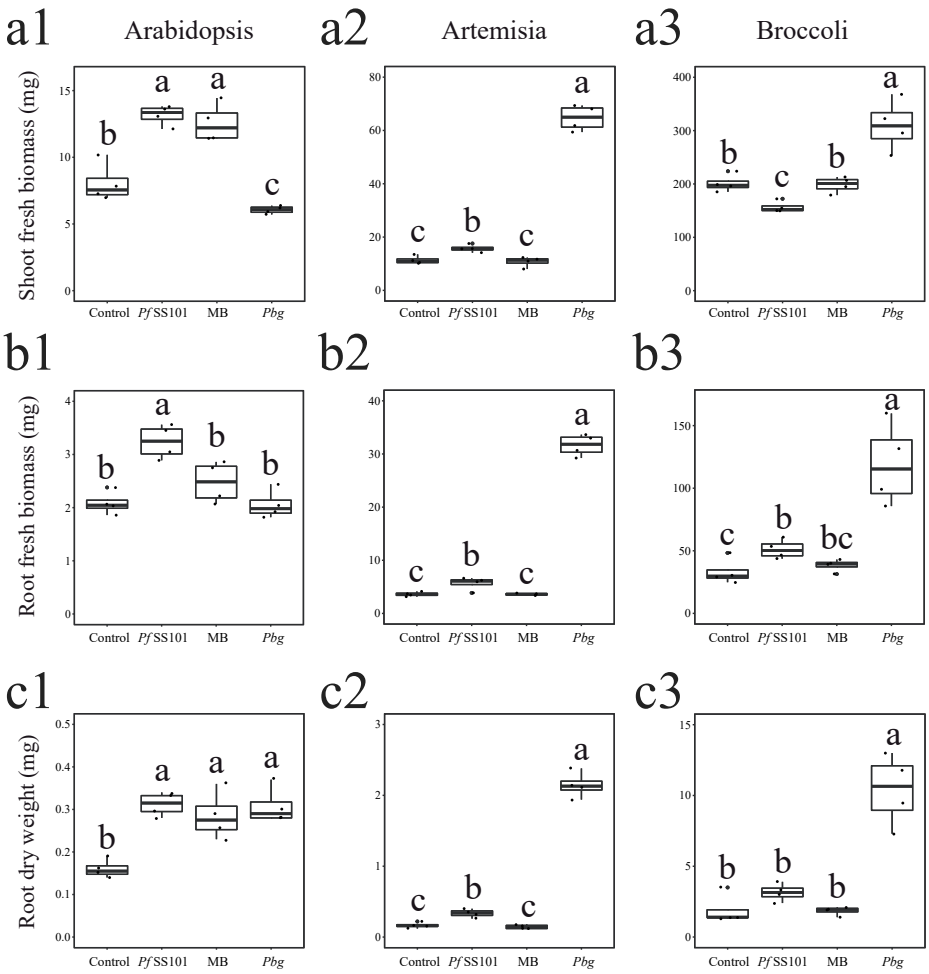

Fig S1. Rhizobacteria-mediated phenotypic changes in three plant species. Change in shoot fresh biomass **(a)**, root fresh biomass **(b)**, and root dry weight **(c)** at 11 dpi for Arabidopsis **(1)** and Broccoli **(3)** and 14 dpi for Artemisia **(2).** *Pf* SS101: *Pseudomonas fluorescens* SS101, MB: *Microbacterium* sp., *Pbg*: *Paraburkholderia graminis.* Box plots represent the average of 4 replicates. Means of percent changes with a different letter are significantly different from each other according to One-way ANOVA (Tukey, $P<0.05$).

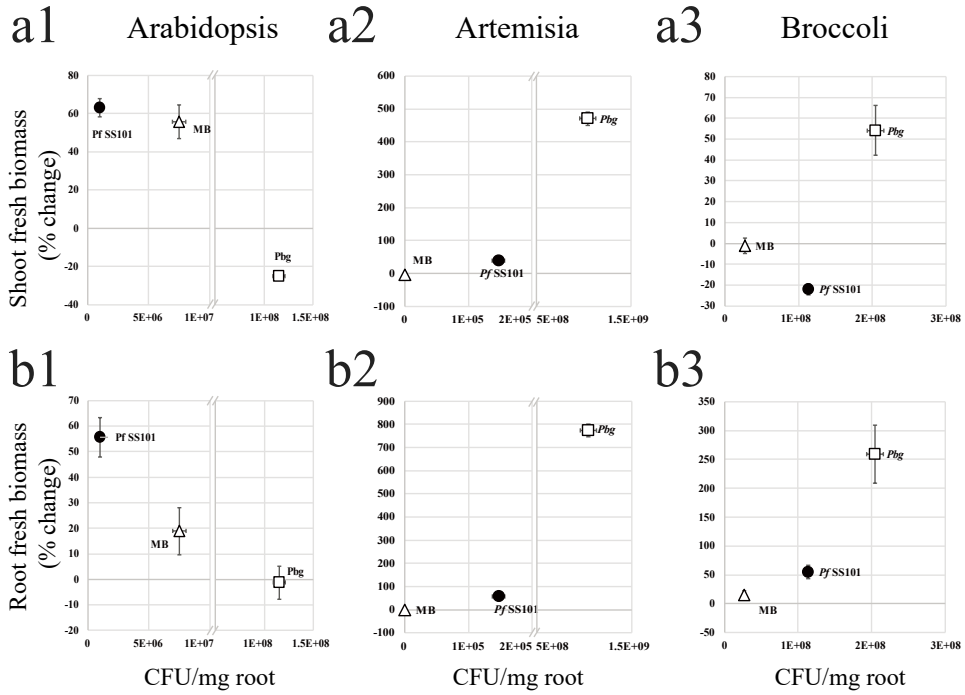

Fig S2. Correlation between rhizobacteria root colonization and host phenotypes. Correlation rhizobacterial population density (CFU/mg root) and percent changes of shoot fresh biomass **(a)** and root fresh biomass **(b)** of Arabidopsis; 11dpi **(1)**, Artemisia; 14dpi **(2)**, and Broccoli; 11dpi **(3)**. *Pf* SS101: *Pseudomonas fluorescens* SS101, MB: *Microbacterium* sp., *Pbg*: *Paraburkholderia graminis.*

Table S4. Annotation of Arabidopsis metabolites that showed significant change in their abundance after inoculation with rhizobacteria. *Pf* SS101: *Pseudomonas fluorescens* SS101, MB: *Microbacterium* sp., *Pbg*: *Paraburkholderia graminis*. Fold changes of each metabolites were calculated against non-treated control. Clustering numbers are associated with metabolite ID in **Fig 3.**

Cluster Number	Metabolite ID	RT (m)	m/z	Mass(D)	Compound	Formula	Δ ppm to DB	Classification	data base	Fold change		
										MB	*Pbg*	*Pf* SS101
1	AT_51	23.33	[M-H]-	393.176544	cis-3-Hexenyl b-primeveroside	C17H30O10	-0.2	Fatty acyl lycoside	HMDB	3.3	1.3	15.0
2	AT_02	50.35	[M-H]-	476.108398	8-Methylthiooctyl glucosinolate (8MTO)	C16H31O9S3N1	-0.9	Aliphatic GLS	KEGG	-1.0	-11.5	2.1
2	AT_01	41.47	[M-H]-	462.092896	7-(Methylthio)heptyl glucosinolate	C15H29O9S3N1	-0.5	Aliphatic GLS	KEGG	-1.0	-16.4	1.7
2	AT_03	20.40	[M-H]-	492.103516	Glucohirsutin	C16H31O10S3N1	-0.4	Aliphatic GLS	KEGG	3.1	-5.7	4.5
2	AT_05	2.25	[M-H]-	436.040771	Glucoraphanin	C12H23NO10S3	-0.8	Aliphatic GLS	KEGG	1.4	-25.1	1.2
3	AT_24	7.07	[M-H]-	138.055923	Gabaculine	C7H9NO2	-0.7	Benzoic acid	KEGG	-1.9	-54.5	-2.3
3	AT_72	2.49	[M+H]+	98.984619	Phosphoric acid	H3PO4	4.5	non-metal phosphate	KEGG	-2.2	-79.8	-1.5
3	AT_06	39.73	[M-H]-	416.105316	Heptylglycosinolate	C14H27O9S2N1	-1.9	Aliphatic GLS	Metlin	-3.2	-13.1	-2.9
4	AT_46	38.73	[M+H]+	207.065094	Scoparone	C11H10O4	-0.4	Coumarin	KEGG	-1.0	-23.6	1.4
4	AT_04	32.48	[M-H]-	448.077271	Glucolesquerellin	C14H27O9S3N1	-0.6	Aliphatic GLS	KEGG	-1.4	-14.5	-1.1
4	AT_76	2.98	[M+H]+	308.091278	Glutathione	C10H17N3O6S	0.7	Peptide	KEGG	-1.5	-25.6	-1.2
5	AT_07	42.55	[M+H]+	201.047867	Camalexin	C11H8N2S	2.2	Alkaloid	PubChem	12.8	64.2	20.5
5	AT_08	43.99	[M+H]+	176.070618	Indole-3-acetic acid (IAA)	C10H9NO2	0.2	Alkaloid	KEGG	14.4	39.9	8.4
5	AT_09	2.17	[M+H]+	132.101974	Leucine	C6H13NO2	0.7	Amino acid	KEGG	2.7	4.0	1.6
5	AT_10	3.57	[M+H]+	166.086349	Phenylalanine	C9H11NO2	0.4	Amino acid	KEGG	2.0	3.2	1.4
5	AT_11	6.92	[M+H]+	205.097031	Tryptophan	C11H12N2O2	-0.7	Amino acid	KEGG	1.8	6.0	1.1
5	AT_12	28.40	[M+H]+	741.222412	Anthocyanin			Anthocyanin	UV	1.2	3.3	1.3
5	AT_13	19.52	[M+H]+	757.217773	Cyanidin 3-rutinoside 5-glucoside	C33H41O20+	-0.9	Anthocyanin	KEGG	2.2	45.3	1.4
5	AT_14	27.72	[M+H]+	741.222839	Anthocyanine unidentified			Anthocyanin	UV	1.4	5.1	1.2
5	AT_15	23.22	[M+H]+	741.222961	Anthocyanine unidentified			Anthocyanin	UV	1.4	5.8	1.2
5	AT_16	27.03	[M+H]+	741.223083	Anthocyanine unidentified			Anthocyanin	UV	1.5	6.4	1.2
5	AT_18	24.81	[M+H]+	1343.349731	Cyanidin 3-O-[2-O-(2-O-(sinapoyl)-bata-D-xylopyranosyl) 6-O-(4-O-(beta-D-glucopyranosyl)-p-coumaroyl-bata-D-glucopyranoside] 5-O-[6-O-(malonyl) bata-D-glucopyranoside] I	C61H67O34	-4.1	Anthocyanin	KNApSAck +UV	87.5	1605.5	1.1
5	AT_17	26.86	[M+H]+	1344.353638	Cyanidin 3-O-[2-O-(2-O-(sinapoyl)-bata-D-xylopyranosyl) 6-O-(4-O-(beta-D-glucopyranosyl)-p-coumaroyl-bata-D-glucopyranoside] 5-O-[6-O-(malonyl) bata-D-glucopyranoside] II	C61H67O34	-4.1	Anthocyanin	KNApSAck +UV	3.6	15.2	1.0
5	AT_19	21.16	[M+H]+	741.222717	Pelargonidin 3-(2glu glucosylrutinoside)	C33H41O19	-2.0	Anthocyanin	HMDB	2.6	10.4	1.5
5	AT_20	21.78	[M+H]+	595.165222	Cyanidin 3-O-rutinoside I	C27H31O15+	-0.7	Anthocyanin	KEGG	3.9	25.9	1.6
5	AT_21	25.94	[M+H]+	595.165283	Cyanidin 3-O-rutinoside II	C27H31O15+	-0.6	Anthocyanin	KEGG	1.9	16.1	1.0
5	AT_22	23.03	[M+H]+	611.160217	Delphinidin 3-O-rutinoside	C27H31O16+	-0.5	Anthocyanin	KEGG	2.0	18.9	-1.0
5	AT_23	12.34	[M-H]-	299.077118	4-Hydroxybenzoate-O-glucoside	C13H16O8	-0.4	Benzoic acid	KEGG	1.6	7.4	-1.1
5	AT_25_2	29.40	[M-H]-	333.145416	3'-N'-Acetylfusarochromanone I	C17H22N2O5	-0.5	Benzoic acid	HMDB	2.6	16.1	1.3

Table S4. (Continued)

Cluster Number	Metabolite ID	RT (m)	m/z	Mass(D)	Compound	Formula	Δ ppm to DB	Classification	data base	Fold change		
										MB	*Pbg*	*Pf* SS101
5	AT_25	29.39	[M+H]+	335.160034	3'-N'-Acetylfusarochromanone I	C17H22N2O5	-0.3	Benzoic acid	HMDB	2.5	16.3	1.2
5	AT_26	32.68	[M+H]+	335.160065	3'-N'-Acetylfusarochromanone II	C17H22N2O5	-0.2	Benzoic acid	HMDB	2.5	18.5	1.2
5	AT_26_2	32.68	[M-H]-	333.145386	3'-N'-Acetylfusarochromanone II	C17H22N2O5	-0.6	Benzoic acid	HMDB	2.6	18.1	1.3
5	AT_27	16.45	[M-H]-	431.118896	Apiosylglucosyl 4-hydroxybenzoate	C18H24O12	-1.4	Benzoic acid	HMDB	3.1	17.2	-1.6
5	AT_28	14.66	[M-H]-	343.066803	Theogallin	C14H16O10	-0.6	Benzoic acid	KEGG	1.5	12.6	1.4
5	AT_29	11.52	[M-H]-	285.061493	Uralenneoside	C12H14O8	-0.3	Benzoic acid	HMDB	1.8	7.0	1.3
5	AT_31	12.67	[M+H]+	163.075394	Methyl cinnamate	C10H10O2	0.1	Hydroxycinnamate	KEGG	7.2	27.5	2.1
5	AT_32	36.98	[M-H]-	591.171753	1,2-Bis-O-sinapoyl-beta-D-glucoside	C28H32O14	-0.3	Hydroxycinnamate	KEGG	1.6	6.2	-2.2
5	AT_33_2	16.61	[M-H]-	385.113647	1-O-Sinapoyl beta-D-glucoside	C17H22O10	-1.0	Hydroxycinnamate	KEGG	3.0	17.8	-1.1
5	AT_33	16.60	[M+H]+	387.128021	1-O-Sinapoyl beta-D-glucoside	C17H22O10	-1.4	Hydroxycinnamate	KEGG	2.6	13.1	-1.3
5	AT_34	18.18	[M-H]-	385.1138	4-O-beta-D-Glucosyl-sinapate	C17H22O10	-0.6	Hydroxycinnamate	KEGG	1.4	3.2	-1.3
5	AT_63	11.94	[M-H]-	371.097992	Dihydroferulic acid 4-O-glucuronide	C16H20O10	-1.0	Hydroxycinnamate	HMDB	5.4	24.9	1.1
5	AT_35	37.62	[M-H]-	591.171692	Di-O-sinapoyl-beta-D-glucoside I	C28H32O14	-0.4	Hydroxycinnamate	KEGG	2.9	26.9	1.4
5	AT_36	34.73	[M-H]-	591.171753	Di-O-sinapoyl-beta-D-glucoside II	C28H32O14	-0.3	Hydroxycinnamate	KEGG	1.7	13.7	-1.5
5	AT_37	36.19	[M-H]-	591.171753	Di-O-sinapoyl-beta-D-glucoside III	C28H32O14	-0.3	Hydroxycinnamate	KEGG	1.7	12.3	-1.1
5	AT_38	33.65	[M-H]-	591.171814	Di-O-sinapoyl-beta-D-glucoside iV	C28H32O14	-0.2	Hydroxycinnamate	KEGG	2.2	13.2	1.1
5	AT_39	38.15	[M-H]-	591.17157	Di-O-sinapoyl-beta-D-glucoside V	C28H32O14	-0.6	Hydroxycinnamate	KEGG	5.0	36.3	-1.1
5	AT_66	8.41	[M+H]+	307.176392	Feruloylagmatine I	C15H22N4O3	-0.3	Hydroxycinnamate	KEGG	5.5	17.9	1.8
5	AT_66_2	8.33	[M+H]+	307.176392	Feruloylagmatine II	C15H22N4O3	-0.3	Hydroxycinnamate	KEGG	2.7	28.9	2.6
5	AT_64	36.97	[M+H]+	369.117798	O-Feruloylquinic acid	C17H20O9	-0.5	Hydroxycinnamate	KEGG	1.5	6.7	-2.4
5	AT_40_2	10.89	[M-H]-	275.151337	p-Coumaroylagmatine I	C14H20N4O2	0.0	Hydroxycinnamate	KEGG	12.2	64.0	5.2
5	AT_40	10.89	[M+H]+	277.165802	p-Coumaroylagmatine I	C14H20N4O2	-0.3	Hydroxycinnamate	KEGG	3.9	16.9	2.4
5	AT_41_2	11.34	[M-H]-	275.151337	p-Coumaroylagmatine II	C14H20N4O2	0.0	Hydroxycinnamate	KEGG	12.2	43.8	3.2
5	AT_43	10.18	[M+H]+	191.033707	Ayapin	C10H6O4	-0.9	Coumarin	KEGG	5.2	10.7	1.4
5	AT_44	10.19	[M-H]-	207.02977	Fraxetin	C10H8O5	-0.7	Coumarin	KEGG	5.3	11.4	1.4
5	AT_45	21.50	[M-H]-	369.082428	Fraxin	C16H18O10	-0.8	Coumarin	KEGG	2.1	8.4	1.4
5	AT_47	14.88	[M+H]+	355.102295	Scopolin	C16H18O9	-0.2	Coumarin	KEGG	8.6	24.8	3.3
5	AT_49	2.35	[M+H]+	244.092712	gamma-Glutamyl-beta-cyanoalanine	C9H13N3O5	-0.3	Dipeptide	KEGG	2.9	20.5	-1.1
5	AT_50	49.03	[M-H]-	545.26001	Canavalioside	C26H42O12	-0.6	Diterpene glycoside	HMDB	2.0	43.4	-1.1
5	AT_52	22.30	[M+H]+	381.175415	Prenyl arabinosyl-(1->6)-glucoside	C16H28O10	-0.3	Fatty acyl glycoside	HMDB	2.6	12.9	-1.4
5	AT_53	25.56	[M+H]+	595.1651	Kaempferol 3-galactoside-7-rhamnoside	C27H30O15	-2.0	Flavonoid	KNApSAck	2.7	9.7	1.6
5	AT_54	21.79	[M-H]-	639.156311	flavonoid di glycoside	C28H32O17	-0.6	Flavonoid	HMDB	4.0	29.4	1.5
5	AT_55	33.88	[M-H]-	609.18219	Hesperidin	C28H34O15	-0.5	Flavonoid	KEGG	-1.2	23.0	-1.1
5	AT_56	28.70	[M-H]-	623.161194	Isorhamnetin 3-neohesperidoside	C28H32O16	-0.9	Flavonoid	HMDB	2.3	3.9	1.5
5	AT_57	26.33	[M-H]-	623.161438	Isorhamnetin 3-O-[b-L-rhamnofuranosyl-(1->6)-D-glucopyranoside]	C28H32O16	-0.5	Flavonoid	HMDB	4.1	19.0	1.1

Table S4. (Continued)

Cluster Number	Metabolite ID	RT (m)	m/z	Mass(D)	Compound	Formula	Δ ppm to DB	Classification	data base	Fold change		
										MB	*Pbg*	*Pf* SS101
5	AT_58	28.68	[M+H]+	579.169983	Kaempferitrin	C27H30O14	-1.5	Flavonoid	KEGG	2.3	6.2	1.5
5	AT_53_2	25.55	[M-H]-	593.151062	Kaempferol 7-rhamnoside-4'-glucoside	C27H30O15	-0.3	Flavonoid	KEGG	2.3	4.4	1.6
5	AT_59	21.17	[M-H]-	739.20874	Robinin	C33H40O19	-0.5	Flavonoid	KEGG	2.9	8.2	1.5
5	AT_60	23.02	[M-H]-	609.145447	Rutin	C27H30O16	-1.1	Flavonoid	KEGG	2.2	21.2	-1.0
5	AT_61	3.40	[M+H]+	226.070786	4-Amino-4-deoxychorismate	C10H11NO5	-0.8	Benzoic acid	KEGG	1.3	4.9	-1.2
5	AT_41	11.35	[M+H]+	277.165771	p-Coumaroylagmatine II	C14H20N4O2	-0.4	Coumaric acids	KEGG	6.4	18.3	2.4
5	AT_65	18.17	[M+H]+	225.075516	Sinapic acid	C11H12O5	-1.2	Hydroxycinnamate	KEGG	1.5	6.0	-1.3
5	AT_62	14.89	[M-H]-	399.092651	Sinapinic acid-O-glucuronide isomer	C17H20O11	-1.6	Hydroxycinnamate	HMDB	9.0	27.3	3.2
5	AT_41_2	42.25	[M-H]-	237.076706	Trimethoxycinnamic acid I	C12H14O5	-0.6	Coumaric acids	HMDB	2.7	53.8	1.0
5	AT_41	42.22	[M+H]+	239.091248	Trimethoxycinnamic acid I	C12H14O5	-0.6	Coumaric acids	HMDB	6.7	100.3	1.4
5	AT_42	27.24	[M+H]+	239.091248	Trimethoxycinnamic acid II	C12H14O5	-0.6	Coumaric acids	HMDB	2.0	7.8	1.3
5	AT_67	18.70	[M-H]-	403.124268	Gardenoside	C17H24O11	-0.9	Iridoid	KEGG	2.3	16.6	1.3
5	AT_68	10.03	[M-H]-	549.182373	Genipin 1-beta-gentiobioside	C23H34O15	-0.3	Iridoid	KEGG	6.2	18.0	1.9
5	AT_69	12.66	[M-H]-	387.129913	Geniposide	C17H24O10	0.7	Iridoid	KEGG	8.0	30.9	2.1
5	AT_70	40.41	[M-H]-	541.192505	Deoxyloganin tetraacetate	C25H34O13	-0.2	iridoids	KEGG	-1.1	3.7	-1.9
5	AT_71	17.79	[M+H]+	124.075829	p-Anisidine	C7H9NO	1.2	Methoxyaniline	KEGG	1.3	19.7	-1.3
5	AT_74	30.98	[M-H]-	137.024216	Salicylic acid	C7H6O3	-1.5	Benzoic acid	KEGG	6.2	40.7	1.4
5	AT_75	44.69	[M-H]-	319.176056	525178	C15H28O7	-2.1	Pentaethylene glycol, monoallyl ether	PubChem	19.6	44.2	1.8
5	AT_77	20.45	[M-H]-	551.176575	(Z)-Resveratrol 3,4'-diglucoside	C26H32O13	-0.8	Resveratrol	HMDB	1.8	2.9	-1.0
8	AT_48	2.99	[M-H]-	191.019669	5-Dehydro-4-deoxy-D-glucarate	C6H8O7	-0.3	Dicarboxylic acid	KEGG	3.5	3.0	1.6
9	AT_73	3.22	[M-H]-	115.003578	Fumaric acid	C4H4O4	-1.1	Organic acid	HMDB	4.7	1.6	1.8

Table S5. Annotation of Broccoli metabolites that showed significant change in their abundance after inoculation with rhizobacteria. *Pf* SS101: *Pseudomonas fluorescens* SS101, MB: *Microbacterium* sp., *Pbg*: *Paraburkholderia graminis*. Fold changes of each metabolites were calculated against non-treated control. Clustering numbers are associated with metabolite ID in **Fig 3.**

Cluster Number	Metabolite ID	RT (m)	m/z	Mass(D)	Compound	Formula	Δ ppm to DB	Classification	data base	Fold change		
										MB	*Pbg*	*Pf* SS101
1	BO_36	2.2	[M+H]+	261.037109	Hexose 1-phosphate	C6H13O9P	0.5	Hexose phosphate	KEGG	11.4	-2.2	-1.1
2	BO_09	6.54	[M+H]+	205.097321	Tryptophan	C11H12N2O2	0.7	amino acid	KEGG	-3.0	-2.1	-2.3
2	BO_71	43.18	[M+H]+	631.276428	Brassica napus non-fluorescent chlorophyll catabolite 3	C34H38N4O8	0.3	Tetrapyrrole	HMDB	-3.0	-3.6	-4.4
2	BO_62	2.15	[M-H]-	351.10257	Benzylpenicilloic acid	C16H20N2O5S	1.6	Penicilloic acid	KEGG	-2.2	-3.9	-3.6
2	BO_05	3.20	[M-H]-	152.986389	3-Sulfolactaldehyde	C3H6O5S	0.4	Alkanesulfonic acid	KEGG	-2.8	-10.3	-8.2
3	BO_59	2.16	[M-H]-	175.047012	Allantoic acid	C4H8N4O4	-1.8	n-Carbamoyl-alpha amino acid	KEGG	-1.7	-4.9	-4.7
3	BO_34	2.98	[M-H]-	188.056656	N-Acetyl-L-glutamic acid	C7H11NO5	-2.2	Glutamic acid	KEGG	-1.7	-3.7	-3.9
3	BO_24_2	23.99	[M-H]-	609.146423	Kaempferol 3-O-beta-D-sophoroside or (C05625), (C17563), (C19796)	C27H30O16	0.5	Flavonoid	KEGG	-1.5	-8.0	-3.3
3	BO_06	1.62	[M+H]+	175.119202	Arginine	C6H14N4O2	1.3	Amino acid	KEGG	-1.2	-2.3	-2.3
3	BO_08	1.84	[M-H]-	154.062424	Histidine	C6H9N3O2	-2.9	Amino acid	KEGG, Metlin	-1.2	-2.0	-2.1
4	BO_58	33.49	[M-H]-	385.150909	Methylsyringin	C18H26O9	-0.4	Monolignol	Metlin	-1.3	-2.3	-1.4
4	BO_61	26.98	[M-H]-	593.209412	Zizybeoside II	C25H38O16	1.2	Oligosaccharide	KEGG	-1.5	-3.2	-1.2
4	BO_02	17.16	[M-H]-	380.156464	cis-Zeatin-O-glucoside	C16H23N5O6	-2.8	6-alkylaminopurines	KEGG	-1.1	-3.0	1.0
4	BO_73	12.29	[M-H]-	222.077393	Acetyl-L-tyrosine	C11H13NO4	-2.1	Tyrosine	Metlin	-1.2	-3.1	-1.2
4	BO_04	15.40	[M-H]-	436.041565	Glucoraphanin	C12H23NO10S3	1.0	Aliphatic glucosinolate	KEGG	-1.1	-2.1	1.1
4	BO_51	21.12	[M-H]-	172.098099	N-Acetylleucine	C8H15NO3	-2.7	Leucine	Metlin	1.0	-2.8	1.1
4	BO_17	19.70	[M-H]-	536.17804	4-Demethylsimmondsin 2'-(E)-ferulate	C25H31NO12	1.3	Coumaric acid	HMDB	-1.1	-2.1	1.1
4	BO_13	18.01	[M-H]-	329.088043	1-O-Vanilloyl-beta-D-glucose	C14H18O9	0.7	Benzoic acid	KEGG	-1.2	-4.6	-1.4
4	BO_60	2.53	[M+H]+	98.984688	Phosphoric acid	H3PO4	-1.5	non-metal phosphate	KEGG	-1.1	-3.0	-1.1
6	BO_72	3.00	[M-H]-	191.019897	Citric acid	C6H8O7	-2.4	Tricarboxylic acid	KEGG, Metlin	2.7	3.9	2.9
6	BO_69	34.13	[M-H]-	469.081787	(Z)-Resveratrol 3-(3''-sulfoglucoside) or (HMDB37073), (HMDB37076)	C20H22O11S	1.7	Stilbene	HMDB	1.2	2.3	2.8
6	BO_15	4.33	[M-H]-	173.009323	Dehydroascorbic acid	C6H6O6	-3.1	Bbutenolide	KEGG	1.5	2.7	3.4
6	BO_56	37.93	[M+H]+	369.118317	O-Feruloylquinic acid	C17H20O9	0.9	Hydrocinnamate	KEGG	1.1	1.9	2.2
6	BO_48	21.69	[M-H]-	447.054474	Glucobrassicin	C16H20O9S2N2	1.7	Indolic glucosinonate	KEGG	1.5	4.0	5.1
6	BO_16	17.91	[M-H]-	385.11441	1-O-Sinapoyl beta-D-glucoside	C17H22O10	1.0	Coumaric acid	KEGG	1.3	3.0	3.7
6	BO_46	21.72	[M+H]+	369.11145	Desulfoglucobrassicin	C16H20N2O6S	-0.1	Indolic glucosinolate	KEGG	1.5	3.4	3.9
6	BO_14	2.24	[M+H]+	177.039734	Ascorbic acid	C6H8O6	2.0	Butenolide	KEGG	2.0	3.7	4.5
6	BO_43	19.89	[M+H]+	195.065308	Ferulic acid or (C12204), (C10477)	C10H10O4	0.7	Hydroxycinnamate	KEGG	1.1	1.9	2.2
6	BO_40	11.40	[M+H]+	181.049728	Caffeic acid	C9H8O4	0.8	Hydroxycinnamate	KEGG	1.4	2.5	3.2
6	BO_41	11.42	[M-H]-	341.088074	Caffeic acid 3-glucoside or (C10433)	C15H18O9	0.7	Hydroxycinnamate	KEGG	1.3	2.3	2.9

Table S5. (Continued)

Cluster Number	Metabolite ID	RT (m)	m/z	Mass(D)	Compound	Formula	Δ ppm to DB	Classification	data base	Fold change		
										MB	*Pbg*	*Pf* SS101
6	BO_01	5.76	[M+H]+	298.096924	Methylthioadenosine	C11H15N5O3S	0.2	5'-deoxy-5'-thionucleoside	KEGG	1.4	2.2	2.1
7	BO_67	33.14	[M-H]-	577.156799	Glucofrangulin A	C27H30O14	0.8	Quinone	KEGG	-2.7	1.5	3.2
7	BO_50	24.09	[M+H]+	306.097595	Ascorbigen	C15H15NO6	1.2	Isosorbide	HMDB	2.2	6.4	7.1
7	BO_65	38.88	[M+H]+	339.107605	Hydrojuglone glucoside	C16H18O8	0.5	Phenolic glycoside	HMDB	2.4	4.5	8.8
7	BO_31	38.85	[M-H]-	561.162048	Flavonol 3-O-beta-D-glucosyl-(1->2)-beta-D-glucoside	C27H30O13	1.3	Flavonoid	KEGG	2.2	4.6	10.3
7	BO_42	18.74	[M+H]+	195.065338	Ferulic acid	C10H10O4	0.8	Hydroxycinnamate	KEGG	1.3	1.9	3.2
7	BO_68	18.74	[M-H]-	355.103821	Gentiopicroside	C16H20O9	1.1	Iridoid	KEGG	1.4	2.0	3.5
7	BO_07	2.04	[M-H]-	132.03035	Aspartic acid	C4H7NO4	-2.8	amino acid	KEGG	1.7	2.6	3.5
7	BO_70	2.09	[M-H]-	195.050842	D-Gluconic acid	C6H12O7	-0.9	Sugar acid	KEGG	1.3	1.8	3.2
7	BO_27	17.99	[M+H]+	935.245972	Quercetin 3-[p-coumaroyl-(->6)-glucosyl-(1->2)-glucosyl-(1->2)-glucoside] or (HMDB0029268)	C42H46O24	0.8	Flavonoid	HMDB	-1.1	1.2	2.1
7	BO_27_2	17.98	[M-H]-	933.231323	Quercetin 3-[p-coumaroyl-(->6)-glucosyl-(1->2)-glucosyl-(1->2)-glucoside]	C42H46O24	0.7	Flavonoid	HMDB	-1.1	1.2	2.3
7	BO_23	20.77	[M-H]-	947.247437	Kaempferol 3-(2-feruloylsophoroside) 7-glucoside	C43H48O24	1.2	Flavonoid	HMDB	-1.0	1.2	2.4
7	BO_25	20.78	[M+H]+	949.261597	Kaempferol 3-sophoroside 7-(2-feruloylglucoside) or (HMDB0040801), (HMDB29269)	C43H48O24	0.8	Flavonoid	HMDB	-1.1	1.3	2.3
7	BO_32	14.56	[M+H]+	773.213074	Kaempferol 3-sophorotrioside	C33H40O21	-0.5	Flavonoid	KEGG	-1.1	1.3	2.3
7	BO_53	37.39	[M-H]-	693.204773	Neocuscutoside C	C32H38O17	0.7	Lignan glycoside	Metlin	1.4	2.4	5.9
7	BO_38	40.02	[M-H]-	929.27356	2-Feruloyl-1,2'-disinapoylgentiobiose	C44H50O22	1.6	Hydroxycinnamate	HMDB	1.1	1.4	2.6
7	BO_64	26.64	[M-H]-	415.125183	2-Hydroxybenzaldehyde O-[xylosyl-(1->6)-glucoside]	C18H24O11	1.4	Phenolic glycosides	HMDB	1.7	2.1	5.7
7	BO_52	36.17	[M-H]-	693.204773	Sesaminol glucosyl-(1->2)-glucoside	C32H38O17	1.7	Lignan	HMDB	1.4	2.0	4.2
7	BO_29	20.33	[M-H]-	609.146667	Rutin	C27H30O16	0.9	Flavonoid	KEGG	1.2	1.9	3.4
7	BO_57	14.87	[M+H]+	339.107605	p-Coumaroyl quinic acid or (C10432), (C10441)	C16H18O8	0.4	Hydroxycinnamate	KEGG	1.3	2.3	3.9
7	BO_57_2	14.89	[M-H]-	337.093689	p-Coumaroyl quinic acid or (C10441), (C10432)	C16H18O8	0.4	Hydroxycinnamate	KEGG	1.3	2.3	4.2
7	BO_22	35.44	[M-H]-	723.21521	Flavonol 3-O-beta-D-glucosyl-(1->2)-beta-D-glucosyl-(1->2)-beta-D-glucoside	C33H40O18	1.4	Flavonoid	KEGG	1.5	2.6	4.3
7	BO_21	33.33	[M-H]-	577.15686	Daidzein 4',7-diglucoside	C27H30O14	1.0	Flavonoid	HMDB	1.5	2.4	5.2
7	BO_19	17.22	[M+H]+	355.102661	Scopolin or (C00852), (C08996)	C16H18O9	0.8	Coumarin	KEGG	1.2	1.9	3.1
7	BO_54	12.99	[M-H]-	371.098541	Dihydroferulic acid 4-O-glucuronide	C16H20O10	0.5	Flavonoid	HMDB	1.5	2.9	4.7
7	BO_55	10.15	[M+H]+	355.102448	Chlorogenic acid	C16H18O9	0.2	Flavonoid	KEGG	1.3	2.6	3.9
7	BO_24	20.34	[M+H]+	611.160583	Kaempferol 3-O-beta-D-sophoroside or (C05625), (C17563)	C27H30O16	-0.2	Flavonoid	KEGG	1.3	2.3	3.7
7	BO_30	28.87	[M-H]-	665.173584	sudachiin B or (HMDB0039088)	C30H34O17	1.9	Flavonoid	HMDB	1.4	2.4	5.0
7	BO_26	30.48	[M-H]-	739.210815	Mauritianin	C33H40O19	2.3	Flavonoid	HMDB	1.2	2.1	3.4

Table S5. (Continued)

Cluster Number	Metabolite ID	RT (m)	m/z	Mass(D)	Compound	Formula	Δ ppm to DB	Classification	data base	Fold change		
										MB	*Pbg*	*Pf* SS101
7	BO_45	16.68	[M+H]+	225.075836	Sinapic acid	C11H12O5	0.3	Hydroxycinnamate	KEGG	1.1	1.5	2.0
7	BO_55_2	16.11	[M+H]+	355.102692	Chlorogenic acid or (C01527), (C08996)	C16H18O9	0.9	Hydroxycinnamate	HMDB	1.7	2.9	4.5
7	BO_10	17.79	[M-H]-	278.067352	N-[4'-hydroxy-(E)-cinnamoyl]-L-aspartic acid	C13H13NO6	1.2	Aspartic acid	HMDB	1.3	2.2	3.3
7	BO_28	30.14	[M-H]-	739.210693	Robinin	C33H40O19	2.1	Flavonoid	KEGG	1.4	3.4	5.4
8	BO_49	34.54	[M-H]-	477.064697	neoglucobrassicin	C17H22O10S2N2	0.8	Indolic glucosinonate	KEGG	-1.1	1.1	3.5
8	BO_12	4.46	[M-H]-	315.072632	Ginnalin B	C13H16O9	-0.7	Benzoic acid	Metlin	1.3	1.4	7.2
8	BO_11	13.50	[M-H]-	299.077423	4-(beta-D-Glucosyloxy)benzoate	C13H16O8	0.7	Benzoic acid	KEGG	1.3	6.0	40.0
8	BO_47	27.80	[M-H]-	477.064667	4-Methoxyglucobrassicin	C17H22N2O10S2	0.7	Indolic glucosinonate	KEGG	-1.0	1.0	2.3
8	BO_33	33.93	[M-H]-	547.146606	Puerarin xyloside	C26H28O13	1.6	Flavonoids	KEGG	1.9	3.3	12.8
8	BO_20	34.36	[M+H]+	191.14299	beta-Damascenone	C13H18O	-0.3	Enone	HMDB	1.1	1.4	2.6
8	BO_03	12.11	[M-H]-	406.031067	Glucoiberverin	C11H21NO9S3	1.3	Aliphatic glucosinolate	KEGG	1.3	-1.1	2.3
8	BO_37	2.18	[M-H]-	289.033173	Sedoheptulose phosphate or (C19882)	C7H15O10P	0.5	Hexose phosphate	KEGG	1.3	-1.1	4.1
8	BO_39	16.21	[M-H]-	325.093597	4-O-beta-D-Glucosyl-4-hydroxycinnamate or (C16827)	C15H18O8	0.1	Hydroxycinnamate	KEGG	1.6	1.4	2.9
8	BO_44	16.22	[M+H]+	165.054794	p-Coumaric acid or (C00166), (C12621), (C01772)	C9H8O3	1.3	Hydroxycinnamate	KEGG	1.7	1.5	2.3
9	BO_66	2.25	[M-H]-	110.985336	Hydroxymethylphosphonate	CH5O4P	-3.5	Phosphonic acid	KEGG	1.7	3.7	3.0
9	BO_35	2.18	[M-H]-	209.066757	Coriose or (C21043), (C02076)	C7H14O7	-2.9	Glycoside	KEGG	1.8	2.9	2.2
9	BO_63	2.19	[M-H]-	306.076965	Glutathione	C10H17N3O6S	-0.7	Peptide	Metlin	1.8	2.5	1.6
9	BO_18	15.82	[M+H]+	193.049622	Scopoletin, Isoscopoletin, 4-Methyldaphnetin, 5,7-dihydroxy-4-methylcoumarin (Coumarins)	C10H8O4	0.2	Coumarin	KEGG	1.5	3.9	-8.9

Table S6. Annotation of Artemisia metabolites that showed significant change in their abundance after inoculation with rhizobacteria. *Pf* SS101: *Pseudomonas fluorescens* SS101, MB: *Microbacterium* sp., *Pbg*: *Paraburkholderia graminis*. Fold changes of each metabolites were calculated against non-treated control. Clustering numbers are associated with metabolite ID in **Fig 3.**

Cluster Number	Metabolite ID	RT (m)	m/z	Mass(D)	Compound	Formula	Δ ppm to DB	Classification	data base	Fold change		
										MB	*Pbg*	*Pf* SS101
1	AA_53	21.01	[M+H]+	209.153366	Carvyl propionate	C13H20O2	-1.1	Terpenoid	magma	1.0	-15.0	-1.7
1	AA_33	21.87	[M+H]+	565.155151	Neoschaftoside	C26H28O14	-0.1	Flavonoid	Knapsack	-1.2	-2.2	-1.2
1	AA_80	49.98	[M+H]+	235.169189	(+)-12-Hydroxy-alpha-cyperone	C15H22O2	-0.3	Terpenoid	KEGG	-1.1	-2.4	-1.3
1	AA_11	1.74	[M+H]+	104.107407	Choline	C5H14NO	4.1	Choline	metlin	1.1	-6625.2	-1.2
1	AA_01	2.12	[M+H]+	177.061813	Allantoic acid	C4H8N4O4	-0.1	Alpha amino acid	magma	1.1	-2.2	1.4
1	AA_07	3.12	[M+H]+	206.102081	N-Acetyl-D-fucosamine	C8H15NO5	-0.9	Amino sugar	magma	1.0	-373.0	1.4
1	AA_57	2.51	[M+H]+	98.984627	Phosphoric acid	H3O4P	4.6	non-metal phosphate	HMDB	1.1	-11.3	1.2
1	AA_29	44.85	[M-H]-	271.061066	4',5,8-Trihydroxyflavanone	C15H12O5	-0.9	Flavonoid	HMDB	-1.2	-2.3	-1.3
1	AA_30	38.32	[M-H]-	287.05603	3',5,5',8-Tetrahydroxyflavanone; (S)-form	C15H12O6	-0.3	Flavonoid	Dictionary of natural compound	-1.1	-2.6	-1.6
1	AA_79	41.18	[M+H]+	235.169098	Dihydrodeoxyarteannuin B	C15H22O2	-0.7	Terpenoid	Knapsack	-1.2	-2.0	-1.3
1	AA_34	29.35	[M+H]+	641.171082	Patuletin 3-O-rutinoside	C28H32O17	-0.2	Flavonoid	Knapsack	-1.1	-2.5	-1.3
1	AA_34_2	29.34	[M-H]-	639.15625	Patuletin 3-O-rutinoside	C28H32O17	-0.7	Flavonoid	Knapsack	-1.0	-2.5	-1.3
1	AA_31	43.45	[M+H]+	347.076202	5,6,3',4'-Tetrahydroxy-3,7-dimethoxyflavone	C17H14O8	0.2	Flavonoid	Knapsack	-1.1	-2.5	-1.3
1	AA_76	41.87	[M+H]+	235.169098	Artemisinic acid	C15H22O2	-0.7	Terpenoid	magma	-1.3	-4.4	-1.7
1	AA_90	34.22	[M-H]-	507.114197	11-O-Syringylbergenin	C23H24O13	-1.0	Benzoic acid	Pubchem	1.1	-2.4	1.1
1	AA_62	40.98	[M-H]-	517.134705	Medicarpin 3-O-glucoside-6'-malonate	C25H26O12	-0.9	Pterocarpan	magma	-1.0	-2.3	-1.2
1	AA_81	22.00	[M+H]+	105.070274	Styrene	C8H8	3.8	Styrene	magma	1.2	-10.5	-1.0
1	AA_15	16.88	[M-H]-	243.134827	Leucyl-Hydroxyproline	C11H20N2O4	-0.8	Dipeptide	HMDB	-1.3	-25.0	-1.7
1	AA_49	47.25	[M-H]-	551.213013	Prupaside	C27H36O12	-0.7	Lignan glycoside	HMDB	-1.1	-2.0	-1.1
1	AA_84	29.21	[M-H]-	347.170929	Foeniculoside V	C16H28O8	-0.6	Terpene glycoside	HMDB	-1.0	-3.6	-1.1
1	AA_10	6.94	[M-H]-	138.055939	Gabaculine	C7H9NO2	-0.6	Benzoic acid	KEGG	-1.1	-13.0	-1.5
1	AA_27	32.91	[M-H]-	415.197205	Ethyl 7-epi-12-hydroxyjasmonate glucoside	C20H32O9	-0.4	Fatty acyl glycosides of mono- and disaccharides	Metlin	1.0	-3.3	-1.2
1	AA_85	23.11	[M-H]-	347.170959	Nepetariaside	C16H28O8	-0.5	Terpene glycoside	HMDB	1.0	-3.1	-1.2
1	AA_38	32.21	[M-H]-	243.123566	4-Oxododecanedioic acid	C12H20O5	-0.9	Hydroxy fatty acid	Metlin	-1.1	-4.4	-1.2
1	AA_16	13.28	[M+H]+	245.149445	Isoleucyl-Hydroxyproline	C11H20N2O4	-0.6	Dipeptide	HMDB	-1.1	-8.6	-1.3
1	AA_17	5.81	[M+H]+	231.133804	Valyl-Hydroxyproline	C10H18N2O4	-0.6	Dipeptide	HMDB	-1.1	-10.0	-1.4
1	AA_91	26.11	[M+H]+	227.127609	1-Acetoxy-7-hydroxy-3,7-dimethyl-2E,5E-octadien-4-one	C12H18O4	-0.8		Knapsack	-1.1	-5.4	-1.5
1	AA_87	28.32	[M+H]+	175.148239	1,2,3,4-Tetrahydro-1,4,6-trimethyl-naphthalene	C13H18	-0.2	Tetralin	HMDB	-1.0	-3.4	-1.3
1	AA_22	42.91	[M-H]-	469.22879	3-Hydroxy-6-methylheptyl 2-O-?-D-glucopyranosyl-?-D-glucopyranoside	C20H38O12	-0.5	Fatty acyl glycosides of mono- and disaccharide	Metlin	-1.1	-13.1	-1.9
1	AA_71	24.93	[M-H]-	311.113586	p-Coumaryl alcohol 4-O-glucoside	C15H20O7	-0.4	monolignol_cinnamyl alcohol beta-D-glucosid	magma	1.1	-3.3	-1.3

Table S6. (Continued)

Cluster Number	Metabolite ID	RT (m)	m/z	Mass(D)	Compound	Formula	Δ ppm to DB	Classification	data base	Fold change		
										MB	*Pbg*	*Pf* SS101
1	AA_21	51.43	[M-H]-	333.191803	3,7-Dimethyl-5-octene-1,7-diol 1-glucoside	C10H20O2	-0.2	Fatty acyl glycosides of mono- and disaccharide	HMDB	1.0	-6.4	-1.7
1	AA_59	22.32	[M-H]-	297.097839	Picein	C14H18O7	-0.5	Phenolic glycosides	KNAPSACK	1.1	-6.5	-1.4
1	AA_50	41.38	[M-H]-	187.097504	Azelaic acid or (C17878)	C9H16O4	-0.4	Medium-chain fatty acid	magma	1.1	-4.5	-1.4
1	AA_48	19.59	[M-H]-	172.097855	N-Acetyl-L-leucine or (C10173)	C8H15NO3	-0.4	Leucine and derivative	magma	-1.0	-3.4	1.0
1	AA_72	21.99	[M-H]-	461.166443	Verbasoside or (HMDB39233)	C20H30O12	0.0	Monolignol	HMDB	1.1	-6.9	-1.1
1	AA_02	6.39	[M-H]-	315.10849	Hydroxytyrosol 1-O-glucoside	C14H20O8	-0.2	o-glycosyl compound	HMDB	1.0	-2.3	-1.0
1	AA_25	19.29	[M+H]+	403.196198	D-Linalool 3-(6''-malonylglucoside) or (HMDB0031763)	C19H30O9	-0.2	Fatty acyl glycoside	HMDB	-1.0	-2.0	-1.1
1	AA_36	2.33	[M+H]+	261.037048	Glucose 6-phosphate	C6H13O9P	0.2	Hexose phosphate	HMDB	-1.0	-4.7	-1.1
2	AA_56	53.51	[M+H]+	137.132401	beta-Pinene	C10H16	-0.6	Monoterpen	magma	1.8	2.6	1.3
2	AA_74	54.32	[M+H]+	233.153412	Isoalloalantolactone (Helenin)	C15H20O2	-0.7	Terpenoid	KEGG	-796.2	2.2	-2.3
2	AA_73	12.94	[M-H]-	353.087616	Scopolin or (C00852)	C16H18O9	-0.3	Hydroxycinnamate	magma	-1.4	3.5	-1.0
2	AA_05	3.75	[M+H]+	118.086517	Valine	C5H11NO2	2.2	Amino acid	HMDB	-1.0	90.3	1.1
2	AA_08	42.95	[M+H]+	135.116821	p-Cymene	C10H14	0.0	Terpenoids	HMDB	1.4	2.6	1.3
2	AA_63	33.27	[M-H]-	515.119141	1,3-Dicaffeoylquinic acid I	C25H24O12	-0.7	Hydroxycinnamate	Metlin	1.3	3.2	-1.1
2	AA_54	30.97	[M-H]-	417.176422	2-[4-(3-Hydroxypropyl)-2-methoxyphenoxy]-1,3-propanediol 1-glucoside	C19H30O10	-0.5	Hydroxycinnamate	HMDB,DNP	1.3	6.1	2.1
2	AA_18	51.66	[M+H]+	179.085541	2,12-Tetradecadiene-4,6,8,1-tetrayne	C14H10	0.1	Enyme	HMDB	2.6	14.5	5.4
2	AA_61	5.78	[M+H]+	167.070328	3-Hydroxyhydrocinnamic acid	C9H10O3	0.4	Phenylpropanoic acid	ChemSpider	24.4	179.8	51.7
2	AA_64_2	29.92	[M-H]-	515.119141	1,3-Dicaffeoylquinic acid II	C25H24O12	-0.7	Hydroxycinnamate	HMDB	1.3	5.5	1.3
2	AA_55	33.39	[M-H]-	371.134491	Syringin	C17H24O9	-0.6	Hydroxycinnamate	Knapsack	-1.0	2.0	1.1
2	AA_88	4.05	[M-H]-	173.009048	Aconitic acid	C6H6O6	-0.7	Tricarboxylic acid	Metline	-1.0	4.7	-1.1
2	AA_86	49.47	[M-H]-	403.197113	Pisumionoside	C19H32O9	-0.6	Terpene glycoside	HMDB	1.0	4.6	1.2
2	AA_44	5.09	[M+H]+	265.154816	Feruloylputrescine	C14H20N2O3	0.6	Hydroxycinnamate	magma	-1.1	5.9	1.3
2	AA_77	50.95	[M+H]+	221.189926	Artemisinic alcohol	C15H24O	-0.3	Sesquiterpenoid	magma	1.1	2.5	1.0
2	AA_75	46.14	[M-H]-	285.170746	1,2,6,7-Tetraoxaspiro[7.11]nonadecan-3-one	C15H26O5	0.0	Sesquiterpenoid	Chemspider	1.2	3.7	1.4
2	AA_39	32.43	[M-H]-	193.0504	Methyl caffeate	C10H10O4	-1.2	Hydroxycinnamate	KEGG	1.0	4.7	-1.2
2	AA_78	45.50	[M-H]-	283.154999	Dihydroartemisinin or Arteannuin H	C15H24O5	-0.3	Sesquiterpenoid	metlin_HMDB	-1.2	2.9	-1.1
2	AA_20	13.34	[M-H]-	393.176544	cis-3-Hexenyl b-primeveroside	C17H30O10	-0.2	Fatty acyl glycoside	HMDB	1.0	2.3	1.0
2	AA_83	5.79	[M-H]-	391.124542	Shanzhiside	C16H24O11	-0.1	Terpene glycoside	ChemSpider	1.1	6.7	1.9
2	AA_45	15.65	[M-H]-	419.155731	Lamioside	C18H28O11	-0.5	Iridoid	KEGG	1.0	3.1	1.2
2	AA_24	46.98	[M+H]+	401.180481	Corchoionoside B	C19H28O9	-0.3	Fatty acyl glycoside	HMDB	-1.1	3.7	-1.1
2	AA_13	29.86	[M+H]+	163.038605	7-Hydroxycoumarin	C9H6O3	-2.2	Coumarin	Knapsack	-1.1	69.2	-1.1
2	AA_26	40.84	[M-H]-	501.233978	Eriojaposide A	C24H38O11	-0.3	Fatty acyl glycoside	HMDB	1.0	5.1	1.3

Table S6. (Continued)

Cluster Number	Metabolite ID	RT (m)	m/z	Mass(D)	Compound	Formula	Δ ppm to DB	Classification	data base	Fold change		
										MB	*Pbg*	*Pf* SS101
2	AA_14	16.21	[M-H]-	129.055664	Mevalonolactone	C6H10O3	-0.4	Delta valerolactone	HMDB	-1.2	2.2	-1.2
2	AA_37	9.38	[M-H]-	175.061066	3-Propylmalate	C7H12O5	-0.9	Hydroxy fatty acid	magma	-1.1	5.9	1.6
2	AA_04	1.97	[M-H]-	132.030121	Aspartic acid	C4H7NO4	-0.8	Amino acid	HMDB	1.1	3.8	1.2
2	AA_42	13.68	[M-H]-	341.087555	Caffeic acid 3-glucoside	C15H18O9	-0.5	Hydroxycinnamate	magma	1.2	4.7	1.3
2	AA_35	27.63	[M-H]-	447.092834	Luteolin 7-glucoside	C21H20O11	-1.0	Flavonoid	HMDB	-1.1	2.3	-1.2
2	AA_66	36.03	[M-H]-	529.134766	1-Feruloyl-5-caffeoylquinic acid	C26H26O12	-0.7	Hydroxycinnamate	Metlin, HMDB	1.1	170.1	5.6
2	AA_64	41.77	[M-H]-	543.150513	1,5-Diferuloylquinic acid	C27H28O12	-0.5	Hydroxycinnamate	HMDB	-1.7	29.4	-1.7
2	AA_68	24.36	[M+H]+	369.118042	5-O-Feruloylquinic acid	C17H20O9	0.2	Hydroxycinnamate	Metlin	-1.2	5.8	-1.0
2	AA_40	21.96	[M-H]-	367.10321	O-Feruloylquinate	C17H20O9	-0.6	Hydroxycinnamate	KEGG	-1.3	13.5	-1.1
2	AA_40_2	21.96	[M+H]+	369.118011	O-Feruloylquinate	C17H20O9	0.1	Hydroxycinnamate	KEGG	-1.3	13.5	-1.1
2	AA_47	26.19	[M-H]-	389.108795	Monotropein	C16H22O11	-0.4	Iridoid o-glycoside	magma	1.0	13.8	1.0
2	AA_09	17.77	[M-H]-	308.077576	N-Feruloylaspartic acid	C14H15NO7	0.0	Aspartic acid	HMDB	1.1	49.6	1.0
2	AA_58	2.41	[M-H]-	133.01416	Malic acid	C4H6O5	-0.7	Organic acid	MSMS	-1.4	6.7	-1.4
2	AA_65	36.37	[M-H]-	529.134766	1-Caffeoyl-5-feruloylquinic acid	C26H26O12	-0.7	Hydroxycinnamate	HMDB, PubChem	-1.1	10.8	1.1
2	AA_69	14.88	[M+H]+	355.102203	Chlorogenic Acid	C16H18O9	-0.4	Hydroxycinnamate	Metlin	-1.1	2.6	-1.1
2	AA_67	36.03	[M+H]+	531.149231	4-O-Caffeoyl-3-O-feruloylquinic acid	C26H26O12	-0.9	Hydroxycinnamate	HMDB	-19.4	13.3	-1.6
2	AA_46	15.65	[M+H]+	213.112045	7-Deoxyloganetin	C11H16O4	-0.6	Terpenoid	KEGG	-1.0	2.7	1.1
2	AA_89	2.99	[M-H]-	191.019699	Citric acid	C6H8O7	-0.1	Tricarboxylic acid	HMDB	1.0	9.5	-1.5
2	AA_12	33.63	[M+H]+	357.118011	1-Feruloyl-D-glucose	C16H20O9	0.1	Coumaric acid	KEGG	-1.3	9.5	-1.1
2	AA_52	3.54	[M-H]-	159.029785	Oxoadipic acid	C6H8O5	-0.9	Medium-chain keto acids and derivatives, Carboylic acid	KEGG	2.2	60.3	2.2
2	AA_82	3.68	[M-H]-	191.019745	2,5-Diketogulonic acid	C6H8O7	0.1	Sugar acid	HMDB	1.3	9.4	-1.2
2	AA_70	33.14	[M+H]+	339.1073	p-Coumaroyl quinic acid	C16H18O8	-0.4	Hydroxycinnamate	magma	-1.3	22.5	-1.1
2	AA_41	33.15	[M+H]+	357.118011	1-O-Feruloyl-beta-D-glucose	C16H20O9	0.0	Hydroxycinnamate	ChemSpider	-1.3	21.8	-1.1
2	AA_51	18.07	[M-H]-	131.071274	6-Hydroxyhexanoate	C6H12O3	-0.7	Medium-chain hydroxy acid	HMDB	1.1	6.6	-1.4
2	AA_43	26.72	[M+H]+	165.054703	p-Coumaric acid	C9H8O3	0.5	Hydroxycinnamate	HMDB	1.2	6.2	1.0
3	AA_28	42.78	[M+H]+	129.127426	octanal/1-Octen-3-ol (C14272)	C8H16O	0.4	Fatty alcohol	Metlin, KNApSAck	-1.2	9.3	11.0
3	AA_19	26.99	[M-H]-	503.249634	Blumenol C O-[apiosyl-(1->6)-glucoside], (3S,7E,9R)-4,7-Megastigmadiene-3,9-diol 9-[apiosyl-(1->6)-glucoside]	C24H40O11	-0.4	Fatty acyl glycoside	Metlin	1.2	6.3	8.7
3	AA_60	31.57	[M+H]+	331.138672	(±)-3-(4-Hydroxyphenyl)-1,2-propanediol 4'-O-glucoside	C15H22O8	-0.3	Phenylpropanod	Metlin	1.2	2.1	2.4
3	AA_06	2.97	[M-H]-	128.035217	Pyroglutamic acid, Pyrroline hydroxycarboxylic acid, 4-Oxoproline	C5H7NO3	-0.8	Amino acid	Metlin	-1.1	1.2	2.1
3	AA_03_2	1.70	[M-H]-	173.104233	Arginine	C6H14N4O2	-1.0	Amino acid	Metlin, HMDB	1.1	-2.3	2.4
3	AA_03	1.59	[M+H]+	175.118973	Arginine	C6H14N4O2	0.1	Amino acid	Metlin, HMDB	1.2	-1.6	2.5

Table S7. Fold changes of metabolites in shoots of Arabidopsis (Arab), Broccoli (Bro) and Artemisia (Art) upon treatment of the roots with different rhizobacterial genera. The metabolites listed here have been associated with human health. *Pf* SS101: *Pseudomonas fluorescens* SS101, MB: *Microbacterium* sp., *Pbg*: *Paraburkholderia graminis*.

Plant	Compound	Compound classification	Fold changes			Health treat	Reference
			MB	Pbg	*Pf* SS101		
Arab	Glucoerucin	Aliphatic GLS	-1.43	-1.71	-1.18	Fungicidal (soil born pathogen) activity of enzyme derivered production of glucoiberin, Cancer prevention: inhibition of cell demage indeced by H2O2 in hepa1c1c7 cell line by myrosinase treated this glucosinlate, oomycete, antioxidative, cancer chemopreventive	(Manici *et al*., 1999; Manici *et al*., 2000; Zhu & Loft, 2003; Barillari *et al*., 2005; Razis *et al*., 2011)
Arab	Glucohirsutin	Aliphatic GLS	3.07	-5.71	4.48	Resistance to insect hervivory	(Beekwilder *et al*., 2008)
Arab	Glucoraphanin	Aliphatic GLS	1.39	-25.11	1.19	Cancer prevention: inhibition of cell demage indeced by H2O2 in hepa1c1c7 cell line by myrosinase treated this glucosinlate, Anticarcinogen sulforaphane (catalized by myrosinase)	(Matusheski & Jeffery, 2001; Zhu & Loft, 2003)
Arab	Camalexin	Alkaloid	12.8	64.2	20.5	Antiproliferative activity against a human breast cancer cell line	(Glawischnig, 2007)
Arab	Indole-3-acetic acid	Alkaloid	14.4	39.9	8.4	Plant growth regulator	(Spaepen *et al*., 2007)
Arab	Cyanidin delivatives	Anthocyanin	2.2	45.3	1.4	Antioxidants, which help to prevent neuronal diseases, cardiovascular illnesses, cancer, diabetes, inflammation, and many such others diseases	(Yousuf *et al*., 2016)
Arab	Gabaculine	Benzoic acid	-1.94	-54.55	-2.32	GABA transaminase inhibitor	(Rando & Bangerter, 1977)
Arab	Phenylacetic acid	Carboxylic acid ester	4.25	46.04	2.21	Natural auxin	(Wightman & Lighty, 1982)
Arab	Trimethoxycinnamic acid	Coumaric acid	6.7	100.3	1.4	Antidepressant-like effects on mice in forced swimming test and anti-stress effects on rat	(Nakazawa *et al*., 2003; Kawashima *et al*., 2004)
Arab	Ayapin	Coumarin	5.2	10.7	1.4	Antifungal activity	(Urdangarin *et al*., 1999)
Arab	Fraxetin	Coumarin	5.32	11.39	1.36	Neuroprotective effect, antioxidative, Antihyperglycemic effect, Antitumor and antimetastatic actions	(Martín-Aragón *et al*., 1997; Molina-Jiménez *et al*., 2004; Murali *et al*., 2013; Kimura & Sumiyoshi, 2015)
Arab	Fraxin	Coumarin	2.06	8.45	1.37	Antioxidative	(Whang *et al*., 2005)
Arab	Scoparone	Coumarin	-1.0	-23.6	1.4	Antioomycete, prevention and therapy of liver injury	(Afek & Sztejnberg, 1988; Zhang *et al*., 2013)
Arab	Hesperidin	Flavonoid	-1.21	22.99	-1.05	Anti-inflammatory	(Guardia *et al*., 2001)
Arab	Isorhamnetin glycosides	Flavonoid	2.28	3.93	1.54	free radical scavenging, cancer cell apoptosis induction	(Hyun *et al*., 2006; Antunes-Ricardo *et al*., 2014)
Arab	Kaempferitrin	Flavonoid	2.3	6.2	1.5	inhibits insulin stimulated GLUT4 translocation and glucose uptake in 3T3-L1 adipocytes	(Prasad *et al*., 2009)
Arab	Rutin	Flavonoid	2.23	21.22	-1.03	Antioxidative, Anti-inflammatory, cancer chemopreventive	(Deschner *et al*., 1991; Guardia *et al*., 2001; Yang *et al*., 2008)
Arab	Sinapic acid	Hydroxycinnamate	1.5	6.0	-1.3	Anti-Inflammatory Effects, Anxiolytic-like effects, Cerebral protective and cognition-improving effects	(Karakida *et al*., 2007; Yoon *et al*., 2007; Yun *et al*., 2008)
Arab	Geniposide	Iridoid	8.01	30.89	2.14	Anti-inflammatory, Antithrombotic, hypoglycemic effect	(Suzuki *et al*., 2001; Koo *et al*., 2006; Wu *et al*., 2009)
Arab	Fumaric acid	Organic acid	4.69	1.57	1.80	Treatment for Psoriasis vulgaris and decrease of multifocal leukoencephalopathy (PML)	(Ermis *et al*., 2013)
Arab	Salicylic Acid	Organic acid	6.22	40.65	1.37	Provoke SAR	(Delaney *et al*., 1994)

Table S7. (Continued)

Plant	Compound	Compound classification	Fold changes			Health treat	Reference
			MB	Pbg	*Pf* SS101		
Bro	Glucoraphanin	Aliphatic GLS	-1.06	-2.05	1.11	Cancer prevention: inhibition of cell demage indeced by H2O2 in hepa1c1c7 cell line by myrosinase treated this glucosinlate, Anticarcinogen sulforaphane (catalized by myrosinase)	(Matusheski & Jeffery, 2001; Zhu & Loft, 2003)
Bro	Ascorbic acid	Butenolide	2.01	3.73	4.53	Antioxidative, Anticancer activities	(Fraga *et al*., 1991; Arrigoni & De Tullio, 2002; Chen *et al*., 2005)
Bro	Dehydroascorbic acid	Butenolide	1.47	2.73	3.38	Cerebroprotection	(Huang *et al*., 2001)
Bro	Scopoletin	Coumarin	1.49	3.91	-8.88	Inhibited PC3 proliferation by inducing apoptosis of PC3 cells (human prostate cancer cell line), antithyroid, antioxidative and antihyperglycemic activity	(Liu *et al*., 2001; Panda & Kar, 2006)
Bro	beta-Damascenone	Enones	1.09	1.42	2.64	Antispasmodic activity	(Pongprayoon *et al*., 1992)
Bro	Kaempferol glycosides	Flavonoid	-1.00	1.25	2.40	Neuroinflammation, anti-obesity and anti-diabetic effects, inflammation, allelopathic role	(Fang *et al*., 2005; Fiorentino *et al*., 2009; Zhu *et al*., 2011; Yu *et al*., 2013; Zang *et al*., 2015)
Bro	Rutin	Flavonoid	1.16	1.91	3.36	Antioxidative, Anti-inflammatory, cancer chemopreventive activities	(Deschner *et al*., 1991; Guardia *et al*., 2001; Yang *et al*., 2008)
Bro	Caffeic acid	Hydroxycinnamate	1.39	2.52	3.23	Antimitogenic, anticarcinogenic, antiinflammatory, and immunomodulatory properties, antioxidative activities	(Huang *et al*., 1988; Natarajan *et al*., 1996; Gülçin, 2006)
Bro	Ferulic acid	Hydroxycinnamate	1.30	1.90	3.15	Cancer chemopreventive effect	(Huang *et al*., 1988)
Bro	Sinapic acid	Hydroxycinnamate	1.08	1.51	2.02	Anti-Inflammatory, Anxiolytic-like, Cerebral protective and cognition-improving effects	(Karakida *et al*., 2007; Yoon *et al*., 2007; Yun *et al*., 2008)
Bro	4-Methoxyglucobrassicin	Indolic GLS	-1.02	1.01	2.30	Antioxidative effect	(Kim & Ishii, 2006)
Bro	Glucobrassicin	Indolic GLS	1.51	3.96	5.09	Cancer chemopreventive effect	(Park *et al*., 2013)
Bro	Neoglucobrassicin	Indolic GLS	-1.15	1.15	3.51	Breakdown products induce cancer chemopreventinve activity	(Haack *et al*., 2010)
Bro	Gentiopicroside	Iridoid	1.37	2.01	3.54	Hepatoprotective effect	(Kondo *et al*., 1994)
Bro	Ascorbigen	Isosorbide	2.24	6.44	7.05	Degraded product has anticarcinogenic effect, induction of phase I and II enzyme involved in the detoxification of xenobiotics	(Wagner & Rimbach, 2009)
Bro	Chlorogenic acid	Quinic acid	1.29	2.60	3.88	Cancer chemopreventive, antioxidative activities	(Huang *et al*., 1988; Sato *et al*., 2011)
Art	Gabaculine	Benzoic acid	-1.13	-13.04	-1.48	GABA transaminase inhibitor	(Rando & Bangerter, 1977)
Art	7-Hydroxycoumarin	Coumarin	-1.06	69.18	-1.08	Anti-tumour activity	(Lopez-Gonzalez *et al*., 2004)
Art	Octanal	Fatty alcohol	-1.16	9.30	10.95	Antifungal activity	(Zhou *et al*., 2014)
Art	Luteolin 7-glucoside	Flavonoid	-1.08	2.28	-1.25	Anti-inflammatory activity	(Hu & Kitts, 2004)
Art	Puerarin xyloside	Flavonoid	1.22	13.05	2.36	Anti-osteoporotic , Antitumour activities	(Chen *et al*., 2016; Li *et al*., 2016; Zhang *et al*., 2018)
Art	Caffeic acid 3-glucoside	Hydroxycinnamate	1.18	4.73	1.26	Anti-inflammatory activity, increases osteoblastic bone formation and prevents bone loss in ovariectomized mice	(Wang *et al*., 2014; Zhang *et al*., 2016)
Art	p-Coumaric acid	Hydroxycinnamate	1.19	6.16	1.03	Protects rats hearts against doxorubicin-induced oxidative stress in the heart and H82 Antioxidative, Antibacterial activities	(Zang *et al*., 2000; Abdel-Wahab *et al*., 2003; Lou *et al*., 2012)
Art	Methyl caffeate	Hydroxycinnamate	1.03	4.67	-1.17	Antimicrobial and Antimycobacterial Activities	(Balachandran *et al*., 2012)
Art	Azelaic acid	Medium-chain fatty acid	1.08	-4.46	-1.36	Treatment on melasma	(Baliña & Graupe, 1991)
Art	Syringin	Phenolic glycoside	-1.04	2.05	1.11	Anti-inflammatory, antinociceptive and hypoglycemic effect, Antifeedant property, and anti-allergic effect	(Cho *et al*., 2001; Choi *et al*., 2004; Cis *et al*., 2006; Niu *et al*., 2008)
Art	Chlorogenic acid	Quinic acid	-1.08	2.61	-1.11	Cancer chemopreventive, antioxidative activities	(Huang *et al*., 1988; Sato *et al*., 2011)

Table S7. (Continued)

Plant	Compound	Compound classification	Fold changes			Health treat	Reference
			MB	Pbg	*Pf* SS101		
Art	Artemisinic alcohol	Sesquiterpenoid	1.09	2.48	1.03	Precousor of Artemisinin	
Art	Artemisinin	Sesquiterpenoid	-1.10	1.09	-1.14	Antimalarial and Anticancer activities, inhibitors of hepatitis B virus	(Singh & Lai, 2004; Romero *et al.*, 2005; Dondorp *et al.*, 2009)
Art	Dihydroartemisinin	Sesquiterpenoid	-1.25	2.95	-1.10	Antimalarial activity, induction of cytotoxicity on Human breast cancer cells, induction of apaotosis on ovarian cancer cells, inhibition of angiogenesis, pancreatic cancer cells	(Singh & Lai, 2001; Chen *et al.*, 2004; Chen, H *et al.*, 2009; Chen, T *et al.*, 2009)

Chapter 4

Steering the Broccoli shoot metabolome by root-colonizing *Paraburkholderia* species: impacts on growth and defense

Je-Seung Jeon, Natalia Carreno-Quintero, Ric De Vos,
Jos M. Raaijmakers and Desalegn W. Etalo

Manuscript submitted for publication

Abstract

Beneficial rhizobacteria can promote plant growth and induce resistance. Recent advances in analytical chemistry allow to study the impact of rhizobacteria on primary and secondary metabolism in plants and how these changes associate with the plant phenotypic changes. In this study, a new strategy integrating GC/LC-MS-based metabolomics was firstly employed to elucidate changes in primary and secondary metabolite networks in the shoots of two Broccoli cultivars upon root colonization by three *Paraburkholderia* species, *P. graminis* (*Pbg*), *P. hospita* (*Pbh*), and *P. terricola* (*Pbt*). Results showed that *Pbt* was a poor colonizer of the roots of Malibu cultivar and did not promote plant growth in contrast to other combinations of the two Broccoli cultivars and *Paraburkholderia* species. *Pbh* and *Pbt* induced resistance in Malibu cultivar to infections by the bacterial leaf pathogen *Xanthomonas campestris*. Subsequent metabolomics exhibited that soluble sugar levels were much higher in leaves of Malibu cultivar most likely providing resources for the biosynthesis of phenylpropanoid downstream metabolites such as hydroxycinammates, flavonoids, and stilbenoids, metabolites with antimicrobial activities. In addition to enhancement of key precursors for growth and secondary metabolite biosynthesis, treatment of *Paraburkholderia* also induced metabolite remobilization. The metabolite remobilization involved both suppression of resource competing metabolite pathways such as amino acids and rechanneling of existing primary metabolite-derivatives and other secondary metabolites to other metabolite pathways. Flavonoids, hydroxycinnamates, stilbenoids, coumarins and lignins showed substantial accumulation upon treatments with the *Paraburkholderia* species, metabolites with direct antimicrobial effects and that can act as a physical barrier against pathogenic bacteria such as *Xanthomonas campestris*. The integrated primary and secondary metabolome profiling conducted in this study further suggests that rhizobacteria could avert the negative impact of defense priming on the host fitness by generating substantial amounts of soluble sugars and by remobilizing other metabolites to compensate for the high energy and carbon skeleton demand associated with growth and defense priming.

Keywords: broccoli metabolites; *Paraburkholderia*; beneficial rhizobacteria; non-targeted metabolomics; secondary metabolites, primary metabolites.

Introduction

Plants are fine-tuned factories of more than 100,000 secondary metabolites (Wink, 2010). Many plant species exhibit pharmaceutical activities, providing valuable scaffolds for the development of new pharmaceuticals (Cragg & Newman, 2013; Bauer & Brönstrup, 2014). For the plant itself, secondary metabolites are involved in adaptation to environmental changes (Bourgaud *et al.*, 2001) including tolerance to biotic stresses such as insect herbivory and pathogen infections (Bennett & Wallsgrove, 1994; Rattan, 2010; Boulogne *et al.*, 2012). Therefore, steering plant chemistry to elevate specific metabolites has been a major direction in plant breeding. Recent studies have shown that rhizobacteria, i.e. bacteria colonizing the surface and internal plant root tissue, can enhance plant growth, induce systemic resistance and alter changes in plant chemistry, providing new avenues to enhance the levels of specific plant secondary metabolites of interest.

Plants photosynthetically fix carbon and metabolize it for growth and defense. Both processes appear incompatible due to limited resources and is referred to as the "defense-growth trade-off" (Huot *et al.*, 2014). However, several studies have shown that specific rhizobacteria can parallelly induce both growth and defense. For instance, our previous studies demonstrated that *Pseudomonas fluorescens* SS101 enhanced biomass of Arabidopsis as well as resistance against a bacterial leaf pathogen and insect herbivory (van de Mortel *et al.*, 2012; Cheng *et al.*, 2017). Similar results were observed in *Oryza sativa* (Chamam *et al.*, 2013), *Panax ginseng* (Gao *et al.*, 2015), *Piper betle* (Lavania *et al.*, 2006), *Pisum sativum* (Mabrouk *et al.*, 2007), and *Salvia officinalis* (Ghorbanpour *et al.*, 2016) upon inoculation with various rhizobacterial genera. However, how specific rhizobacteria induce defense and enhance growth simultaneously is not well understood. Here, we studied the impact of root-colonizing *Paraburkholderia* species on growth and defense of two Broccoli cultivars. Broccoli (*Brassica olearacea* var. italica) is a crop plant consumed worldwide, known to have high value natural compounds including glucosinolates and flavonoids (Naguib *et al.*, 2012). The Broccoli cultivars used in present study were Coronado and Malibu, bred to possess high and lower levels of glucosinolates (glucoiberin, glucoraphanin and glucobrassicin), respectively. *Paraburkholderia* is a diverged monophyletic clade from the genus *Burkholderia* (Sawana *et al.*, 2014). A number of rhizospheric and endophytic *Paraburkhoderia* species, in particular *Paraburkholderia phytofirmans* PsJN, *P. fungorum* and *P. graminis,* can promote growth of maize, strawberry and Arabidopsis (Ledger *et al.*, 2016; Mitter *et al.*, 2017; Rahman *et al.*, 2018) and suppress pathogen infections (Timmermann *et al.*, 2017; Carrión *et al.*, 2018). Also various *Paraburkholderia* species are typically found in the mycosphere consuming organic acids released from the fungi and using the hyphae as 'highways' for translocation (Nazir *et al.*, 2009). The *Paraburkholderia* species used in our work presented here are *Paraburkholderia graminis* (*Pbg*), *P. hospita* (*Pbh*), and *P. terricola* (*Pbt*) which exhibited plant protection against the fungal root pathogen *Rhizoctonia solani.* For *P. graminis*, we further showed that the production of sulfurous volatiles was a key mechanism in disease

suppression (Carrión *et al.*, 2018).

In the present study, we monitored the effects of different root-colonizing *Paraburkholderia* species on phenotypes of two Broccoli cultivars, in particular growth promotion and defense against the bacterial leaf pathogen *Xanthomonas campestris*. At two different time points during the *Paraburkholderia*-Broccoli interactions we conducted untargeted metabolomics to map the systemic changes in primary and secondary metabolomism in the shoots of Broccoli. Our results show that, in the partnerships of *Paraburkholderia* species with the two Broccoli cultivars, there were common and specific signatures in both primary and secondary metabolism. The results suggest that the enhanced accumulation of soluble sugars in shoots of Broccoli cultivars upon *Paraburkholderia* root colonization translate into distinct changes in secondary metabolism that in turn associate with distinctive changes in plant growth and defense. The integrated strategy adopted in this study enhanced our fundamental understanding of metabolic fluxes associated with plant growth and defense.

Materials and Methods

Bacterial strains and culture conditions

The rhizobacterial strains *Paraburkholderia graminis* (*Pbg*), *P. hospita* (*Pbh*), and *P. terricola* (*Pbt*) used in this study were originally isolated from rhizospheric soil of *Beta vulgaris* grown in *Rhizoctonia solani* suppressive soil (Carrión *et al.*, 2018). Culture of *Paraburkholderia* species were maintained in Luria Bertani (LB)-medium (Lennox, Carl Roth) at 25 °C. After incubation for 16 hours, bacteria cells were spun down to make bacteria pellets. These pellets were then washed three times with 10 mM $MgSO_4$ and resuspended in 10 mM $MgSO_4$ to a final density of OD_{600} = 1.0 (~10^9 cells per ml).

Plant Materials and growth conditions

Seeds of two Broccoli cultivars (*Brassica olearacea* var. italica), Coronado and Malibu, were kindly provided by Bejo Seeds (Warmenhuizen, The Netherlands). The seeds were surface sterilized for 30 minutes by immersing them in 1% (v/v) sodium hypochlorite amended with 0.1 % (v/v) of Tween 20, and rinsed three times with ample sterile distilled water. Thereafter, five seeds were sown on 100 X 100 mm square petri dishes containing 50 ml of half-strength Murashige and Skoog (0.5 X MS) agar media with 0.5% sucrose (w/v) and 1.2% plant agar (w/v). Five days after germination and vegetative growth in petri dishes, the root tips of the seedlings from the two Broccoli cultivars were inoculated with 2 µl cell suspension (±10^9 cells per ml) of each three *Paraburkholderia* species. Plants treated with 2 µl 10 mM $MgSO_4$ served as controls. The plates with the control and inoculated plants were then sealed and incubated in a climate chamber (21 °C / 21 °C day/night temperature; 180 µmol light $m^{-2}s^{-1}$ at plant level during 16 h/d; 70% relative humidity) until harvest (11 days post inoculation).

Temporal changes in shoot fresh biomass were measured every two days until harvest.

Rhizobacteria root colonization assay

Bacterial root colonization was determined at 6 and 11 dpi for each of the three *Paraburkholderia* species on each of the two Broccoli cultivars. Briefly, treated roots were collected at 6 and 11 dpi and placed in sterile 50 mL Falcon tube and its biomass was measured. Then the root samples were vortexed (60 s) in 10 mM $MgSO_4$, sonicated (60 s), and again vortexed (15 s) to resuspend the bacteria adhering to the root. The suspensions were serial dilution plated onto PSA plates containing 100 µg ml^{-1} delvocid (DSM) to inhibit fungal growth. Plates were incubated at 25 ℃ in the dark for 3 days, colonies were counted and the number of colony-forming units (cfu) per gram of root fresh weight was calculated.

Plant phenotyping

Fresh biomass of the Broccoli shoots was measured to determine the effect of the rhizobacteria on plant growth. For Broccoli, shoot fresh biomass from the respective treatments was weighed every two day after bacterial inoculation until the last harvest at 11 dpi. The average weight of 5 Broccoli seedlings was considered as one independent biological replicate. The roots were carefully removed from the MS-agar and washed with distilled water to eliminate adhering agar, blotted dry on filter paper and their fresh weight was recorded.

Induced resistance assays

To assess the impact of *Paraburkholderia* species on induced resistance, the two Broccoli cultivars were inoculated with the three *Paraburkholderia* species and grown for 11 days. Thereafter, leaves were inoculated with the bacterial leaf pathogens *Xanthomonas campestris* pv. Armoraciae P4216 (*Xc*a) and *Xanthomonas campestris* pv. Campestris P4014 (*Xc*c). To do that, *Xc*a and *Xc*c were cultured in LB-medium at 25 ℃. After 16 hours, bacterial cells were washed following similar procedure for *Paraburkholderia* as described above. A 2 µl suspension of *Xc*a or *Xc*c (~1 X 10^9 cell per ml) was inoculated on the first true leaf of the Broccoli seedlings after scratching the leaf surface with sterile 20 µl pipet tips. Ten days after pathogen challenge, disease severity of the shoots was assessed by determining the migration of the lesion from the inoculation spot to the other parts of the shoot following an ordinal scale from 0 - 5 as shown in supplementary **Fig S2**. Severity values were converted to 0 to 100 Disease severity index (DSI) using the equation (Kobriger & Hagedorn, 1983). DSI (%) = ∑(severity class x no. plants in class)/(total no. of plants x the highest class No.)

Plant metabolomics

Sample collection

Shoots from the control plants and plants treated with three *Paraburkholderia* species were harvested at 6 and 11 dpi. For each plant cultivar x *Paraburkholderia* combination, 4 biological replicates of 5 plants each were considered. Briefly, shoots were snap frozen in liquid nitrogen and ground to fine powder under continuous cooling and kept at -80 °C until further use.

Polar primary metabolite extraction and analysis

Polar primary metabolite sample preparation was performed as described by (Weckwerth *et al.*, 2004; Carreno-Quintero *et al.*, 2012). Briefly, a total of 1.4 mL of methanol containing ribitol (0.2mg/mL) as an internal standard was added to a 2 mL Eppendorf tube containing a total of 200 mg Broccoli leaf powder. After vortexing (10 s) and shaking in a thermomixer at 950 rpm for 10 min, the samples were centrifuged at maximum speed for 10 min. 500 uL of the supernatant was transferred to a new 2 mL Eppendorf tube and 370 µl of chloroform and 750 µl of distilled water were added. The mixture was vigorously mixed by vortexing and centrifuging for 10 min at maximum speed (14,000 rpm). 50 µl of the upper polar phase was transferred to an insert in a 2 mL vial. The solvent was then vacuum dried (speedvac) for 16 h at room temperature and sealed under an argon atmosphere. The dried samples were derivatized online as described by Lisec *et al*. (2006) using a Combi PAL autosampler (CTC Analytics). Initially, 12.5 µl methoxyamine (20 mg mL^{-1} pyridine) was added to each of the samples and incubated for 30 min at 40 °C under agitation. The samples were then derivatized for one hour by adding 17.5 µl of *N*-methyl-*N*-(trimethylsilyl) trifluoroacetamide (MSTFA). An alkane mixture (C11-C21 and C24-C33) was added to determine the retention indices of metabolites. The derivatized samples were analyzed by a GC-TOF-MS system consisting of an Optic 3 high-performance injector (ATAS) and an Agilent 6890 gas chromatograph (Agilent Technologies) coupled to a Pegasus III time-of-flight mass spectrometer (Leco Instruments).

2 uL of each sample was subjected to the injector at 70 °C using a split flow of 19 mL min^{-1}. The chromatographic separation was performed using a VF-5ms capillary column (Varian; 30 m x 0.25 mm x 0.25 mm) including a 10-m guardian column with helium as carrier gas at a flow rate of 1 mL min^{-1}. The temperature was isothermal for 2 min at 70 °C, followed by a 10 °C min^{-1} ramp to 310 °C, and was held for 5 min. The transfer line temperature was set at 270 °C. The column effluent was ionized by electron impact at 70 eV. Mass spectra were acquired at 20 scans s^{-1} within a mass-to-charge ratio range of 50 to 600 at a source temperature of 200 °C. A solvent delay of 295 s was set. The detector voltage was set to 1,400 V.

Semi-polar secondary metabolite extraction and analysis

For extraction of semi-polar secondary metabolites, 300 µL of 99.89% methanol containing 0.13% (v/v) formic acid was added to 100 mg plant material in 2 ml round bottom Eppendorf tubes, and sonicated for 15 min followed by centrifugation for 15 min at 20,000 X *g*. The supernatants containing predominantly the semi-polar metabolites were transferred to 96-well filter plate (AcroPrepTM, 350 µL, 0.45µm, PALL), vacuum filtrated to the 96-deep-well autosampler plates (Waters) using a Genesis Workstation (Tecan Systems).

An UltiMate 3000 U-HPLC system (Dionex) was used to create a 45 minutes linear gradient of 5-35% acetonitrile in 0.1% formic acid (FA) in water at a flow rate of 0.19 ml min^{-1}. 5 µl of each extract was injected and compounds were separated on a Luna C18 column (2.0 X 150 mm, 3µm; Phenomenex) maintained at 40 °C (De Vos *et al.*, 2007). The detection of compounds eluting from the column was performed with a Q-Exactive Plus Orbitrap FTMS mass spectrometer (Thermo Scientific). Full scan MS data were generated with electrospray in switching positive/negative ionization mode at a mass resolution of 35,000 (FWHM at m/z 200) in a range of *m/z* 95-1350. Subsequent MS/MS experiments for identification of selected metabolites were performed with separate positive or negative electrospray ionization at a normalized collision energy of 27 and a mass resolution of 17,500. The ionization voltage was optimized at 3.5 kV for positive mode and 2.5 kV for negative mode; capillary temperature was set at 250 °C; the auxiliary gas heater temperature was set to 220 °C; sheath gas, auxiliary gas and the sweep gas flow were optimized at 36, 10 and 1 arbitrary units, respectively. Automatic gain control was set a 3^{e6} and the injection time at 100 ms. External mass calibration with formic acid clusters was performed in both positive and negative ionization modes before each sample series.

Data processing and analysis

GC-TOF-MS

Raw data was primarily processed by Chroma TOF software 2.0 (Leco Instruments) and MassLynx software (Waters), and subjected to MetAlign software to extract and align the mass signal whose signal-to-noise ratio larger than 3 as described by Carreno-Quintero *et al*. (2012). The mass features were considered as a signal if they were detected in at least 3 biological replicates. Mass features fragments originating from the same metabolites were clustered together by MSClust software into 138 representative primary metabolites. Further, data transformation and scaling were performed in GeneMaths XT 1.6 (www.applied-maths.com). This then used for hierarchical cluster analysis using Pearson's correlation coefficient and Unweighted Pair Group Method with Arithmetic Mean (UPGMA). To identify metabolites, the reconstructed mass spectra file was introduced to NIST MS search software (v 2.2) with Wiley spectral libraries and in-house library, followed by comparison with

retention indices determined by a series of alkanes. Metabolite annotations were manually curated. The mass intensity of the representative metabolites was normalized by the internal standard, ribitol.

LC-MS

Peak picking, baseline correction, and mass signal alignment of the LC-MS data was performed using Metalign software (Lommen, 2009). The mass features were considered as a signal if they were detected in at least 3 biological replicates of a treatment with signal intensity 3 times of the noise value. Then, mass features originating from the same metabolites were clustered based on retention window and their correlation across all measured samples, using MSClust software (Tikunov *et al.*, 2012). After this, so-called centrotypes, representing reconstructed putative metabolites mass spectra were selected, of which relative abundance was represented by the Measured Ion Count (MIC) representing the sum of the ion count values (corrected by their membership) for all measured cluster ions in a given sample. The samples were batch corrected to reduce batch effect of large series of samples during the LCMS analysis according to (Wehrens *et al.*, 2016). ANOVA and fold changes > 2.0 were applied to identify mass signals that were significantly changed between the treatments. Data transformation and scaling was performed in GeneMaths XT 1.6 (www.applied-maths.com). Transformed and scaled values were used for hierarchical cluster analysis using Pearson's correlation coefficient and Unweighted Pair Group Method with Arithmetic Mean (UPGMA).

Annotation of differential metabolites was performed based on selection of pseudomolecule ions from the masses in the MSClust-reconstructed metabolites, first by matching their accurate masses plus retention times to previously reported metabolites present in Arabidopsis and Broccoli on the same LC-MS system and similar chromatographic conditions. Second, if compounds were not yet present in this experimentally obtained database, detected masses were matched with compound libraries, including Metabolomics Japan (www.metabolomics.jp), the Dictionary of Natural Products (http://dnp.chemnetbase.com), KNApSAcK (http://kanaya.naist.jp/KNApSAcK), and Metlin (http:// metlin.scripps.edu/) using a maximum deviation of observed mass from calculated of 5 ppm. The identity of potential candidate metabolites was further verified using Magma online tool (Ridder *et al.*, 2013) that compares the Insilco fragmentation patterns of a given metabolites to the experimentally obtained fragmentation patterns.

Statistical analysis

The relative changes in shoot biomass, root biomass in the combinations of two Broccoli cultivars and *Paraburkholderia* species was analyzed with R Studio software (Version 3.6.1). First, the normality and homogeneity of variance of the data was assessed and when the two assumptions were not met the data was transformed using Box-Cox or log transformation

using a package MASS. Differences were tested by two-way analysis of variance (ANOVA). A Tukey-HSD test was used to separate group mean values when the ANOVA was significant at $p < 0.05$. The ANOVA table is shown in Supplementary Material, **Table S1**. Differences in phenotypic parameters between the rhizobacterial treatments and non-treated controls were assessed by Student's *t*-Test.

Results

Paraburkholderia species promote growth of Broccoli

In general, root tip inoculation of the Broccoli cultivars with different *Paraburkholderia* species led to changes in leaf color (deep green leaves), shoot biomass, root biomass and root architecture (**Fig 1a**). Percent change in biomass was used as a standard measure to assess the growth-promoting effects of the *Paraburkholderia* species in two Broccoli cultivars. The percent change in biomass was calculated by dividing the biomass difference between rhizobacteria-treated plants and the control to the biomass of the control plants. Two-way analysis of variance was conducted to assess the influence of the two independent variables (*Paraburkholderia* species and Broccoli cultivars) on shoot and root biomass. The *Paraburkholderia* species included three levels (*Pbg*, *Pbh* and *Pbt*) and the Broccoli cultivars consisted of two levels (Coronado and Malibu). Furthermore, two-tailed student's *t*-test was used to assess the impact of the *Paraburkholderia* species inoculation on shoot and root biomass when compared to the control plants.

Results showed that all but *Pbt*-Malibu interaction resulted in significant increase in shoot biomass when compared to the control plants (**Fig1b**). All three *Paraburkholderia* species significantly increased the root biomass in both Broccoli cultivars when compared to the control (**Fig 1c**). In general, the relative impact of *Paraburkholderia* species was up to 3 times higher for root biomass than for shoot biomass (**Fig 1b** and **1c**). The two-way ANOVA showed highly significant interactions between *Paraburkholderia* species and Broccoli cultivars regarding the percent change in shoot and root biomass (Supplementary **Table S1**). Overall, for cultivar Coronado the percent change in shoot biomass was not significantly different between the three *Paraburkholderia* species. Whereas, in Malibu the percent change in shoot biomass was significantly higher for *Pbg* and *Pbh* inoculated plants as compared to *Pbt*. Furthermore, inoculation of plants with *Pbh* led to a significantly higher increase in shoot biomass in Malibu than in cultivar Coronado. When it comes to percent change in root biomass, only inoculation of *Pbt* showed significant differences between the two Broccoli cultivars. Over a period of 11 days, both *Pbg* and *Pbh* inoculated Broccoli cultivars showed significantly higher shoot and root biomass from 7 dpi onwards. Whereas, *Pbt* inoculated plants showed significantly higher shoot biomass in Coronado cultivar from 9 dpi onward. As indicated above, the shoot biomass of Malibu cultivar inoculated with *Pbt* was not significantly different from the untreated plants (**Fig 1d**).

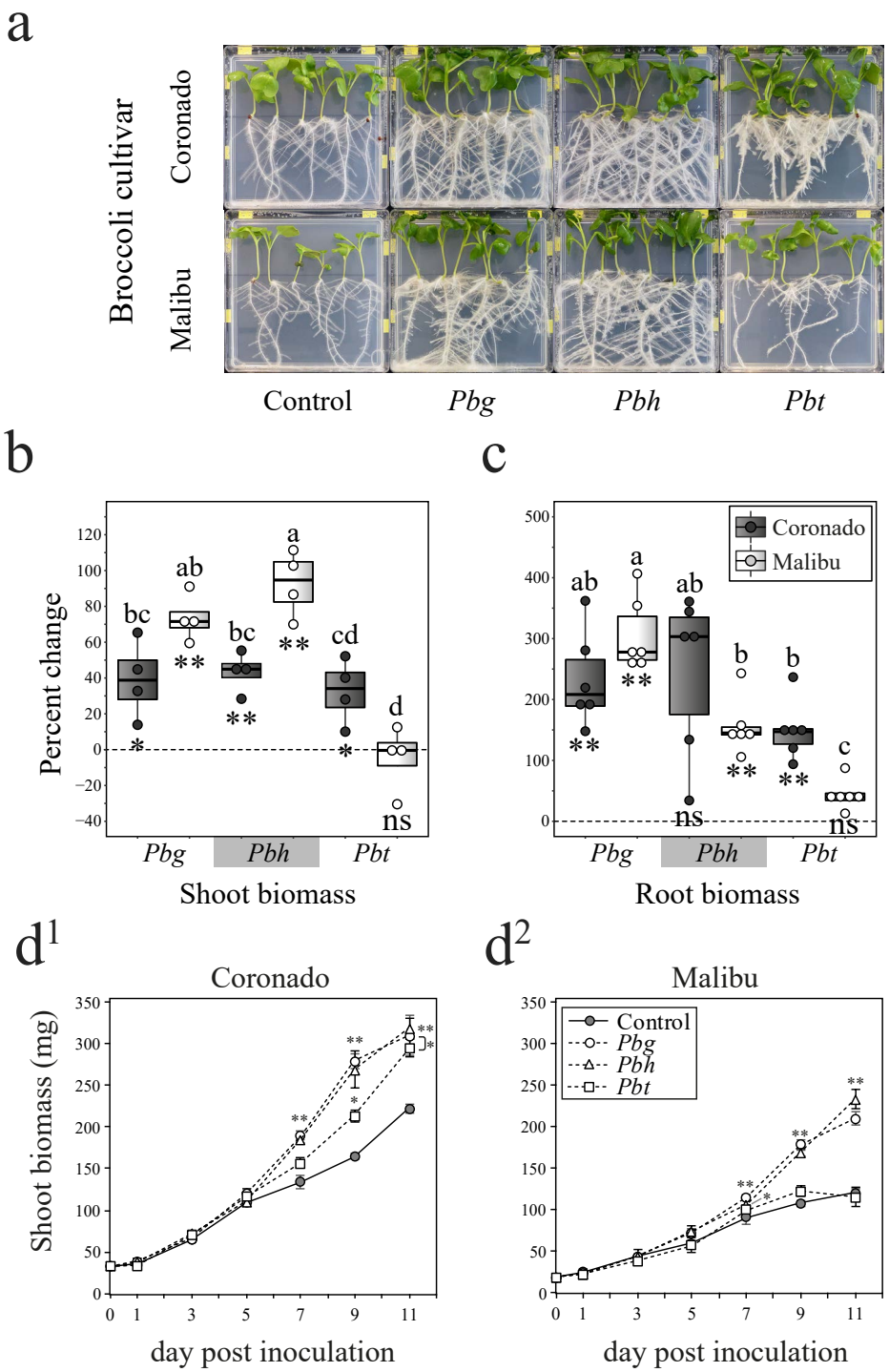
a
Broccoli cultivar
Coronado
Malibu
Control
Pbg
Pbh
Pbt
b
Percent change
Shoot biomass
c
Coronado
Malibu
Root biomass
d1
Coronado
Shoot biomass (mg)
day post inoculation
d2
Malibu
Control
Pbg
Pbh
Pbt
day post inoculation

Fig 1.

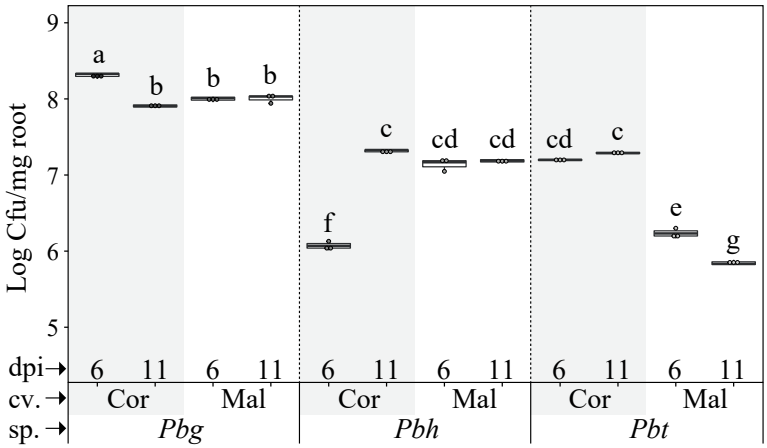

Fig 2. Root colonization ability of three *Paraburkholderia* species on two Broccoli cultivars at 6 and 11 dpi. Means of 3 replicates are shown. Different letters indicate significant differences based on three-ways ANOVA (Broccoli cultivars and Bacteria species, $P < 0.05$). Broccoli cultivars (Cor: Coronado, Mal: Malibu) and *Paraburkholderia* species, *Pbg*: *Paraburkholderia graminis*, *Pbh*: *P. hospita*, and *Pbt*: *P. terricola*.

Relation between root colonization and plant growth promotion

Root colonization of the three *Paraburkholderia* species was assessed for the two Broccoli cultivars at the early and late seedling growth stages. The data was log-transformed as the data did not meet both criteria for homogeneity of variance and normality. Three-way analysis of variance was conducted on the interaction effect of *Paraburkholderia* species, Broccoli cultivars and time after inoculation on root colonization. The *Paraburkholderia* species included three levels (*Pbg*, *Pbh* and *Pbt*), the Broccoli cultivars included two levels (Coronado and Malibu) and time after inoculation consisted of two levels (6 dpi and 11 dpi). There was highly significant three-way interaction effect on root colonization

◀◀◀ **Fig 1**. Biomass and phenotypic changes in Broccoli cultivars in response to root tip inoculation with three *Paraburkholderia* species. (a) Pictures of MS agar plate with two Broccoli cultivars (Coronado and Malibu) at 11 days post inoculation with the three *Paraburkholderia* species. (b) Percent changes in shoot biomass (mean ± standard error, n = 4) and (c) Percent changes in root biomass (mean ± standard error, n = 6) of two broccoli cultivars inoculated with the *Paraburkholderia* species. *Pbg*: *Paraburkholderia graminis*, *Pbh*: *P. hospita*, and *Pbt*: *P. terricola.* Different letters show significant difference between the treatments (Two-way ANOVA, Tukey's HSD *post hoc* test, $P < 0.05$). Asterisks denote statistical differences between non-bacteria treated control (two-tailed Student's t test): * $P< 0.05$; ** $P< 0.01$. (d) Temporal changes in shoot biomass of two Broccoli cultivars (d^1: Coronado and d^2: Malibu) inoculated with the *Paraburkholderia* species. Asterisks denote statistical differences (two-tailed Student's t test): * $P< 0.05$; ** $P< 0.01$. *Pbg*: *Paraburkholderia graminis*, *Pbh*: *P. hospita*, and *Pbt*: *P. terricola*.

(Supplementary **Table S3**). In general, compared to the other two *Paraburkhoderia* species, *Pbg* showed significantly higher root colonization in both cultivars at both time points (**Fig 2**) In addition, *Pbg* showed significantly higher root colonization in Coronado cultivar at early time point, while in Malibu the root colonization by *Pbg* was not significantly different between the two time points. In contrast, *Pbh* showed significantly lower root colonization at 6 dpi on Coronado cultivar. However, at the later time point, it showed significant increase in root colonization. Whereas, its root colonization was not significantly different between the two time points in Malibu cultivar. On the other hand, *Pbt* showed significantly lower root colonization in Malibu cultivar at both time points. Furthermore, *Pbt* on Malibu showed significant decline in root colonization at the later time point. Hence, ineffective growth promotion in combination of Malibu-*Pbt* seemed to have a strong correlation with cultivar specific lower root colonization capacity of *Pbt*.

Paraburkholderia **species altered primary and secondary metabolism of Broccoli shoot**

Considering the extent of species and cultivar-dependent variations in root colonization and plant growth promotion, we investigated the systemic effect of the different *Paraburkholderia* species on the shoot metabolome of the two Broccoli cultivars at 6 and 11 dpi. We specifically looked into the association between primary and secondary metabolism affected by the *Paraburkholderia* species. GC-MS- and LC-MS-based non-targeted metabolomics were used to profile polar primary metabolites and semi-polar secondary metabolites in shoot extracts, respectively. The data was subjected to ANOVA with correction for multiple testing (Benjamini-Hochberg) and metabolites that were significantly different ($P < 0.05$ and fold change >2) between at least two treatments were used for multivariate analysis. Principal Component Analysis (PCA) and Hierarchical Cluster Analysis (HCA) were used to reduce the dimensionality of the data and explore specific patterns between the different plant–rhizobacterial interactions.

Effect of Paraburkholderia on shoot primary metabolism

GC-MS-based non-targeted metabolomics demonstrated that out of 138 polar metabolites, 68 metabolites were significantly different at least between two treatments in shoots of the two Broccoli cultivars upon inoculation with three rhizobacterial species at 6 and 11 dpi. At 6 dpi, PCA indicated that the first three principal components (PC) explained 67.7% of the total variance (**Fig 3a1**). The first PC (PC1), explained 34.8% of the total variance and corresponded to either enhanced or reduced metabolites in the Broccoli cultivars by the *Paraburkholderia* treatment when compared to the controls (**Fig 3b1,** Clusters **1**, **5, 8** and **9**). Out of the three *Paraburkhoderia* species, root tip inoculation by *Pbg* had the greatest impact on shoot primary metabolism of both Broccoli cultivars. Inoculation with *Pbh* and *Pbt* resulted in changes in the shoot primary metabolome in a cultivar-dependent manner. For *Pbh*, the impact on shoot primary metabolome was more extensive for Malibu than for

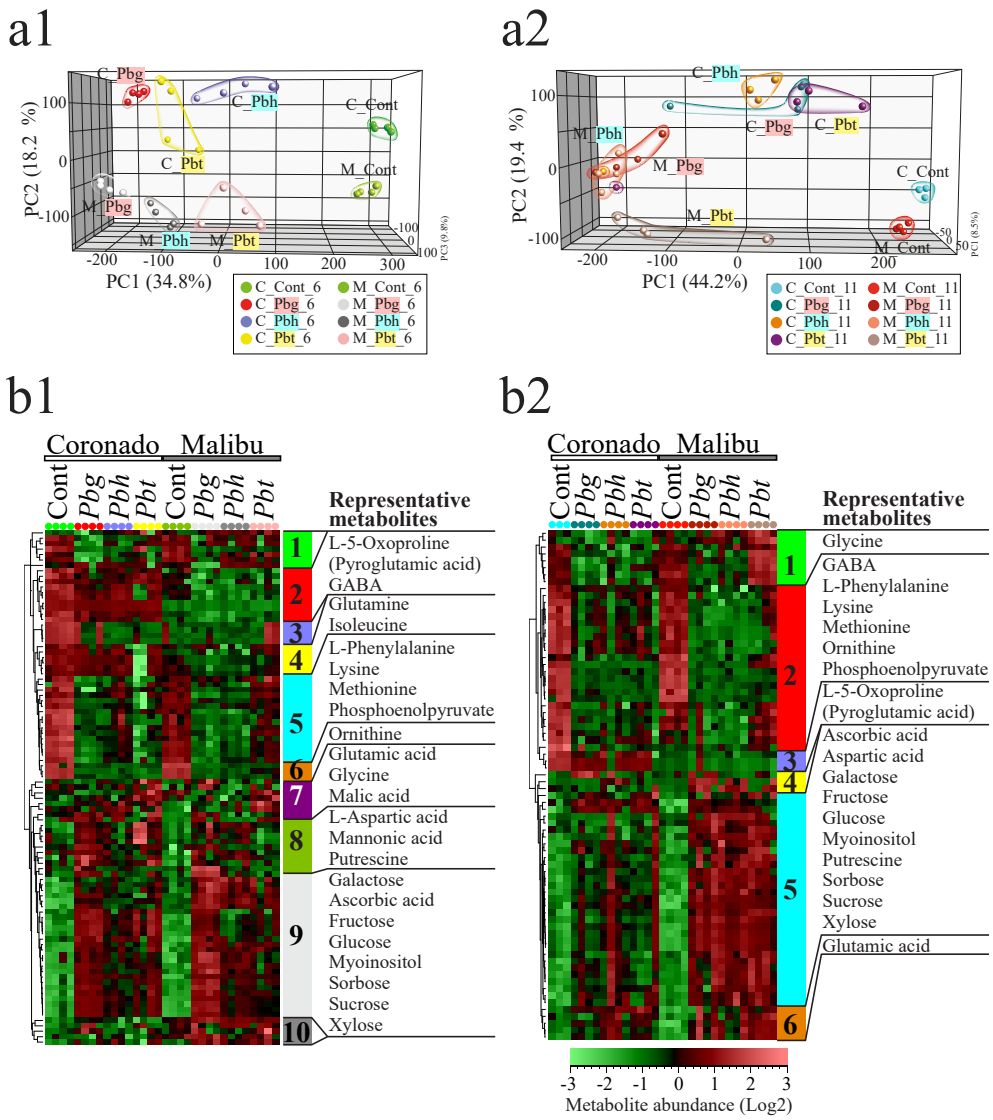

Fig 3. Rhizobacteria-mediated changes in shoot primary metabolites in two Broccoli cultivars. (**a**) Principal Component Analysis (PCA) and (**b**) Hierarchical Cluster Analysis (HCA) based on differentially regulated metabolites of the samples at 6 dpi (**1**) and 11 dpi (**2**). In the HCA, metabolite clusters are indicated by different colors. Information on the representative metabolites of each clusters is given on the right side, if the metabolites are annotated. (**c**) Impact of *Paraburkholderia* species on sugar generation and utilization of two Broccoli cultivars. Broccoli cultivars (Cor: Coronado, Mal: Malibu), Cont.: non-rhizobacteria treated control, *Pbg*: *Paraburkholderia graminis*, *Pbh*: *P. hospita*, and *Pbt*: *P. terricola*.

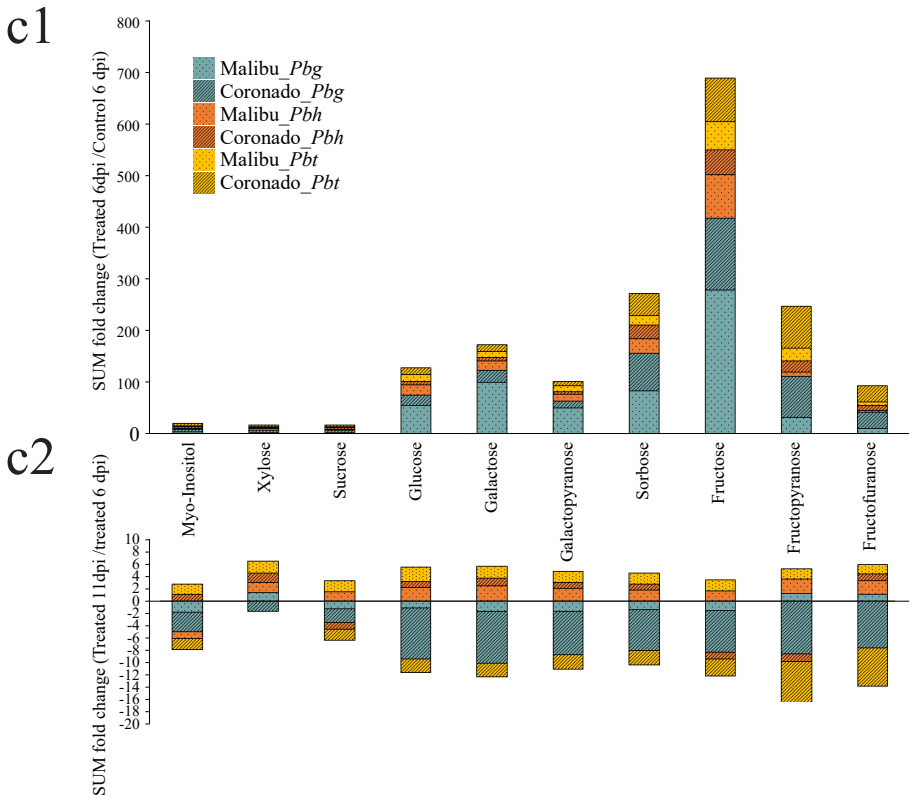

Fig 3. (continued)

Coronado, while for *Pbt* more extensive changes in the shoot primary metabolome were observed for Coronado (**Fig 3a1**). The major changes in primary metabolism induced by *Paraburkholderia* included accumulation of sugars (Cluster **9**) and depletion of amino acids (Cluster **5**, phenylalanine, lysine, methionine) and of the phosphate ester, phosphoenolpyruvate (PEP), a key intermediate in glycolysis and gluconeogenesis.

Some of the representative metabolites in cluster **8** that showed accumulation in all interactions, except in the ineffective *Pbt*-Malibu interaction, include aspartic acid, mannonic acid and putrescine. The second principal component (PC2) explained 18.2% of the total variance and associated with metabolites that showed variation between the two cultivars. Furthermore, treatment of the two cultivars with *Pbg* and *Pbh* widened the inherent variation in the level of some of the metabolites between the two Broccoli cultivars. (**Fig 3b1** Clusters **2** and **3**). Amino acids such as glutamine, oxoproline (pyroglutamic acid), GABA (γ-aminobutyric acid) and isoleucine were intrinsically higher in Coronado when compared to Malibu.

At the later seedling growth stage (11 dpi), inoculation of the Broccoli cultivars with the three *Paraburkholderia* species continued to have substantial impact on shoot primary metabolism.

PCA showed that the first three principal component explained 72.0% of the total variance (**Fig 3a2**). Here, the impact of all three *Paraburkholderia* species on the shoot metabolome was Broccoli cultivar dependent and was greater in Malibu (**Fig 3a2**). The first principal component (PC1) explained 44.2% of the total variance and corresponded to metabolites that were enhanced (**Fig 3b2** Cluster **5**) or reduced (Cluster **2**) in the *Paraburkholderia* treatments. The depleted Broccoli shoot metabolites upon inoculation with the three rhizobacterial species encompassed amino acids such as lysine, phenylalanine, methionine, the non-proteinogenic amino acids ornithine and GABA, as well as the important metabolic intermediate phosphoenolpyruvate (PEP). In all but the ineffective partnership between *Pbt*-Malibu, the important intermediate phosphoenolpyruvate, showed 11-14 fold decreases (Supplementary excel, **Table S6**). On the other hand, sugars and other metabolites, including ascorbic acid and aspartic acid, represent the induced metabolites by the *Paraburkholderia* treatments when compared to the control plants (Cluster **5**). Sugars showed greater abundance in Malibu cultivar treated with *Paraburkholderia* than in Coronado. However, at 11 dpi, sugars in *Paraburkholderia*-treated plants showed dramatic depletion in Coronado cultivar as compared to 6 dpi. Whereas in Malibu cultivar the temporal variation in the level of the sugars was less pronounced (**Fig 3b2** Cluster **5,** Supplementary **Fig S3** and **S4**). The PC2, representing 19.4% of the total variance, was associated with metabolites in cluster **1** including glycine that were depleted in all treatment combinations except in the controls and in the ineffective partnership between *Pbt* and Malibu (**Fig 3b2** Cluster **1**). Oxoproline and some other metabolites shown in cluster **3** were intrinsically abundant in the shoots of Coronado.

Paraburkholderia's impact on Broccoli primary metabolism is associated with soluble sugars

As sugars are the primary drivers of plant growth, we looked into their temporal dynamics, particularly related to sugar generation and utilization in the shoots of the two Broccoli cultivars with or without the influence of the *Paraburkholderia* species. The fold change in sugar level between *Paraburkholderia* treated and control plants at 6dpi was used as a measure of sugar generation. While the temporal fold change in sugar level of treated plants from 6 to 11 dpi was used as a measure of sugar utilization. In control plants, sugars showed no significant change between the two Broccoli cultivars at 6 dpi (supplementary **Fig S3**). In contrast, treatment with the *Paraburkholderia* species showed unprecedented impact on the sugar generation in shoots of both Broccoli cultivars resulting in significant increases in the level of fructose and its derivatives, glucose, sorbose, galactose and galactopyranose at 6 dpi. Moreover, the magnitude of sugar generation showed remarkable difference between the *Paraburkholderia* species-Broccoli cultivar combinations (**Fig 3c1**). *Pbg* showed the highest sugar generation when compared to *Pbh* and *Pbt* and its sugar generation ability was significantly higher in Malibu cultivar. The ineffective partnership between *Pbt* and Malibu had the least significant impact on sugar generation. Similarly, the sugar utilization also showed noticeable differences among the *Paraburkholderia* species-Broccoli cultivar

combinations. In Coronado, *Pbg* inoculation led to greater sugar utilization when compared to cultivar Malibu. The ineffective partnership between *Pbt* and Malibu showed reduced sugar utilization when compared to the effective partnership of *Pbt* with Coronado (**Fig 3c2**).

Effects of Paraburkholderia on shoot secondary metabolism

From the total of 1868 metabolites detected in positive or negative ionization mode, 1386 metabolites were significantly different between at least two treatments. PCA of the metabolites at 6 dpi demonstrated distinct clustering of the samples based on the *Paraburkholderia* species-Broccoli cultivar combination (**Fig 4a1**). The first PC explained 33.2% of the total variation and was associated with metabolites that were intrinsically abundant in one of the two Broccoli cultivars (Clusters **3**, **5** and **12**). Treatment of the two Broccoli cultivars with the *Paraburkhoderia* species also widened the variation in the level of the metabolites that were intrinsically different between the two Broccoli cultivars. Metabolites that were intrinsically abundant in Coronado included aliphatic glucosinolates such as 2-methylbutyl glucosinolate and glucoiberverin as well as the aromatic glucosinolates glucotropaeolin and gluconasturtiin. The levels of aliphatic glucosinolates 2-methylbutyl glucosinolate and glucoiberverin were 147 and 209 times higher in Coronado when compared to Malibu, respectively (Cluster **3**). In Malibu, on the other hand, a number of metabolites from the phenylpropanoid pathway were intrinsically abundant (Clusters **5** and **12**). The second principal component (PC2) explained 20.9% of the total variance and was associated with metabolites that were reduced (**Fig 4b1** Clusters **2** and **4**) or induced (Clusters **7** and **11**) by the *Paraburkholderia* treatments. Inoculation of *Pbg* had the greatest impact on the shoot secondary metabolome profile of both Broccoli cultivars, whereas the ineffective partnership between *Pbt* and Malibu had less pronounced impact on the shoot metabolome. Metabolites in cluster **2,** comprising amino acids such as arginine, asparagine, tryptophan and N-acetylated glutamic acid/fucosamine, showed greater reduction in their abundance upon treatment with *Paraburkholderia* species. Cluster **4** encompassed metabolites that were more abundant in Malibu than Coronado and included ascorbic acid ethyl ester, N-acetyl-tryptophan, and terpenoids such as S-furanopetasitin and sonchuionoside C. The metabolites in clusters **7** and **11** were induced by all the *Paraburkholderia* species and were dominated by phenylpropanoids. In Malibu, inoculation of *Pbg* led to greater accumulation of phenylpropanoids such as flavonoids glycosides (kaempferol-di/tri-(feruloyl/coumaroyl) glycosides and robinin), hydroxycinnamates (ferulic acid and its derivatives, caffeic acid derivatives such as chlorogenic acid) and an indole acetic acid derivative such as indole-3-acetic-acid-O-glucuronide when compared to the other two *Paraburkholderia* species. PC3 explained 4.9% of the total variance and was represented by *Pbg*-triggered (Clusters **8** and **10**) or *Pbt*-induced (Cluster **13**) metabolites in both Broccoli cultivars. *Pbg*-induced metabolites in cluster **8** consisted of the flavonoid kaempferol 3-sophorotrioside. Whereas *Pbt*-triggered metabolites in cluster **13** included the hydroxycinnamate 1,2-bis-O-sinapoyl-beta-D-glucoside and resveratrol-sulfoglucoside, a stilbenoid.

Similarly, at 11dpi, inoculation with *Paraburkholderia* species led to substantial changes in the shoot metabolite profiles of the two Broccoli cultivars (**Fig 4a2** and **4b2**). In the PCA, the first three PCs explained 51.1% of the total variance. The first PC, explaining 29.1% of the total variance is associated with metabolites that accumulated or were reduced in response to *Paraburkholderia* and the change in these group of metabolites was more pronounced in Malibu cultivar (**Fig 4b2** Clusters **1**, **2**, **3**, **4** and **5**: up, **10** and **11**: down). The induced metabolites in the above-mentioned clusters included flavonoids i.e. flavonol-di/tri-glycosides, kaempferol-di/tri-glycosides (feruloyl/caffeoyl/coumaroyl), robinin, medicarpin-O-glucoside-malonate, as well as hydroxycinnamates i.e. ferulic acid, caffeic acid and various derivatives of these metabolites. Furthermore, coumarins such as eupatoriochromene and mahaleboside and mevalonate, a precursor of mevalonate pathways that goes to terpenoid biosynthesis was also induced by the *Paraburkholderia* treatment. The reduced metabolites in both Broccoli cultivars included amino acids such as arginine, asparagine and acetyl/valyl conjugated amino acids i.e. valyl-methionine, and N-acetylglutamic acid (Cluster **10**). Meanwhile, metabolites in cluster **11** were also reduced by the *Paraburkhoderia* treatment and these metabolites were intrinsically abundant in Coronado cultivar. Some of the metabolites in cluster **11** included sulfur-containing metabolites such as the aliphatic glucosinolates 2-methylbutyl glucosinolate and glucoiberverin, derivatives of sulfurous amino acids including leucyl-cysteine and methionyl-isoleucine, as well as precursor or breakdown products of glucosinolates, for instance, 6-methylthiohexanaldoxime and 3-methylsulfinylpropyl isothiocyanate. The second PC (PC2) explained 23.8% of the total variance and was associated with metabolites that were intrinsically more abundant in cultivar Malibu (**Fig 4b2** Clusters **6**, **7**, **8** and **9**). Metabolites in clusters **6**, **7**, **8** and **9** showed significant depletion in all effective partnerships between the *Paraburkholderia* species and Broccoli cultivars. Tryptophan, a building block for indolic glucosinolate and the growth hormone indole-3-acetic acid, N-acetylated amino acid including N-acetyl phenylalanine/tryptophan, terpenoids i.e. S-furanopetasitin and sonchuionoside C, and sulforaphane an isothiocyanate are some of the metabolites in these cluster worth mentioning. PC3 explained 6.2% of the total variance and was associated with yet unknown metabolites that showed *Pbg* specific alteration in both Broccoli cultivars (Clusters **13**).

Paraburkholderia induces systemic resistance against the bacterial leaf pathogen *Xanthomonas campestris* in a cultivar-dependent manner

As shown above, the two Broccoli cultivars exhibited inherent differences in their shoot chemistry (**Fig 4**). Furthermore, treatment of the plant roots with different *Paraburkholderia* species led to substantial alteration of the shoot metabolome including metabolome signatures specific to the individual combination of *Paraburkholderia* species and Broccoli cultivar (**Fig 4**). Based on this, we hypothesized that the inherent and induced differences in shoot chemistry between the two cultivars could contribute to a differential defense response against leaf pathogens. To address this hypothesis, treated and control plants of the two

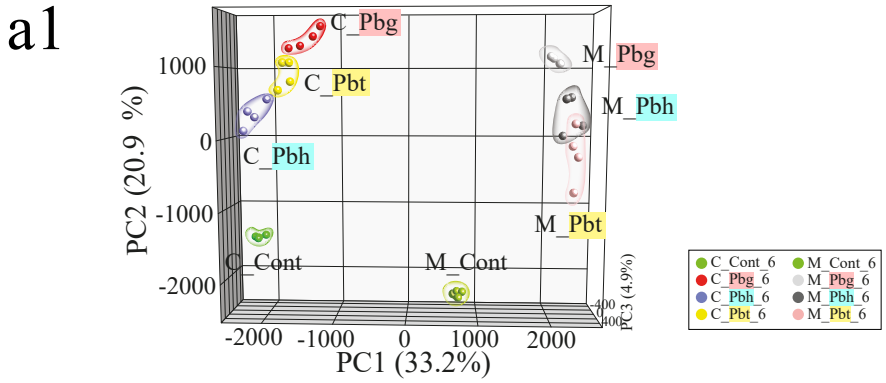

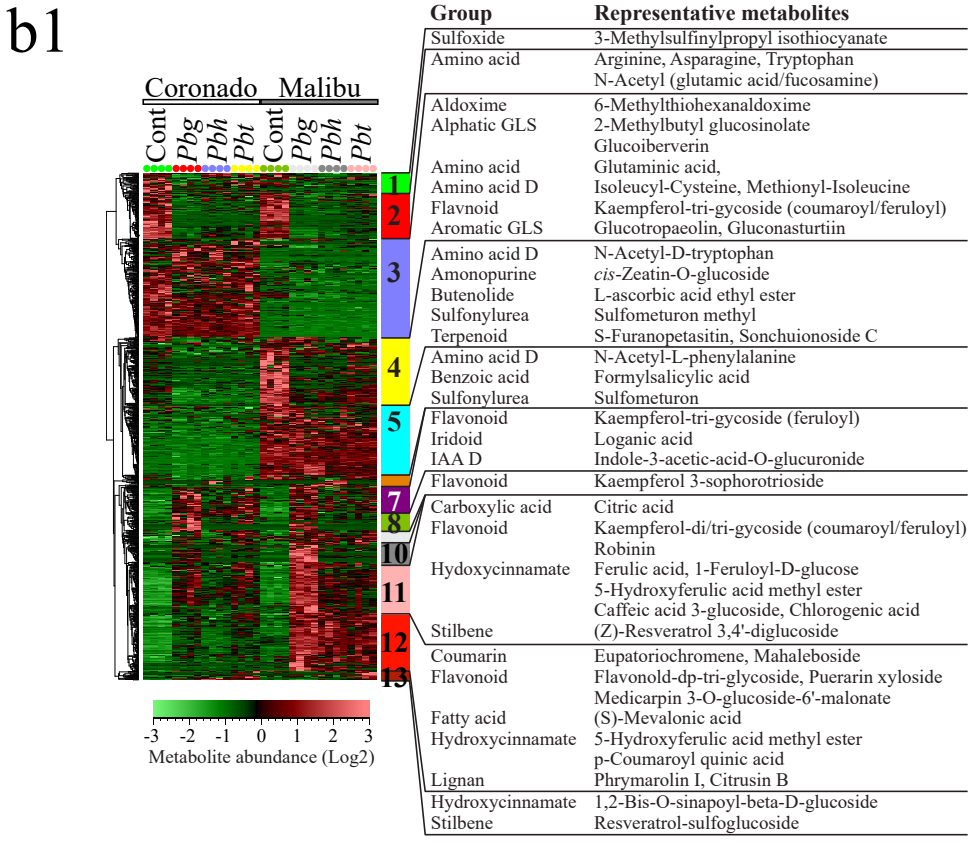

Fig 4. Rhizobacteria-mediated changes in the shoot secondary metabolites in Broccoli cultivars. (**a**) Principal component analysis (PCA) and (**b**) Hierarchical cluster analysis (HCA) based on differentially regulated metabolites of the samples at 6 dpi (**1**) and 11 dpi (**2**). In the HCA, metabolite clusters are indicated by different colors. Information on the representative metabolites of each clusters is given on the right side, if the metabolites are annotated. Broccoli cultivars (Cor: Coronado, Mal: Malibu), Cont.: non-rhizobacteria treated control, *Pbg*: *Paraburkholderia graminis*, *Pbh*: *P. hospita*, and *Pbt*: *P. terricola*. * GLS=glucosinolate, ** D=derivative.

a2

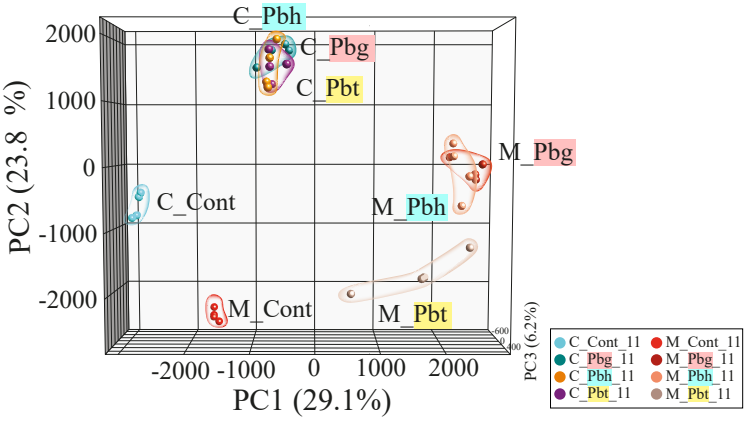

b2

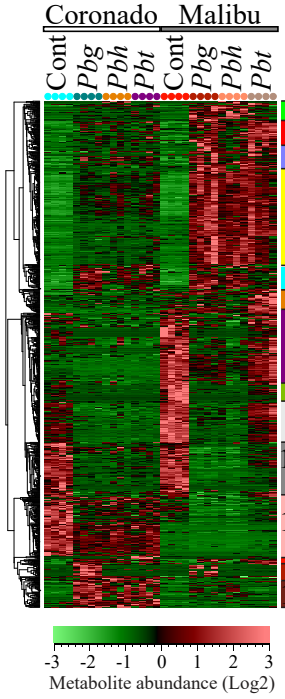

Group	Representative metabolites
Flavonoid	Kaempferol 3-sophorotrioside
Sulfonylurea	Sulfometuron methyl
Carboxylic acid	Citric acid
Hydroxycinnamate	5-O-Caffeoylshikimic acid
	Trimethoxycinnamic acid
Stilbene	(Z)-Resveratrol 3,4'-diglucoside
	Resveratrol-sulfoglucoside
Hydroxycinnamate	5-Hydroxyferulic acid methyl ester
IAA D*	Indole-3-acetic-acid-O-glucuronide
Coumarin	Eupatoriochromene, Mahaleboside
Flavonoid	Flavonol-di/tri-glycosides
	Kaempferol-di/tri-glycosides
	Kaempferol-tri-glycosides (feruloyl/caffeoyl/coumaroyl)
	Kaempferol 3-sophorotrioside
	Puerarin xyloside, Robinin
	Medicarpin 3-O-glucoside-6'-malonate
Fatty acid	(S)-Mevalonic acid
Hydroxycinnamate	Ferulic acid, 1-Feruloyl-D-glucose
	2-Feruloyl-1,2'-disinapoylgentiobiose
	5-Hydroxyferulic acid methyl ester
	Caffeic acid 3-glucoside
	Chlorogenic acid
	p-Coumaroyl quinic acid
Lignan	Citrusin B
Aromatic GLS**	Gluconasturtiin
Iridoid	Loganic acid
Amino acid D	N-Acetyl-L-phenylalanine
Sulfoxide	Sulforaphane
Amino acid	Tryptophan
Amino acid D	N-Acetyl-D-tryptophan
Amonopurine	*cis*-Zeatin-O-glucoside
Sulfonylurea	Sulfometuron
Terpenoid	S-Furanopetasitin, Sonchuionoside C
Amino acid	Arginine, Asparagine
Amino acid D	Valyl-Methionine
	N-Acetylglutamic acid
Aldoxime	6-Methylthiohexanaldoxime
Aliphatic GLS	2-Methylbutyl glucosinolate
	Glucoiberverin
Amino acid D	Leucyl-Cysteine, Methionyl-Isoleucine
Sulfoxide	3-Methylsulfinylpropyl isothiocyanate
Benzoic acid	Formylsalicylic acid

Fig 4. (Continued)

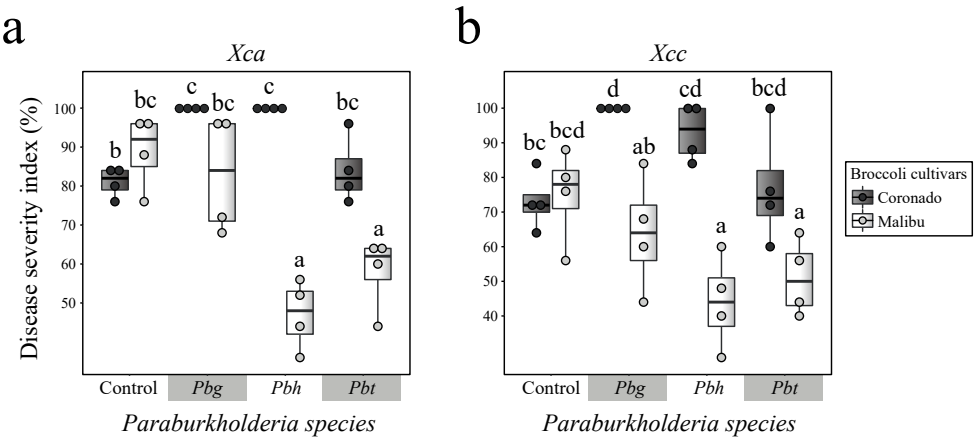

Fig 5. Impact of root-colonizing *Paraburkholderia* species on defense of Broccoli cultivars against two bacterial leaf pathogens. Disease severity index of two broccoli cultivars treated with either one of the three *Paraburkholderia* species and challenged with two bacterial leaf pathogens (a) *Xanthomonas campestris* pv. armoraciae P4216 (*Xc*a) and (b) *Xanthomonas campestris* pv. campestris P4014 (*Xcc*). Broccoli cultivars (Cor: Coronado, Mal: Malibu), Control: non-treated control, *Pbg*: *Paraburkholderia graminis*, *Pbh*: *P. hospita*, and *Pbt*: *P. terricola*. Different letters show statistically significant differences between the treatments (Two-way ANOVA, Tukey's HSD *post hoc* test, $P < 0.05$).

cultivars were challenged with two bacterial leaf pathogens, i.e. *Xanthomonas campestris* pv. armoraciae P4216 (*Xca*) and *Xanthomonas campestris* pv. campestris P4014 (*Xcc*).

Regression analysis was employed to examine the interaction effect of two independent variables (*Paraburkholderia* species and Broccoli cultivars) on disease severity of the two bacterial pathogens using the "betareg" package in R. The *Paraburkholderia* species included three levels (*Pbg*, *Pbh* and *Pbt*) and the Broccoli cultivars consisted of two levels (Coronado and Malibu). There was a highly significant interaction effect of the *Paraburkholderia* species and Broccoli cultivars on disease severity for both *Xanthomonas* pathovars (Supplementary **Table S4**). No significant inherent variation in disease severity was observed between the two Broccoli cultivars when they were challenged with the two bacterial pathogens (**Fig 5**). However, treatment of the roots of the two Broccoli cultivars with the *Paraburkholderia* species led to a reduction or an enhancement of disease severity. For example, treatment with *Pbg* and *Pbh* enhanced disease severity in Coronado cultivar challenged by both bacterial pathogens, whereas *Pbh* and *Pbt* significantly reduced disease severity in cultivar Malibu challenged by each of the two bacterial pathogens (**Fig 5**).

Discussion

Our results showed that root-colonizing *Paraburkholderia* species altered shoot primary and secondary metabolism of Broccoli seedlings, promoted growth and induced systemic defense

against bacterial leaf pathogens. The magnitude of the alteration of these traits is dependent on the *Paraburkholderia* species and Broccoli cultivar combinations. The widely accepted "defense-growth tradeoff" concept asserts that activation of plant defense comes at the expense of plant growth due to resource limitations (Huot *et al.*, 2014). Here we showed that rhizobacteria treatment of plant roots promotes growth and at the same time primes the plant defense against biotic stress factors. Rhizobacteria defense priming is considered to have lower cost when compared to activation of direct defense (Martinez-Medina *et al.*, 2016). However, judging the cost of defense priming by only assessing some key physiological process such as seed production, number of flowers, pollen quality and number, and plant growth does not necessarily explain the energy and carbon costs associated with defense priming. Hence, to understand the underlying mechanisms by which rhizobacteria promote growth and prime the plant's defense without compromising plant fitness, it requires a comprehensive investigation of the host metabolome network.

Root colonization by rhizobacteria is an important trait required for establishing beneficial effect on plant growth and health (Lugtenberg *et al.*, 2001; Compant *et al.*, 2010). In line with this, our study showed an association between root colonization ability of the *Paraburkholderia* species, their impact on the host metabolome and their ability to promote plant growth. For example, *Pbh* showed significantly reduced root colonization for cultivar Coronado at 6 dpi and its impact on both primary and secondary metabolism was the lowest when compared to *Pbg* and *Pbt* treated plants. Interestingly, at 11dpi, *Pbh* exhibited enhanced root colonization which coincided with an elevated impact on the shoot metabolome, comparable to that of plants treated with *Pbg* and *Pbt* (**Fig 3** and **4** PCA). Similarly, *Pbt* showed significantly reduced root colonization for cultivar Malibu at both 6 and 11dpi with no significant growth promotion effect and the least impact on the shoot primary and secondary metabolism as compared to plants inoculated with *Pbg* and *Pbh*. The two Broccoli cultivars used in this study showed inherent differences in their shoot metabolome profile. Phenylpropanoids were more abundant in Malibu and glucosinolate and other sulfur-containing compounds showed higher abundance in Coronado. Assuming this variation in shoot chemistry may be reflected in differences in root chemistry, these intrinsic differences between the two cultivars might have influenced the root colonization ability of *Paraburkholderia* species and the effectiveness of the partnerships. Although the root exudate profile of the two Broccoli cultivars was not assessed in our study, exudate composition of plant species has a major impact on microbiome assembly and functions in the rhizosphere (Philippot *et al.*, 2013; Pérez-Jaramillo *et al.*, 2016; Hu *et al.*, 2018; Lundberg & Teixeira, 2018; Pérez-Jaramillo *et al.*, 2018; Stringlis, Ioannis A *et al.*, 2018; Huang *et al.*, 2019). Assessing the root exudate profile of the two broccoli cultivars in combination with bioassay-guided fractionation of the exudates will be instrumental to identify metabolite signatures that govern the differences in root colonization by the *Paraburkholderia* species and the effectiveness of their partnership with different Broccoli cultivars.

The *Paraburkholderia* species exerted a substantial impact on the host primary and secondary metabolism at both early and late stages of seedling growth. Their biggest impact on primary metabolism was reflected in soluble sugar generation and utilization and both parameters showed significant variation across the *Paraburkholderia* species - Broccoli cultivar combinations (**Fig 3c**). All combinations, except *Pbt*-Malibu, resulted in effective partnership, i.e. plant growth promotion. Effective partnerships showed higher soluble sugar generation at the early stage of seedling growth and high sugar utilization at the later stage of seedling growth, whereas the ineffective partnership between Malibu and *Pbt* showed reduced sugar generation and utilization. Soluble sugars are fuel for growth and for the biosynthesis of secondary metabolites involved in defense (Herrmann & Weaver, 1999; Hartmann & Trumbore, 2016). Moreover, soluble sugars such as galactose, glucose, sorbose, fructose, sucrose and xylose have been reported to be effective chemotaxis agents for bacteria (Adler *et al.*, 1973; Ordal *et al.*, 1979). Their increased production under effective partnership between plants and rhizobacteria could provide both the plants and rhizobacteria with fuel for energy production to sustain growth and secondary metabolite production. In general, low sugar concentration promotes 'source' activities such as photosynthesis, nutrient mobilization and export, while high sugar level enhances 'sink' activities such as growth and sugar storage (Rolland *et al.*, 2006). Hence, we postulate that the enhancement of the sugar levels is a key mechanism that determines the effectiveness of the partnership between rhizobacteria and plants. Furthermore, under effective partnership, there was significantly higher depletion (>11-fold) of PEP, a key substrate for the TCA cycle and the shikimate pathway (**Fig 6**), whereas PEP depletion was only about 2-fold under ineffective partnership. Furthermore, greater depletion of GABA under the effective partnership suggests catabolism of GABA to succinyl semialdehyde followed by its conversion to succinate to feed the greater demand of pyruvate in the TCA cycle. Key intermediates in the TCA cycle such as citric acid and malic acid showed increased abundance under effective partnership. In the TCA cycle, citrate is converted to malate and used in the mitochondria for energy production (Fernie *et al.*, 2004). Hence, these observations most likely meet the greater demand for carbon and energy occurring during enhanced growth and defense priming in the effective *Paraburkholderia*-Broccoli interactions.

For the soluble sugars, *Paraburkholderia* species showed their biggest impact on fructose abundance. *Pbg*-Malibu interaction showed the highest root colonization and had the highest impact on shoot fructose level (~>280 folds). In contrast, *Pbt*-Malibu and *Pbh*-Coronado interactions showed the lowest root colonization levels and had the lowest impact on shoot fructose generation at the early stages of seedling growth. Interestingly, the biggest impact on shoot fructose abundance by *Pbg* also showed the biggest impact on secondary metabolism in general and phenolic compounds accumulation in particular when compared to *Pbh* and *Pbt* at 6 dpi (**Fig 6**). This suggests that the effects of elevated levels of soluble sugars are not only limited to plant growth but also extend to secondary metabolites biosynthesis. For example, fructose is the primary substrates for fructose-6-phospate, a key substrate for the

biosynthesis of both PEP and erythros-4-phosphate (**Fig 6**). These two intermediates are channeled to the shikimate pathway that bridges carbohydrate metabolism to biosynthesis of aromatic primary and secondary metabolites (Herrmann & Weaver, 1999). The shikimate pathway provides all the important precursors for the biosynthesis of phenylpropanoids including hydroxycinnamates, flavonoids, stilbenoids, coumarins and lignins that showed significant accumulation in plants treated with *Paraburkholderia* species (**Fig 4b** and **6**). A study on the *pho3* mutant of Arabidopsis that accumulates soluble sugars to high levels, showed large increases in the expression of transcriptional factors and enzymes involved in anthocyanin biosynthesis (Lloyd & Zakhleniuk, 2004). Another study also showed greater accumulation of fructose (~10 fold) and flavonoids in quinoa cotyledons in response to UV-B radiation (Hilal *et al.*, 2004). Considering our results and the aforementioned findings by other studies, we postulate that one of the key mechanisms by which rhizobacteria modulate host secondary metabolism is by soluble sugar generation.

In addition to enhancement of key precursors for growth and secondary metabolite biosynthesis, treatment of *Paraburkholderia* also induced metabolite remobilization. The metabolite remobilization involved both suppression of resource competing metabolite pathways such as amino acids and rechanneling of existing primary metabolite-derivatives and other secondary metabolites to other metabolite pathways. For example, aromatic glucosinolate, amino acids and their derivatives, some terpenoids showed more depletion in effective partnerships (**Fig 6** and **Fig 4b2**). Hence, remobilization of the existing metabolites towards targeted metabolite pathways could be an additional strategy used by rhizobacteria to reduce the cost of *de novo* biosynthesis of metabolites.

Our results also showed that rhizobacteria-mediated reorganization of the host metabolome landscape not only affects plant growth but also the defense response of Broccoli cultivars to bacterial leaf pathogens. In general, inoculation of the *Paraburkholderia* species showed greater suppression of pathogen proliferation in cultivar Malibu that intrinsically has more phenolic compounds (**Fig 5**). The phenylpropanoid pathway appears to be the central target by the *Paraburkholderia* species and was altered to a greater extent in Malibu than in Coronado (**Fig 6**). All metabolite classes belonging to this pathway including flavonoids, hydroxycinnamates, stilbenoids, coumarins and lignins showed substantial accumulation upon treatments with the *Paraburkholderia* species (**Fig 6**). These metabolites were reported to have direct antimicrobial effects and/or act as a physical barrier against pathogenic microorganisms (Dixon *et al.*, 2002; Cvikrova *et al.*, 2006). Hydroxycinnamic acids and flavonoid were shown to negatively affect the disease symptom development in Chinese cabbage challenged by *Xanthomonas campestris* pv. campestris (*Xcc*) (Islam *et al.*, 2018). Of all the *Paraburkholderia* species-Broccoli cultivars combinations, treatment of roots of cultivar Coronado with *Pbg* resulted in higher disease severity (**Fig 5**). However, we could not find a specific metabolic signature that corresponds to the increased pathogen susceptibility of Coronado treated with *Pbg*.

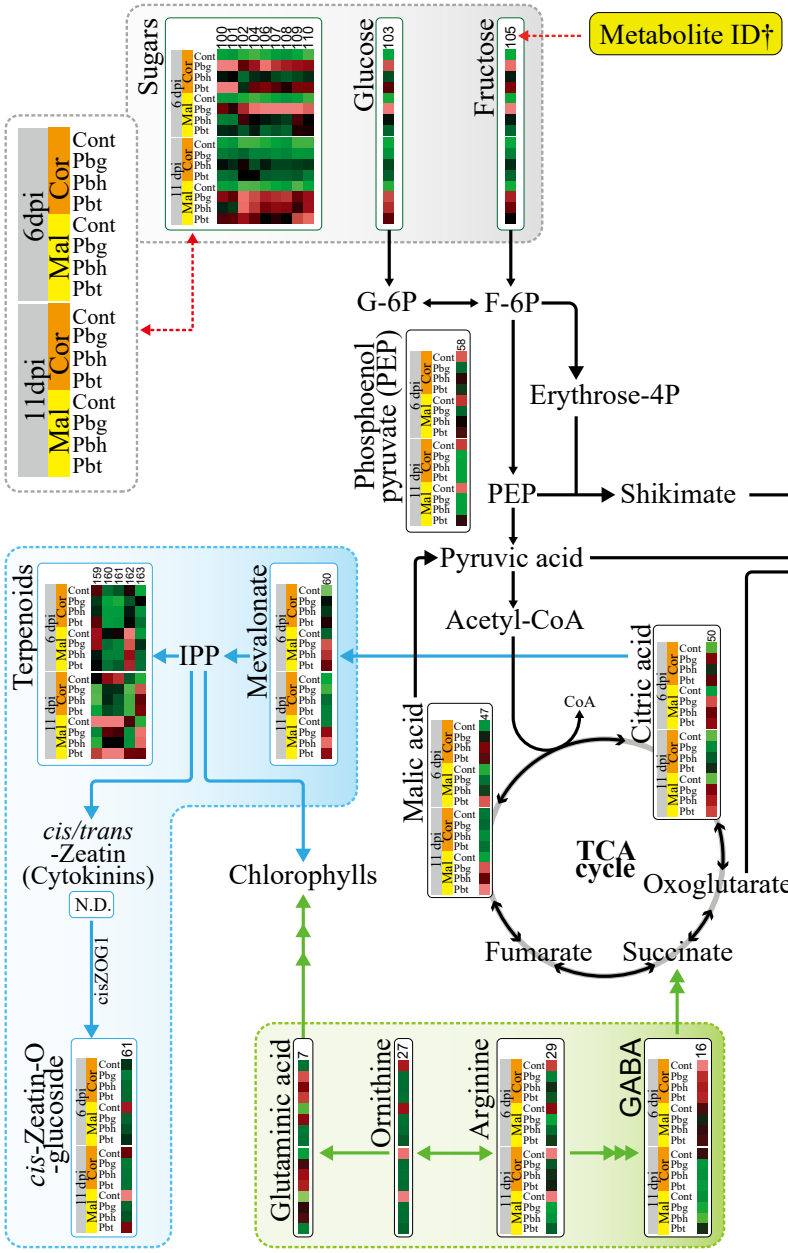

Fig 6. Alteration of core primary and secondary metabolite pathways by *Paraburkholderia* species in Broccoli. The metabolite pathways are organized as modules inside different colored boxes and the abundance of the significantly altered metabolites is represented by the heat map where each cells representing the abundance of a metabolite of a sample for *Paraburkholderia* species-Broccoli cultivar and time combinations. The metabolite ID corresponding to each metabolites is indicated at the top of the heat map and detailed information on the identity of the individual metabolites is provided in the supplementary excel **Table S9**. G-6P (Glucose 6-phosphate), F-6P (Fructose 6-phosphate), CHS

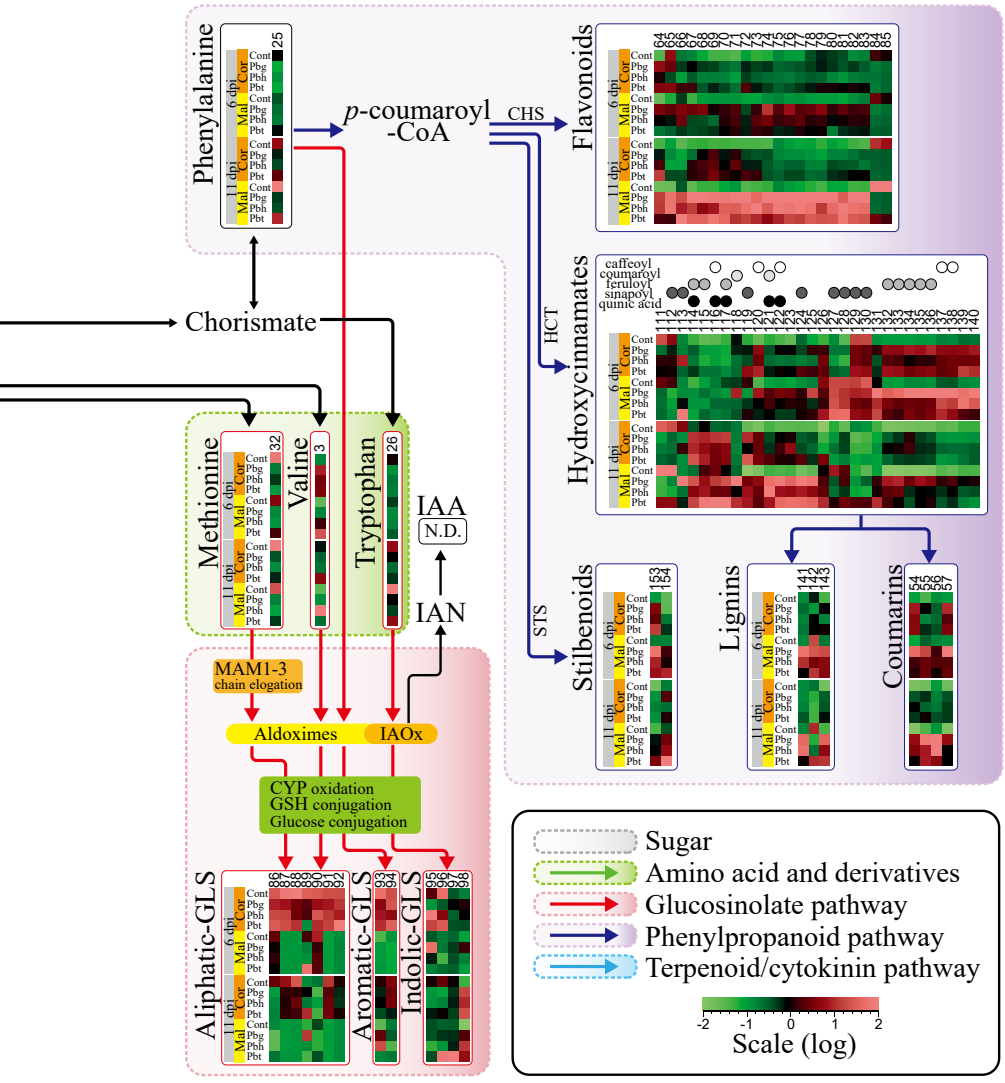

(Chalcone synthase), cisZOG1 (Cis-zeatin O-glucosyltransferase 1), CYP (Cytochrome P450), GABA (γ-aminobutyric acid), GLS (Glucosinolates), GSH (Glutathione), HCT (hydroxycinnamoyl-CoA shikimate/quinate hydroxy-cinnamoyl transferase), IAA (indole-3-acetic acid), IAN (indole-3-acetonitrile), IAOx (indole-3-acetaldoxime), IPP (isopentenyl pyrophosphate), MAM (methylthioalkylmalate synthase), and STS (stilbene synthase). Broccoli cultivars (Cor: Coronado, Mal: Malibu), Cont.: non-rhizobacteria treated control, *Pbg*: *Paraburkholderia graminis*, *Pbh*: *P. hospita*, and *Pbt*: *P. terricola*. Multiple-headed arrows indicate hidden intermediate processes in the pathways.

Defense priming is not a low-cost defensive measure as postulated but could cost substantial amounts of energy and carbon resources. This is shown by the massive accumulation of phenylpropanoids and other defensive compounds in plants primed by *Paraburkholderia* species even before the plants were challenged with the bacterial leaf pathogens. The integrated primary and secondary metabolome profiling of primed plants suggests that rhizobacteria could avert the negative impact of defense priming on the host fitness by generating massive amount of soluble sugars and remobilizing other metabolites to accommodate for the high energy and carbon skeleton demand associated with growth and defense priming. This could indicate that defense costs can be regulated if resources are not limiting and aligns with studies that showed the inevitability of defense-growth trade-off occurs primarily under resource-limiting conditions (Bergelson & Purrington, 1996; van Dam & Baldwin, 1998).

The magnitude of the impact of the rhizobacteria on plant growth, metabolism and defense priming showed an association with the level of root colonization by the rhizobacteria. On the other hand, the plant genotype and its intrinsic chemical composition could affect the ability of the rhizobacteria to colonize the host root and could determine the impact rhizobacteria have on different phenotypic traits of the host. Hence, breeding of plant for different traits should consider its impact on the host chemistry and its associated effect on the recruitment of beneficial microbes for the plant functioning. Furthermore, investigating the underlying mechanism of rhizobacteria-mediated generation of soluble sugars in plants could be instrumental for breeding programs that aim to produce high yielding and stress-resilient crops. Hence, further studies on beneficial bacterial traits involved in the modulation of the host metabolism could provide information on the underlying mechanisms of rhizobacteria-mediated alteration of host metabolism, growth and defense priming.

Acknowledgements

Seeds of two Broccoli cultivars (*Brassica olearacea* var. italic), Coronado and Malibu, were kindly provided by Bejo seed company (Warmenhuizen, The Netherlands). We are grateful to Bert Schipper and Henriëtte Vaneekelen for their help with LC MS analysis and pre-processing of metabolomics data.

Supplementary materials

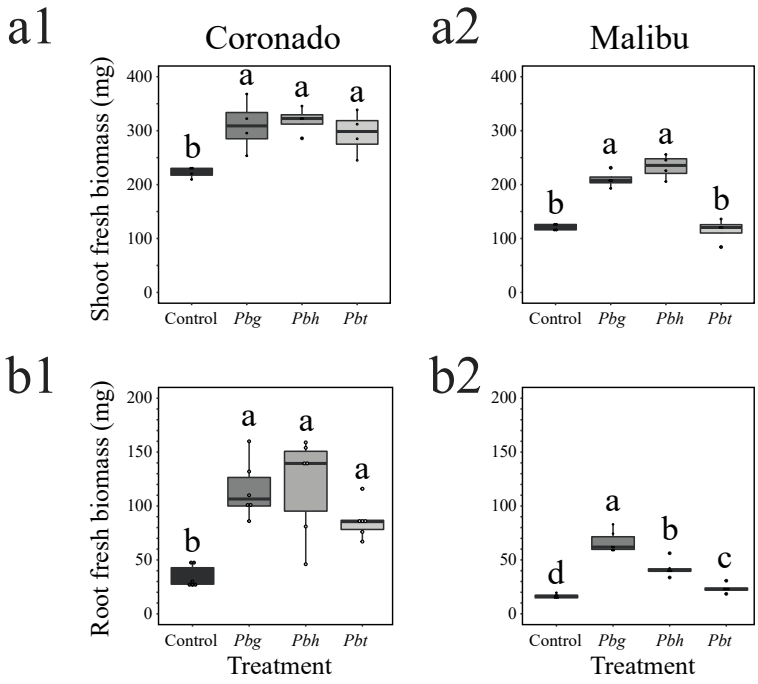

Fig S1. Absolute changes in shoot (**a**) and root (**b**) biomass of Broccoli cultivars Coronado (**1)** and Malibu (**2)** at 11 dpi with *Paraburkholderia* species. *Pbg*: *Paraburkholderia graminis*, *Pbh*: *P. hospita*, and *Pbt*: *P. terricola.* Different letters show significant statistical difference between the treatments (One-way ANOVA, Tukey's HSD *post hoc* test, $P < 0.05$).

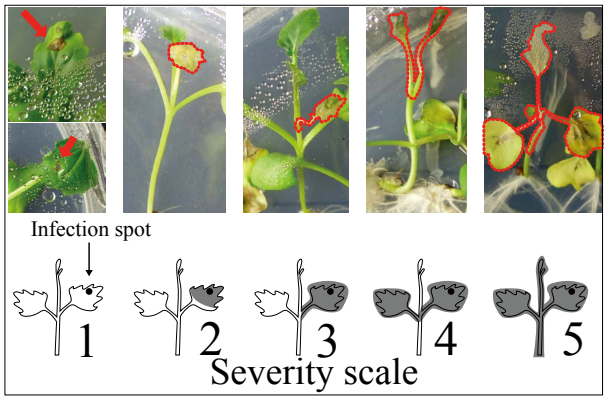

Fig S2. Disease severity scale. For the severity (**c**), each Broccoli seedlings from four biological replicates were individually scored (n = 20). Disease severity was scored by determining the migration of the lesion from the inoculation spot to the other parts of the shoot following an ordinal scale from 1- 5, where 1 = no necrosis or migration, 2 = full infection of the treated leaf, 3 = migration to the leafstalk of the treated leaf, 4 = infection of the neighboring leaf, and 5 = infection of the entire seedling.

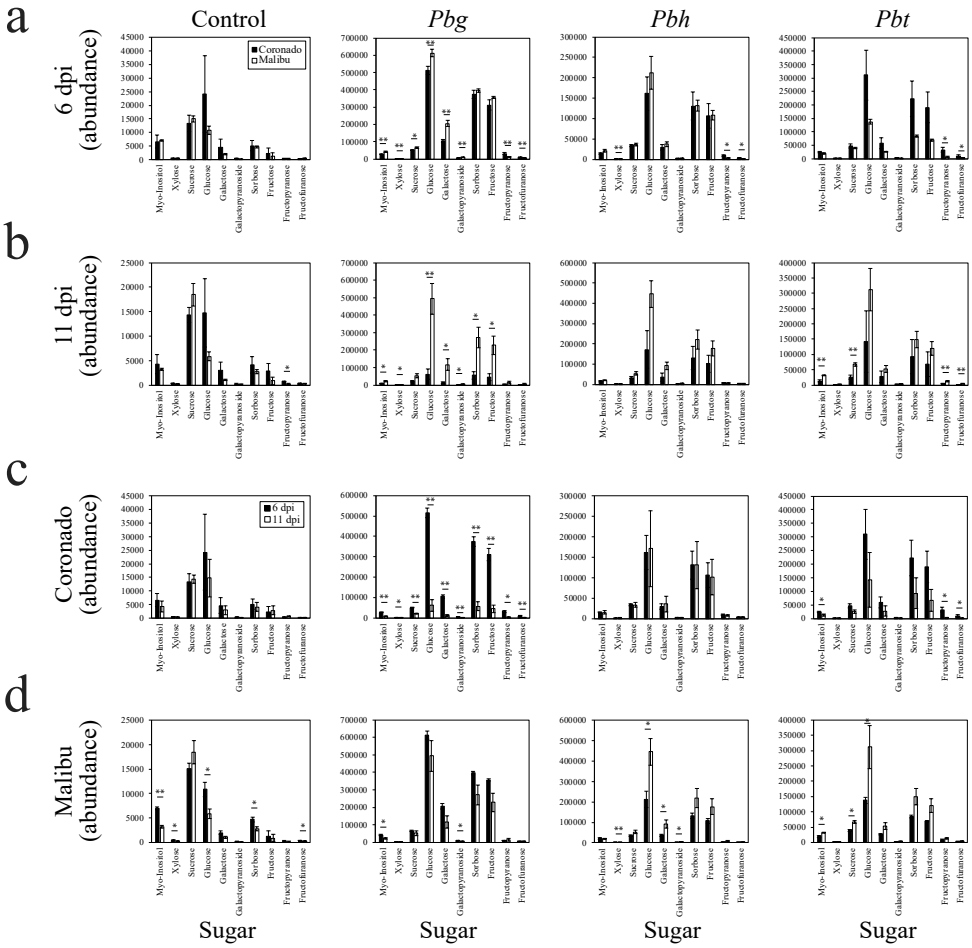

Fig S3. Absolute abundance of soluble sugars in two Broccoli cultivars upon *Paraburkholderia* inoculation at two time points (6 and 11 dpi). Comparative analysis of the of abundance of soluble sugars between the two cultivars at 6 dpi (**a)** and at 11 dpi (**b**). Comparative analysis of the abundance of soluble sugars at two time points in Coronado (**c**) and Malibu (**d**) cultivars. *Pbg*: *Paraburkholderia graminis*, *Pbh*: *P. hospita*, and *Pbt*: *P. terricola*. Asterisks denote significant statistical differences between Broccoli cultivars, Coronado and Malibu (two tailed Student's t test): * $P < 0.05$; ** $P < 0.01$.

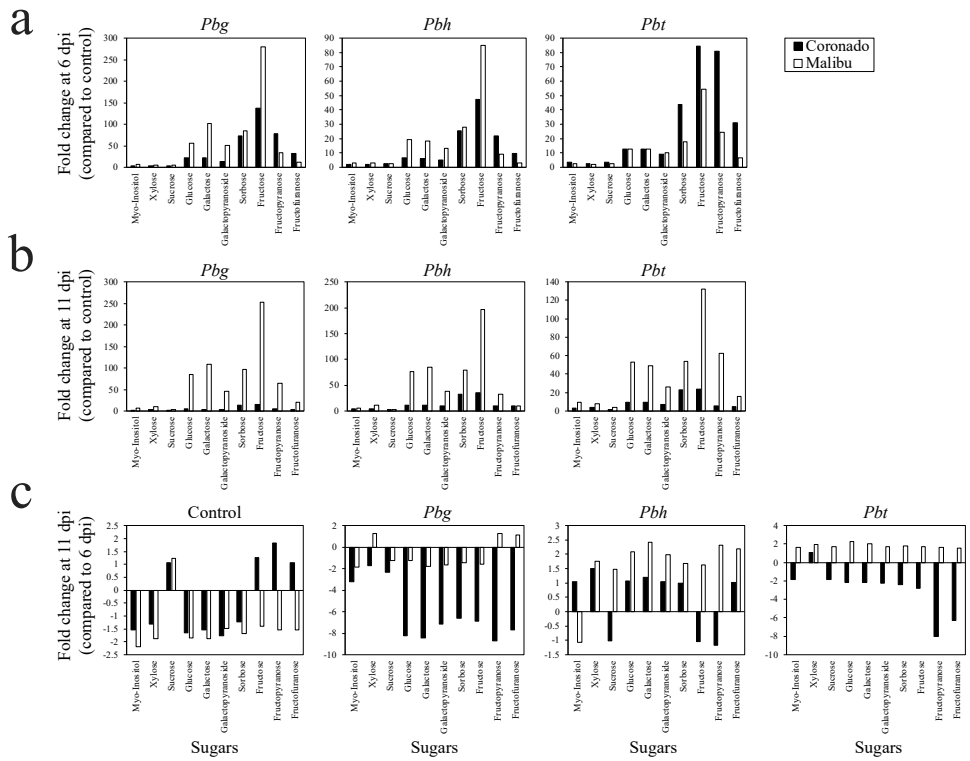

Fig S4. *Paraburkholderia* species-mediated changes in shoot soluble sugar abundance in two Broccoli cultivars, Coronado and Malibu, at 6 dpi (**a**), 11 dpi (**b**), and relative fold change between the two time points (**c**). In (**a**) and (**b**), fold change was calculated by dividing the abundance of each soluble sugars in treated plants to that of the non-treated control. *Pbg*: *Paraburkholderia graminis*, *Pbh*: *P. hospita*, and *Pbt*: *P. terricola*.

Table S1. Analysis of variance ANOVA (type II) of percent changes in shoot and root biomass in two Broccoli cultivars inoculated with three *Paraburkholderia* genera at 11 dpi.

Sample	Factor	Sum Sq	Df	F value	Pr(>F)	
Shoot fresh biomass relative change	Broccoli cultivars	1425	1	4.882	0.040333	*
	Bacteria species	12949	2	22.182	1.39E-05	***
	Broccoli cultivars: Bacteria species	8561	2	14.665	0.000166	***
	Residuals	5254	18			
Root fresh biomass relative change	Broccoli cultivars	1210.18	2	19.711	3.42E-06	***
	Bacteria species	142.42	1	4.6394	0.039404	*
	Broccoli cultivars: Bacteria species	400.55	2	6.5241	0.004441	**
	Residuals	920.94	30			

Significance codes: *** 0, ** 0.001, * 0.01.

Table S2. Population density of three *Paraburkholderia* species on roots of two Broccoli cultivars. *Pbg*: *Paraburkholderia graminis*, *Pbh*: *P. hospita*, and *Pbt*: *P. terricol*a.

Broccoli cultivar	Rhizobacteria	Population density (Cfu/mg roots)	
		6 dpi	11 dpi
Coronado	*Paraburkholderia graminis*	$2.05 \pm 0.11 \times 10^{8}$	$8.10 \pm 0.28 \times 10^{7}$
	P. hospita	$1.18 \pm 0.09 \times 10^{6}$	$2.06 \pm 0.08 \times 10^{7}$
	P. terricola	$1.58 \pm 0.03 \times 10^{7}$	$1.95 \pm 0.04 \times 10^{7}$
Malibu	*P. graminis*	$1.00 \pm 0.05 \times 10^{8}$	$1.02 \pm 0.07 \times 10^{8}$
	P. hospita	$1.40 \pm 0.15 \times 10^{7}$	$1.53 \pm 0.06 \times 10^{7}$
	P. terricola	$1.72 \pm 0.16 \times 10^{6}$	$7.02 \pm 0.35 \times 10^{5}$

Cfu: Colony forming unit
*Values represent the average of 3 replicates ± SE of three replicates

Table S3. Analysis of variance ANOVA (type II) of root colonization of three *Paraburkholderia* species in two Broccoli cultivars at two time points (6 dpi, 11 dpi). Data was log transformed using the package MASS in R.

Factor	Sum Sq	Df	F value	Pr(>F)	
Day post inoculation	0.0887	1	41.745	1.11E-06	***
Broccoli cultivar	0.7069	1	332.569	1.44E-15	***
Bacteria species	13.4135	2	3155.343	< 2.2e-16	***
Day post inoculation: Broccoli cultivar	0.4061	1	191.066	6.35E-13	***
Day post inoculation: Bacteria species	1.3366	2	314.421	< 2.2e-16	***
Broccoli cultivar: Bacteria species	4.353	2	1023.972	< 2.2e-16	***
Day post inoculation: Broccoli cultivar: Bacteria species	0.9733	2	228.966	2.33E-16	***
Residuals	0.051	24			

Signif. codes: 0 =***, 0.001 = **, 0.01 = *

Table S4. Beta regression analysis of disease severity in twoBroccoli cultivars (Coronado and Malibu) primed with *Paraburkholderia* species and treated with*Xanthomonas, a* Broccoli leaf pathogen. Different *Paraburkholderia* species were used to induced systemic resistance. *Xca*: *Xanthomonas campestris* pv. Armoraciae P4216 and *Xcc*: *X. campestri*s pv. Campestris P4014.

Pathovar	model term	df1	df2	F.ratio	p.value
Xca	Rhizobacteria	3	Inf	11.74	<.0001
	Broccoli cultivar	1	Inf	64.893	<.0001
	Rhizobacteria:Broccoli cultivar	3	Inf	20.627	<.0001
Xcc	Rhizobacteria	3	Inf	3.811	0.0096
	Broccoli cultivar	1	Inf	49.535	<.0001
	Rhizobacteria:Broccoli cultivar	3	Inf	7.604	<.0001

Table S5. *Paraburkholderia* species-mediated changes in shoot polar primery metabolites (GC-MS) in two Broccoli cultivars (Coronado and Malibu) at 6 dpi. The tabulated data corresponds to the hierarchical cluster analysis (HCA) showen in **Fig 3b1** of the manuscript. The fold changecorresponding to each metabolites was calculated by dividing the abundance of each metabolites in Paraburkholderia treated plants to the non-treated control. *Pbg*: *Paraburkholderia graminis*, *Pbh*: *P. hospita*, and *Pbt*: *P. terricola*.

Cluster Number	Mapping Number	RT(m)	Mass	RI		Annotation	Fold change					
				Obse-rved	in DB		Coronado			Malibu		
							Pbg	*Pbh*	*Pbt*	*Pbg*	*Pbh*	*Pbt*
1		16.6	73	1848	1846	4-(2-Aminoethyl)-2-methoxyphenol, 3TMS derivative	-8.54	-6.92	-1.48	-8.19	-5.17	-5.01
2		13.0	55	1529	1529	Hexamethylene diacrylate	-1.58	-1.8	-1	-5.82	-5.37	-3.47
2	18	12.8	73	1520	1522	L-5-Oxoproline	-1.4	-1.38	-1.43	-3.07	-2.81	-2.28
2	16	12.9	73	1523	1525	GABA	-1.23	-1.26	-1.25	-1.74	-1.64	0.67
4	10	9.8	73	1286	1286	Isoleucine	-2.16	-2.82	-3.21	0.49	0.25	0.43
4		11.2	174	1387	1386	Ethyl 2,4-Dimethylbenzoate	-1.16	-1.21	-1.7	0.4	-2.84	0.69
4	12	15.7	73	1767	1768	Glutamine	-1.36	-1.32	-2.65	-3.67	-3.38	-2.24
5	25	14.1	73	1623	1624	L-Phenylalanine	-1.94	-1.6	-1.93	-1.31	-1.47	1.01
5		8.5	73	1192		Methyl 7-Trimethylsilylheptanoate	-5.11	-2.09	-2.81	-3.99	-2.64	-2.32
5	31	17.2	73	1910	1912	Lysine	-3.61	-2.87	-4.21	-2.54	-2.89	-2.23
5		13.5	73	1573		Trimethyl[(2E/Z)-6-(2-thienyl)-2,6-heptadienyl]silane	-2.52	-1.94	-3.12	-2.53	-1.95	-1.64
5		12.0	73	1453	1452	N,N-Diethyl 6-oxoheptamide	-16.07	-4.09	-16.43	-18.08	-10.83	-10.08
5	32	12.8	176	1514	1515	Methionine	-2.85	-2.19	-3.51	-3.09	-2.9	-1.85
5		13.7	73	1591	1595	Diethyl (2R/S,3R)-2-Allyl-3-(trimethylsiloxy)succinate	-3.45	-2.42	-3.28	-4.1	-3.7	-2.73
5		14.6	73	1669	1673	7,8-Dehydro-8-deoxocurcumen-11-ol	-3.05	-2.05	-3.23	-3.1	-2.56	-1.96
5	58	9.5	73	1263	1263	Phosphoenolpyruvate	-3.81	-2.05	-2.63	-3.48	-2.32	-1.76
6	27	16.1	73	1805		DL-Ornithine	-12.52	-10.61	-13.78	-11.85	-8.33	-6.05
7	47	12.3	73	1479	1480	Malic acid	1.31	1.57	1.48	1.12	1.48	1.71
7	22	10.0	73	1299	1300	Glycine	-1.08	1.23	1.03	0.77	1.01	1.28
7	6	13.9	73	1611	1612	Glutamic acid	1.28	1.14	1.13	1.24	-1.35	0.99
8	4	11.6	73	1420	1420	L-Aspartic acid	2.3	1.67	4.18	2.96	2.67	1.97
8	146	17.9	73	1977	1981	Mannonic acid, lactone	1.96	-1.24	4.08	1.59	0.87	0.62
8		9.4	73	1259	1260	TMS 4-DI-TMS-AMINOBUTYRATE	3.22	1.55	1.7	1.68	1.86	1.76
8	8	15.3	73	1729	1731	Putrescine	1.44	1.09	1.42	1.18	1.02	0.95
9	45	16.5	73	1839	1863	Ascorbic acid	1.5	1.34	1.46	1.85	1.49	1.71
9		16.9	191	1877	1877	2-Amino-3-cyano-4-(2'-furyl)-4-thioxobut-2-ene	28.8	5.29	24.23	20.2	2.46	4.7
9	101	16.1	73	1801	1802	D-(-)-Fructopyranose (isomer 2)	78.58	22.07	80.8	26.95	10.85	15.98
9	100	16.0	73	1795	1792	D-(-)-Fructofuranose (isomer 1)	32.09	9.51	31.1	15.76	5.46	7.45
9	102	14.3	73	1640	1634	Xylose	3.71	2.08	2.64	4.77	2.75	2.96
9	105	16.7	73	1863	1865	Fructose	138.02	47.19	84.47	157.82	40.86	37.71
9	109	18.8	73	2074	2077	Myo-Inositol	4.06	2.18	3.69	6.29	2.58	3.45
9	110	23.3	73	2606	2611	Sucrose	3.8	2.52	3.57	4.89	2.76	2.86
9	106	16.6	73	1854	1854	Sorbose	73.61	25.66	43.78	77.87	21.94	20.4
9	107	18.2	73	2010	2010	D-Galactopyranoside	14.23	5.01	9.38	23.53	5.31	5.29
9	108	17.1	73	1899	1898	d-Galactose, 2,3,4,5,6-pentakis-O-(trimethylsilyl)-, o-methyloxyme, (1E)-	22.64	6.32	12.58	44.36	6.79	6.93
9	103	16.9	73	1879	1881	Glucose	21.19	6.66	12.81	25.26	6.97	7.46

Table S6. *Paraburkholderia* species-mediated changes in shoot polar primery metabolites (GC-MS) in two Broccoli cultivars (Coronado and Malibu) at 11 dpi. The tabulated data corresponds to the hierarchical cluster analysis (HCA) showen in **Fig 3b2** of the manuscript. The fold changecorresponding to each metabolites was calculated by dividing the abundance of each metabolites in Paraburkholderia treated plants to the non-treated control. *Pbg*: *Paraburkholderia graminis*, *Pbh*: *P. hospita*, and *Pbt*: *P. terricola*.

Cluster Number	Mapping Number	RT(m)	Mass	RI		Annotation	Fold change					
				Obse-rved	in DB		Coronado			Malibu		
							Pbg	*Pbh*	*Pbt*	*Pbg*	*Pbh*	*Pbt*
1	22	10.0	73	1299	1300	Glycine	-1.16	-1.84	-1.29	-2.4	-1.22	-1.14
2	32	12.8	176	1514	1515	Methionine	-2.37	-3.18	-2.1	-2.59	-3.39	-1.95
2		13.5	73	1573		Trimethyl[(2E/Z)-6-(2-thienyl)-2,6-heptadienyl]silane	-2.22	-2.21	-2.41	-2.06	-2.12	-1.4
2		14.6	73	1669	1673	7,8-Dehydro-8-deoxocurcumen-11-ol	-2.27	-2.16	-2.36	-2.31	-2.49	-1.7
2		12.0	73	1453	1452	N,N-Diethyl 6-oxoheptamide	-11.7	-4.59	-3.09	-11.19	-10.7	-4.25
2		13.7	73	1591	1595	Diethyl (2R/S,3R)-2-Allyl-3-(trimethylsiloxy)succinate	-2.14	-2.12	-2.35	-2.7	-2.95	-2.89
2	25	14.1	73	1623	1624	L-Phenylalanine	-1.05	-1.17	-0.83	-2.72	-2.86	-1.63
2	58	9.5	73	1263	1263	Phosphoenolpyruvate	-14.18	-11.91	-12.75	-11.43	-11.3	-2.13
2	31	17.2	73	1910	1912	Lysine	-2.71	-2.55	-2.75	-3.47	-3.4	-2.92
2	27	16.1	73	1805		DL-Ornithine	-10.86	-14.9	-10.33	-23.84	-22.03	-13.68
2		16.6	73	1848	1846	4-(2-Aminoethyl)-2-methoxyphenol, 3TMS derivative	-6.71	-10.66	-10.6	-11.9	-13.78	-8.23
2		8.5	73	1192		Methyl 7-Trimethylsilylheptanoate	-7.85	-3.95	-3.55	-2.19	-3.16	-1.29
2	16	12.9	73	1523	1525	GABA	-2.38	-2.31	-2.44	-1.13	-1.27	1.31
3		13.0	55	1529	1529	Hexamethylene diacrylate	-9.3	-13.75	-12.34	1.09	1.07	1.44
3	18	12.8	73	1520	1522	L-5-Oxoproline	-2.49	-2.15	-2.3	1.03	-1.11	1.01
5	8	15.3	73	1729	1731	Putrescine	1.42	1.36	1.32	4.01	3.62	2.83
5		9.4	73	1259	1260	TMS 4-DI-TMS-AMINOBUTYRATE	3.61	2.89	3.65	2.61	2.84	2.16
5	4	11.6	73	1420	1420	L-Aspartic acid, 2TMS derivative	1.74	2.07	1.77	3.03	4.77	3.4
5	110	23.3	73	2606	2611	Sucrose	1.63	2.47	1.91	2.84	2.89	3.65
5	102	14.3	73	1640	1634	Xylose	2.13	3.11	2.88	10.9	10.76	7.98
5	105	16.7	73	1863	1865	Fructose	20.05	45.02	30.13	252.76	196.15	132.07
5	109	18.8	73	2074	2077	Myo-Inositol	1.26	2.26	2.03	7.05	6.12	9.87
5	106	16.6	73	1854	1854	Sorbose	11.13	25.71	18.28	97.3	79.09	53.56
5	107	18.2	73	2010	2010	D-Galactopyranoside, methyl 2,3,4-tris-O-(trimethylsilyl)-, acetate	1.99	5.2	4.14	45.56	38.49	25.88
5	103	16.9	73	1879	1881	Glucose	2.57	7.06	5.83	84.07	75.88	53.04
5	108	17.1	73	1899	1898	d-Galactose, 2,3,4,5,6-pentakis-O-(trimethylsilyl)-, o-methyloxyme, (1E)-	2.68	7.65	5.92	107.78	84.51	48.95
5	45	16.5	73	1839	1863	Ascorbic acid	1.19	1.39	0.91	2.13	2.33	2.55
6	6	13.9	73	1611	1612	Glutamic acid	1.05	1.12	1.22	1.66	1.57	1.69
6	5	12.7	73	1511	1512	ASPARTIC ACID-TRITMS	-1.47	1.1	1.04	2.22	1.78	2.46
6	101	16.1	73	1801	1802	D-(-)-Fructopyranose (isomer 2)	9.02	18.82	10.12	64.34	32.8	62.32
6	100	16.0	73	1795	1792	D-(-)-Fructofuranose (isomer 1)	4.18	9.7	4.95	20.31	10.47	15.98

Table S7. *Paraburkholderia* species-mediated changes in shoot semi-polar secondary metabolites (LC-MS) in two Broccoli cultivars (Coronado and Malibu) at 6 dpi. The tabulated data corresponds to the hierarchical cluster analysis (HCA) showen in **Fig 4b1** of the manuscript. The fold changecorresponding to each metabolites was calculated by dividing the abundance of each metabolites in Paraburkholderia treated plants to the non-treated control. *Pbg*: *Paraburkholderia graminis*, *Pbh*: *P. hospita*, and *Pbt*: *P. terricola*.

Cluster number	Mapping number	RT (m)	m/z	Mass (D)	Compound	Formula	Δ ppm to DB	Classification	data base	Fold change					
										Coronado			Malibu		
										Pbg	*Pbh*	*Pbt*	*Pbg*	*Pbh*	*Pbt*
1	157	17.46	[M+H]+	164.019562	3-Methylsulfinylpropyl isothiocyanate	C5H9NOS2	-1.64	Sulfoxide	HMDB	-3.4	-2.3	-3.0	-1.2	-1.4	-1.4
2		3.00	[M+H]+	114.054932	1-Pyrroline-2-carboxylic acid	C5H7NO2	-0.39	Pyrroline	HMDB	-1063.2	-146.0	-16.1	-1425.4	-1410.1	-23.4
2	111	20.19	[M-H]-	536.176819	4-Demethylsimmondsin 2'-(E)-ferulate	C25H31NO12	-0.99	Coumaric acid	HMDB	-1.8	-1.4	-1.5	-1.4	-1.4	-1.4
2	29	1.63	[M+H]+	175.118820	Arginine	C6H14N4O2	-0.89	Amino acid	KEGG	-3.3	-2.0	-2.4	-4.6	-2.2	-1.7
2		1.80	[M-H]-	173.104156	Arginine	C6H14N4O2	-1.55	Amino acid	KEGG	-3.0	-1.6	-2.3	-4.6	-2.3	-1.8
2	30	1.97	[M-H]-	131.045929	Asparagine	C4H8N2O3	-2.25	Amino acid	KEGG	-3.7	-2.3	-2.8	-3.8	-2.3	-2.1
2	85	23.64	[M-H]-	609.144470	Flavonoid di glycoside or (C12634), (C05625), (C17563)	C27H30O16	-2.72	Flavonoid	KEGG	-5.1	-4.4	-4.2	-5.9	-4.1	-3.2
2	84	23.63	[M+H]+	611.158447	Flavonoid di glycoside or (C05625), (C19796)	C27H30O16	-3.65	Flavonoid	KEGG	-7.3	-5.7	-7.8	-9.3	-4.7	-3.8
2	42	7.21	[M-H]-	138.055878	Gabaculine	C7H9NO2	-1.06	Benzoic acid	KEGG	-1.2	-1.1	1.0	-2.6	-2.6	-1.2
2	148	3.12	[M+H]+	286.138916	Glycylprolylhydroxyproline	C12H19N3O5	-2.90	Oligopeptide	HMDB	-2.6	-1.7	-1.2	-3.4	-2.3	-1.1
2	145	2.98	[M-H]-	204.087799	N-Acetyl-D-fucosamine	C8H15NO5	0.37	Monosaccharide	KEGG	-5.5	-4.7	-4.2	-8.6	-7.1	-5.4
2	28	2.95	[M-H]-	188.056519	N-Acetylglutamic acid	C7H11NO5	0.39	Glutamic acid	HMDB	-5.0	-3.8	-4.5	-5.3	-4.1	-3.7
2	26	7.80	[M-H]-	203.082779	Tryptophan	C11H12N2O2	0.76	Amino acid	KEGG	-3.3	-2.2	-2.5	-2.2	-2.0	-1.2
2	149	28.71	[M-H]-	593.208496	Zizybeoside II	C25H38O16	-0.38	Oligosaccharide	KEGG	-2.2	-1.9	-1.8	-3.2	-2.9	-2.3
3	170	21.27	[M-H]-	278.107025	2-Acetamido-3-hexylsulfonylpropanoic acid	C11H21NO5S	1.08		PubChem	1.1	-1.0	-1.0	-1.4	-1.3	-1.5
3	88	20.01	[M-H]-	388.074219	2-Methylbutyl glucosinolate	C12H23NO9S2	0.24	Aliphatic GLS	Metlin, KEGG	-2.1	-2.1	-1.5	-1.7	1.2	1.4
3	176	29.31	[M+H]+	162.094620	6-Methylthiohexanaldoxime	C7H15NOS	-0.35		KEGG	-1.1	-1.1	-1.9	-2.5	-3.5	-1.8
3	92	10.13	[M-H]-	406.030487	Glucoiberverin	C11H21NO9S3	-0.09	Aliphatic GLS	KEGG	-1.1	-1.2	1.5	3.9	1.9	1.6
3	93	23.98	[M-H]-	422.058563	Gluconasturtiin	C15H21NO9S2	0.09	Other GLS	KEGG	-1.4	-1.3	-1.2	1.7	1.7	1.7
3	94	15.94	[M-H]-	408.042725	Glucotropaeolin	C14H19NO9S2	-0.24	Other GLS	KEGG	1.0	-1.3	1.1	-1.4	-1.3	-1.2
3	7	2.00	[M-H]-	146.045837	Glutaminic acid	C5H9NO4	-0.60	Amino acid	KEGG	1.8	1.4	1.7	2.1	1.4	1.4
3	13	4.25	[M+H]+	235.110428	Isoleucyl-Cysteine, Leucyl-Cysteine	C9H18N2O3S	-2.81	Dipeptide	HMDB	-2.5	-1.7	-1.1	1.1	1.1	1.2
3	53	3.31	[M+H]+	246.169876	Isovalerylcarnitine	C12H23NO4	-0.41	Carnitine	KEGG	-1.5	-1.4	-1.2	-1.1	-1.5	-1.2
3	80	20.47	[M-H]-	947.247437	Kaempferol 3-(2-feruloylsophoroside) 7-glucoside	C43H48O24	1.23	Flavonoid	HMDB	1.0	-1.3	1.2	1.8	1.7	1.2
3	65	20.90	[M+H]+	919.249146	Kaempferol 3-O-[6-(4-coumaroyl)-beta-D-glucosyl-(1->2)-beta-D-glucosyl-(1->2)-beta-D-glucoside]	C42H46O23	-1.23	Flavonoid	KEGG	-1.1	-1.5	-1.0	2.0	1.7	1.4
3		20.91	[M-H]-	917.235291	Kaempferol 3-O-[6-(4-coumaroyl)-beta-D-glucosyl-(1->2)-beta-D-glucosyl-(1->2)-beta-D-glucoside]	C42H46O23	-0.47	Flavonoid	KEGG	-1.2	-1.6	1.0	2.1	2.0	1.8
3	17	2.96	[M+H]+	263.141815	Methionyl-Isoleucine	C11H22N2O3S	-2.18	Dipeptide	HMDB	-1.6	-1.6	-1.6	-1.3	-1.3	-1.2
3	112	33.28	[M-H]-	385.150146	Methylsyringin	C18H26O9	-0.68	Phenolic glycoside	HMDB	-1.4	-1.3	-1.3	-2.3	-2.0	-1.7
3	44	33.29	[M+H]+	225.111435	Olivetolic acid	C12H16O4	-3.29	Benzoic	KEGG	-1.6	-1.6	-1.5	-3.0	-2.2	-2.1
3	52	6.20	[M-H]-	305.087860	Starch acetate	C12H18O9	0.18	Carboxylic acid	HMDB	-1.2	-1.3	1.0	-1.0	-1.5	-1.0

Table S7. (Continued)

Cluster number	Mapping number	RT (m)	m/z	Mass (D)	Compound	Formula	Δ ppm to DB	Classification	data base	Fold change					
										Coronado			Malibu		
										Pbg	*Pbh*	*Pbt*	*Pbg*	*Pbh*	*Pbt*
4	172	3.87	[M-H]-	276.988342	2-C-Methyl-D-erythritol 2,4-cyclodiphosphate	C5H12O9P2	-0.30		KEGG	-1.8	-1.1	-1.2	-1.6	-1.9	-2.2
4		33.64	[M-H]-	333.145691	3'-N'-Acetylfusarochromanone	C17H22N2O5	0.29	Benzopyran	HMDB	2.0	-1.0	1.8	-1.1	-1.1	1.3
4	165	43.28	[M-H]-	629.261658	Brassica napus non-fluorescent chlorophyll catabolite 3	C34H38N4O8	-0.05	Tetrapyrrole	HMDB	-4.3	-2.7	-4.0	-5.5	-5.7	-3.5
4	61	16.87	[M-H]-	380.156128	cis-Zeatin-O-glucoside	C16H23N5O6	-3.67	Fattyacyl glycoside	KEGG	-2.0	-1.5	-1.5	-3.3	-2.8	-2.2
4	35	12.05	[M-H]-	222.077301	Dioxacarb	C11H13NO4	0.35	Benzene	KEGG	-1.7	-1.3	-1.3	-1.7	-1.6	-1.3
4	46	26.20	[M-H]-	203.056168	L-ascorbic acid ethyl ester	C8H12O6	0.22	Butenolide	metlin	-2.5	-1.5	-2.4	-11.8	-4.7	-4.9
4	23	27.97	[M+H]+	247.107407	N-Acetyl-D-tryptophan	C13H14N2O3	-1.09	Amino acid	KEGG	-2.0	-1.8	-1.6	-1.8	-1.8	-1.4
4	164	12.04	[M+H]+	224.091324	Salsolinol 1-carboxylate	C11H13NO4	-1.83	Quinoline	HMDB	-1.9	-1.5	-1.4	-2.1	-1.7	-1.4
4	160	19.07	[M-H]-	431.191284	S-Furanopetasitin	C24H32O5S	3.51	Terpenoid	HMDB	-49.1	-5.3	-4.7	-2.0	-3.0	-2.2
4	161	20.25	[M+H]+	387.200470	Sonchuionoside C	C19H30O8	-2.26	Terpenoid	HMDB	-1.7	-1.4	-1.4	-1.6	-1.5	-1.3
4	24	4.14	[M+H]+	384.113953	Succinyladenosine	C14H17N5O8	-2.70	Purine nucleoside	HMDB	-2.3	-1.6	-1.4	-2.0	-1.9	-1.3
4	156	34.23	[M-H]-	363.075562	Sulfometuron methyl	C15H16N4O5S	-3.48	Sulfonylurea	KEGG	-3.0	-2.6	-3.3	-6.5	-3.2	-1.5
5	36	17.69	[M-H]-	329.087708	1-O-Vanilloyl-beta-D-glucose	C14H18O9	-0.35	Phenolic glycoside	KEGG	-2.1	-1.7	-1.7	-1.6	-1.9	-1.7
5	21	23.98	[M+H]+	252.085983	4-Hydroxy-3-methoxy-cinnamoylglycine	C12H13NO5	-2.75	Amino acid	KEGG	-1.6	-1.5	-1.3	1.0	-1.1	-1.0
5	41	24.57	[M-H]-	165.019363	Formylsalicylic acid or (C14096), (C14100)	C8H6O4	0.24	Benzoic acid	KEGG	1.0	-1.2	1.1	-1.2	-1.0	1.2
5	20	23.98	[M-H]-	206.082062	N-Acetyl-L-phenylalanine	C11H13NO3	-0.79	Phenylalanine	KEGG, Metlin	-1.4	-1.3	-1.2	1.1	-1.1	1.0
5	155	27.17	[M-H]-	349.059875	Sulfometuron	C14H14N4O5S	-3.86	Sulfonylurea	KEGG	-1.2	-1.1	-1.0	-1.1	-1.3	-1.1
7	63	23.89	[M+H]+	225.148117	(6S,9R)-Vomifoliol	C13H20O3	-1.59	Fatty acyl glycoside	KEGG	1.7	1.5	1.5	1.6	1.4	1.4
7	120	21.34	[M-H]-	335.077667	5-O-Caffeoylshikimic acid	C16H16O8	1.32	Coumaric acid	Metlin, KEGG	4.8	4.5	5.3	3.9	2.7	2.6
7	72	33.14	[M-H]-	577.156250	Flavonoid-di-glycoside or (C16981), (C12628), (C12627)	C27H30O14	-0.13	Flavonoid	KEGG	2.4	2.2	3.2	2.2	2.5	2.5
7	147	4.77	[M-H]-	375.093384	Furaneol 4-(6-malonylglucoside)	C15H20O11	0.26	O-Glycosyl comp.	HMDB	1.4	1.1	1.4	1.4	1.4	1.5
7	48	23.68	[M-H]-	350.088165	Indole-3-acetic-acid-O-glucuronide	C16H17NO8	0.07	O-Glucuronides	HMDB	6.4	1.8	3.3	3.1	1.9	1.8
7	67	17.00	[M-H]-	963.241943	Kaempferol 3-O-hydroxyferuloylsophoroside 7-O-glucoside	C43H48O25	1.27	Flavonoid	PubChem	1.5	1.2	1.6	2.7	1.9	1.9
7	163	20.31	[M+H]+	377.144623	Loganic acid	C16H24O10	1.19	Iridoid	KEGG	5.1	1.9	2.9	2.8	2.0	1.9
7		2.40	[M-H]-	133.014084	Malic acid	C4H6O5	-1.05	Hydroxy acid	KEGG	1.8	1.9	1.9	1.6	1.4	1.9
8	59	23.68	[M+H]+	323.122986	Binapacryl	C15H18N2O6	-2.44	Dinoseb	KEGG	6.2	1.9	3.0	3.3	2.1	2.0
8	64	15.09	[M+H]+	773.210571	Kaempferol 3-sophorotrioside	C33H40O21	-3.76	Flavonoid	KEGG	6.7	4.9	6.4	12.9	9.4	6.4
9	124	39.91	[M-H]-	929.272949	2-Feruloyl-1,2'-disinapoylgentiobiose	C44H50O22	0.92	Phenylpropanoid	HMDB	1.1	-1.0	1.3	1.3	1.3	1.3
9	175	33.63	[M+H]+	335.159943	3'-N'-Acetylfusarochromanone	C17H22N2O5	-0.61	Benzopyran	HMDB	3.1	1.9	1.5	1.0	-1.3	-1.1

Table S7. (Continued)

Cluster number	Mapping number	RT (m)	m/z	Mass (D)	Compound	Formula	Δ ppm to DB	Classification	data base	Fold change					
										Coronado			Malibu		
										Pbg	*Pbh*	*Pbt*	*Pbg*	*Pbh*	*Pbt*
11	153	21.46	[M-H]-	551.176697	(Z)-Resveratrol 3,4'-diglucoside	C26H32O13	-0.58	Stilbenoid	HMDB	1.7	1.6	2.0	2.0	1.7	1.6
11	132	18.43	[M-H]-	355.103210	1-Feruloyl-D-glucose	C16H20O9	-0.60	Phenylpropanoid	KEGG	1.8	1.6	1.8	2.1	1.7	1.6
11	37	26.28	[M-H]-	415.124878	2-Hydroxybenzaldehyde O-[xylosyl-(1->6)-glucoside]	C18H24O11	0.70	Phenolic glycoside	HMDB	3.0	2.3	3.2	2.7	1.8	1.9
11	125	43.09	[M+H]+	239.090393	3,4,5-Trimethoxycinnamic acid	C12H14O5	-4.20	Phenylpropanoid	HMDB	2.3	1.5	2.4	2.6	1.4	1.7
11	43	13.33	[M-H]-	299.077576	4-Hydroxybenzoate-O-glucoside	C13H16O8	1.18	Benzoic acid	KEGG	1.3	1.2	1.3	1.8	1.5	1.8
11	135	12.94	[M+H]+	211.059418	5-Hydroxyferulic acid methyl ester I	C10H10O5	-3.12	Phenylpropanoid	KEGG	2.1	1.6	2.0	2.7	1.7	1.7
11	54	18.44	[M+H]+	177.054489	7-Methoxycoumarin or (C03081)	C10H8O3	-0.49	Coumarin	KEGG	2.0	1.9	1.9	2.6	1.7	1.7
11	38	12.10	[M+H]+	138.054703	Anthranilic acid	C7H7NO2	-1.98	Aromatic acid	KEGG	1.9	1.3	1.9	2.4	1.5	1.8
11	138	11.42	[M-H]-	341.087616	Caffeic acid 3-glucoside	C15H18O9	-0.61	Phenylpropanoid	KEGG	2.1	2.0	2.0	2.6	2.0	1.7
11	122	9.97	[M-H]-	353.087585	Chlorogenic acid	C16H18O9	-0.68	Phenylpropanoid	KEGG	2.3	1.7	2.4	2.0	1.7	1.5
11		9.92	[M+H]+	355.101624	Chlorogenic acid	C16H18O9	-2.12	Phenylpropanoid	KEGG	2.3	1.7	2.2	1.9	1.6	1.3
11		15.86	[M-H]-	353.087616	Chlorogenic acid or Coumarin: (C01527) or (C08996)	C16H18O9	-0.59	Phenylpropanoid	KEGG	3.1	2.5	3.2	2.1	1.8	1.5
11	123	15.81	[M+H]+	355.101654	Chlorogenic acid or Coumarin: (C01527) or (C08996)	C16H18O9	-2.03	Phenylpropanoid	KEGG	2.6	2.1	2.7	2.1	1.8	1.6
11	50	2.95	[M-H]-	191.019562	citric acid	C6H8O7	-0.85	Tricarboxylic acid	KEGG	3.9	2.7	3.5	3.4	2.4	2.7
11	136	12.93	[M-H]-	371.097992	Dihydroferulic acid 4-O-glucuronide	C16H20O10	-1.02	Phenylpropanoid	HMDB	2.4	1.8	2.1	2.9	1.9	2.0
11	133	18.43	[M+H]+	195.064651	Ferulic acid	C10H10O4	-2.69	Phenylpropanoid	KEGG	1.7	1.5	1.8	2.2	1.6	1.6
11	51	2.54	[M-H]-	207.014572	Garcinia acid	C6H8O8	-0.33	Carboxylic acid	HMDB	11.1	8.5	27.6	41.4	12.8	8.9
11	104	2.04	[M-H]-	225.061401	Glucoheptonic acid	C7H14O8	-0.99	Glycoside	Metlin	4.9	3.0	4.1	6.2	3.2	2.9
11	68	26.16	[M-H]-	725.194031	Isoschaftoside 4'-glucoside or (HMDB40878)	C32H38O19	0.80	Flavonoid	HMDB	2.9	1.8	2.5	3.8	2.1	2.2
11	83	20.03	[M+H]+	611.159851	Kaempferol 3-O-beta-D-sophoroside or (C05625), (C17563)	C27H30O16	-1.35	Flavonoid	KEGG	1.2	1.1	1.4	1.6	1.5	1.4
11	81	20.46	[M+H]+	949.258301	Kaempferol tri glycoside + feruloyl	C43H48O24	-2.66	Flavonoid	HMDB	-1.0	-1.3	1.2	2.0	1.8	1.6
11	139	15.97	[M-H]-	325.092926	p-Coumaroyl-D-glucose or (C04415), (C05158)	C15H18O8	0.01	Phenylpropanoid	KEGG	2.3	2.0	2.7	4.0	4.1	2.3
11	140	15.99	[M+H]+	165.054581	Phenylpyruvic acid or (C12621), (C00811)	C9H8O3	0.03	Phenylpropanoid	KEGG	2.4	2.0	2.5	4.4	3.7	2.2
11	79	17.75	[M+H]+	935.242615	Quercetin 3-[p-coumaroyl-(->6)-glucosyl-(1->2)-glucosyl-(1->2)-glucoside], Kaempferol 3-O-caffeoyl-sophoroside 7-O-glucoside	C42H46O24	-2.74	Flavonoid	HMDB	1.0	-1.2	1.1	2.3	1.9	1.8
11	69	29.93	[M-H]-	739.210144	Robinin	C33H40O19	1.38	Flavonoid	KEGG	2.3	1.8	2.4	1.8	1.3	1.6
11	57	12.94	[M+H]+	193.048950	Scopoletin, or (C10290), (C18077), (C01938)	C10H8O4	-3.24	Coumarin	KEGG	2.4	1.9	2.1	2.9	1.8	1.8
12	60	3.85	[M-H]-	147.066345	(S)-Mevalonic acid	C6H12O4	0.14	Hydroxy fatty acid	KEGG	2.1	2.0	2.3	1.7	1.6	1.3
12	137	13.27	[M-H]-	341.087585	1-Caffeoyl-beta-D-glucose or (C10431)	C15H18O9	-0.70	Phenylpropanoid	KEGG	2.4	2.1	2.1	3.0	2.3	2.1
12	131	23.26	[M-H]-	195.029892	3,4-Dihydroxyphenylpyruvate	C9H8O5	-0.16	Phenylpropanoid	KEGG	2.7	1.8	2.1	2.5	1.7	1.9
12	99	19.52	[M-H]-	401.109009	4-Hydroxy-5-(3',5'-dihydroxyphenyl)-valeric acid-O-glucuronide	C17H22O11	0.18	Glucuronide	HMDB	1.6	1.5	1.6	2.0	1.8	1.8

Table S7. (Continued)

Cluster number	Mapping number	RT (m)	m/z	Mass (D)	Compound	Formula	Δ ppm to DB	Classification	data base	Fold change					
										Coronado			Malibu		
										Pbg	*Pbh*	*Pbt*	*Pbg*	*Pbh*	*Pbt*
12	74	22.70	[M+H]+	341.138000	5-Deoxykievitone or (C09832), (C18023), (C09753), (C15510)	C20H20O5	-1.10	Flavonoid	KEGG	2.4	1.9	2.3	3.0	2.4	2.0
12	134	14.64	[M+H]+	211.059479	5-Hydroxyferulic acid methyl ester II	C10H10O5	-2.83	Phenylpropanoid	KEGG	2.4	1.8	2.1	2.9	1.8	1.9
12	143	27.39	[M-H]-	567.207886	Citrusin B	C27H36O13	-0.76	Phenylpronanoid	HMDB	2.6	1.8	2.7	2.3	1.9	1.9
12	55	27.40	[M+H]+	219.101242	Eupatoriochromene	C13H14O3	-1.52	Coumarin	KEGG	2.6	1.7	2.4	2.0	1.5	1.6
12	82	20.06	[M-H]-	609.145386	Flavonoid-di-glycoside or (C12634), (C05625), (C18942))	C27H30O16	-1.21	Flavonoid	KEGG	1.3	1.1	1.6	1.7	1.7	1.5
12	73	38.75	[M-H]-	561.160889	Flavonol 3-O-beta-D-glucosyl-(1->2)-beta-D-glucoside	C27H30O13	-0.78	Flavonoid	KEGG	3.9	3.4	4.6	3.7	4.0	3.7
12	70	35.31	[M-H]-	723.213989	Flavonol 3-O-beta-D-glucosyl-(1->2)-beta-D-glucosyl-(1->2)-beta-D-glucoside	C33H40O18	-0.32	Flavonoid	KEGG	2.2	1.9	2.5	2.0	1.9	1.8
12	71	38.58	[M-H]-	723.213928	Flavonol 3-O-beta-D-glucosyl-(1->2)-beta-D-glucosyl-(1->2)-beta-D-glucoside tri glycoside	C33H40O18	-0.41	Flavonoid	KEGG	1.9	1.6	2.0	1.9	1.8	1.7
12	76	39.79	[M-H]-	531.150269	Flavonol 3-O-D-xylosylglucoside	C26H28O12	-1.04	Flavonoid	KEGG	11.7	7.3	14.0	18.4	12.7	8.5
12	78	17.76	[M-H]-	933.231506	Kaempferol 3-O-caffeoyl-sophoroside 7-O-glucoside/ Quercetin 3-[p-coumaroyl-(->6)-glucosyl-(1->2)-glucosyl-(1->2)-glucoside]	C42H46O24	0.94	Flavonoid	HMDB	1.1	-1.1	1.2	2.4	2.1	1.9
12	56	33.73	[M+H]+	325.091370	Mahaleboside	C15H16O8	-1.30	Coumarin	HMDB	3.2	2.8	3.7	5.0	5.3	4.2
12	75	34.36	[M-H]-	517.134094	Medicarpin 3-O-glucoside-6'-malonate	C25H26O12	-1.99	Flavonoid	KEGG	26.1	18.8	30.3	28.1	24.0	15.0
12	121	38.74	[M+H]+	339.106934	p-Coumaroyl quinic acid	C16H18O8	-1.60	Phenylpronanoid	KEGG	3.5	3.0	4.2	3.8	3.7	3.0
12	141	33.28	[M-H]-	487.125000	Phrymarolin I	C24H24O11	0.77	Lignan	KEGG	13.1	3.8	8.4	67.3	48.7	20.0
12	77	33.75	[M-H]-	547.145325	Puerarin xyloside	C26H28O13	-0.73	Flavonoid	KEGG	3.5	2.9	4.2	4.4	4.5	3.7
12	150	22.62	[M-H]-	135.045029	Simple phenolic or (C05613), (C07086), (C07215) or (C01454)	C8H8O2	-0.70	Phenolica aicd	KEGG	3.4	2.2	2.3	2.3	1.7	1.7
13	119	37.81	[M-H]-	591.171875	1,2-Bis-O-sinapoyl-beta-D-glucoside	C28H32O14	-0.08	Phenylpronanoid	KEGG	1.4	1.3	1.8	-1.4	-1.1	-1.0
13	154	31.87	[M-H]-	469.080780	Resveratrol-sulfoglucoside	C20H22O11S	-0.48	Stilbenoid	Metlin, HMDB	1.2	3.7	4.9	1.8	1.7	2.5

Table S8. *Paraburkholderia* species-mediated changes in shoot semi-polar secondary metabolites (LC-MS) in two Broccoli cultivars (Coronado and Malibu) at 11 dpi. The tabulated data corresponds to the hierarchical cluster analysis (HCA) showen in **Fig 4b2** of the manuscript. The fold changecorresponding to each metabolites was calculated by dividing the abundance of each metabolites in Paraburkholderia treated plants to the non-treated control. *Pbg*: *Paraburkholderia graminis*, *Pbh*: *P. hospita*, and *Pbt*: *P. terricola*.

Cluster number	Mapping number	RT(m)	m/z	Mass (D)	Compound	Formula	Δ ppm to DB	Classification	data base	Fold change					
										Coronado			Malibu		
										Pbg	*Pbh*	*Pbt*	*Pbg*	*Pbh*	*Pbt*
1	64	15.09	[M+H]+	773.210571	Kaempferol 3-sophorotrioside	C33H40O21	-3.76	Flavonoid	KEGG	3.5	4.4	6.3	22.8	22.6	16.0
1	118	23.80	[M+H]+	438.238007	N1,N10-Dicoumaroylspermidine	C25H31N3O4	-1.66	Phenylpronanoid	HMDB	-1.1	-1.7	1.0	10.7	2.3	5.3
1	156	34.23	[M-H]-	363.075562	Sulfometuron methyl	C15H16N4O5S	-3.48	sulfonylurea	KEGG	-1.6	1.0	-1.5	1.2	1.4	6.9
2	153	21.46	[M-H]-	551.176697	(Z)-Resveratrol 3,4'-diglucoside	C26H32O13	-0.58	Stilbenoid	HMDB	1.6	1.7	1.6	1.7	1.8	2.2
2	125	43.09	[M+H]+	239.090393	3,4,5-Trimethoxycinnamic acid	C12H14O5	-4.20	Phenylpronanoid	HMDB	3.1	2.8	3.3	7.9	5.7	7.6
2	120	21.34	[M-H]-	335.077667	5-O-Caffeoylshikimic acid	C16H16O8	1.32	Phenylpronanoid	Metlin, KEGG	7.4	7.5	7.8	8.5	7.7	7.4
2	38	12.10	[M+H]+	138.054703	Anthranilic acid	C7H7NO2	-1.98	aromatic acid	KEGG	1.9	1.8	2.1	3.4	2.9	4.8
2	50	2.95	[M-H]-	191.019562	citric acid	C6H8O7	-0.85	Carboxylic acid	KEGG	2.2	2.9	3.3	4.8	5.4	6.1
2		2.40	[M-H]-	133.014084	Malic acid	C4H6O5	-1.05	Hydroxy acid	KEGG	1.6	1.4	2.0	2.3	2.3	2.4
2	154	31.87	[M-H]-	469.080780	Resveratrol-sulfoglucoside	C20H22O11S	-0.48	Stilbenoid	Metlin, HMDB	1.8	1.1	1.6	1.6	1.7	2.9
3	134	14.64	[M+H]+	211.059479	5-Hydroxyferulic acid methyl ester II	C10H10O5	-2.83	Phenylpronanoid	KEGG	4.2	4.4	3.5	6.8	5.2	4.7
3	59	23.68	[M+H]+	323.122986	Binapacryl	C15H18N2O6	-2.44	Dinoseb	KEGG	7.0	6.9	7.8	10.3	7.9	8.7
3	48	23.68	[M-H]-	350.088165	Indole-3-acetic-acid-O-glucuronide	C16H17NO8	0.07	o-glucuronides	HMDB	5.8	5.9	6.2	10.8	6.7	10.1
4	63	23.89	[M+H]+	225.148117	(6S,9R)-Vomifoliol	C13H20O3	-1.59	Fattyacyl glycoside	KEGG	2.4	2.6	2.2	2.9	2.6	2.8
4	60	3.85	[M-H]-	147.066345	(S)-Mevalonic acid	C6H12O4	0.14	Hydroxy fatty acid	KEGG	-1.1	1.2	1.2	1.6	2.0	1.6
4	137	13.27	[M-H]-	341.087585	1-Caffeoyl-beta-D-glucose or (C10431)	C15H18O9	-0.70	Phenylpronanoid	KEGG	3.0	4.2	2.8	5.9	4.8	4.1
4	132	18.43	[M-H]-	355.103210	1-Feruloyl-D-glucose	C16H20O9	-0.60	Phenylpronanoid	KEGG	2.1	2.4	2.1	3.6	3.1	3.0
4	124	39.91	[M-H]-	929.272949	2-Feruloyl-1,2'-disinapoylgentiobiose	C44H50O22	0.92	Phenylpronanoid	HMDB	1.4	1.5	1.8	2.9	2.3	2.7
4	37	26.28	[M-H]-	415.124878	2-Hydroxybenzaldehyde O-[xylosyl-(1->6)-glucoside]	C18H24O11	0.70	Phenolic glycoside	HMDB	3.0	4.6	4.2	5.4	4.6	5.1
4	131	23.26	[M-H]-	195.029892	3,4-Dihydroxyphenylpyruvate	C9H8O5	-0.16	Phenylpronanoid	KEGG	2.2	3.8	2.8	3.7	3.5	5.8
4	74	22.70	[M+H]+	341.138000	5-Deoxykievitone or (C09832), (C18023), (C09753), (C15510)	C20H20O5	-1.10	Flavonoid	KEGG	3.5	3.4	3.5	6.8	5.7	4.4
4	135	12.94	[M+H]+	211.059418	5-Hydroxyferulic acid methyl ester I	C10H10O5	-3.12	Phenylpronanoid	KEGG	2.7	2.9	2.7	5.7	4.3	4.3
4	54	18.44	[M+H]+	177.054489	7-Methoxycoumarin or (C03081)	C10H8O3	-0.49	Coumarin	KEGG	2.4	2.8	2.6	4.0	3.9	3.2
4	138	11.42	[M-H]-	341.087616	Caffeic acid 3-glucoside	C15H18O9	-0.61	Phenylpronanoid	KEGG	2.4	3.0	2.5	5.1	4.4	4.0
4		9.92	[M+H]+	355.101624	Chlorogenic acid	C16H18O9	-2.12	Phenylpronanoid	KEGG	2.8	3.0	3.0	4.5	3.4	3.8
4	122	9.97	[M-H]-	353.087585	Chlorogenic acid	C16H18O9	-0.68	Phenylpronanoid	KEGG	2.8	3.0	2.9	4.3	3.2	4.0

Table S8. (Continued)

Cluster number	Mapping number	RT(m)	m/z	Mass (D)	Compound	Formula	Δ ppm to DB	Classification	data base	Fold change					
										Coronado			Malibu		
										Pbg	*Pbh*	*Pbt*	*Pbg*	*Pbh*	*Pbt*
4	123	15.81	[M+H]+	355.101654	Chlorogenic acid or Coumarin: (C01527) or (C08996)	C16H18O9	-2.03	Phenylpronanoid	KEGG	2.7	3.4	2.7	3.5	2.8	3.6
4		15.86	[M-H]-	353.087616	Chlorogenic acid or Coumarin: (C01527) or (C08996)	C16H18O9	-0.59	Phenylpronanoid	KEGG	2.8	3.5	2.9	3.6	2.8	3.9
4	143	27.39	[M-H]-	567.207886	Citrusin B	C27H36O13	-0.76	Phenylpronanoid	HMDB	4.3	4.5	5.3	4.6	3.5	4.0
4	136	12.93	[M-H]-	371.097992	Dihydroferulic acid 4-O-glucuronide	C16H20O10	-1.02	Phenylpronanoid	HMDB	3.0	3.3	3.1	6.6	5.0	5.4
4	55	27.40	[M+H]+	219.101242	Eupatoriochromene	C13H14O3	-1.52	Coumarin	KEGG	4.3	3.7	4.8	5.0	3.9	3.9
4	133	18.43	[M+H]+	195.064651	Ferulic acid	C10H10O4	-2.69	Phenylpronanoid	KEGG	2.2	2.4	2.1	3.6	3.1	2.8
4	82	20.06	[M-H]-	609.145386	Flavonoid-di-glycoside (C12634) or (C05625), (C18942)	C27H30O16	-1.21	Flavonoid	KEGG	1.7	1.8	2.2	4.4	4.2	3.9
4	72	33.14	[M-H]-	577.156250	Flavonoid-di-glycoside (C16981) or (C12628), (C12627)	C27H30O14	-0.13	Flavonoid	KEGG	4.9	5.5	7.0	19.1	17.7	14.9
4	73	38.75	[M-H]-	561.160889	Flavonol 3-O-beta-D-glucosyl-(1->2)-beta-D-glucoside	C27H30O13	-0.78	Flavonoid	KEGG	6.7	8.3	10.3	16.0	18.2	12.8
4	70	35.31	[M-H]-	723.213989	Flavonol 3-O-beta-D-glucosyl-(1->2)-beta-D-glucosyl-(1->2)-beta-D-glucoside	C33H40O18	-0.32	Flavonoid	KEGG	2.6	2.8	3.0	4.5	4.1	4.2
4	71	38.58	[M-H]-	723.213928	Flavonol 3-O-beta-D-glucosyl-(1->2)-beta-D-glucosyl-(1->2)-beta-D-glucoside tri glycoside	C33H40O18	-0.41	Flavonoid	KEGG	2.5	2.8	2.4	3.2	2.8	2.5
4	76	39.79	[M-H]-	531.150269	Flavonol 3-O-D-xylosylglucoside	C26H28O12	-1.04	Flavonoid	KEGG	12.1	35.8	47.3	127.5	119.5	96.3
4	104	2.04	[M-H]-	225.061401	Glucoheptonic acid	C7H14O8	-0.99	Glycoside	Metlin	2.0	2.6	3.1	6.3	5.9	4.4
4	68	26.16	[M-H]-	725.194031	Isoschaftoside 4'-glucoside or Schaftoside 4'-glucoside	C32H38O19	0.80	Flavonoid	HMDB	4.7	5.6	5.4	13.1	7.4	10.5
4	80	20.47	[M-H]-	947.247437	Kaempferol 3-(2-feruloylsophoroside) 7-glucoside	C43H48O24	1.23	Flavonoid	HMDB	1.2	1.5	1.6	3.6	3.1	2.9
4	65	20.90	[M+H]+	919.249146	Kaempferol 3-O-[6-(4-coumaroyl)-beta-D-glucosyl-(1->2)-beta-D-glucosyl-(1->2)-beta-D-glucoside]	C42H46O23	-1.23	Flavonoid	KEGG	1.1	1.0	1.4	4.3	4.3	2.8
4		20.91	[M-H]-	917.235291	Kaempferol 3-O-[6-(4-coumaroyl)-beta-D-glucosyl-(1->2)-beta-D-glucosyl-(1->2)-beta-D-glucoside]	C42H46O23	-0.47	Flavonoid	KEGG	1.0	1.1	1.3	4.5	4.8	3.4
4	83	20.03	[M+H]+	611.159851	Kaempferol 3-O-beta-D-sophoroside or (C05625), (C17563)	C27H30O16	-1.35	Flavonoid	KEGG	2.1	1.9	2.5	4.3	3.9	3.6
4	78	17.76	[M-H]-	933.231506	Kaempferol 3-O-caffeoyl-sophoroside 7-O-glucoside or (HMDB37938)	C42H46O24	0.94	Flavonoid	HMDB	1.1	1.4	1.5	5.2	4.9	4.5
4	67	17.00	[M-H]-	963.241943	Kaempferol 3-O-hydroxyferuloylsophoroside 7-O-glucoside	C43H48O25	1.27	Flavonoid	PubChem	1.6	2.3	2.3	5.4	4.4	4.9
4	81	20.46	[M+H]+	949.258301	Kaempferol tri glycoside + feruloyl	C43H48O24	-2.66	Flavonoid	HMDB	1.3	1.5	1.7	2.8	3.1	3.0
4	56	33.73	[M+H]+	325.091370	Mahaleboside	C15H16O8	-1.30	Coumarin	HMDB	4.5	5.8	9.8	40.6	46.2	22.5
4	75	34.36	[M-H]-	517.134094	Medicarpin 3-O-glucoside-6'-malonate	C25H26O12	-1.99	Flavonoid	KEGG	7.5	38.7	59.3	476.8	401.1	264.0
4	121	38.74	[M+H]+	339.106934	p-Coumaroyl quinic acid	C16H18O8	-1.60	Phenylpronanoid	KEGG	6.3	6.9	9.9	15.4	17.1	11.4
4	77	33.75	[M-H]-	547.145325	Puerarin xyloside	C26H28O13	-0.73	Flavonoid	KEGG	5.2	9.6	11.8	27.6	27.4	20.6
4	79	17.75	[M+H]+	935.242615	Quercetin 3-[p-coumaroyl-(->6)-glucosyl-(1->2)-glucosyl-(1->2)-glucoside], Kaempferol 3-O-caffeoyl-sophoroside 7-O-glucoside	C42H46O24	-2.74	Flavonoid	HMDB	1.2	1.5	1.7	4.8	3.6	3.9
4	69	29.93	[M-H]-	739.210144	Robinin	C33H40O19	1.38	Flavonoid	KEGG	2.9	3.0	3.2	4.5	3.4	4.5
4	57	12.94	[M+H]+	193.048950	Scopoletin or (C10290), (C18077), (C01938)	C10H8O4	-3.24	Coumarin	KEGG	3.1	3.3	3.3	7.4	5.5	5.4

Table S8. (Continued)

Cluster number	Mapping number	RT(m)	m/z	Mass (D)	Compound	Formula	Δ ppm to DB	Classification	data base	Fold change					
										Coronado			Malibu		
										Pbg	*Pbh*	*Pbt*	*Pbg*	*Pbh*	*Pbt*
4	150	22.62	[M-H]-	135.045029	Benzylformate or (C07086), (C07215) or (C01454)	C8H8O2	-0.70	Phenolica aicds	KEGG	2.6	4.5	2.9	3.1	3.2	4.6
5	119	37.81	[M-H]-	591.171875	1,2-Bis-O-sinapoyl-beta-D-glucoside	C28H32O14	-0.08	Phenylpronanoid	KEGG	2.3	1.8	2.5	2.7	2.9	2.9
5	175	33.63	[M+H]+	335.159943	3'-N'-Acetylfusarochromanone	C17H22N2O5	-0.61	Benzopyran	HMDB	17.2	4.5	11.5	7.5	6.4	2.8
5		33.64	[M-H]-	333.145691	3'-N'-Acetylfusarochromanone	C17H22N2O5	0.29	Benzopyran	HMDB	16.8	4.7	10.7	5.9	4.0	2.9
5	99	19.52	[M-H]-	401.109009	4-Hydroxy-5-(3',5'-dihydroxyphenyl)-valeric acid-O-glucuronide	C17H22O11	0.18	Glucuronide	HMDB	2.2	2.4	1.7	2.4	2.2	1.9
5	147	4.77	[M-H]-	375.093384	Furaneol 4-(6-malonylglucoside)	C15H20O11	0.26	o-glycosyl comp.	HMDB	1.5	1.3	1.5	2.6	2.2	1.9
5	93	23.98	[M-H]-	422.058563	Gluconasturtiin	C15H21NO9S2	0.09	other GLS	KEGG	-1.2	-1.1	-1.3	4.7	6.4	2.5
5	163	20.31	[M+H]+	377.144623	Loganic acid	C16H24O10	1.19	Iridoid	KEGG	16.6	10.7	11.5	21.0	20.1	12.0
7	21	23.98	[M+H]+	252.085983	4-Hydroxy-3-methoxy-cinnamoylglycine	C12H13NO5	-2.75	Amino acid	KEGG	-1.8	-2.2	-2.0	-1.9	-1.9	-1.1
7	148	3.12	[M+H]+	286.138916	Glycylprolylhydroxyproline	C12H19N3O5	-2.90	Oligopeptides	HMDB	-1.2	-1.9	-1.4	-1.6	-2.3	-1.0
7	20	23.98	[M-H]-	206.082062	N-Acetyl-L-phenylalanine	C11H13NO3	-0.79	Phenylalanine	KEGG, Metlin	-1.9	-2.1	-1.9	-2.0	-2.0	-1.2
7	158	19.33	[M+H]+	178.035156	Sulforaphane	C6H11NOS2	-1.83	Sulfoxides	HMDB	-17.3	-2.9	-2.8	-12.0	-8.4	-1.7
8	165	43.28	[M-H]-	629.261658	Brassica napus non-fluorescent chlorophyll catabolite 3	C34H38N4O8	-0.05	Tetrapyrrole	HMDB	-11.2	-10.9	-11.0	-29.9	-37.4	-6.8
9	36	17.69	[M-H]-	329.087708	1-O-Vanilloyl-beta-D-glucose	C14H18O9	-0.35	Benzoic acid	KEGG	-6.0	-4.8	-3.7	-5.9	-4.7	-2.2
9	61	16.87	[M-H]-	380.156128	cis-Zeatin-O-glucoside	C16H23N5O6	-3.67	Fatty acyl glycoside	KEGG	-3.5	-3.3	-3.1	-7.2	-6.1	-2.5
9	35	12.05	[M-H]-	222.077301	Dioxacarb	C11H13NO4	0.35	Benzenes	KEGG	-2.6	-2.6	-2.7	-3.9	-3.1	-1.7
9	85	23.64	[M-H]-	609.144470	Flavonoid di glycoside (C12634) or (C05625), (C17563), (C19796))	C27H30O16	-2.72	Flavonoid	KEGG	-6.1	-6.4	-6.9	-18.6	-17.6	-4.4
9	84	23.63	[M+H]+	611.158447	Flavonoid di glycoside (C12634) or (C05625), (C17563), (C19796)	C27H30O16	-3.65	Flavonoid	KEGG	-5.4	-5.8	-6.4	-13.8	-15.1	-3.0
9	42	7.21	[M-H]-	138.055878	Gabaculine	C7H9NO2	-1.06	Benzoic acid	KEGG	-3.5	-2.6	-2.6	-4.7	-5.4	-1.2
9	23	27.97	[M+H]+	247.107407	N-Acetyl-D-tryptophan	C13H14N2O3	-1.09	Amino acid	KEGG	-3.0	-3.1	-3.7	-3.8	-3.9	-1.6
9	44	33.29	[M+H]+	225.111435	Olivetolic acid	C12H16O4	-3.29	Benzoic derivative	KEGG	-2.2	-2.2	-2.1	-4.0	-5.4	-1.9
9	164	12.04	[M+H]+	224.091324	Salsolinol 1-carboxylate	C11H13NO4	-1.83	Quinoline	HMDB	-2.5	-2.5	-2.6	-3.4	-3.1	-1.6
9	160	19.07	[M-H]-	431.191284	S-Furanopetasitin	C24H32O5S	3.51	Terpenoid	HMDB	-2.2	-2.1	-2.6	-2.2	-3.2	1.1
9	161	20.25	[M+H]+	387.200470	Sonchuionoside C	C19H30O8	-2.26	Terpenoid	HMDB	-1.7	-1.8	-1.9	-1.9	-2.1	-1.1
9	24	4.14	[M+H]+	384.113953	Succinyladenosine	C14H17N5O8	-2.70	Purine nucleoside	HMDB	-3.1	-2.2	-2.2	-3.1	-2.5	-1.4
9	155	27.17	[M-H]-	349.059875	Sulfometuron	C14H14N4O5S	-3.86	Sulfonylurea	KEGG	-1.7	-1.8	-1.5	-1.9	-2.2	-1.1
9	26	7.80	[M-H]-	203.082779	tryptophan	C11H12N2O2	0.76	Amino acid	KEGG	-1.6	-2.9	-2.0	-3.9	-4.9	-2.3
9	149	28.71	[M-H]-	593.208496	Zizybeoside II	C25H38O16	-0.38	Oligosaccharides	KEGG	-2.6	-3.2	-2.8	-5.1	-5.3	-2.2
10		3.00	[M+H]+	114.054932	1-Pyrroline-2-carboxylic acid	C5H7NO2	-0.39	Pyrrolines	HMDB	-1091.0	-1044.4	-1099.5	-1494.1	-1572.9	-1495.0
10	172	3.87	[M-H]-	276.988342	2-C-Methyl-D-erythritol 2,4-cyclodiphosphate	C5H12O9P2	-0.30		KEGG	-4.3	-2.7	-3.8	-8.0	-4.6	-1.7
10	111	20.19	[M-H]-	536.176819	4-Demethylsimmondsin 2'-(E)-ferulate	C25H31NO12	-0.99	Phenylpronanoid	HMDB	-2.3	-2.0	-1.9	-3.1	-3.0	-1.4
10	29	1.63	[M+H]+	175.118820	Arginine	C6H14N4O2	-0.89	Amino acid	KEGG	-3.0	-2.5	-2.4	-6.7	-5.2	-3.1

Table S8. (Continued)

Cluster number	Mapping number	RT(m)	m/z	Mass (D)	Compound	Formula	Δ ppm to DB	Classification	data base	Fold change					
										Coronado			Malibu		
										Pbg	*Pbh*	*Pbt*	*Pbg*	*Pbh*	*Pbt*
10		1.80	[M-H]-	173.104156	Arginine	C6H14N4O2	-1.55	Amino acid	KEGG	-2.9	-2.5	-2.2	-8.1	-5.4	-4.0
10	30	1.97	[M-H]-	131.045929	Asparagine	C4H8N2O3	-2.25	Amino acid	KEGG	-2.5	-2.9	-2.7	-4.3	-4.0	-4.9
10	112	33.28	[M-H]-	385.150146	Methylsyringin	C18H26O9	-0.68	Phenylpronanoid	HMDB	-2.1	-2.1	-1.9	-3.2	-4.2	-1.6
10	145	2.98	[M-H]-	204.087799	N-Acetyl-D-fucosamine	C8H15NO5	0.37	Monosaccharide	KEGG	-4.6	-6.2	-6.6	-8.4	-8.0	-5.3
10	28	2.95	[M-H]-	188.056519	N-Acetylglutamic acid	C7H11NO5	0.39	Glutamic acid	HMDB	-4.0	-5.3	-4.8	-9.2	-7.2	-7.4
10	34	7.09	[M-H]-	161.968781	Raphanusamic acid	C4H5NO2S2	-0.88	Alpha amino acid	Metlin, HMDB	-1.6	-2.0	-1.7	-3.4	-2.7	-2.0
10	52	6.20	[M-H]-	305.087860	Starch acetate	C12H18O9	0.18	Carboxylic acid	HMDB	-3.0	-2.9	-2.4	-2.2	-2.0	1.0
10	33	10.80	[M-H]-	247.111847	Valyl-Methionine/ Methionyl-Valine	C10H20N2O3S	-1.38	Dipeptide	HMDB	-3.1	-2.5	-2.3	-8.7	-3.8	-2.8
11	170	21.27	[M-H]-	278.107025	2-acetamido-3-hexylsulfonylpropanoic acid	C11H21NO5S	1.08		PubChem	-1.5	-1.5	-1.6	-2.2	-1.9	-1.3
11	88	20.01	[M-H]-	388.074219	2-Methylbutyl glucosinolate	C12H23NO9S2	0.24	Aliphatic GLS	Metlin, KEGG	-2.2	-1.7	-2.0	-2.4	-2.2	-1.2
11	157	17.46	[M+H]+	164.019562	3-Methylsulfinylpropyl isothiocyanate	C5H9NOS2	-1.64	Sulfoxide	HMDB	-5.3	-2.2	-2.8	-3.8	-4.7	-1.4
11	176	29.31	[M+H]+	162.094620	6-Methylthiohexanaldoxime	C7H15NOS	-0.35		KEGG	-1.7	-1.7	-2.9	-1.7	-2.0	1.7
11	92	10.13	[M-H]-	406.030487	glucoiberverin	C11H21NO9S3	-0.09	Aliphatic GLS	KEGG	-1.4	-1.6	-1.0	2.1	3.2	2.1
11	13	4.25	[M+H]+	235.110428	Isoleucyl-Cysteine, Leucyl-Cysteine	C9H18N2O3S	-2.81	Dipeptide	HMDB	-2.6	-2.0	-1.8	-1.3	-1.7	1.1
11	53	3.31	[M+H]+	246.169876	Isovalerylcarnitine	C12H23NO4	-0.41	Carnitine	KEGG	-1.5	-1.8	-1.5	-2.0	-1.7	-1.0
11	17	2.96	[M+H]+	263.141815	Methionyl-Isoleucine	C11H22N2O3S	-2.18	Dipeptide	HMDB	-3.3	-1.9	-2.7	-1.4	-1.9	1.2
14	41	24.57	[M-H]-	165.019363	Formylsalicylic acid or (C14100)	C8H6O4	0.24	Benzoic acid	KEGG	4.4	2.2	2.4	1.3	1.2	-1.3
14	7	2.00	[M-H]-	146.045837	Glutaminic acid	C5H9NO4	-0.60	Amino acid	KEGG	1.6	1.8	1.9	2.3	2.4	1.8

Table S9. Polar primary and semi-polar secondary metabolites classes and their metabolites ID used in **Fig 6** of the manuscript. GC: Gas chromatography- mass spectrometry, LC: Liquid chromatography- mass spectrometry.

Mapping #	Compound	Tool
	Amino acid	
1	Serine	GC
2	Threonine	GC
3	Valine	LC
4	L-Aspartic acid	GC
5	ASPARTIC ACID-TRITMS	GC
6	Glutamic acid	GC
7	Glutaminic acid	LC
8	Putrescine	GC
9	Tryptophan or (C07839), (C14916)	LC
10	Isoleucine	GC
11	Proline	GC
12	Glutamine	GC
13	Isoleucyl-Cysteine	LC
14	5-Hydroxyindoleacetylglycine	LC
15	L-Asparagine	GC
16	GABA	GC
17	Methionyl-Isoleucine	LC
18	L-5-Oxoproline	GC
19	L-Serine	GC
20	N-Acetyl-L-phenylalanine	LC
21	4-Hydroxy-3-methoxy-cinnamoylglycine	LC
22	Glycine	GC
23	N-Acetyl-D-tryptophan	LC
24	Succinyladenosine	LC
25	L-Phenylalanine	GC
26	tryptophan	LC
27	Ornithine	GC
28	N-Acetylglutamic acid	LC
29	Arginine	LC
30	Asparagine	LC
31	Lysine	GC
32	Methionine	GC
33	Valyl-Methionine	LC
34	Raphanusamic acid	LC
	Benzene, Benzoic acid	
35	Dioxacarb	LC
36	1-O-Vanilloyl-beta-D-glucose	LC
37	2-Hydroxybenzaldehyde O-[xylosyl-(1->6)-glucoside]	LC
38	Anthranilic acid	LC
39	Apiosylglucosyl 4-hydroxybenzoate	LC
40	dihydroxybenzoic acid glucoside	LC
41	Formylsalicylic acid	LC
42	Gabaculine	LC
43	4-Hydroxybenzoate-O-glucoside	LC
44	Olivetolic acid	LC
	Butenolide	
45	Ascorbic acid	GC
46	L-ascorbic acid ethyl ester	LC
	Carboxylic acid	
47	Malic acid	GC
48	Indole-3-acetic-acid-O-glucuronide	LC
49	Indole-3-acetaldehyde or (C10663), (C06345)	LC
50	Citric acid	LC
51	Garcinia acid	LC
52	Starch acetate	LC
	Carnitines	
53	Isovalerylcarnitine	LC
	Coumarin	
54	7-Methoxycoumarin or (C03081)	LC
55	Eupatoriochromene	LC
56	Mahaleboside	LC
57	Scopoletin or (C10290), (C18077), (C01938)	LC
	Ester	
58	Phosphoenolpyruvate	GC
59	Binapacryl	LC
	Fatty acid, Fatty acyl glycoside	
60	(S)-Mevalonic acid	LC
61	cis-Zeatin-O-glucoside	LC
62	Ethyl 7-epi-12-hydroxyjasmonate glucoside	LC
63	(6S,9R)-Vomifoliol	LC
	Flavonoid	
64	Kaempferol 3-sophorotrioside	LC
65	Kaempferol 3-O-[6-(4-coumaroyl)-beta-D-glucosyl-(1->2)-beta-D-glucosyl-(1->2)-beta-D-glucoside]	LC
66	Kaempferol 3-(2'''-sinapoylsophoroside) 7-glucoside	LC
67	Kaempferol 3-O-hydroxyferuloylsophoroside 7-O-glucoside	LC
68	Isoschaftoside 4'-glucoside/ Schaftoside 4'-glucoside	LC
69	Robinin	LC
70	Flavonol 3-O-beta-D-glucosyl-(1->2)-beta-D-glucosyl-(1->2)-beta-D-glucoside	LC
71	Flavonol 3-O-beta-D-glucosyl-(1->2)-beta-D-glucosyl-(1->2)-beta-D-glucoside tri glycoside	LC
72	Flavonoid-di-glycoside_ Kaempferitrin (C16981)/ Vitexin 2''-rhamnoside (C12628)/ Apigenin 7-O-neohesperidoside (C12627)	LC
73	Flavonol 3-O-beta-D-glucosyl-(1->2)-beta-D-glucoside	LC
74	5-Deoxykievitone/ 6-Prenylnaringenin (C09832)/ Flavaprenin (C18023)/ Glepidotin B (C09753)/ 4-Glyceollidin (C15510)	LC
75	Medicarpin 3-O-glucoside-6'-malonate	LC
76	Flavonol 3-O-D-xylosylglucoside	LC
77	Puerarin xyloside	LC
78	Kaempferol 3-O-caffeoyl-sophoroside 7-O-glucoside/ Quercetin 3-[p-coumaroyl-(->6)-glucosyl-(1->2)-glucosyl-(1->2)-glucoside]	LC

Table S9. (Continued)

Mapping #	Compound	Tool
79	Quercetin 3-[p-coumaroyl-(->6)-glucosyl-(1->2)-glucosyl-(1->2)-glucoside], Kaempferol 3-O-caffeoyl-sophoroside 7-O-glucoside	LC
80	Kaempferol 3-(2-feruloylsophoroside) 7-glucoside	LC
81	Kaempferol tri glycoside + feruloyl	LC
82	Flavonoid-di-glycoside:(C12634) or (C05625), (C18942))	LC
83	Kaempferol 3-O-beta-D-sophoroside or (C05625), (C17563)	LC
84	Flavonoid di glycoside: (C12634) or (C05625), (C17563), (C19796)	LC
85	Flavonoid di glycoside: (C12634) or (C05625), (C17563), (C19796))	LC
	Glucosinolate	
86	Glucoraphanin	LC
87	hexyl glucosinolate (3-Methylpentyl glucosinolate/ 4-Methylpentyl glucosinolate)	LC
88	2-Methylbutyl glucosinolate	LC
89	4-Methylthiobutyl-desulfoglucosinolate	LC
90	Glucoalyssin	LC
91	Glucoiberin	LC
92	Glucoiberverin	LC
93	Gluconasturtiin	LC
94	Glucotropaeolin	LC
95	4-Hydroxyglucobrassicin	LC
96	4-methoxyglucobrassicin	LC
97	Desulfoglucobrassicin	LC
98	Glucobrassicin	LC
	Glucuronide	
99	4-Hydroxy-5-(3',5'-dihydroxyphenyl)-valeric acid-O-glucuronide	LC
	Glycoside	
100	D-(-)-Fructofuranose, pentakis(trimethylsilyl) ether (isomer 1)	GC
101	D-(-)-Fructopyranose	GC
102	Xylose	GC
103	Glucose	GC
104	Glucoheptonic acid	LC
105	Fructose	GC
106	Sorbose	GC
107	D-Galactopyranoside, methyl 2,3,4-tris-O-(trimethylsilyl)-, acetate	GC
108	d-Galactose, 2,3,4,5,6-pentakis-O-(trimethylsilyl)-, o-methyloxyme, (1E)-	GC
109	Myo-Inositol	GC
110	Sucrose	GC
	Hydroxycinnamate	
111	4-Demethylsimmondsin 2'-(E)-ferulate	LC
112	Methylsyringin	LC
113	Sinapine	LC
114	5-O-Feruloylquinic acid	LC
115	6-Feruloylglucose 2,3,4-trihydroxy-3-methylbutylglycoside	LC
116	3-O-Caffeoyl-4-O-methylquinic acid	LC
117	O-Feruloylquinate	LC

Mapping #	Compound	Tool
118	N1,N10-Dicoumaroylspermidine	LC
119	1,2-Bis-O-sinapoyl-beta-D-glucoside	LC
120	5-O-Caffeoylshikimic acid	LC
121	p-Coumaroyl quinic acid	LC
122	Chlorogenic acid	LC
123	Chlorogenic acid or Coumarin: (C01527) or (C08996)	LC
124	2-Feruloyl-1,2'-disinapoylgentiobiose	LC
125	3,4,5-Trimethoxycinnamic acid	LC
126	Urolithin A-3-O-glucuronide	LC
127	1,2,2'-Trisinapoylgentiobioside	LC
128	3',6-Disinapoylsucrose	LC
129	1-O-Sinapoyl beta-D-glucoside or 4-O-beta-D-Glucosyl-sinapate	LC
130	Sinapic acid	LC
131	3,4-Dihydroxyphenylpyruvate	LC
132	1-Feruloyl-D-glucose	LC
133	Ferulic acid	LC
134	5-Hydroxyferulic acid methyl ester II	LC
135	5-Hydroxyferulic acid methyl ester I	LC
136	Dihydroferulic acid 4-O-glucuronide	LC
137	1-Caffeoyl-beta-D-glucose or (C10431)	LC
138	Caffeic acid 3-glucoside	LC
139	p-Coumaroyl-D-glucose or (C04415), (C05158)	LC
140	Phenylpyruvic acid or (C12621), (C00811)	LC
	Lignan	
141	Phrymarolin I	LC
142	Syringin	LC
143	Citrusin B	LC
	Methoxyphenol	
144	4-Heptyloxyphenol	LC
	Monosaccharide	
145	N-Acetyl-D-fucosamine	LC
	Oraganic acid	
146	Mannonic acid, lactone	GC
	O-glycosyl compound	
147	Furaneol 4-(6-malonylglucoside)	LC
	Oligopeptide	
148	Glycylprolylhydroxyproline	LC
	Oligosaccharide	
149	Zizybeoside II	LC
	Phenolic acid	
150	Simple phenolic: (C05613) or (C07086), (C07215), (C01454)	LC
	Quinoline	
151	Quinoline	LC
	Saccharide	
152	(3S,7E,9S)-9-Hydroxy-4,7-megastigmadien-3-one 9-glucoside	LC
	Stilbenoid	
153	(Z)-Resveratrol 3,4'-diglucoside	LC
154	Resveratrol-sulfoglucoside	LC
	Sulfonylurea	
155	Sulfometuron	LC
156	Sulfometuron methyl	LC

Table S9. (Continued)

Mapping #	Compound	Tool
	Sulfoxide	
157	3-Methylsulfinylpropyl isothiocyanate	LC
158	Sulforaphane	LC
	Terpenoid	
159	(4R,5S,7R,11S)-11,12-Dihydroxy-1(10)-spirovetiven-2-one 11-glucoside	LC
160	S-Furanopetasitin	LC
161	Sonchuionoside C	LC
162	10-Deoxygeniposidic acid	LC
163	Loganic acid	LC
	Others	
164	Salsolinol 1-carboxylate	LC
165	Brassica napus non-fluorescent chlorophyll catabolite 3	LC
166	1-Methyl-4-(1-methyl-2-propenyl)-benzene/ alpha-Ionene/ 1,2,3,4,Tetrahydro-1,5,7-trimethylnapthalene/ 5,7alpha-Dihydro-1,4,4,7a-tetramethyl-4H-indene	LC
167	2-(3-Phenylpropyl)tetrahydrofuran	LC
168	2,5-Dihydro-2,4,5-trimethyloxazole/ 2-Acetylpyrrolidine	LC
169	2,6-Dimethoxy-4-propylphenol	LC
170	2-acetamido-3-hexylsulfonylpropanoic acid	LC
171	2-Amino-2-deoxyisochorismate	LC
172	2-C-Methyl-D-erythritol 2,4-cyclodiphosphate	LC
173	O-Demethylpuromycin	LC
174	pantothenic acid (vitamin B5)	LC
175	3'-N'-Acetylfusarochromanone	LC
176	6-Methylthiohexanaldoxime	LC

Chapter 5

Effects of sulfur assimilation in *Pseudomonas fluorescens* on growth, shoot metabolome and defense of Brassica species

Je-Seung Jeon, Desalegn W. Etalo, Natalia Carreno-Quintero,
Ric De Vos, and Jos M. Raaijmakers

Manuscript submitted for publication

Abstract

Genome-wide analysis of plant growth-promoting *Pseudomonas fluorescens* strain SS101 (*Pf* SS101) combined with site-directed mutagenesis recently revealed that sulfur assimilation plays an important role in growth promotion and induced systemic resistance of the model plant Arabidopsis. Here we investigated how sulfur metabolism of *Pf* SS101 affects the shoot metabolome of Arabidopsis and of the related Brassica crop Broccoli. To this end, we treated roots of Arabidopsis and Broccoli seedlings with *Pf* SS101 or mutant 20H12 disrupted in the adenylsulfate reductase gene *cysH,* a key gene involved in sulfur assimilation and the biosynthesis of cysteine and methionine. Sulfur assimilation in *Pf* SS101 significantly affected growth of Arabidopsis but showed an adverse effect on shoot biomass of two Broccoli cultivars. In Arabidopsis, sulfur assimilation by *Pf* SS101 affected the levels of sulfurous as well as non-sulfurous metabolites in the shoot. The impact on the sulfur-containing metabolites was mainly reflected in long chain aliphatic glucosinolates. Arabidopsis treated with the *cysH* mutant showed significantly higher levels of short and medium chain aliphatic glucosinolates as compared to plants treated with wild type *Pf* SS101. Moreover, both *Pf* SS101 and *cysH* mutant treatments significantly enhanced the levels of indole metabolites such as camalexin and indole-3-acetic acid in the Arabidopsis shoot. In Broccoli, *Pf* SS101 triggered significant changes in the shoot metabolome towards defensive metabolites such as indole glucosinolates and phenylpropanoids. Furthermore, root tip treatment of two Broccoli cultivars with *Pf* SS101 significantly reduced disease severity caused by the bacterial leaf pathogen *Xanthomonas campestris* pv. armoraciae (*Xca*) but not for *Xanthomonas campestris* pv. campestris (*Xcc*). Treatment of the root tips with the *cysH* mutant only reduced disease severity in Broccoli cultivar Malibu. In conclusion, sulfur assimilation by *Pf* SS101 had a significant impact on the biosynthesis of sulfurous and non-sulfurous metabolites in the plant shoots. These changes in the host metabolome are likely associated with the observed systemic defense against bacterial infections of the leaves, but the success and magnitude thereof depend on the plant cultivar and the pathogen pathovar.

Keywords: *Pseudomonas fluorescens*; sulfur metabolism; plant growth promotion; induced systemic resistance; plant metabolomics; glucosinolates; flavonoids.

Introduction

The genus *Pseudomonas* is an abundant member of the plant microbiome, particularly of the rhizosphere. Various studies have shown that different strains of root-associated *Pseudomonas* species can promote plant growth, alter root architecture and induce systemic resistance (Vessey, 2003; Pieterse *et al.*, 2014; Etalo *et al.*, 2018). Recent studies also revealed that some root-colonizing *Pseudomonas* strains can significantly alter shoot and root chemistry. More specifically, we demonstrated that plant growth-promoting *Pseudomonas fluorescens* strain SS101 (*Pf* SS101) altered the levels of glucosinolates, coumarins, flavonoids, and camalexin in shoots and roots of Arabidopsis (van de Mortel *et al.*, 2012). Also, *P. fluorescens* strain N21.4 was shown to enhance the level of isoflavonoids in soybean (Algar *et al.*, 2014). Another interesting recent finding was that *Pseudomonas simiae* strain WCS417 induced root exudation of scopoletin, an iron-mobilizing coumarin with antimicrobial activity, suppressing the growth of fungal root pathogens but supporting root colonization by beneficial *Pseudomonas* strains (Stringlis, Ioannis A *et al.*, 2018). For most root-associated *Pseudomonas* strains, however, the specific traits that trigger phenotypic and metabolome changes in different host plants are yet unknown.

By screening a genome-wide library of approximately 7,500 random transposon mutants, we identified specific genes in *Pf* SS101 that were associated with growth promotion and induced systemic resistance in Arabidopsis (Cheng *et al.*, 2017). Twenty-one mutants were identified with a compromised ability to promote plant growth, to alter root architecture or to trigger systemic resistance against the bacterial leaf pathogen *Pseudomonas syringae* pv. tomato (Pst). Subsequent validation by site-directed mutagenesis and genetic complementation of the mutants demonstrated that the phosphogluconate dehydratase gene *edd*, the response regulator gene *colR* and the adenylsulfate reductase gene *cysH* play important roles in plant growth promotion, alteration of root architecture and induced systemic resistance (ISR) by *Pf* SS101. *CysH* is a gene involved in sulfur assimilation and the biosynthesis of the amino acids cysteine and methionine. Transcriptome analysis of Arabidopsis further revealed that biosynthetic processes associated with sulfur compounds (in particular cysteine and glucosinolates) were the most significantly enriched in seedlings treated with *Pf* SS101 as compared to the control plants and to plants treated with the *cysH* mutant (Cheng *et al*. 2017). These results indicated that *Pf* SS101 modulates sulfur metabolism in Arabidopsis confirming and extending results from Meldau *et al.* (2013) and Aziz *et al*. (2016) who attributed modulation of sulfur metabolism as a key mechanism of growth promotion and induction of lateral roots of tobacco and Arabidopsis by different *Bacillus* strains.

In the present study, we investigated the effects of sulfur metabolism (i.e. effects of the *cysH* mutation) in *Pf* SS101 on the shoot metabolome of Arabidopsis. To that end, we adopted a nontargeted metabolomics approach to assess the differences between the shoot metabolomes of Arabidopsis seedlings treated with either *Pf* SS101 or with *cysH*-mutant 20H12. Furthermore, we investigated if strain *Pf* SS101 can induce similar phenotypic and

metabolome changes in shoots of the related Brassicaceous crop plant Broccoli and if also for Broccoli these changes are associated with sulfur metabolism. The *Pf* SS101-mediated phenotypic responses investigated for two Broccoli cultivars include root and shoot growth as well as induced resistance against two pathovars of *Xanthomonas campestris*, an important bacterial leaf pathogen of Broccoli and other cruciferous crops (Monteiro *et al.*, 2005).

Materials and methods

Plant material and growth

Seeds of *Arabidopsis thaliana* Columbia (Col-0) were surface-sterilized as previously described (van de Mortel *et al.*, 2012). Seeds of the two Broccoli (*Brassica olearacea* var. italica) cultivars Coronado and Malibu were kindly provided by Bejo Seeds (Trambaan1, 1749 CZ Warmenhuizen, The Netherlands). Surface sterilization of the Broccoli seeds was performed by immersing 2 - 3 g of seeds for 30 min in 30 ml of 1% (v/v) sodium hypochlorite supplemented with 0.1% (v/v) of Tween 20 followed by 3 washes with ample sterile distilled water. For the Arabidopsis assays, sterile seeds were sown on 90-mm-diameter Petri dishes containing 20 ml half-strength Murashige and Skoog (MS) agar media, containing 0.5% sucrose (w/v) and 1.2% plant agar (w/v). For the Broccoli assays, five sterile seeds were sown on 140-mm-diameter petri dishes containing 50 ml of half-strength MS agar. The plates were then placed in a climate chamber maintained at 21°C /21°C day/night; 180 µmol light $m^{-2}s^{-1}$, 16 h light/8 h dark cycle and 70% relative humidity. After a week of Arabidopsis growth and five days of Broccoli growth, roots of each seedling were inoculated with a 2 µl of bacteria suspension (~10^9 cells ml^{-1}). After inoculation, plants were placed back in the same growth chamber until harvest.

Bacterial strains and culture conditions

Pseudomonas fluorescens strain SS101 (*Pf* SS101) was originally isolated from the wheat rhizosphere (de Souza *et al.*, 2003). *CysH*-mutant 20H12 of *Pf* SS101 was generated by site-directed mutagenesis as described by Cheng *et al*. (2017). *Pf* SS101 and mutant 20H12 were cultured in King's medium B (KB) at 25°C for 16h. Broccoli leaf pathogens *Xanthomonas campestris* pv. armoraciae (*Xca*) and *Xanthomonas campestris* pv. campestris (*Xcc*) were kindly provided by Bejo Seeds and were cultured in Luria Bertani (LB) medium (Lennox, Carl Roth) at 25°C for 16h. Bacterial cells were collected by centrifugation, washed three times with 10 mM $MgSO_{4,}$ and resuspended in 10 mM $MgSO_4$ to a final density of 10^9 cells ml^{-1} (OD_{600} = 1.0).

Disease assay for induced resistance against the leaf pathogen *Xanthomonas*

For infection, the first true leaves of the Broccoli seedlings were pierced and 2 µl (10^9 cells

ml^{-1}) of the bacterial pathogens *Xca* and *Xcc* inoculum was applied at 11 days post inoculation (dpi) of *Pf* SS101 or the *cysH* mutant to the roots. Ten days after pathogen challenge, disease severity on the shoot was assessed by determining the migration of the lesion from the inoculation spot to other parts of the shoot based on a 0-5 ordinal scale as shown in the Supplementary Material (**Figure S3**): 1 = no necrosis or migration, 2 = necrosis of the treated leaf, 3 = migration of the lesion to the leafstalk of the treated leaf, 4 = visible necrotic or water-soaked lesions of the neighboring (nontreated) leaf, and 5 = infection of the entire shoot. Severity values were converted to 0 to 100 Disease severity index (DSI) according to the following equation used by (Vieira *et al.*, 2012). DSI (%) = ∑ (scores of all plants)/ [Maximum disease score x (total number of plants)] x 100. Next to this disease severity assessment, treated Broccoli shoots were collected, ground in a sterile mortar and suspended in 50 mL Falcon tube to measure its biomass. Samples were then vortexed for 60 s in 10 mM MgSO4, sonicated for 60 s, and again vortexed for 15 s. The suspension was serially dilution plated onto KB agar plates containing 100 µg ml^{-1} delvocid (DSM) to inhibit fungal growth and incubated for 3 days at 25 °C. Colonies with the typical phenotype of *Xca* and *Xcc* were counted and expressed as colony-forming units (cfu) mg^{-1} of shoot fresh weight.

Plant metabolite analysis

Sample preparation

Shoots of Arabidopsis and Broccoli were harvested at 11 days after root treatment with buffer (control), *Pf* SS101 or with mutant 20H12. For each plant species/cultivar X rhizobacteria combination, 4 biological replicates were used with ten Arabidopsis and five Broccoli seedlings per replicate. In brief, shoots were snap frozen in liquid nitrogen and ground to fine powder under continuous cooling and kept at -80 °C until further use. To extract semi-polar secondary metabolites, 300 µL of 99.89% methanol containing 0.13% (v/v) formic acid was added to 100 mg plant material in 2 ml round bottom Eppendorf tubes, and sonicated for 15 min followed by centrifugation for 15 min at 20,000 x *g*. The supernatants were transferred to 96-well filter plates (AcroPrepTM, 350 µl, 0.45µm, PALL), vacuum filtrated to the 96-deep-well autosampler plates (Waters) using a Genesis Workstation (Tecan Systems).

Metabolite analysis

An UltiMate 3000 U-HPLC system (Dionex) was employed to create a 45-minutes linear gradient of 5-35% (v/v) acetonitrile in 0.1% (v/v) formic acid (FA) in water at a flow rate of 0.19 ml per min. 5 µl of each extract was injected and compounds were separated on a Luna C18 column (2.0 x 150 mm, 3µm; Phenomenex) maintained at 40 °C (De Vos *et al.*, 2007). The detection of compounds eluting from the column was carried out with a Q-Exactive Plus Orbitrap FTMS mass spectrometer (Thermo Scientific). Full scan MS data were generated with electrospray in switching positive/negative ionization mode at a mass resolution of

35,000 (FWHM at m/z 200) in a range of m/z 95-1350. Subsequent MS/MS experiments for identification of selected metabolites were performed with separate positive or negative electrospray ionization at a normalized collision energy of 27 and a mass resolution of 17,500. The ionization voltage was optimized at 3.5 kV for positive mode and 2.5 kV for negative mode; capillary temperature was set at 250 °C; the auxiliary gas heater temperature was set to 220 °C; sheath gas, auxiliary gas and the sweep gas flow were optimized at 36, 10 and 1 arbitrary units, respectively. Automatic gain control was set a 3e6 and the injection time at 100 ms. External mass calibration with formic acid clusters was performed in both positive and negative ionization modes before each sample series.

LC-MS data processing and analysis

Peak picking, baseline correction, and mass signal alignment of the LC-MS data were performed using Metalign software (Lommen, 2009). The mass features were considered as a signal if they were detected in at least 3 biological replicates of a treatment with a signal intensity 3 times higher than the background noise value. Then, mass features originating from the same metabolites were clustered based on retention window and their correlation across all measured samples, using MSClust software (Tikunov *et al.*, 2012). After this, so-called centrotypes representing reconstructed putative metabolites mass spectra were selected, of which relative abundance was represented by the Measured Ion Count (MIC), which is the sum of the ion count values (corrected by their membership) for all measured cluster ions in a given sample. ANOVA with Benjamini–Hochberg false discovery rate (BH-FDR) correction ($P < 0.05$) and fold changes more or less than 2.0 were applied to identify mass signals that were significantly changed in bacteria-treated to control samples. Then, the bootstrapping analysis we performed to weed out duplicate signals within each mass mode and between two mass modes (positive and negative). Data transformation and scaling were performed in GeneMaths XT 1.6 (www.applied-maths.com). Transformed and scaled values were used for hierarchical cluster analysis using Pearson's correlation coefficient and Unweighted Pair Group Method with Arithmetic Mean (UPGMA).

Metabolites annotation of MS signals was carried out based on selection of pseudomolecule ions from the masses in the MSClust-reconstructed metabolites, first by matching their accurate masses plus retention times to previously reported metabolites present in Arabidopsis and Broccoli on the same LC-MS system and similar chromatographic conditions. Second, if compounds were not yet present in this experimentally obtained dedicated database, KEGG and HMDB databases basis MS/MS annotation that were mounted on MAGMa online tool (Ridder *et al.*, 2013) were primarily applied with a maximum deviation of observed mass from calculated of 5 ppm. In addition, some annotations were complemented by the aid of other publicly available compound libraries, including PubChem (https://pubchem.ncbi.nlm.nih.gov/) and Metlin (http:// metlin.scripps.edu/).

Statistical analysis

Changes in shoot biomass and pathogen incidence between treatments were analyzed with R Studio software (Version 3.6.1). The data for plant shoot and root biomass were statistically analyzed by two-way analysis of variance (ANOVA). A Tukey-HSD test was used to separate group mean values when the ANOVA was significant at $P < 0.05$. For the disease severity data, beta regression analysis was employed to examine the interaction effect of two independent variables (Rhizobacteria and Broccoli cultivars) on disease severity of the two bacterial pathogens using ("betareg") package in R.

Results

Role of the *cysH* gene of *P. fluorescens* SS101 in plant growth promotion

Treatment of Arabidopsis roots with *Pf* SS101 led to a significant increase in total plant biomass (62.8% ± 4.6) (**Fig 1b1**). Inoculation with *cysH*-mutant 20H12 also increased plant biomass (35.1% ± 4.8) relative to the untreated control, but the magnitude of the growth promotion was significantly less than that observed for wild type *Pf* SS101. *Pf* SS101 significantly increased root biomass (44.5% ± 0.6) whereas *cysH*-mutant 20H12 did not affect root biomass and did not have major effects on root architecture as observed for wild type *Pf* SS101 which reduces the length of the primary root and enhances lateral root formation (**Fig 1a** and **1b3**).

For the two Broccoli cultivars, the impact of *Pf* SS101 and mutant 20H12 on plant growth was different from that observed for Arabidopsis. In Broccoli, there was a significant interaction effect between the Broccoli cultivars and the rhizobacteria (wild type/mutant) for the shoot, root and total biomass (Supplementary **Table S1**). Overall, the total biomass of both Broccoli cultivars upon root treatment with *Pf* SS101 showed no significant changes relative to the non-treated controls. However, *Pf* SS101 significantly affected biomass allocation to shoot and roots with significant reductions of the shoot biomass in both cultivars (-22.1% ± 2.6 and -15.6% ± 5.1 in Coronado and Malibu, respectively) and significant increases in root biomass (71.7% ± 14.2 in Coronado and 29.0% ± 5.0 in Malibu) (**Fig 1**). Mutant 20H12 significantly enhanced total biomass of Broccoli cultivar Malibu but not of cultivar Coronado. The change in biomass allocation to shoot and roots was not as apparent for mutant 20H12 as it was for wild type *Pf* SS101. Compared to wild type *Pf* SS101, however, the total biomass of both Broccoli cultivars was significantly higher in the 20H12 treatment. Collectively these results suggest that sulfur assimilation in *Pf* SS101 contributes positively to growth promotion of Arabidopsis, whereas for Broccoli it has a neutral to negative effect on growth depending on the cultivar.

To determine if these differential effects on plant biomass were associated with differences

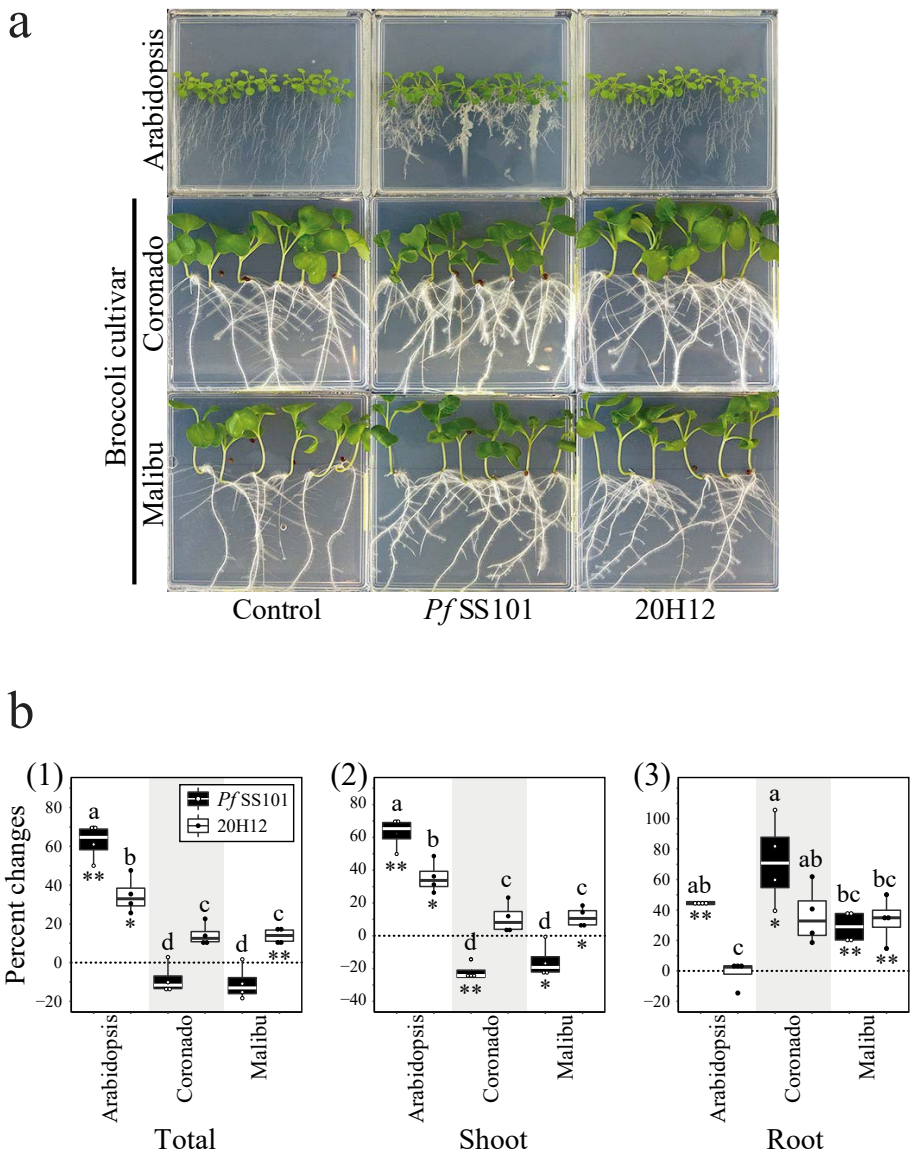

Fig 1. Phenotypic changes in Arabidopsis and Broccoli seedlings upon root treatment by *P. fluorescens* SS101 or its *cysH* mutant 20H12. Photographs of MS agar plates with Arabidopsis, and two Broccoli cultivars (Coronado, Malibu) treated on the root tip with *Pf* SS101 (wild type) or its *cysH* mutant (20H12) (**a**). Percent change in fresh biomass of shoot and root of plants treated with rhizobacteria when compared to untreated plants (11dpi) (**b**). Means of percent changes in biomass with a different letter are significantly different among treatments according to two-way ANOVA (Tukey, $P<0.05$). Asterisks denote statistically significant differences (two-tailed Student's t test): * $P < 0.05$; ** $P < 0.01$ of rhizobacteria treated plants when compared to the controls. For each plant species, four independent biological replicates were used with 10 seedlings of Arabidopsis and 5 of Broccoli per biological replicate. *Pf* SS101: *Pseudomonas fluorescens* SS101, 20H12: *cysH* gene mutant of *Pf* SS101.

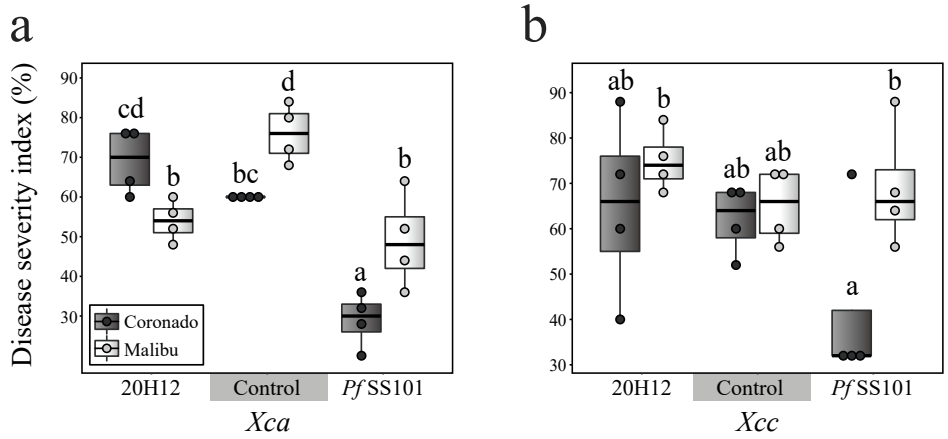

Fig 2. Rhizobacteria-mediated resistance in two Broccoli cultivars, Coronado and Malibu, against the bacterial leaf pathogens *Xanthomonas campestris*: *Xanthomonas campestris* pv. armoraciae (*Xc*a) (**a**) and *Xanthomonas campestris* pv. campestris (*Xcc*) (**b**). Prior to pathogen inoculation on the leaves, roots of each Broccoli cultivar were treated with *P. fluorescens* SS101 or its *cysH*-mutant 20H12 and incubated for 11 days. For the disease severity caused by *Xca* or *Xcc*, Broccoli seedlings from four biological replicates were individually scored (n = 20). Disease severity was scored on a scale from 0-5, where 1 = no necrosis or migration, 2 = full infection of the treated leaf, 3 = migration of the infection to the leafstalk of the treated leaf, 4 = infection of the neighboring leaf, and 5 = infection of the entire seedling (see supplementary material **Fig S3**). Different letters above bars indicate statistically significant differences based on beta regression analysis followed by Tukey test ($P < 0.05$).

in root colonization, rhizosphere population densities of *Pf* SS101 and *cysH*-mutant 20H12 were assessed at 11 dpi. The results showed that for Arabidopsis and for the two Broccoli cultivars, mutant 20H12 generally established up to 10-fold higher rhizosphere population densities than *Pf* SS101: 20H12 established population densities ranging from 2.0 ± 0.1 x 10^6 to 5.3 ± 0.3 x 10^6 CFU mg^{-1} whereas densities of *Pf* SS101 ranged from 2.2 ± 0.3 x 10^5 to 9.9 ± 0.5 x 10^5 CFU mg^{-1} (Supplementary **Table S2**). These results indicate that the *cysH* gene adversely affects root colonization of Arabidopsis and Broccoli by *Pf* SS101. When we plotted the different rhizobacterial densities against the plant biomass changes relative to the non-treated controls (Supplementary **Fig S2**), no overall consistent pattern was found: higher rhizobacterial population densities were associated with positive, negative or no changes in shoot and root biomass of the treated plants.

Role of the *cysH* gene of *P. fluorescens* SS101 in induced resistance

For the two Broccoli cultivars, we also looked into the effect of root inoculation with *Pf* SS101 or the *cysH*-mutant 20H12 on infection of the leaves by two pathovars of the bacterial leaf pathogen *Xanthomonas campestris*. Broccoli cultivar Coronado treated with *Pf* SS101 and challenged by *Xanthomonas campestris* pv. armoraciae (*Xca*) showed significant reduction in disease severity, whereas root treatment with mutant 20H12 was not effective

(**Fig 2a**). By contrast, both *Pf* SS101 and mutant 20H12 induced resistance in cultivar Malibu against *Xca* (**Fig 2**). However, *Pf* SS101 and mutant 20H12 had no significant impact on *Xcc* severity for both Broccoli cultivars (**Fig 2B**). The results further showed that the qualitative disease severity index correlated, in most cases, with the cell density of the two *Xanthomonas* pathovars, i.e. a higher disease severity index corresponded to a higher cell density of the *Xc* pathovars in the leaves (Supplementary **Fig S4**). An exception was the density of *Xcc* in leaves of *Pf* SS101-treated Malibu seedlings where a 50-fold reduction of the *Xcc* density in the leaves relative to the nontreated control was not accompanied by a lower disease severity (Supplementary **Fig S4**).

Effect of *P. fluorescens* SS101 and the *cysH* gene on the plant metabolome

Untargeted metabolome analysis was employed to investigate the impact of the *cysH* gene mutation of *Pf* SS101 on changes in the shoot secondary metabolome and to identify potential associations with the phenotypic changes induced by these rhizobacteria as descirbed above. The shoot metabolites that were significantly altered (fold change (FC) >2, $p < 0.05$ in ANOVA (Benjamini and Hochberg)) upon root treatment by *Pf* SS101 or its *cysH*-mutant 20H12 were used for principal component analysis (PCA) and hierarchical cluster analysis (HCA) for Arabidopsis and Broccoli.

Arabidopsis

From the total of 725 metabolites detected in Arabidopsis shoots in positive or negative ionization mode, 128 (18%) metabolites were significantly different between the treatments. Abundance and fold changes of each plant metabolite are shown in Supplementary Material, **Table S5**. PCA of the metabolites revealed a clear discrimination between treatments with the first three principal components explaining 90.3% of the total variance (**Fig 3a**). The first principal component (PC1) accounted for 58.3% of the total variance and associated with metabolites that showed greater depletion or accumulation in plants treated with *Pf* SS101 and 20H12 when compared to the control (**Fig 3b**, clusters **1-2** (depleted) and clusters **4-5 (**accumulated)). Metabolites in cluster **1** showed significant depletion in plants treated with *Pf* SS101 and include the short chain (C-4) isoleucine-derived aliphatic 2-methylbutyl glucosinolate (glucocleomin), amino acids and derivatives such as arginine and N-acetyl-L-tyrosine, and fattyl acyl glycosides such as (R)-pantothenic acid 4'-O-b-D-glucoside. Cluster **2** comprises metabolites that were depleted in plants treated with both *Pf* SS101 and the mutant 20H12, and the depletion was more pronounced on plants treated with *Pf* SS101. Some of the identified metabolites in this cluster include an amino acid and derivatives such as glutamine and N-(1-deoxy-1-fructosyl)proline, 5-oxoproline, fatty acyl glycosides and a hydroxycinnamic acid O-feruloylquinic acid. Metabolites that were increased by the *Pf* SS101 treatment are shown in Cluster **4** and include a long chain (C-8) aliphatic glucosinolate 8-methylthiooctyl glucosinolate, a hydroxycinnamic acid glucuronide sinapinic acid-O-

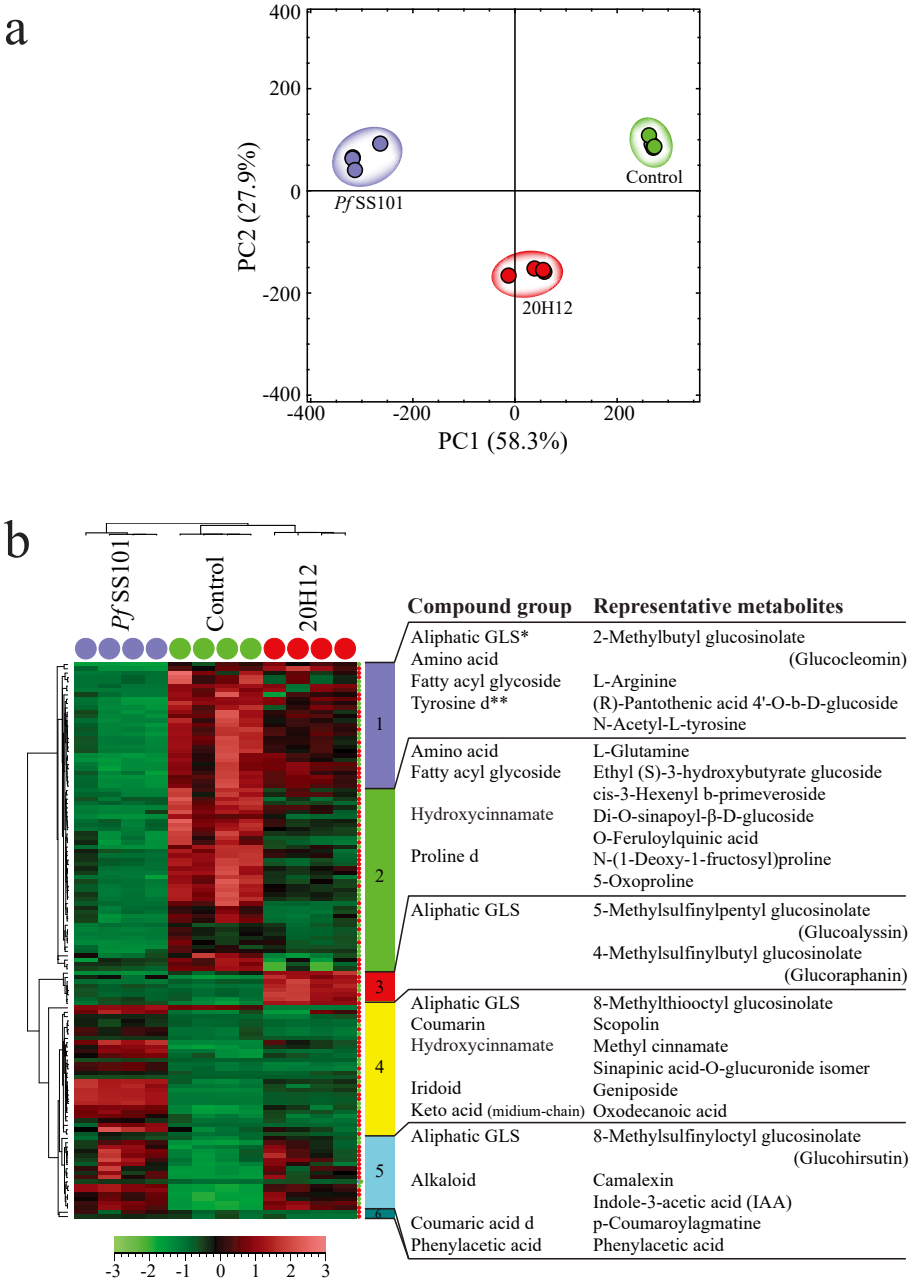

Fig 3. Metabolome changes in Arabidopsis shoots upon root treatment by *P. fluorescens* SS101 or its *cysH* mutant 20H12. Shown are the results of the principal component analysis (PCA) (**a**) and hierarchical cluster analysis (HCA) (**b**) based on differentially regulated semi-polar metabolites. In the HCA, various metabolite clusters are indicated by different colors and when none of the metabolites in a given cluster was annotated, the cluster number was omitted (Clusters 3, 5, and 10 in **Fig b**). * GLS=glucosinolate. ** d=derivative.

glucuronide, a medium chained keto acid oxodecanoic acid and the coumarin scopolin (see cluster **4**). Cluster **5** represents metabolites that were enhanced in both *Pf* SS101 and 20H12 treatments and include a long chain (C-8) aliphatic glucosinolate 8-methylsulfinyloctyl glucosinolate (glucohirsutin), a hydroxycinnamic acid amide coumaroylagmatine, and stress-associated alkaloids such as camalexin (20.5-fold up in *Pf* SS101 and 17.3-fold up in 20H12) and indole-3-acetic acid (IAA) (8.4-fold in *Pf* SS101 and 6.9-fold in 20H12). The second principal component (PC2) explained 27.9% of the total variance and includes metabolites accumulated only in the 20H12 treatment (Cluster **3**). Here, 4-methylsulfinylbutyl glucosinolate (glucoraphanin) and 5-methylsulfinylpentyl glucosinolate (glucoalyssin), middle chained (C-4 and C-5, respectively) aliphatic glucosinolate, displayed 20H12-specific accumulation.

In conclusion, the most prominent similarities in shoot metabolome changes induced in Arabidopsis shoots by *Pf* SS101 and mutant 20H12 are enhanced levels of the plant growth hormone IAA and the stress- associated alkaloid camalexin. The most prominent differences in shoot metabolome affected by the *cysH* mutation involve medium chain keto acid and the long chain (C-8) aliphatic glucosinolate 8-methylthiooctyl glucosinolate (enhanced in the *Pf* SS101 treatment to greater level) and the middle chain (C-4 and C-5) aliphatic glucosinolates 4-methylsulfinylbutyl glucosinolate and 5-methylsulfinylpentyl glucosinolate (enhanced in the 20H12 treatment to greater level).

Broccoli

The *cysH* mutation in *Pf* SS101 also had substantial impact on Broccoli shoot metabolism (**Fig 4**). Detailed information about abundance and fold change of each metabolite is shown in Supplementary Material, **Table S6**. From the total of 1908 metabolites that were detected in the Broccoli shoot samples, 830 (44%) metabolites were significantly different between the *Pf* SS101 and 20H12 treatments. In PCA, the first three PCs explained 73.7% of the total variation. The first PC explained 33.9% of the total variation and corresponds to Broccoli metabolites that were enhanced or reduced in plants treated with *Pf* SS101 and the mutant 20H12. The magnitude of the alteration of these metabolites was greater in *Pf* SS101 treatment (i.e. cluster **5**: 307 metabolites; cluster **1**: 55 metabolites). Cluster **5**, the largest cluster of *Pf* SS101-enhanced metabolites, comprised metabolites associated with plant defense-related phenylpropanoid biosynthesis such as the flavonoids kaempferol-di/tri-(feruloyl/ caffeoyl/ coumaroyl) glycosides, quercetin-tri-coumaroyl glycoside, rutin, the hydroxycinnamates caffeic acid, ferulic acid, feruloylquinic acid, sinapic acid, chlorogenic acid, neocuscutoside C, and their derivatives, and resveratrol sulfoglucoside. In addition, some phenolic glucosides including ginnalin B, hydroxybenzaldehyde diglycoside, hydrojuglone glucoside, as well as antioxidant butenolides such as ascorbic acid (vitamin C) and dehydroascorbic acid also belonged to this metabolite cluster that was accumulated in the *Pf* SS101 treatment. Among the identified glucosinolates in cluster 5, the indole glucosinolate glucobrassicin and its

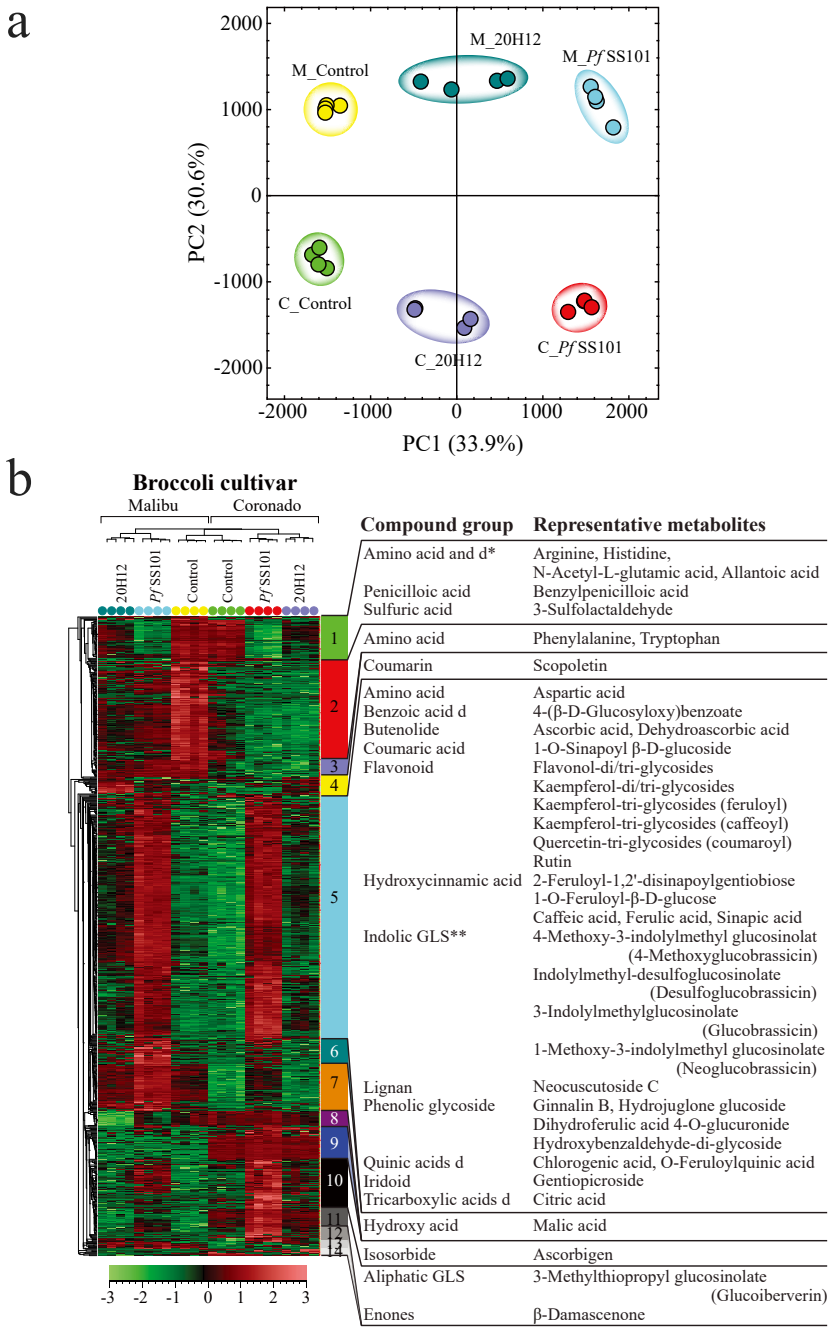

Fig 4. Metabolome changes in the shoots of two Broccoli cultivars, Coronado and Malibu upon root treatment by *P. fluorescens* SS101 or its *cysH* mutant 20H12. Shown are the results of the PCA (**a**) and HCA (**b**) based on differentially regulated semi-polar metabolites. In the HCA, various metabolite clusters are indicated by different colors; when none of the metabolites in a given cluster was annotated, the cluster number was omitted (Clusters 3, 6, 8, 9, 12, 13 and 14 in **Fig b**). * GLS=glucosinolate. ** d=derivative.

derivatives showed significant increases in the *Pf* SS101 treatment. Cluster **1** encompasses metabolites that were reduced in the *Pf* SS101 treatment and include some amino acids and derivatives, allantoic acid, benzylpenicilloic acid, as well as 3-sulfolactaldehyde. PC2 explained 30.6% of the total variation and was associated with metabolites that were intrinsically different in abundance between the two Broccoli cultivars (Clusters **2** and **7** (high in Malibu) and clusters **9** and **11** (high in Coronado). Furthermore, metabolites clusters **7**, **9** and **11** showed higher accumulation in plants treated with *Pf* SS101 when compared to the mutant 20H12. Metabolites that decreased in both Broccoli cultivars were grouped together in cluster **2** and encompassed phenylalanine and tryptophan, the building blocks for phenylpropanoid and indolic glucosinolate biosynthesis, respectively. In addition, malic acid was most abundant in Malibu (cluster **7**) while the level of the aliphatic glucosinolate glucoiberverin was much higher in Coronado (cluster **11**). The third PC explained 9.2% of the total variation and was associated with metabolites that were accumulated (cluster **4**) in both Broccoli cultivars or decreased in Malibu (cluster **8**) in plants treated with 20H12. In summary, the *cysH* mutation in *Pf* SS101 enhanced metabolites in Broccoli shoots that are associated with flavonoid, hydroxycinnamate, and indolic glucosinolate biosynthesis.

Discussion and conclusions

We previously showed that the rhizobacterium *Pf* SS101 promoted growth and altered root architecture of Arabidopsis, induced systemic resistance (ISR) and enhanced glucosinolate levels in roots and shoots (Van de Mortel *et al*. 2012). By screening a genome-wide mutant library of *Pf* SS101, we then identified the adenylsulfate reductase gene *cysH* as one of the key genes associated with growth promotion and ISR (Cheng *et al*., 2017). *CysH* is involved in sulfur assimilation and the biosynthesis of cysteine and methionine. Results from Cheng *et al*. (2017) further showed that addition of cysteine to the growth medium induced lateral root formation in Arabidopsis in a concentration dependent manner and triggered ISR against the bacterial leaf pathogen *Pseudomonas syringae.* Cysteine can enter into the glucosinolate biosynthesis pathway of plants by different routes including i) direct donation of reduced sulfur to glucosinolate biosynthesis, ii) incorporation of cysteine into methionine that, through a series of side chain elongation, S-glycosylation and other secondary modifications, ends up in the glucosinolate pool, and iii) conjugation of cysteine, glutamate and glycine to form glutathione (GSH) (Meister, 1995) which in turn acts as a sulfur donor for glucosinolate biosynthesis (Geu-Flores *et al.*, 2011). The results of our study confirmed that methionine-derived glucosinolate levels were increased in shoots of Arabidopsis upon root treatment with *Pf* SS101 and further showed higher levels of the long chain (C-8) aliphatic glucosinolates i.e. 8-methylthiooctyl glucosinolate and glucohirsutin. In leaves of Arabidopsis seedlings treated with the *cysH* mutant, the levels of long chain (C-8) aliphatic glucosinolates were lower and, instead, we observed higher levels of the C-4 and C-5 short chain aliphatic glucosinolates 4-methylsulfinylbutyl glucosinolate and 5-methylsulfinylpentyl glucosinolate,

respectively. The isoleucine-derived short chain (C-4) aliphatic glucosinolate 2-methylbutyl glucosinolate showed significant reduction in plants treated with *Pf* SS101. In Arabidopsis, side chain elongation of aliphatic glucosinolates is catalyzed by the MAM1/MAM3 proteins which condense 2-oxo acids and acetyl-CoA to extend the alkane C chain (Textor *et al.*, 2004; Textor *et al.*, 2007). Oxodecanoic acid that could be a potential substrate for chain elongation also showed greater accumulation in plants treated with *Pf* SS101. Interestingly, transcriptome analysis from our previous study also revealed that plants treated with *Pf* SS101 showed significantly higher expression of both MAM1 and MAM3 genes when compared to plants treated with mutant 20H12 or untreated plants (Cheng *et al.*, 2017). Collectively these results indicate that the *cysH* gene of *Pf* SS101 contributes to chain elongation of aliphatic glucosinolates in leaves of Arabidopsis.

For Broccoli, however, sulfur metabolism of *Pf* SS101 appeared to adversely affect shoot biomass as root treatment with the *cysH* mutant resulted in higher total biomass for both cultivars than observed for wild type *Pf* SS101. Overall, the total biomass of both Broccoli cultivars upon root treatment with *Pf* SS101 showed no significant changes relative to the non-treated controls, but *Pf* SS101 significantly affected biomass allocation to shoot and roots with significant reductions of the shoot biomass in both cultivars and significant increases in root biomass. Mutant 20H12 significantly enhanced total biomass of Broccoli cultivar Malibu but not of cultivar Coronado. The change in biomass allocation to shoot and roots was not as apparent for mutant 20H12 as it was for wild type *Pf* SS101. Collectively these results suggest that sulfur assimilation in *Pf* SS101 has a neutral to negative effect on growth depending on the cultivar. In the Broccoli shoot metabolome, *Pf* SS101 enhanced defense-associated metabolites mainly from the phenylpropanoid pathway such as flavonols including kaempferol and quercetin glycosides, various hydroxycinnamates such as caffeic acid and ferulic acid as well as antioxidants such as ascorbic acid and the indole glucosinolate glucobrassicin, indolylmethyl-desulfoglucosinolate (desulfoglucobrassicin) and 4-methoxy-3-indolylmethyl glucosinolate (4-methoxyglucobrassicin). By contrast, the levels of flavonoids, hydroxycinnamates and the indole glucosinolates showed slight to moderate increases in seedlings treated with the mutant 20H12. The enhanced level of glucobrassicin and its derivatives in *Pf* SS101-treated seedlings suggests that sulfur assimilation in *Pf* SS101 might gear tryptophan metabolism in Broccoli towards the biosynthesis of indolic glucosinolates instead of the growth-promoting phytohormone IAA. Furthermore, the high abundance of flavonoids particularly the flavonol subclass in plants treated with *Pf* SS101 might impact auxin biosynthesis, transport (Besseau *et al.*, 2007), distribution and its conjugation/degradation (Kuhn *et al.*, 2016) thereby affecting plant growth. Additionally, the higher accumulation of phenylpropanoids and other carbon and energy costly secondary metabolites in Broccoli seedlings treated with *Pf* SS101 could pose resource limitation to plant growth-related processes and lead to an adverse effect on plant growth.

Although sulfur assimilation by *Pf* SS101 adversely affected overall growth in Broccoli, it

led to enhanced defense against *Xca* in a Broccoli cultivar-specific manner. When cultivar Coronado was treated on the roots with *Pf* SS101 and challenged on the leaves with *Xca,* a significantly reduced disease severity was observed while root treatment with mutant 20H12 was not effective. By contrast, both *Pf* SS101 and mutant 20H12 reduced disease severity caused by *Xca* in cultivar Malibu. The extent of *Pf* SS101-mediated changes in the Broccoli shoot metabolome, particularly towards defensive secondary metabolites such as flavonoids, hydroxycinnamates, lignin, iridoid glycosides and indolic glucosinolates was substantial. These classes of metabolites significantly increased in the shoots of both Broccoli cultivars upon root tip treatment with *Pf* SS101. Moreover, cultivar Malibu treated with mutant 20H12 also showed higher levels of these classes of metabolites, while in cultivar Coronado the level of these metabolites remained unchanged or showed reduced increase. Phenolic compounds can have direct or indirect inhibitory effect on bacterial pathogens. The direct effect involves disruption of growth- and reproduction-related processes in the pathogens (Maddox *et al.*, 2010; Xie, Y *et al.*, 2015), while the indirect effect involves limiting the pathogen ingress by fortifying the plant cell wall (Reimers & Leach, 1991; Miedes *et al.*, 2014). Similarly, the indolic glucosinolate glucobrassicin was reported to have inhibitory activity against *Xcc* in *Brassica oleracea* (Madloo *et al.*, 2019) and 4-methoxyglucobrassicin was implicated as a signal molecule in plant defense against bacteria and fungi (Bednarek *et al.*, 2009). Hence, *Pf* SS101-mediated systemic resistance in Broccoli against *Xca* and to some extent against *Xcc* is likely related, at least in part, to the observed changes in these shoot secondary metabolites. In conclusion, our result showed that sulfur assimilation in *Pf* SS101 can affect its interaction with the host and exhibit growth-promoting or growth-retarding effects in a plant species- and even cultivar-dependent manner. Furthermore, sulfur assimilation by *Pf* SS101 had significant impact on both sulfur-containing and non-sulfur containing metabolites such as glucosinolates and phenylpropanoids, respectively. These changes in the shoot metabolome are likely associated with pathogen defense and their impact is dependent on the pathovar (*Xca/Xcc*) of the pathogen.

Interestingly, there were other metabolite changes observed in Broccoli shoots that appear to be disconnected from sulfur assimilation in *Pf* SS101. For example, the level of ascorbic acid (vitamin C), an antioxidant element (Foyer, 2017; Smirnoff, 2018), was enhanced in *Pf* SS101-treated seedlings, suggesting an upregulation of the l-galactose pathway of ascorbate synthesis. In addition, a significant increase of scopolin, a coumarin glycoside, was detected in our study. Recent work on Arabidopsis treated with growth-promoting *Pseudomonas simiae* strain WCS417 revealed enhanced levels of scopoletin in root exudates (Stringlis et al. 2018). They further showed that scopoletin is an iron-mobilizing phenolic compound with selective antimicrobial activity that shapes the root-associated microbial community (Stringlis, Ioannis A *et al.*, 2018). Our results show that scopolin accumulates also in the leaves. If these coumarins also have antibacterial activity against leaf pathogenic *Pseudomonas syringae* tested in our previous study or against the two *Xanthomonas campestris* pathovars of Broccoli tested in this study will be subject of future investigations to unravel the importance of coumarins in

the observed ISR response. Integration of metabolomics with transcriptomics followed by targeted gene editing of pathways in the host plant will be needed to validate the functional importance of several of the metabolome changes observed in the shoots of Arabidopsis and other plant species following treatment with growth-promoting rhizobacteria.

Acknowledgements

Seeds of two Broccoli cultivars (*Brassica olearacea* var. italic), Coronado and Malibu, together with Broccoli leaf pathogen *Xanthomonas* spp. were kindly provided by Bejo seed company (Trambaan1, 1749 CZ Warmenhuizen, The Netherlands). We are grateful to Bert Schipper and Henriëtte Vaneekelen for their help with LC MS analysis and pre-processing of metabolomics data.

Supplementary materials

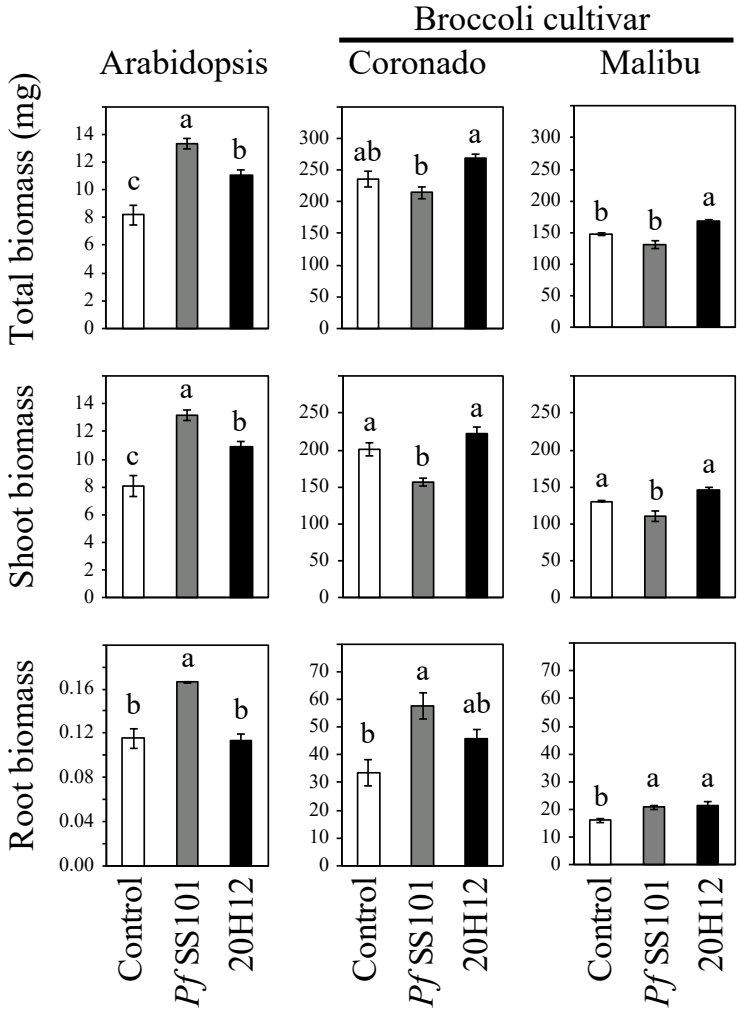

Fig S1. Biomass changes (absolute) of the whole plant, shoot and root after rhizobacteria treatment (11 dpi). Bars with different letters are significantly different among treatments according to one-way ANOVA (Tukey, $P<0.05$). For each plant species, four independent biological replicates were used with 10 seedlings of Arabidopsis and 5 of Broccoli per replicate. *Pf* SS101: *Pseudomonas fluorescens* SS101, 20H12: *cysH* gene mutant of *Pf* SS101.

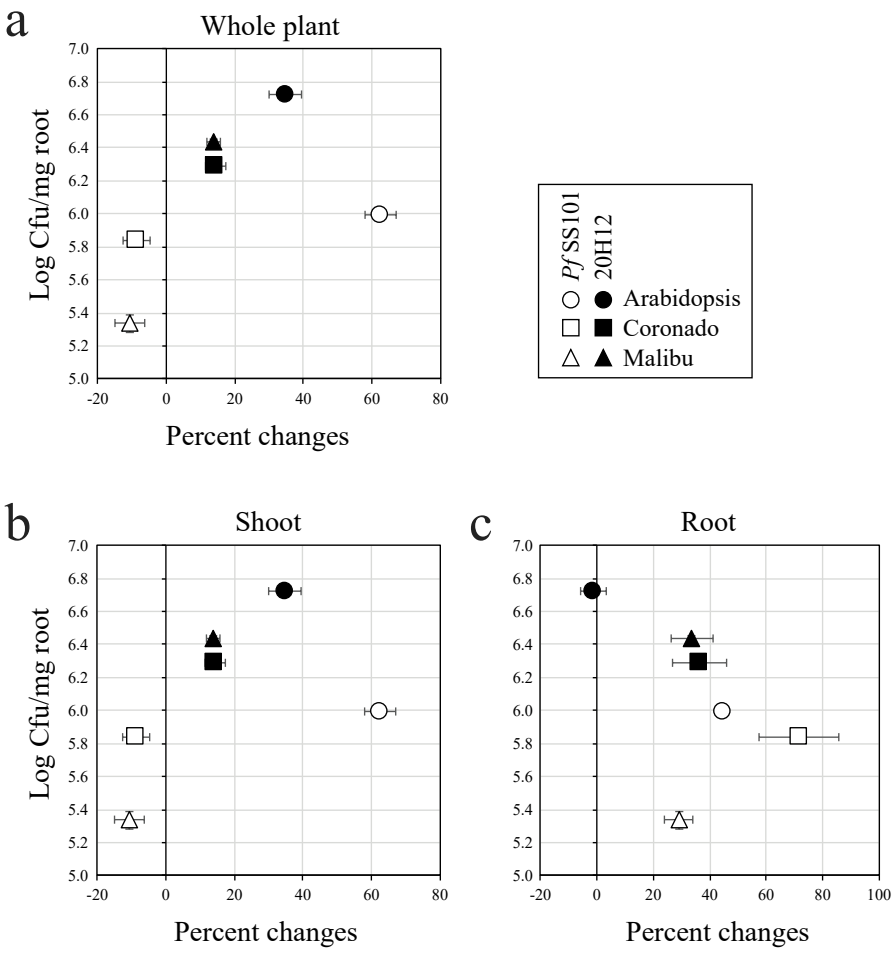

Fig S2. Correlation between host phenotypic changes and root colonization of *Pseudomonas fluorescens* SS101 and *cysH* mutant 20H12. Correlation between the rhizosphere population density of rhizobacteria (Log Cfu/mg root) and percent changes of biomass of whole plant (**a**), shoot (**b**) and root (**c**) of Arabidopsis and two Broccoli cultivars: Coronado and Malibu at 11dpi. *Pf* SS101: *Pseudomonas fluorescens* SS101, 20H12: *cysH* mutant of *Pf* SS101.

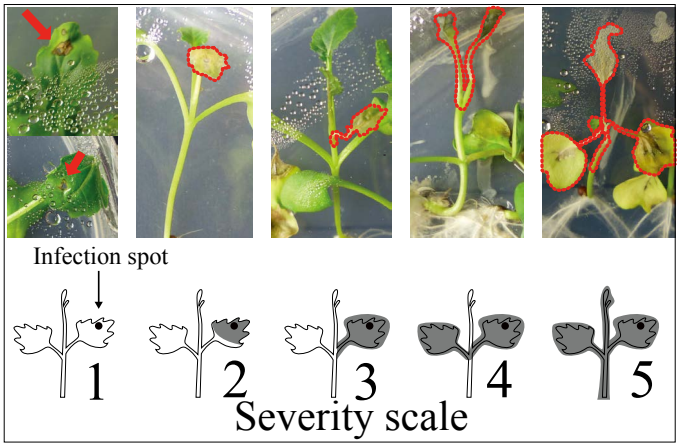

Fig S3. Disease severity scale used to assess the level of induced resistance in Broccoli at 11 dpi. 1 = no necrosis, no migration of the bacterial leaf pathogen *Xanthomonas campestris*, 2 = dispersal of the infection symptoms over the treated leaf, 3 = migration of the pathogen to the leafstalk of the treated leaf, 4 = migration to the neighboring leaf, and 5 = migration to the entire seedlings after infestation.

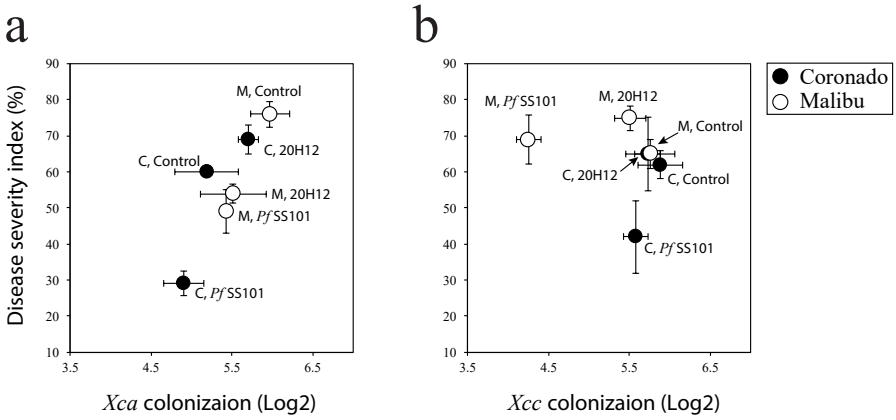

Fig S4. Correlation between disease severity of Broccoli and cell density of the bacterial pathogen *Xca* (**a**): *Xanthomonas campestris* pv. armoraciae, and *Xcc* (**b**): *Xanthomonas campestris* pv. campestris. C: Coronado, M: Malibu, Control: Broccoli without bacteria treatment, *Pf* SS101: *Pseudomonas fluorescens* SS101; 20H12: *cysH*-mutant of *Pf* SS101.

Table S1. Results of the analysis of variance ANOVA (type II) of phenotypic changes induced in tow Broccoli cultivars by root inoculation by *Pseudomonas fluorescens* strain SS101 or its *cysH* mutant 20H12. Shown are whole plant, shoot and root biomass changes in the two broccoli cultivars after root inoculation with *Pf* SS101: *Pseudomonas fluorescens* SS101, 20H12: *cysH*-mutant of *Pf* SS101.

Sample	Factor	Df	Sum Sq	Mean Sq	F value	Pr(>F)	
Whole plant fresh biomass relative change	Broccoli cultivars	2	11513	5757	94.559	2.83E-10	***
	Bacteria (WT vs Mutant)	1	260	260	4.263	0.0537	.
	Broccoli cultivars: Bacteria	2	3536	1768	29.043	2.32E-06	***
	Residuals	18	1096	61			
Shoot fresh biomass relative change	Broccoli cultivars	2	15124	7562	103.416	1.35E-10	***
	Bacteria	1	699	699	9.554	0.0063	**
	Broccoli cultivars: Bacteria	2	4373	2186	29.899	1.90E-06	***
	Residuals	18	1316	73			
Root fresh biomass relative change	Broccoli cultivars	2	4453	2226	8.477	0.00255	**
	Bacteria	1	3883	3883	14.783	0.00119	**
	Broccoli cultivars: Bacteria	2	2829	1415	5.386	0.01468	*
	Residuals	18	4728	263			

Significance codes: *** 0, ** 0.001, * 0.01. Bacteria (Wild type when compared to the mutant)

Table S2. Population density of *Pseudomonas fluorescens* SS101 and *cysH*-mutant 20H12 on roots of Arabidopsis and two Broccoli cultivars, Coronado and Malibu, at 11 dpi. *Pf* SS101: *Pseudomonas fluorescens* SS101, 20H12: *cysH*-mutant of *Pf* SS10*1*.

Plant species		Population density (Cfu/mg*)	
		***Pf* SS101**	**20H12**
Arabidopsis thaliana		$9.9 \pm 0.5 \times 10^5$	$5.3 \pm 0.3 \times 10^6$
Brassica oleracea var. italica	Coronado	$6.9 \pm 0.5 \times 10^5$	$2.0 \pm 0.1 \times 10^6$
	Malibu	$2.2 \pm 0.3 \times 10^5$	$2.7 \pm 0.1 \times 10^6$

CFU: Colony forming unit

*Values represent the average of 3 replicates ± SE of three replicates

Table S3. Effects of root treatment of two Broccoli cultivars with the beneficial rhizobacterium *Pseudomonas fluorescens* SS101, or with its *cysH*-mutant on the phylosphere population density of two pathovars of the bacterial leaf pathogen *Xanthomonas campestris* at 11 dpi. The two Broccoli cultivars are Coronado and Malibu; the two pathovars of *X. campestris* are *Xca*: *X. campestris* pv. armoraciae, and *Xcc*: *X. campestris* pv. campestris

Broccoli cultivars	Rhizobacteria pretreatments	Population density (Cfu/mg*)	
		Xca	*Xcc*
Coronado	Control	$4.4 \pm 3.3 \times 10^5$	$1.5 \pm 1.0 \times 10^6$
	Pf SS101	$1.2 \pm 0.6 \times 10^5$	$4.5 \pm 1.5 \times 10^5$
	20H12	$5.8 \pm 1.9 \times 10^5$	$6.4 \pm 2.1 \times 10^5$
Malibu	Control	$1.6 \pm 1.1 \times 10^6$	$1.1 \pm 6.2 \times 10^6$
	Pf SS101	$2.7 \pm 0.3 \times 10^5$	$2.1 \pm 0.1 \times 10^4$
	20H12	$8.5 \pm 5.4 \times 10^5$	$4.0 \pm 1.2 \times 10^5$

Cfu: Colony forming unit

*Values represent the average of 3 replicates ± SE of three replicates

Table S4. Results of the beta regression analysis of disease severity caused by *Xanthomonas* on leaves two Broccoli cultivars (Coronado and Malibu) that were pretreated on the roots with *Pseudomonas fluorescens* SS101 or its *cysH*-mutant.

Pathovar	model term	df1	df2	F.ratio	p.value
Xca	Rhizobacteria	2	Inf	43.681	<.0001
	Genotype	1	Inf	7.058	0.0079
	Rhizobacteria:Genotype	2	Inf	17.234	<.0001
Xcc	Rhizobacteria	2	Inf	2.878	0.0562
	Genotype	1	Inf	6.523	0.0106
	Rhizobacteria:Genotype	2	Inf	2.253	0.105

Table S5. Annotation of Arabidopsis shoot metabolites that showed significant change in their abundance after root inoculation with rhizobacterium *Pf* SS101: *Pseudomonas fluorescens* SS101, or its mutant 20H12: *cysH*-mutant of *Pf* SS101. Fold changes were calculated by dividing the abundance of each metabolite to the non-treated control. Cluster numbers are associated with the cluster in **Fig 3b.**

Cluster	RT(m)	Mass(D)	m/z	Compound	Formula	Δ ppm to data base	Classification	data base	Fold change	
									Pf SS101	20H12
1	19.9	388.0738	[M-H]-	Glucocleomin (2-Methylbutyl glucosinolate)	C12H23NO9S2	-0.78	Aliphatic GLS	KEGG	-2.09	-1.29
1	1.6	175.1189	[M-H]+	L-Arginine	C6H14N4O2	-0.46	Amino acid	KEGG	-2.15	-1.13
1	15.7	380.1559	[M-H]-	(R)-Pantothenic acid 4'-O-b-D-glucoside	C15H27NO10	-0.97	Fatty acyl glycoside	HMDB	-4.20	-1.55
1	11.3	222.0771	[M-H]-	N-Acetyl-L-tyrosine	C11H13NO4	-0.43	Tyrosine and derivative	HMDB	-3.25	-1.63
2	7.2	228.0501	[M-H]+	Stizolobic acid	C9H9NO6	-0.73	Amino acid	KEGG	-2.33	-1.68
2	1.9	145.0617	[M-H]-	L-Glutamine or (C05100)	C5H10N2O3	-1.12	Amino acid	KEGG	-2.27	-1.54
2	7.1	138.0559	[M-H]-	Gabaculine	C7H9NO2	-0.73	Benzoic acid	KEGG	-2.32	-1.63
2	27.7	395.191	[M-H]+	cis-3-Hexenyl b-primeveroside	C17H30O10	-0.34	Fatty acyl glycoside	HMDB	-3.70	-1.88
2	13.8	293.1241	[M-H]-	Ethyl (S)-3-hydroxybutyrate glucoside	C12H22O8	-0.26	Fatty acyl glycoside	HMDB	-2.42	-1.74
2	6.1	278.1234	[M-H]+	N-(1-Deoxy-1-fructosyl)proline	C11H19NO7	-0.16	Proline and	HMDB	-2.35	-1.61
2	3.0	130.05	[M-H]+	5-Oxoproline or (C01877), (C04282)	C5H7NO3	0.86		KEGG	-2.06	-1.66
2	37.0	591.1718	[M-H]-	Di-O-sinapoyl-beta-D-glucoside	C28H32O14	-0.29	Coumaric acid	KEGG	-2.17	-1.40
2	37.0	369.1178	[M+H]+	O-Feruloylquinic acid	C17H20O9	-0.48	Quinic acid	KEGG	-2.44	-1.45
3	3.9	450.0566	[M-H]-	Glucoalyssin (5-methylsulfinylpentyl glucosinolate)	C13H25O10S3N1	-0.41	Aliphatic GLS	KEGG	1.17	2.06
3	3.2	436.0409	[M-H]-	Glucoraphanin (4-Methylsulfinylbutyl glucosinolate)	C12H23O10S3N1	-0.46	Aliphatic GLS	KEGG	1.26	1.47
4	12.7	163.0754	[M+H]+	Methyl cinnamate	C10H10O2	0.11	Cinnamic acid derivative	KEGG	2.08	-1.36
4	14.9	355.1023	[M+H]+	Scopolin	C16H18O9	-0.23	Coumarin	KEGG	3.29	-1.37
4	14.9	399.0927	[M-H]-	Sinapinic acid-O-glucuronide isomer	C17H20O11	-1.59	hydroxycinnamic acid glycoside	HMDB	3.18	-1.45
4	12.7	387.1299	[M-H]-	Geniposide	C17H24O10	0.75	Iridoid	KEGG	2.14	-1.39
4	50.3	476.1084	[M-H]-	8-Methylthiooctyl glucosinolate (8MTO)	C16H31O9S3N1	-0.89	Aliphatic GLS	KEGG	2.12	1.31
4	23.3	187.1331	[M+H]+	3-Oxodecanoic acid	C10H18O3	1.24	Medium-chain keto acid	HMDB	16.49	3.07
5	20.4	492.1035	[M-H]-	Glucohirsutin (8-Methylsulfinyloctyl glucosinolate)	C16H31O10S3N1	-0.42	Aliphatic GLS	KEGG	4.48	3.49
5	42.5	201.0479	[M+H]+	Camalexin	C11H8N2S	2.17	Alkaloid	PubChem	20.51	17.31
5	44.0	176.0706	[M+H]+	Indole-3-acetic acid (IAA)	C10H9NO2	0.24	Alkaloid	KEGG	8.40	6.92
5	11.3	275.1513	[M-H]-	p-Coumaroylagmatine II	C14H20N4O2	0.05	Coumaric acid	KEGG	3.15	2.21
5	21.7	135.0451	[M-H]-	Phenylacetic acid	C8H8O2	-5.85	Phenylacetic acid	KEGG	2.21	2.81

Table S6. Annotation of Broccoli shoot metabolites that showed significant change in their abundance after root inoculation with rhizobacterium *Pf* SS101: *Pseudomonas fluorescens* SS101, or its mutant 20H12: *cysH*-mutant of *Pf* SS101. Fold changes were calculated by dividing the abundance of each metabolite to the non-treated control. Cluster numbers are associated with the cluster in **Fig 4b.**

Cluster number	RT (m)	Mass(D)	m/z	Compound	Formula	Δ ppm	Classification	data base	Fold change			
									Coronado		Malibu	
									Pf SS101	20H12	*Pf* SS101	20H12
1	1.8	154.062424	[M-H]-	Histidine	C6H9N3O2	-2.9	Amino acid	KEGG, Metlin	-2.1	-1.5	-2.0	-1.3
1	1.6	175.119202	[M+H]+	Arginine	C6H14N4O2	1.3	Amino acid	KEGG	-2.3	-1.4	-2.0	-1.3
1	3.0	188.056656	[M-H]-	N-Acetyl-L-glutamic acid	C7H11NO5	-2.2	Glutamic acid	KEGG	-3.9	-2.3	-3.0	-1.9
1	2.2	175.047012	[M-H]-	Allantoic acid	C4H8N4O4	-1.8	Alpha amino acid	KEGG	-4.7	-2.0	-3.0	-1.8
1	2.1	351.10257	[M-H]-	Benzylpenicilloic acid	C16H20N2O5S	1.6	Penicilloic acid	KEGG	-3.6	-2.6	-3.3	-2.2
1	3.2	152.986389	[M-H]-	3-Sulfolactaldehyde	C3H6O5S	0.4	Sulfuric acid	KEGG	-8.2	-4.5	-8.0	-3.1
2	3.1	166.086502	[M+H]+	Phenylalanine	C9H11NO2	0.8	Amino acid	KEGG	-1.5	-1.7	-1.5	-2.1
2	6.5	205.097321	[M+H]+	Tryptophan	C11H12N2O2	0.7	Amino acid	KEGG	-2.3	-3.2	-1.8	-3.8
2	43.2	631.276428	[M+H]+	Brassica napus non-fluorescent chlorophyll catabolite 3	C34H38N4O8	0.3	Tetrapyrrole	HMDB	-4.4	-3.8	-1.9	-2.2
4	15.8	193.049622	[M+H]+	Scopoletin or (C18079)	C10H8O4	0.2	Coumarin	KEGG	-8.9	2.1	19.4	6.5
5	5.8	298.096924	[M+H]+	Methylthioadenosine	C11H15N5O3S	0.2	Thionucleoside	KEGG	2.1	1.5	1.7	1.2
5	2.0	132.03035	[M-H]-	Aspartic acid	C4H7NO4	-2.8	Amino acid	KEGG	3.5	2.1	2.6	2.1
5	17.8	278.067352	[M-H]-	N-[4'-hydroxy-(E)-cinnamoyl]-L-aspartic acid	C13H13NO6	1.2	Aspartic acid	HMDB	3.3	1.9	2.3	1.4
5	13.5	299.077423	[M-H]-	4-(beta-D-Glucosyloxy)benzoate	C13H16O8	0.7	Benzoic acid	KEGG	40.0	1.6	5.0	-1.4
5	2.2	175.025177	[M-H]-	Ascorbic acid	C6H8O6	-1.2	Butenolide	KEGG	2.7	2.4	2.3	2.2
5	2.2	177.039734	[M+H]+	Ascorbic acid	C6H8O6	2.0	Butenolide	KEGG	4.5	3.6	2.5	2.2
5	4.3	173.009323	[M-H]-	Dehydroascorbic acid	C6H6O6	-3.1	Butenolide	KEGG	3.4	2.0	2.5	1.8
5	17.9	385.11441	[M-H]-	1-O-Sinapoyl beta-D-glucoside	C17H22O10	1.0	Coumaric acid	KEGG	3.7	1.6	2.1	1.2
5	17.2	355.102661	[M+H]+	Scopolin or (C00852) or (C08996)	C16H18O9	0.8	Coumarin	KEGG	3.1	1.5	2.3	1.4
5	33.3	577.15686	[M-H]-	Daidzein 4',7-diglucoside	C27H30O14	1.0	Flavonoid	HMDB	5.2	2.1	2.9	1.5
5	35.4	723.21521	[M-H]-	Flavonol 3-O-beta-D-glucosyl-(1->2)-beta-D-glucosyl-(1->2)-beta-D-glucoside	C33H40O18	1.4	Flavonoid	KEGG	4.3	2.1	2.7	1.5
5	20.8	947.247437	[M-H]-	Kaempferol 3-(2-feruloylsophoroside) 7-glucoside	C43H48O24	1.2	Flavonoid	HMDB	2.4	1.2	2.3	1.3
5	20.3	611.160583	[M+H]+	Kaempferol 3-O-beta-D-sophoroside or (C05625), (C17563)	C27H30O16	-0.2	Flavonoid	KEGG	3.7	1.7	2.6	1.5
5	18.0	935.245972	[M+H]+	Kaempferol 3-O-caffeoyl-sophoroside 7-O-glucoside or (HMDB0037938)	C42H46O24	0.8	Flavonoid	HMDB	2.1	1.2	3.0	1.7
5	20.8	949.261597	[M+H]+	Kaempferol 3-sophoroside 7-(2-feruloylglucoside) or (HMDB0040801), (HMDB0029269)	C43H48O24	0.8	Flavonoid	HMDB	2.3	1.2	2.7	1.4
5	30.5	739.210815	[M-H]-	Mauritianin	C33H40O19	2.3	Flavonoid	HMDB	3.4	1.7	2.6	1.4
5	18.0	933.231323	[M-H]-	Quercetin 3-[p-coumaroyl-(->6)-glucosyl-(1->2)-glucosyl-(1->2)-glucoside]	C42H46O24	0.7	Flavonoid	HMDB	2.3	1.2	3.2	1.8
5	30.1	739.210693	[M-H]-	Robinin	C33H40O19	2.1	Flavonoid	KEGG	5.4	2.5	3.0	1.5
5	20.3	609.146667	[M-H]-	Rutin	C27H30O16	0.9	Flavonoid	KEGG	3.4	1.5	3.0	1.6
5	28.9	665.173584	[M-H]-	Sudachiin B or (HMDB39088)	C30H34O17	1.9	Flavonoid	HMDB	5.0	2.0	5.3	2.2
5	38.8	561.162048	[M-H]-	Flavonol 3-O-beta-D-glucosyl-(1->2)-beta-D-glucoside	C27H30O13	1.3	Flavonoid	KEGG	10.3	4.0	5.4	2.5

Table S6. (Continued)

Cluster number	RT (m)	Mass(D)	m/z	Compound	Formula	Δ ppm	Classification	data base	Fold change			
									Coronado		Malibu	
									Pf SS101	20H12	*Pf* SS101	20H12
5	14.6	773.213074	[M+H]+	Kaempferol 3-sophorotrioside	C33H40O21	-0.5	Flavonoid	KEGG	2.3	1.1	1.7	1.2
5	33.9	547.146606	[M-H]-	Puerarin xyloside	C26H28O13	1.6	Flavonoid	KEGG	12.8	3.5	6.3	2.6
5	2.2	289.033173	[M-H]-	Sedoheptulose phosphate or (C19882)	C7H15O10P	0.5	Hexose phosphate	KEGG	4.1	2.0	3.9	1.6
5	40.0	929.27356	[M-H]-	2-Feruloyl-1,2'-disinapoylgentiobiose	C44H50O22	1.6	Hydroxycinnamate	HMDB	2.6	1.3	2.2	1.4
5	19.8	355.103882	[M-H]-	1-O-Feruloyl-beta-D-glucose	C16H20O9	-0.4	Hydroxycinnamate	KEGG	3.2	1.6	1.8	1.4
5	11.4	181.049728	[M+H]+	Caffeic acid	C9H8O4	0.8	Hydroxycinnamate	KEGG	3.2	2.0	2.0	1.7
5	11.4	341.088074	[M-H]-	Caffeic acid 3-glucoside or (C10433)	C15H18O9	0.7	Hydroxycinnamate	KEGG	2.9	1.9	2.0	1.7
5	18.7	195.065338	[M+H]+	Ferulic acid	C10H10O4	0.8	Hydroxycinnamate	KEGG	3.2	1.7	1.8	1.4
5	19.9	195.065308	[M+H]+	Ferulic acid	C10H10O4	0.7	Hydroxycinnamate	KEGG	2.2	1.6	1.4	1.5
5	16.7	225.075836	[M+H]+	Sinapic acid	C11H12O5	0.3	Hydroxycinnamate	KEGG	2.0	1.2	1.8	1.2
5	27.8	477.064667	[M-H]-	4-Methoxyglucobrassicin (4-Methoxy-3-indolylmethyl glucosinolate)	C17H22N2O10S2	0.7	Indolic GLS	KEGG	2.3	-1.1	1.7	-1.0
5	21.7	369.11145	[M+H]+	Desulfoglucobrassicin (Indolylmethyl-desulfoglucosinolate)	C16H20N2O6S	-0.1	indolic GLS	KEGG	3.9	1.8	3.3	1.9
5	21.7	447.054474	[M-H]-	Glucobrassicin (3-Indolylmethylglucosinolate)	C16H20O9S2N2	1.7	Indolic GLS	KEGG	5.1	1.9	3.8	2.0
5	34.5	477.064697	[M-H]-	neoglucobrassicin (1-Methoxy-3-indolylmethyl glucosinolate)	C17H22O10S2N2	0.8	Indolic GLS	KEGG	3.5	1.2	3.6	1.5
5	36.2	693.204773	[M-H]-	Sesaminol glucosyl-(1->2)-glucoside	C32H38O17	1.7	Lignan	HMDB	4.2	1.8	3.7	1.7
5	37.4	693.204773	[M-H]-	Neocuscutoside C	C32H38O17	0.7	Lignan glycoside	Metlin MS	5.9	2.1	4.4	2.0
5	4.5	315.072632	[M-H]-	Ginnalin B	C13H16O9	-0.7	Phenolic glycoside	Metlin MS	7.2	1.2	4.3	1.1
5	26.6	415.125183	[M-H]-	2-Hydroxybenzaldehyde O-[xylosyl-(1->6)-glucoside]	C18H24O11	1.4	Phenolic glycoside	HMDB	5.7	2.0	2.7	1.7
5	13.0	371.098541	[M-H]-	Dihydroferulic acid 4-O-glucuronide	C16H20O10	0.5	Phenolic glycoside	HMDB	4.7	1.9	3.8	2.0
5	38.9	339.107605	[M+H]+	Hydrojuglone glucoside	C16H18O8	0.5	Phenolic glycoside	HMDB	8.8	3.7	5.3	2.6
5	10.2	355.102448	[M+H]+	Chlorogenic acid	C16H18O9	0.2	Quinic acid	KEGG	3.9	1.9	2.3	1.4
5	37.9	369.118317	[M+H]+	O-Feruloylquinic acid I	C17H20O9	0.9	Quinic acid	KEGG	2.2	1.2	1.5	1.2
5	17.6	367.103668	[M-H]-	O-Feruloylquinic acid II	C17H20O9	-0.7	Quinic acid	KEGG	2.1	1.3	1.4	1.1
5	33.1	577.156799	[M-H]-	Glucofrangulin A	C27H30O14	0.8	Quinone	KEGG	3.2	-5.6	1.6	1.9
5	18.7	355.103821	[M-H]-	Gentiopicroside	C16H20O9	1.1	Secoiridoid	KEGG	3.5	1.7	1.9	1.3
5	34.1	469.081787	[M-H]-	(Z)-Resveratrol 3-(3''-sulfoglucoside) or (HMDB37073), (HMDB37076)	C20H22O11S	1.7	Stilbene	HMDB	2.8	2.0	2.3	1.7
5	2.1	195.050842	[M-H]-	D-Gluconic acid	C6H12O7	-0.9	Sugar acid	KEGG	3.2	1.7	2.1	1.5
5	3.0	191.019897	[M-H]-	Citric acid	C6H8O7	-2.4	Tricarboxylic acid	KEGG, Metlin	2.9	2.4	3.1	2.3
5	35.4	501.160126	[M+H]+	Nocardicin A	C23H24N4O9	-4.4		KEGG	4.6	2.2	2.9	1.6
7	14.9	339.107605	[M+H]+	p-Coumaroyl quinic acid or (C10432), (C10441)	C16H18O8	0.4	Quinic acid	KEGG	3.9	1.8	2.1	1.3
7	2.8	133.014282	[M-H]-	Malic acid	C4H6O5	-4.4	Hydroxy acid	KEGG, Metlin	2.0	2.3	2.5	2.0
10	24.1	306.097595	[M+H]+	Ascorbigen	C15H15NO6	1.2	Isosorbide	HMDB	7.1	2.7	6.5	2.7
11	12.1	406.031067	[M-H]-	Glucoiberverin (3-Methylthiopropyl glucosinolate)	C11H21NO9S3	1.3	Aliphatic GLS	KEGG	2.3	1.0	1.3	3.1

Table S6. (Continued)

Cluster number	RT (m)	Mass(D)	m/z	Compound	Formula	Δ ppm	Classification	data base	Fold change			
									Coronado		Malibu	
									Pf SS101	20H12	*Pf* SS101	20H12
11	34.4	191.14299	[M+H]+	beta-Damascenone	C13H18O	-0.3	Enone	HMDB	2.6	1.1	1.5	-1.4
12	16.2	165.054794	[M+H]+	p-Coumaric acid or (C00166), (C12621), (C01772)	C9H8O3	1.3	Hydroxycinnamate	KEGG	2.3	1.7	1.2	1.2
12	16.2	325.093597	[M-H]-	4-O-beta-D-Glucosyl-4-hydroxycinnamate or (C16827), (C05158)	C15H18O8	0.1	Hydroxycinnamate	KEGG	2.9	1.7	-1.1	1.1
12	2.2	209.066757	[M-H]-	Coriose or (C21043), (C02076)	C7H14O7	-2.9	Glycoside	KEGG	2.2	1.7	1.6	1.6
12	2.3	110.985336	[M-H]-	Hydroxymethylphosphonate	CH5O4P	-3.5	Phosphonic acid	KEGG	3.0	1.7	2.0	2.2
13	3.9	173.009308	[M-H]-	trans-Aconitic acid or (C05422)	C6H6O6	-3.2	Tricarboxylic acid	HMDB	2.1	3.7	2.4	1.7

Chapter 6

Transcriptome profiling of *Paraburkholderia graminis* colonizing roots of *Brassica oleracea*

Je-Seung Jeon, Desalegn W. Etalo, Fleur Gawehns-Bruning,
Ben Oyserman, Wilfred van Ijcken, Rutger Brouwer,
Victor J. Carrion, Jos M. Raaijmakers

Abstract

Beneficial rhizobacteria can positively affect plant growth and tolerance to biotic and abiotic stresses, while profiting from nutritious exudates released by the plant roots. To establish such a relationship, a variety of genes from each of the two organisms are expressed. Here we studied gene expression in a strain of *Paraburkholderia graminis* (*Pbg*) that promotes growth of Broccoli. We first show that only live *Pbg* cells enhanced Broccoli biomass whereas dead cells and cell-free culture supernatans and bacterial volatile organic compounds did not. Subsequent transcriptome analysis of *Pbg* colonizing the roots of two Broccoli cultivars showed a total of 380 differently expressed genes (DEGs). Genes involved in flagellar assembly, chemotaxis and motility as well as genes associated with nutrient uptake and (an) ion transport were upregulated in *Pbg* cells colonizing roots of Broccoli seedlings. Genes that were down-regulated involved genes associated with environmental changes and stress. Several *Pbg* genes showed cultivar-specific expression, including *Pbg* genes related to methionine import, symbiotic interaction and nitrate transport. These results suggest specific quantitative or qualitative differences in root traits (i.e. exudates, cellular architecture) between the two Broccoli cultivars. Collectively, our study provides a basis to further unravel the bacterial determinants and molecular mechanisms underlying plant growth promotion by the beneficial rhizobacterium *Pbg*.

Keywords: rhizobacteria-plant interaction; plant growth promotion; root colonization, gene expression

Introduction

The rhizosphere is a dynamic ecosystem where diverse interactions occur at the interface between the plant roots and the soil microbiome. Plants can release up to 21% of photosynthetically fixed carbon into the rhizosphere, thereby influencing microbiome assembly and functions (Clarkson & Hanson, 1980; Mendes *et al.*, 2011; Mendes *et al.*, 2013; Etalo *et al.*, 2018). While many members of the rhizosphere microbiome exert neutral effects on the plant, several members have a beneficial influence on plants (Raaijmakers *et al.*, 2009). The beneficial effects of these rhizobacterial species include plant growth promotion (Van Loon, 2007; van de Mortel *et al.*, 2012), induction of systemic resistance against pathogens or herbivores (Raaijmakers *et al.*, 2009; van de Mortel *et al.*, 2012; Pieterse *et al.*, 2014; Cheng *et al.*, 2017; Stringlis, Ioannis A *et al.*, 2018), and enhanced tolerance to abiotic stresses including salinity and drought (Dimkpa *et al.*, 2009; Bharti *et al.*, 2016; Vurukonda *et al.*, 2016). Several microbial traits involved in these beneficial effects have been identified (Han *et al.*, 2006; Nam *et al.*, 2006; Kim *et al.*, 2007; Sumayo *et al.*, 2013), but for many rhizobacteria there is still limited knowledge of the genes and traits expressed during root colonization and plant growth promotion.

On the plant side, Wang *et al*. (2005) showed for *Pseudomonas fluorescens* FPT9601-T5 enhanced expression of genes related to auxin and disease resistance, whereas genes associated with ethylene synthesis in Arabidopsis were down-regulated (Wang *et al.*, 2005). Pieterse and colleagues further showed that root inoculation with *P. simiae* WCS417r triggered induced systemic resistance (ISR) in Arabidopsis by inducing jasmonic acid or ethylene signaling in the leaves in response to infection by the bacterial leaf pathogen *P. syringae* pv. tomato (*Pst*) DC3000 (Pieterse *et al.*, 2001; Verhagen *et al.*, 2004). Recent studies by Ke *et al*. (2019) elegantly revealed that approximately 42% of a diverse set of rhizobacterial genera were able to quench the local root immune response. They further showed that a plant beneficial *Pseudomonas* strain suppressed plant immunity by lowering the pH via the secretion of gluconic acid which enabled colonization of the plant rhizosphere. For *P. fluorescens* SS101, Cheng *et al.* (2017) demonstrated that growth promotion and induced resistance in Arabidopsis against *Pst* DC3000 was associated with sulfur assimilation, auxin biosynthesis and transport, steroid biosynthesis and carbohydrate metabolism. Also for *Microbacterium* sp. strain EC8, Cordovez *et al*. (2018) showed that growth promotion of Arabidopsis via volatile organic compounds (VOCs) was associated with upregulation of Arabidopsis genes involved in the assimilation and transport of sulfate and nitrate. Interestingly, these plant growth-promoting rhizobacteria (PGPR) could affect gene expression during many developmental stages of the plant. For example, endophytic PGPR strain *Paraburkholderia phytofirmans* PsJN enhanced expression of Arabidopsis genes implicated in phytohormones auxin and gibberellin pathways in early ontogeny, while in later stages this strain triggered genes associated with flowering (Poupin *et al.*, 2013).

While the research focus of bacteria-plant interactions has predominantly been on phenotypic

and transcriptional responses of the plant, insight into the transcriptome of beneficial rhizobacteria on plant roots is still largely elusive for most interactions. Several studies demonstrated the impact of root exudates on bacterial gene expression or bacterial gene regulation. For example, sugar beet root exudates differently regulated genes in *Pseudomonas aeruginosa* involved in chemotaxis and type II secretion (Mark *et al.*, 2005) while maize exudates led to strong induction of *Bacillus amyloliquefaciens* genes involved in nutrient utilization, bacterial chemotaxis, motility and non-ribosomal synthesis of antimicrobial peptides and polyketides (Fan *et al.*, 2012). Collectively these studies suggested that specific constituents of root exudates affect bacterial motility. Contrary to this, it has been shown that genes involved in chemotaxis and motility in *Bacillus subtilis* were significantly suppressed in response to exudates of rice seedlings (Xie, S *et al.*, 2015) while maize root exudates enhanced expression of genes involved in stress responses and in metabolism and transport of nutrients (Fan *et al.*, 2012). By using a randomly barcoded mutagenesis approach, Cole *et al*. (2017) showed that several hundred genes of *Pseudomonas simiae* were involved in colonization of Arabidopsis roots. These included genes involved in carbon metabolism, amino acid transport and metabolism, cell wall biosynthesis, motility and a number of genes with yet unknown functions. Comparative analysis with colonization genes identified previously for *Pseudomonas putida* colonizing tomato roots showed limited overlap (Cole *et al.*, 2017), suggesting that the transcriptional responses in rhizobacteria are plant species and rhizobacterial species specific. Levy *et al*. (2018) sequenced 484 genomes of bacterial isolates from roots of Brassicaceae, poplar, and maize and identified thousands of plant-associated gene clusters by comparing 3,837 bacterial genomes. They discovered that genomes of plant-associated bacteria encode more carbohydrate metabolism functions and harbour fewer mobile elements than related non-plant-associated bacteria. They further validated candidates from sets of plant-associated genes and revealed that two mutants of *Paraburkholderia kururiensis* M130 showed reduced colonization of rice roots as compared to their parental strain. These genes encode an outer membrane efflux transporter from the nodT family, and a *Tir* chaperone protein (*CesT*).

For successful and broad application of beneficial rhizobacterial strains, it is important they can successfully colonize roots of cultivars of the same plant species and preferably also other plant species. Hence identifying common and specific genes involved in root colonization is instrumental in bio-prospecting for beneficial rhizobacteria. In this context, we studied the transcriptome of plant growth-promoting *Paraburkholderia graminis* during colonization of the roots of two Broccoli cultivars. *Paraburkholderia* is a monophyletic clade from the genus *Burkholderia* and classified as non-pathogenic environmental bacteria (Sawana *et al.*, 2014). Several species of this genus such as *P. phytofirmans*, *P. fungorum* and *P. graminis* have shown growth promotion of maize, strawberries and Arabidopsis (Ledger *et al.*, 2016; Mitter *et al.*, 2017; Rahman *et al.*, 2018) and have been implicated in the natural suppressiveness of soils to the soil-borne pathogen *Rhizoctonia solani* (Carrión *et al.*, 2018). In our previous study, we showed that *P. graminis* (*Pbg*) enhanced shoot biomass of Broccoli cultivars

Coronado and Malibu by approximately 70% and 40%, respectively. To begin to identify bacterial genes and mechanisms involved growth promotion, we investigated transcriptional responses in *Pbg* during colonization of roots of these two Broccoli cultivars. We first tested if *Pbg* needs to be alive to promote growth of Broccoli or if also dead cells, culture supernatant or bacterial volatile organic compounds (VOCs) can induce the same plant phenotype. Thereafter, transcriptome analysis of *Pbg* colonizing roots of Broccoli seedlings was performed by RNA-seq. Comparative transcriptome analysis revealed common and cultivar-specific expressions of genes that may play a critical role in plant growth promotion by *Paraburkholderia graminis*.

Materials and methods

Plant material and growth conditions

Seeds of Broccoli (*Brassica oleracea* var. italica) cultivars Coronado and Malibu were kindly provided by Bejo Seeds (Warmenhuizen, The Netherlands). Seed surface disinfection was performed by immersing 2 - 3 g of seeds for 30 min in 30 ml of 1% (v/v) sodium hypochlorite with 0.1% (v/v) Tween 20 followed by 3 subsequent rinses with ample sterile distilled water. After sterilization, five Broccoli seeds were sown on 140-mm-diameter petri dishes containing 50 ml of half-strength Murashige and Skoog agar media, containing 0.5% sucrose (w/v) and 1.2% plant agar (w/v). The plates were placed vertically in a climate chamber at 21 °C /21 °C day/night; 180 µmol light m^{-2} s^{-1}, 16 h light/8 h dark cycle and 70% relative humidity. After five days of Broccoli growth, roots of each seedling were inoculated with a cell suspension of *Paraburkholderia graminis* as described below. After inoculation, plants were vertically grown in the same growth chamber until harvest (11 dpi).

Bacterial treatments

Paraburkholderia graminis (*Pbg*) strain PHS1, originally isolated from the rhizosphere of sugar beet (*Beta vulgaris*) seedlings grown in a *Rhizoctonia*-suppressive soil (Carrión *et al.*, 2018), was cultured in Luria Bertani (LB) medium (Lennox, Carl Roth) at 25 °C for 16 h. Bacterial cells were collected by centrifugation, washed three times with 10 mM $MgSO_4$ and resuspended in 10 mM $MgSO_4$ to a final density of 5 x 10^7 cells ml^{-1}. To determine if growth promotion of the Broccoli seedlings can also be induced with dead cells, the bacterial suspension was placed in 2 mL tubes and pasteurized at 65 °C for 20 min. Cell-free supernatant was prepared by filtration of the bacterial overnight cell culture through a 0.2 µm filter. Dead cells and cell-free culture supernatant were further exposed to UV light for 40 min. For the live cells, 2 µl suspension were inoculated onto roots of 5-day-old Broccoli seedlings; for the heat-killed cell and metabolite, 50 µl suspension was inoculated on the root tips of the 5-day-old seedlings. For the control, the same volumes of 10 mM $MgSO_4$ or LB medium were used.

To examine if volatile organic compounds (VOCs) emitted by *Pbg* are involved in Broccoli shoot growth promotion, we used an experimental design where *Pbg* is physically separated from the Broccoli seedlings while permitting air-to-air contact between the compartments (Supplementary **Fig S1**). To this end, the lids of 140-mm petri dishes were merged face-to-face with holes to allow physical separation of the petri dishes while permitting VOCs exchanges. Broccoli seeds were sown and grown in one plate for 5 days. In the other plate, 50 µl of *Pbg* (10^7 cells ml^{-1}) was inoculated on MS media in a smaller petri dish (Ø60 mm). Then, on the lids of both plates, two holes (Ø10 mm) were made at 2 cm distances from the top and bottom ends, allowing VOCs diffusion to the plate where Broccoli seedlings were grown (Supplementary **Fig S1**). In addition, to determine if sulfurous VOCs produced by *Pbg* are associated with Broccoli growth promotion, we tested mutants C3 and D3 that are disrupted in the genes coding for cysteine desulfurase and for dimethyl sulfoxide reductase, respectively (Carrión *et al.*, 2018).

Bacterial gene expression on roots of Broccoli seedlings

***Paraburkholderia* cell collection**

To begin to identify bacterial traits involved in Broccoli growth promotion, we conducted a comparative transcriptome analysis of *Pbg* colonizing roots of the two Broccoli cultivars. Total RNA was extracted from *Pbg* cells from roots of two Broccoli cultivars and from *Pbg* grown on MS media as a control. To do this, roots of Broccoli seedlings at 6 dpi were detached from MS agar and transferred to a 5 ml falcon tube containing 2 ml of lifeguard (lifeguard®). The tubes were then vortexed (30 s), sonicated (1 min), and vortexed (10 s) again to separate adherent bacteria. Root tissue was removed from the tubes and the bacterial cell suspension was transferred to a 2 mL Eppendorf tube. Meantime, cells of *Pbg* grown on MS media only were scraped off and transferred into 2 ml lifeguard solution. The collected bacterial cell suspensions were spun down at maximum speed at 15,000 rpm at 4 °C for 1 min, and supernatant was removed. Thereafter, the cell pellet was kept at -80 °C until used. Four replicates were used for each treatment.

After thawing the bacterial cell pellet on ice, Trizol reagent (Roti®ZOL RNA. ROTH) was added and the suspension was incubated at 60 °C for 10 min to break the bacterial cells. The RNA was extracted and purified using the NucleoSpin® RNA kit (Macherey-Nagel) according to manufacturer's protocol and stored at -80 °C until sequencing. The quality of RNA was evaluated by NanoDrop and RNA concentration was assessed by Qubit® 3.0 Fluorometer (Invitrogen). Prior to RNA sequencing, a DNase treatment was performed again to remove genomic DNA followed by a purification with the RNeasy MinElute Cleanup Columns (Qiagen). The RNA integrity was determined using an Agilent 2100 Bioanalyzer. The RNA samples were prepared according to the Ovation Complete Prokarotic RNA-Seq DR Multiplex system (Nugen). In brief, 500 ng of total RNA was used for the cDNA

synthesis with retained RNA strand information. The cDNA was generated using non-rRNA selective primers. The cDNA was fragmented using the Covaris S-series System according to the manufacturer's recommendations followed by an Agencourt RNAClean XP beads purification. The fragmented cDNA was end repaired and barcoded Illumina adapters were ligated followed by a two-step strand selection. The sequencing library was ribosomal depleted using Nugen's insert dependent adaptor cleavage technology and enriched by PCR for 18 cycles followed by a RNAClean XP beads purification. The concentration and quality of the sequencing libraries were determined by Agilent 2100 Bioanalyzer using a High Sense assay. The sequencing libraries were pooled and single read 100-bp sequenced with dual 8-bp indices according to the Illumina TruSeq Rapid v2 protocol on the HiSeq2500.

Transcriptome data analysis

Transcriptome analysis was carried out with the workflow engine Snakemake (Köster & Rahmann, 2012) in combination with Trinity (Grabherr *et al.*, 2011) as described in Schulz-Bohm *et al.* (2018). In the pipeline, raw RNA-Seq reads were filtered using Fastq MCF (Aronesty, 2011) and aligned to the genome sequence of *Paraburkholderia graminis* strain PHS1 (https://www.ncbi.nlm.nih.gov/genome/ 1613?genome _assembly_id=390432) with Bowtie 2 (Langmead & Salzberg, 2012). Differential expressed genes (DEG) were analyzed by edgeR V3.2 (Robinson *et al.*, 2010; McCarthy *et al.*, 2012). DEG output was further refined with the significance threshold of P value < 0.05 and a FDR value < 0.05. Functional categorization of genes was performed on EGGNog-Mapper web server (http://eggnog-mapper.embl.de/). Generated GO terms that satisfy the significance threshold were subjected to an R package GoSeq (Young *et al.*, 2010) to perform gene overrepresentation analysis. Pathway analysis was carried out on KEGG ontology in the KEGG web server (https://www.KEGG.jp/KEGG/KEGG2.html). Biological interpretation of the DEGs was performed using Cytoscape software with ClueGO plugin (Bindea *et al.*, 2009)

Statistical analysis

Differences in shoot biomass between *Pbg* treatment and non-treated control were analyzed by Student's *t*-Test. Two-way analysis of variance (ANOVA) of the absolute shoot biomass for the two Broccoli cultivars and different bacterial traits of *Pbg* were performed in R Studio software (V 3.6.1). When the data set could not meet normality and homogeneity of variance, Box-Cox transformation was performed using the package MASS. The ANOVA table is presented in Supplementary **Table S1**.

Results

Cultivar-specific growth promotion

Introduction of *Paraburkholderia graminis* (*Pbg*) strain PSH1 onto Broccoli roots significantly enhanced shoot biomass in both cultivars at 11 dpi (**Fig 1**). The absolute biomass was higher for cultivar Coronado than for Malibu (**Fig 1b** and **c**) but percent changes in shoot biomass induced by *Pbg* relative to the non-treated control was significantly higher (P = 0.03) for Malibu: *Pbg* enhanced Malibu shoot biomass by 73.4% (±6.5) and 39.2 % (±10.8) for cultivar Coronado (**Fig 1d**). *Pbg* colonized roots of both Broccoli cultivars to the same extent with densities of $8.1 \pm 0.3 \times 10^7$ and $1.0 \pm 0.1 \times 10^8$ CFU/g for Coronado and Malibu, respectively.

Identification of bacterial traits contributing to plant growth promotion

To begin to identify the bacterial traits involved in plant growth promotion, we first tested if growth promotion could also be induced by dead *Pbg* cells or cell-free *Pbg* culture supernatant. At 11 dpi, only live *Pbg* cells resulted in significant shoot biomass increases in both Broccoli cultivars, whereas dead *Pbg* cells or cell-free culture supernatant did not (**Fig 2**). Previous studies by Carrión *et al*. (2018) had shown that the production of sulfurous volatiles (VOCs) is one of the key mechanisms of plant protection by *Pbg*. To test if Broccoli growth promotion was due to volatile organic compounds (VOCs) produced by *Pbg*, we conducted bioassays where *Pbg* cells were physically separated from the Broccoli seedlings (Supplementary materials **Fig S1).** In these assays, we also included two *Pbg* mutants disrupted in genes involved in the biosynthesis of sulfurous VOCs: mutant C3 is disrupted in the gene coding for cysteine desulfurase and mutant D3 in the gene coding for dimethyl sulfoxide reductase (Carrión *et al.*, 2018). The results of this dedicated VOCs-bioassay showed that there were no significant biomass changes in Broccoli induced by either *Pbg* wildtype or these two mutants (**Fig 2**). These results indicate that growth promotion is induced by live *Pbg* cells and that VOCs do not play a significant role in growth promotion of Broccoli seedlings.

Transcriptional changes in *Paraburkholderia* during colonization of Broccoli roots

To identify *Pbg* genes expressed in *Pbg*-Broccoli interactions, we set out a genome-wide transcript analysis. To identify the time-point for RNA-seq analysis, we first evaluated the temporal changes in shoot biomass by harvesting seedlings at 1, 3, 5, 7, 9, and 11 dpi after *Pbg* inoculation. The results showed that significant growth promotion was first visible at 7 dpi onward (**Fig 3**). Therefore, we chose 6 dpi as the time-point for *Pbg* transcriptome analyses. A total of 13.7 – 22.1 million reads of high quality were obtained per sample (Supplementary **Fig S3**). Genes with a fold change ≥ 2, and P and FDR ≤ 0.05 were considered as differentially expressed genes (DEGs). Among the total of 2948 annotated *Pbg* genes annotated, 380 genes showed significant expression in the interaction with Broccoli roots. Compared to

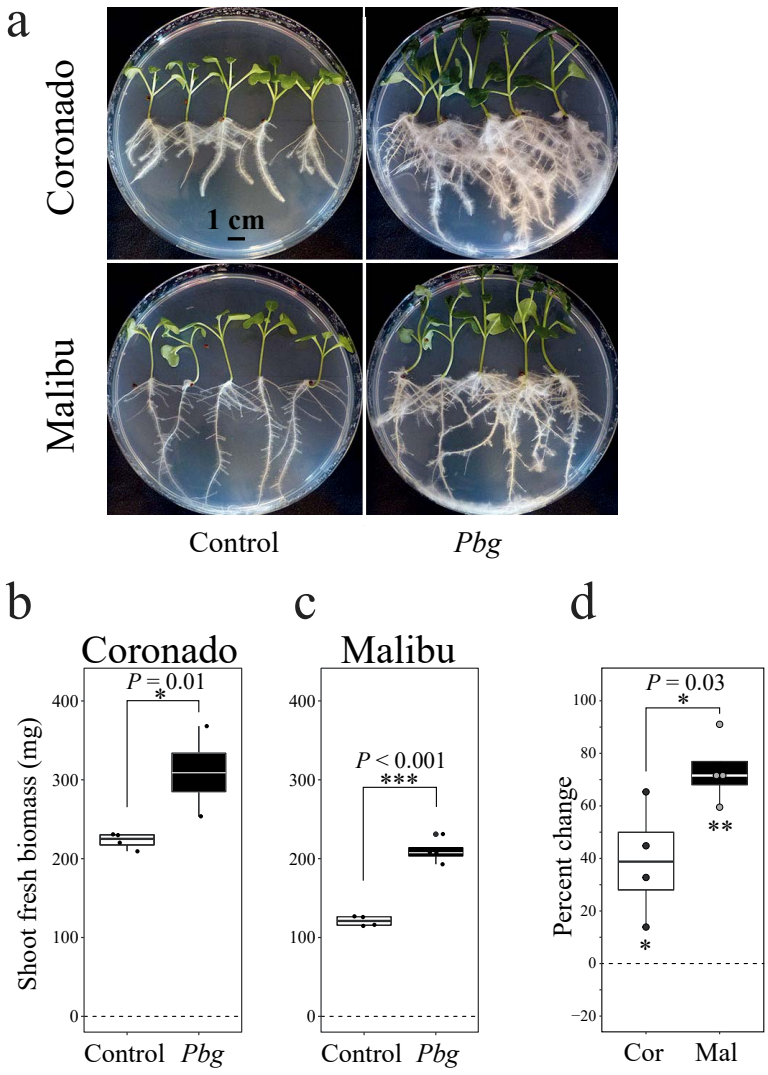

Fig 1. Broccoli phenotype changes in response to root tip inoculation with *Paraburkholderia graminis* (*Pbg*) strain PSH1. (**a**) Photographs of Broccoli cultivars Coronado (Cor) and Malibu (Mal) grown on MS agar plates at 11 days post inoculation (dpi) with *Pbg*. (**b**) Shoot biomass changes of Coronado, (**c**) Malibu. (**d**) shoot biomass changes induced by *Pbg* relative to the non-treated control (mean ± standard error, n = 4) for both Broccoli cultivars. Asterisks above the bars denote statistical differences (two tailed Student's *t* test). * $P < 0.05$; ** $P < 0.01$; ***: $P < 0.001$. Asterisks below the bars in (**d**) indicate statistical differences to the control for the two Broccoli cultivars.

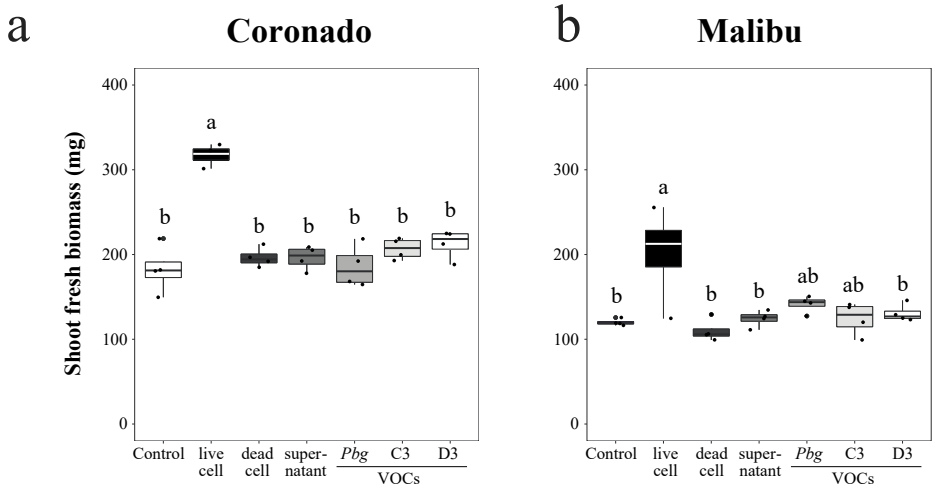

Fig 2. Identification of various traits of *Paraburkholderia graminis* (*Pbg*) involved in growth promotion of the two Broccoli cultivars Coronado (**a**) and Malibu (**b**). At 11 dpi, shoot biomass of Broccoli treated with live *Pbg* cells, heat-killed *Pbg* cells, cell-free *Pbg* culture supernatant and volatile organic compounds (VOCs) from *Pbg*. For determining the potential role of VOCs, Pbg was physically separated from the Broccoli seedlings. Furthermore, two mutants disrupted in sulfurous VOVs production were used; these include a mutant in the gene for cysteine desulfurase (C3) and in the gene for dimethyl sulfoxide reductase (D3). Control: non-treated *Pbg*-free. Means of biomass changes with a different letter are significantly different among the treatments according to one-way ANOVA (Tukey, $P < 0.05$)

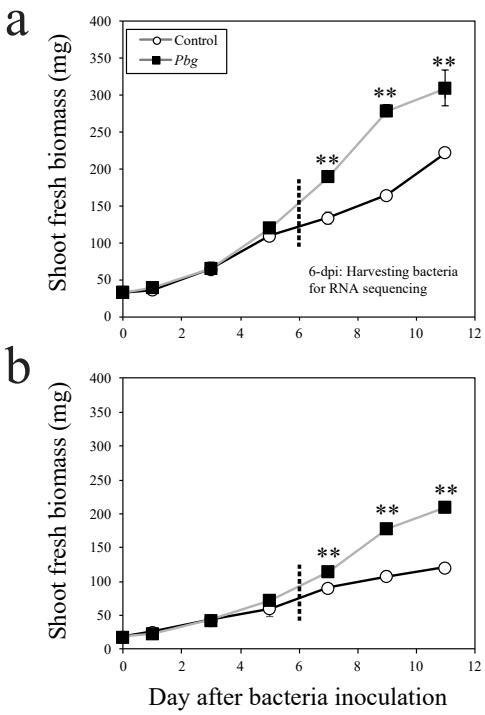

Fig 3. Temporal changes in shoot biomass of Broccoli cultivars Coronado (**a**) and Malibu (**b**) after root inoculation with *Paraburkholderia graminis* (*Pbg*). Asterisks denote statistical differences relative to the untreated Broccoli seedlings (two tailed Student's t test): * $P < 0.05$; ** $P < 0.01$.

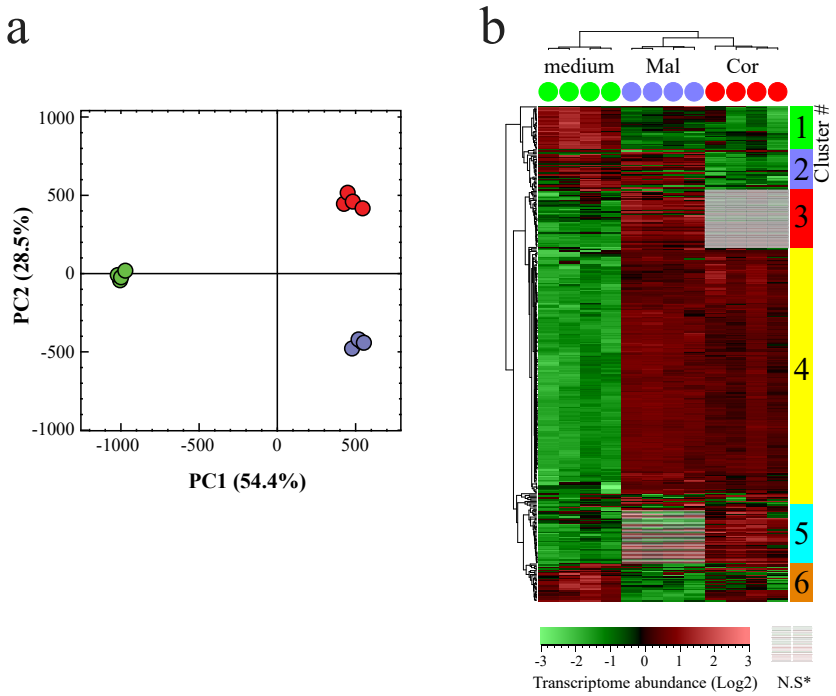

Fig 4. Transcriptome changes of *Paraburkholderia graminis* (*Pbg*) grown on roots of Broccoli cultivars, Coronado (Cor) and Malibu (Mal). The figure depicts the results of a principal component analysis (PCA) (**a**) and hierarchical cluster analysis (HCA) (**b**). Results represent genes that are expressed differentially between *Pbg* grown on MS-agar medium and on the roots of the two Broccoli cultivars. Cluster numbers (Cluster #) are segments where the transcriptomes clustered together after Pearson correction with unweighted pair group method with arithmetic mean (UPGMA). These differentially expressed genes are indicated by different colors in the HCA. *N.S: genes not expressed significantly different.

Pbg grown on MS-agar, 310 DEGs (238 up- and 72 down-regulated) were identified in *Pbg* colonizing roots of Coronado and 310 DEGs (239 up- and 71 down-regulated) on roots of Malibu. Gene Onthology (GO) over-representation analysis using Goseq resulted in 19 different orthologous gene categories (COG). Overall, up-regulated gene clusters in *Pbg* colonizing roots of cultivar Coronado categorized into "Energy production and conversion (C), Cell motility (N), Inorganic ion transport and metabolism (P)" (Supplementary **Table. S2**), while down-regulated genes encompassed genes belonging to "Another part of Energy production and conversion (C), Replication and repair (L), Post-translational modification, protein turnover, chaperone functions (O), and Inorganic ion transport and metabolism (P)" (Supplementary **Table. S3**). Meanwhile, genes expressed in *Pbg* colonizing roots of Malibu grouped into classes "Energy production and conversion (C), Cell motility (N), Inorganic ion transport and metabolism (P), and Signal Transduction (T)" (Supplementary **Table. S4**), whereas down-regulated genes classified into "Another subcategories of Energy production and conversion (C), Amino Acid metabolism and transport (E), Carbohydrate metabolism

and transport (G), Translation (J), Transcription (K), Post-translational modification, protein turnover, chaperone functions (O)" (Supplementary **Table. S5**). To visualize DEGs, principal component analysis (PCA) and hierarchical cluster analysis (HCA) were performed on a total 380 DEGs that showed significant difference between Coronado and the control treatment or between Malibu and control. In PCA, the first two principal components explained 82.9% of the total variance (**Fig 4a**). The first principal component (PC1), representing 54.4% of the total variance, was explained by genes that were highly enriched (**Fig 4b** cluster **3**) or suppressed (clusters **1** and **6**) in the interaction of *Pbg* with both Broccoli cultivars. PC2 explained 28.5% of the total variance and corresponded to DEGs with Coronado-specific expression (**Fig 4b** clusters **5**: up-regulation and **2**: down-regulation) or Malibu-specific expression (Cluster **3**: upregulation).

Among the 380 DEGs, 240 genes (186 up- and 54 down-regulated) were found to be commonly regulated for both Broccoli cultivars (**Fig 5**). DEGs of *Pbg* associated with COG class "Cell motility (N)" accounted for the most enriched genes in both Broccoli cultivars, encompassing genes encoding for flagellar assembly such as *flgA - L*, and for motility such as *motA*, *B* and *C* (**Fig 6** and **Table 1**) with up to 474-fold increases in gene expression relative to the control. This was followed by DEGs belonging to "Energy production and conversion (C) and Inorganic ion transport and metabolism (P)". including genes associated with the phosphate metabolic process (*pstA-C* and *pstS*, **Fig 6**), and with nitrate metabolism such as *narH* (nitrate reductase beta subunit), *narJ* (nitrate reductase beta molybdenum cofactor assembly chaperone), and *narK* (nitrite transporter). In particular *narJ* displayed 1189.3 and 522.0-fold increases in *Pbg* on roots of Coronado and Malibu, respectively, while expression of *narH* increased 492.6 and 240.8-fold, respectively. In addition, *sdhB* and *sdhC* which encode an iron-sulfur protein and the succinate dehydrogenase cytochrome subunit, respectively, were 10.9 to 15.5-fold up-regulated on roots of Coronado and Malibu. Furthermore, several genes such as *atpE, cyoB, glnP, hisJ,* and *qoxA* involved in (an)ion transport displayed increases in expression of 9.2 to 259.6-fold (**Table 1**). Genes down-regulated on roots of Broccoli include genes associated with metabolic adaptation to environmental changes (*aceA*, 6-fold), protein restoration by stress condition (*groL*, up to 4-fold), and the antitoxin component of a toxin-antitoxin (TA) module (*yefM*, more than 2-fold). Collectively these results indicate that *Pbg*-Broccoli interactions are characterized by enhanced expression of *Pbg* genes associated with motility and (an)ion uptake and transport and down-regulation of genes associated with environmental changes and stress.

Next to common genes expressed on roots of both Broccoli cultivars, we also identified DEGs with cultivar-specific enrichments. For example, on roots of Coronado *Pbg* genes related to methionine import (i.e *metN2* and *metN*) were upregulated, whereas genes associated with symbiotic interaction (*ppk2*, 10-fold increase) and a nitrate transporter (*nasF*, 18-fold increase) showed Malibu specific up-regulation (**Table 1**). Other *Pbg* genes showed Broccoli-cultivar specific down-regulation. For example, genes involved in DNA ligase (*lig*, 3.2-fold), guanine

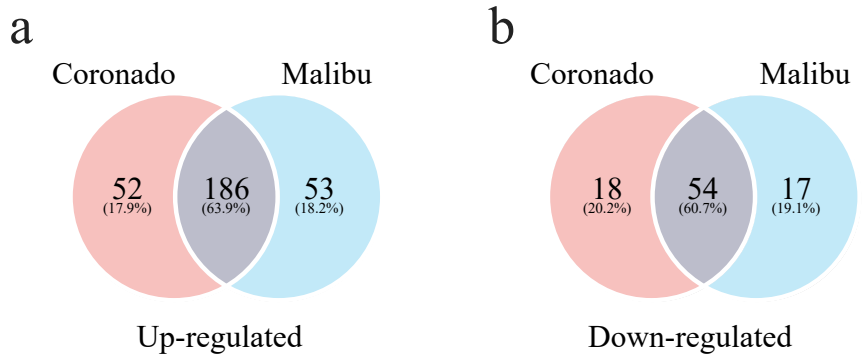

Fig 5. Differently expressed genes (DEGs) of *Paraburkholderia graminis* (*Pbg*) colonizing roots of Broccoli cultivars Coronado and Malibu. Venn diagrams show the number of up- or down-regulated *Pbg* genes expressed commonly or exclusively on roots of each of the two cultivars.

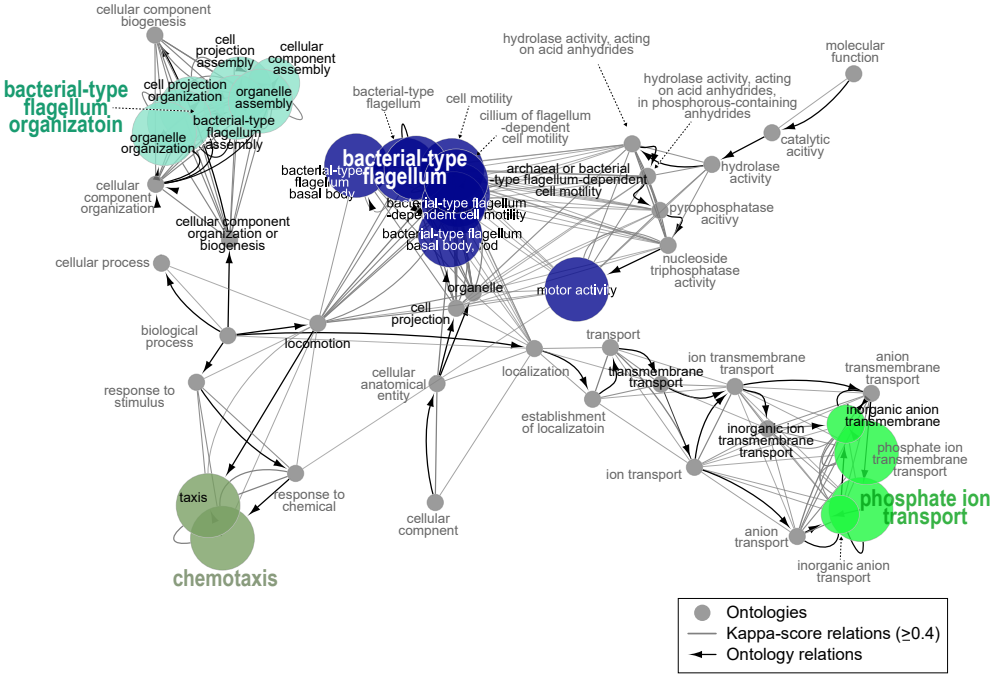

Fig 6. Enrichment analysis of differentially expressed genes (DEGs) of *Paraburkholderia graminis* (*Pbg*) that were commonly up-regulated on roots of both Broccoli cultivars, Coronado and Malibu 6 days after inoculation (6-dpi). Cluster analysis was performed using Cytoscape with ClueGO plugin. Networks with terms functionally grouped with GO pathways are indicated as nodes (two-sided hypergeometric test corrected with Benjamini-Hochberg $P < 0.05$) linked by heir kappa score level (≥ 0.4), with only the label of the most significant term per group. The node size represents the term enrichment significance and node color shows cluster color.

transport (*yjcD*, 3.9-fold), and copper ion homeostasis (*cutC*, 2.7-fold) displayed Coronado specific suppression, while *Pbg*-Malibu interaction led to a significant down-regulation of genes associated with COG classes involved in cytolysis in other organism (*hppD*) and iron-sulfur cluster assembly (*iscA* and *iscU,* 2.0 – 2.2-fold).

Table 1. Differently expressed genes (DEGs) of *Pbg* colonizing roots of two Broccoli cultivars, Coronado and Malibu at 6 dpi. Fold change of gene expression in root colonizing Pbg relative to control was calculated.

DEGs in	RefSeqID	Gene	COG*	Description	Fold change	
					Cor**	Mal**
Up-regulation						
both	WP_006050918.1	*flgA*	N	Flagella basal body p-ring formation protein	14.1	30.0
both	WP_006050919.1	*flgB*	N	Structural component of flagellum, the bacterial motility apparatus. Part of the rod structure of flagellar basal body	84.2	157.2
both	WP_029970946.1	*flgC*	N	Belongs to the flagella basal body rod proteins family	107.0	192.0
both	WP_006050921.1	*flgD*	N	Required for flagellar hook formation. May act as a scaffolding protein	86.3	144.2
both	WP_006050922.1	*flgE*	N	flagellar	137.8	269.6
both	WP_006050923.1	*flgF*	N	Flagellar basal-body rod protein *FlgF*	103.9	171.2
both	WP_006050924.1	*flgG*	N	flagellar basal-body rod protein	283.2	474.3
both	WP_006050925.1	*flgH*	N	Assembles around the rod to form the L-ring and probably protects the motor basal body from shearing forces during rotation	128.0	199.5
both	WP_029970942.1	*flgI*	N	Assembles around the rod to form the L-ring and probably protects the motor basal body from shearing forces during rotation	92.2	185.0
both	WP_107709963.1	*flgJ*	N	Flagellar rod assembly protein muramidase *FlgJ*	35.7	55.2
both	WP_006050930.1	*flgK*	N	flagellar hook-associated protein	63.2	89.8
both	WP_053858870.1	*flgL*	N	Flagellar hook-associated protein 3	63.0	75.0
both	WP_114156561.1	*cheA*	T	Signal transducing histidine kinase homodimeric	27.4	30.8
both	WP_114156560.1	*cheB*	NT	catalyzes the demethylation of specific methylglutamate residues introduced into the chemoreceptors (methyl-accepting chemotaxis proteins) by *CheR*	12.7	14.9
both	WP_053858877.1	*cheD*	NT	Probably deamidates glutamine residues to glutamate on methyl-accepting chemotaxis receptors (MCPs), playing an important role in chemotaxis	16.4	21.5
both	WP_053858878.1	*cheR*	H	Methylation of the membrane-bound methyl-accepting chemotaxis proteins (MCP) to form gamma-glutamyl methyl ester residues in MCP	23.2	27.6
both	WP_006051159.1	*cheV*	T	response regulator	9.4	12.7
both	WP_006050900.1	*cheW*	NT	chemotaxis protein	43.9	46.2
both	WP_006050895.1	*motA*	N	With *MotB* forms the ion channels that couple flagellar rotation to proton sodium motive force across the membrane and forms the stator elements of the rotary flagellar machine	15.2	20.9
both	WP_006050896.1	*motB*	N	PFAM *OmpA MotB* domain protein	13.8	12.5
both	WP_107709453.1	*motC*	N	PFAM *MotA TolQ ExbB* proton channel	21.5	31.9
both	WP_006051988.1	*pstA*	P	TIGRFAM phosphate ABC transporter, inner membrane subunit *PstA*	23.6	37.3
both	WP_006051989.1	*pstB*	P	Esterase-like activity of phytase	17.2	27.3
both	WP_029967734.1	*pstC*	P	probably responsible for the translocation of the substrate across the membrane	14.2	23.0
both	WP_006051986.1	*pstS*	P	Part of the ABC transporter complex PstSACB involved in phosphate import	25.0	56.8
both	WP_114157001.1	*narG*	C	Belongs to the prokaryotic molybdopterin-containing oxidoreductase family	559.0	268.2
both	WP_114157002.1	*narH*	C	nitrate reductase beta subunit	492.6	240.8
both	WP_114157003.1	*narJ*	C	nitrate reductase molybdenum cofactor assembly chaperone	1189.3	522.0
both	WP_114157000.1	*narK*	P	nitrite transporter	370.4	190.9
both	WP_114158013.1	*narK1*	P	PFAM major facilitator superfamily MFS_1	33.4	15.4
both	WP_114156998.1	*narX*	T	Histidine kinase	19.5	37.6
both	WP_114156816.1	*sdhA*	C	Belongs to the FAD-dependent oxidoreductase 2 family. FRD SDH subfamily	12.1	14.8

DEGs in	RefSeqID	Gene	COG*	Description	Fold change	
					Cor**	Mal**
both	WP_114156815.1	*sdhB*	C	Belongs to the succinate dehydrogenase fumarate reductase iron-sulfur protein family	12.1	13.9
both	WP_006047674.1	*sdhC*	C	Succinate dehydrogenase cytochrome b556 subunit	10.9	15.5
both	WP_114157710.1	*odhA*	C	2-oxoglutarate dehydrogenase, E1	17.2	19.1
both	WP_006050844.1	*atpE*	C	F(1)F(0) ATP synthase produces ATP from ADP in the presence of a proton or sodium gradient. F-type ATPases consist of two structural domains, F(1) containing the extramembraneous catalytic core and F(0) containing the membrane proton channel, linked together by a central stalk and a peripheral stalk. During catalysis, ATP synthesis in the catalytic domain of F(1) is coupled via a rotary mechanism of the central stalk subunits to proton translocation	9.9	13.9
both	WP_114156996.1	*cyoB*	C	Belongs to the heme-copper respiratory oxidase family	19.8	30.9
both	WP_029967077.1	*glnP*	P	HEQRo_perm_3TM amino ABC transporter, permease, 3-TM region, His Glu Gln Arg opine family domain protein	9.2	28.1
both	WP_114157834.1	*hisJ*	ET	PFAM extracellular solute-binding protein, family 3	18.8	52.7
both	WP_053859432.1	*qoxA*	C	ubiquinol oxidase subunit	194.6	259.6
Cor	WP_114157622.1	*metN2*	P	Part of the ABC transporter complex MetNIQ involved in methionine import. Responsible for energy coupling to the transport system	6.7	n.s***
Cor	WP_006050267.1	*metN*	P	Part of the ABC transporter complex MetNIQ involved in methionine import. Responsible for energy coupling to the transport system	6.6	n.s
Mal	WP_029971217.1	*atpB*	C	it plays a direct role in the translocation of protons across the membrane	n.s	9.0
Mal	WP_006049611.1	*ppk2*	S	Polyphosphate kinase 2 (PPK2)	n.s	10.3
Mal	WP_114158028.1	*nasF*	P	Nitrate ABC transporter	n.s	17.7
Down-regulation						
Both	WP_006052990.1	*aceA*	C	Isocitrate lyase	-6.2	-6.1
Both	WP_053857609.1	*groL*	O	Prevents misfolding and promotes the refolding and proper assembly of unfolded polypeptides generated under stress conditions	-2.6	-3.6
Both	WP_029971804.1	*yefM*	D	Antitoxin component of a toxin-antitoxin (TA) module	-2.7	-2.3
Cor	WP_107709809.1	*lig*	L	Catalyzes the ATP-dependent formation of a phosphodiester at the site of a single strand break in duplex DNA	-3.3	n.s
Cor	WP_006051136.1	*yjcD*	S	PFAM Xanthine uracil vitamin C permease	-3.9	n.s
Cor	WP_029969539.1	*cutC*	P	Participates in the control of copper homeostasis	-2.7	n.s
Mal	WP_006053048.1	*hppD*	C	4-Hydroxyphenylpyruvate dioxygenase	n.s	-2.3
Mal	WP_029967490.1	*iscA*	S	Belongs to the HesB IscA family	n.s	-2.0
Mal	WP_006051271.1	*iscU*	C	A scaffold on which IscS assembles Fe-S clusters. It is likely that Fe-S cluster coordination is flexible as the role of this complex is to build and then hand off Fe-S clusters	n.s	-2.2

COG*, COG category. Energy production and conversion (C), Cell cycle control and mitosis (D), Amino Acid metabolism and transport (E), Coenzyme metabolism (H), Replication and repair (L), Cell motility (N), Post-translational modification, protein turnover, chaperone functions (O), Inorganic ion transport and metabolism (P), Function Unknown (S), Signal Transduction (T). **Cor, Coronado and Mal, Malibu. n.s.***, not significant.

Discussion

Since Kloepper and colleagues (Kloepper, 1978) first termed plant growth-promoting rhizobacteria (PGPR) in their experiment with radish, a great deal of attention has been paid to unearthing the astonishing number and diversity of rhizobacterial genera that can promote plant growth and trigger systemic resistance, thereby enhancing crop yield and improving plant quality traits. Transcriptome analysis of interacting organisms is providing new insights into mechanisms involved in the beneficial PGPR traits. To date, such approaches have been performed largely in Arabidopsis (Wang *et al.*, 2005; Cartieaux *et al.*, 2008; Lakshmanan *et al.*, 2013; Cordovez *et al.*, 2017), pepper (Lim & Kim, 2013), rice (Drogue *et al.*, 2014), and tomato (Ongena, Marc *et al.*, 2005; Valenzuela-Soto *et al.*, 2010). However, little is known about gene expression in the beneficial bacteria during root colonization. Here, we

showed *Paraburkholderia graminis* (*Pbg*)-mediated growth promotion of Broccoli and gene expression in response to their interaction with the seedlings of two Broccoli cultivars. *Pbg* enhanced plant biomass was already described in our previous study (Chapters 3 and 4), in which *Pbg* root treatment significantly increase shoot biomass of Broccoli and Artemisia but reduced Arabidopsis biomass. These results suggested that *Pbg*-induced growth promotion is host plant specific.

In this study, we first assessed different bacterial states such as live cells, heat-killed cells, filtrate of bacterial liquid culture and volatile organic compounds (VOCs) from *Pbg* to unearth which bacterial traits are associated with plant growth promotion. Our results showed that only viable cells were able to significantly enhance the biomass of both Broccoli cultivars. The importance of bacteria cell viability biomass induction was also displayed other PGPR strains i.e. *Paraburkholderia phytofirmans* PsJN (Poupin *et al.*, 2013), *Pseudomonas fluorescens*, and *P. aeruginosa* (Siddiqui & Shaukat, 2002; Cheng *et al.*, 2017) attested in Arabidopsis. Bacterial culture filtrates may contain phytohormones such as indole-3-acetic acid (IAA) (Idris *et al.*, 2007; Dodd *et al.*, 2010; Calvo *et al.*, 2014; Olanrewaju *et al.*, 2017) that can contribute to growth promotion. Although we did not analyse the chemical composition of the culture filtrates, our results suggest that the *Pbg* suprenatant does not contain sufficient levels of phytohormones to enhance biomass of Broccoli seedlings.

Our genome-wide transcriptome analysis of *Pbg* colonizing roots of two Broccoli cultivars revealed that genes involved in flagellar assembly and motility, phosphate metabolism, nitrate metabolism and ion transport (up-regulation) were highly expressed. Among others, the gene clusters most expressed were those associated with flagellar assembly and motility (**Table 1**), further reinforcing the importance of these traits in successful root colonization (Walsh *et al.*, 2001; de Weert *et al.*, 2002; de Weert *et al.*, 2004). In our study, enriched genes involved in flagella assembly *flg* operons (as *flgA-L*), chemotaxis *che* operons (*cheA, B, D, R, V* and *W*), and mobility *mot* operons (*motA, B* and *C*) indicated that root exudates of both Broccoli cultivars, Coronado and Malibu, contain chemo-attractants or nutrients that trigger *Pbg* to colonize the roots. Such up-regulation of genes involved in flagellar assembly and motility were previous reported in *Bacillus amyloliquefaciens* FZB42 in response to maize root exudate (Fan *et al.*, 2012). Next to bacterial motility, *Pbg* interaction with both Broccoli cultivars also revealed expression of genes associated with nutrition uptakes and ion transport, including the nitrate reductase genes, *narH, narJ,* and *nark,* phosphate ion transport genes such as *pstA* and *pstS*, as well as genes involved in (an)ion transport such as *atpE, cyoB, glnP, hisJ,* and *qoxA*. The *pst* operon functions as part of the ABC transporter complex (Bentley *et al.*, 2002; Lee *et al.*, 2012) whereas the *nar* operon plays an important role in nitrogen assimilation for bacterial energy metabolism (Tang, 2014) (DeMoss & Hsu, 1991). In addition, we found that the *sdh* operon (*sdhA-C*) and *odhA* gene of the TCA cycle (Hederstedt & Rutberg, 1981; McNeil *et al.*, 2012), also displayed up-regulation in *Pbg* colonizing roots of both Broccoli cultivars. These results suggest that root exudates of Broccoli seedlings serve as an energy source for

Pbg by enhancing nutrient uptake and transport in *Pbg*.

Analysis of the differentially expressed genes (DEGs) in the interaction between *Pbg* and roots of the two Broccoli cultivars further suggested that apart from common energy metabolism (i.e. phosphate and nitrate metabolism), there were additional *Pbg* genes whose expression was altered in a cultivar-specific manner. *Pbg* colonizing roots of Coronado specifically induced the expression of an ABC transporter complex involved in methionine import (*metN*). Methionine plays an important role in the biosynthesis of aliphatic glucosinolates in Brassica species including Broccoli. Broccoli cultivar Coronado, compared to Malibu, possesses higher levels of aliphatic glucosinolates (glucoiberin, glucoraphanin and glucobrassicin) and previous primary metabolome analysis demonstrated that Coronado intrinsically had more methionine (Chapter 4). Consequently, *metN* up-regulation in *Pbg*-Coronado combination suggested that Coronado may release more methionine into media promoting import of methionine into the *Pbg* cells. In turn, methionine metabolism in *Pbg* may trigger the biosynthesis of ethylene which in turn may affect growth and defense in the host plant. Follow-up experiments to determine if ethylene is produced by *Pbg* upon methionine addition, during colonization of Broccoli roots and produced at biologically meaningful concentrations will be needed to address this hypothesis. When *Pbg* was interacting with Malibu, genes of the *isc* operon (*iscA* and *iscU*) involved in iron-sulfur cluster demonstrated Malibu-specific down-regulation. This may due to relatively less sulfurous compounds in the root exudates of Malibu, which intrinsically possesses less glucosinolates than Coronado. Also, one of the genes in the *atp* operon (*atpB*), which regulate ATP transport (von Meyenburg *et al.*, 1982; Santana *et al.*, 1994), exhibited Malibu-specific induction. Collectively these results suggest cultivar-specific differences in rhizodeposition that in turn differently alter gene expression in this beneficial rhizobacterium. They confirm and extend results of previous transcriptome analysis of *Pseudomonas aeruginosa* PA01 colonizing roots of two sugar beet cultivars with different root exudate compositions (Mark *et al.*, 2005). The signaling compounds in the Broccoli root exudates that induce or repress *Pbg* gene expression as well as the functional role of several bacterial traits identified in this study remain to be further examined. Detailed chemical profiling of the root exudate of the two Broccoli cultivars and site-directed mutagenesis of specific DEGs will help further discovering mechanisms underlying root colonization and plant growth promotion by *Pbg*.

Acknowledgements

We are grateful to Dr. Gabriela Bindea for her help with technical support in ClueGO (Cytoscape plugin) enrichment analysis and to Prof. Dr. Hyo Jung Lee for advices in functional categorization of genes.

Supplementary materials

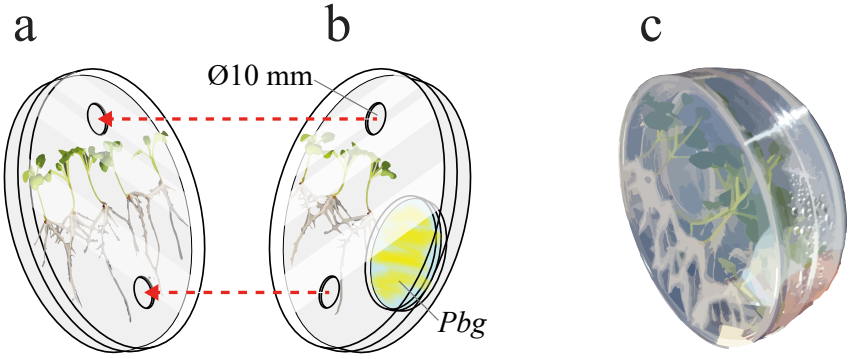

Fig S1. Scheme for VOCs exposure experiment. Five Broccoli seedlings grown on 140-mm-diameter petri dishes containing 50 ml of a half-strength Murashige and Skoog agar media, including 0.5% sucrose (w/v) and 1.2% plant agar (w/v) (**a**), and *Paraburkholderia graminis* (*Pbg*) grown on 60-mm-diameter petri dishes containing the same media (**b**). The holes of two petri dishes were placed face-to-face to allow gas exchanges (**c**).

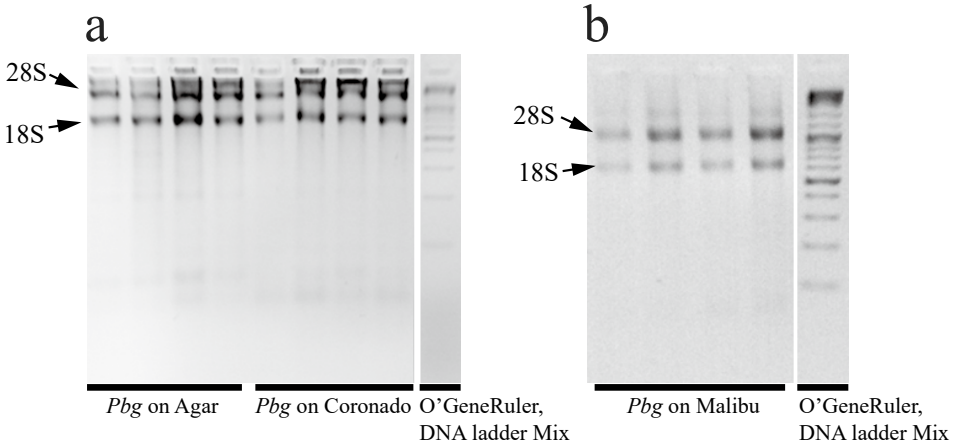

Fig S2. Agarose gel of total RNA extracted from *Paraburkholderia graminis* grown on media or on roots of two Broccoli cultivars at 6 dpi. Pbg grwon on MS-agar and root of Coronado (**a**) and Malibu (**b**) O'GeneRuler DNA ladder mix was used as size marker.

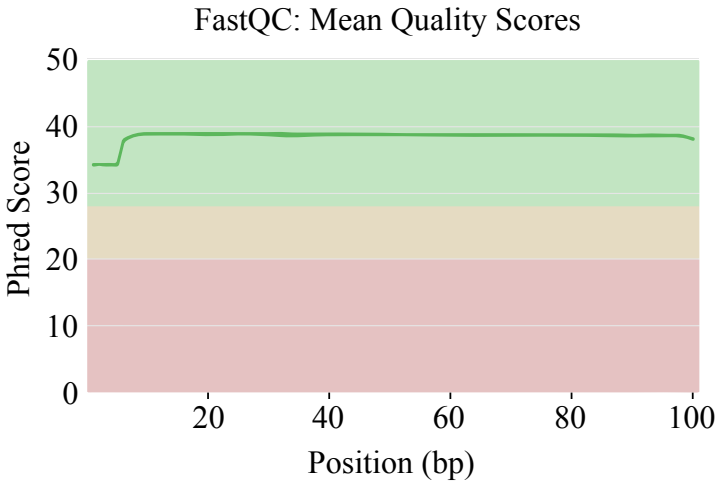

Fig S3. Quality score plot of FastQC per base sequence of *Paraburkholderia graminis* grown on MS-agar or on roots of Broccoli cultivars Coronado and Malibu. The lines (all were imposed) shown in the plot are all located in green area displaying a high quality of the RNA sequencing reads.

Table S1. Quantification of RNA extracted from *Paraburkholderia graminis* (*Pbg*) grown on MS-agar medium or on roots of Broccoli cultivars Coronado or Malibu grown on MS.

***Pbg* grown on**	**Replicate.**	**Nano drop measurement**		
		Ratio 260/280	**Ratio 260/230**	**RNA (ng/µl)**
MS-agar	1	2.15	2.36	562.4
	2	2.21	2.40	770.2
	3	2.18	2.42	2252.0
	4	2.2	2.50	787.1
Coronado roots	1	2.18	2.32	378.8
	2	2.18	2.39	1206.9
	3	2.19	2.33	941.3
	4	2.19	2.42	1082.7
Malibu roots	1	2.15	2.42	1494.6
	2	2.16	2.41	2013.0
	3	2.15	2.33	1167.3
	4	2.16	2.42	1587.4

Table S2. Output of gene set enrichment analysis (GSEA) performed for the up-regulated genes of *Paraburkholderia graminis* colonizing the roots of Coronado, a cultivar of Broccoli, seedlings. GSEA was performed using Goseq using $P < 0.05$.

GO term	Ontology	Description	NO. DE in list	NO. in reference	P-value
GO:0009055	C	electron transfer activity	7	19	0.000
GO:0022900	C	electron transport chain	8	30	0.001
GO:0045333	C	cellular respiration	9	38	0.001
GO:0000104	C	succinate dehydrogenase activity	4	8	0.001
GO:0070469	C	respiratory chain	4	8	0.001
GO:0070470	C	plasma membrane respiratory chain	4	8	0.001
GO:0098803	C	respiratory chain complex	4	8	0.001
GO:0009060	C	aerobic respiration	6	22	0.005
GO:0042126	C	nitrate metabolic process	2	2	0.006
GO:0019645	C	anaerobic electron transport chain	2	2	0.006
GO:0008940	C	nitrate reductase activity	2	2	0.006
GO:0045273	C	respiratory chain complex II	3	6	0.006
GO:0045274	C	plasma membrane respiratory chain complex II	3	6	0.006
GO:0045281	C	succinate dehydrogenase complex	3	6	0.006
GO:0045282	C	plasma membrane succinate dehydrogenase complex	3	6	0.006
GO:0020037	C	heme binding	3	7	0.007
GO:0022904	C	respiratory electron transport chain	5	18	0.007
GO:0015980	C	energy derivation by oxidation of organic compounds	9	48	0.009
GO:0015002	C	heme-copper terminal oxidase activity	2	3	0.016
GO:0009061	C	anaerobic respiration	3	8	0.018
GO:0016661	C	oxidoreductase activity, acting on other nitrogenous compounds as donors	2	4	0.025
GO:0098797	C	plasma membrane protein complex	5	25	0.026
GO:0051538	C	3 iron, 4 sulfur cluster binding	2	4	0.027
GO:2001057	C	reactive nitrogen species metabolic process	2	4	0.030
GO:0016627	C	oxidoreductase activity, acting on the CH-CH group of donors	4	17	0.031
GO:0006091	C	generation of precursor metabolites and energy	9	60	0.032
GO:0006099	C	tricarboxylic acid cycle	4	16	0.033
GO:0006101	C	citrate metabolic process	4	16	0.033
GO:0046906	C	tetrapyrrole binding	3	12	0.042
GO:0001666	C	response to hypoxia	2	5	0.044
GO:0036293	C	response to decreased oxygen levels	2	5	0.044
GO:0070482	C	response to oxygen levels	2	5	0.044
GO:0071944	CDEGH-MNPQST	cell periphery	42	385	0.001
GO:0005886		plasma membrane	38	336	0.001
GO:0016020		membrane	41	376	0.002
GO:0006544	CE	glycine metabolic process	2	5	0.046
GO:0051179	CEGMNPT	localization	29	156	0.000
GO:0006811	CEGMPT	ion transport	10	63	0.012
GO:1990204	CF	oxidoreductase complex	7	16	0.000
GO:0044459	CGNPQ	plasma membrane part	13	107	0.049
GO:0040011	CHMNT	locomotion	22	26	0.000
GO:0001539	CMN	cilium or flagellum-dependent cell motility	16	19	0.000
GO:0071973	CMN	bacterial-type flagellum-dependent cell motility	16	19	0.000
GO:0097588	CMN	archaeal or bacterial-type flagellum-dependent cell motility	16	19	0.000
GO:0006928	CMN	movement of cell or subcellular component	16	20	0.000
GO:0048870	CMN	cell motility	16	20	0.000
GO:0051674	CMN	localization of cell	16	20	0.000
GO:0044780	CN	bacterial-type flagellum assembly	4	5	0.000
GO:0044781	CN	bacterial-type flagellum organization	4	5	0.000
GO:0030030	CN	cell projection organization	4	8	0.002
GO:0030031	CN	cell projection assembly	4	8	0.002
GO:0098660	CP	inorganic ion transmembrane transport	5	26	0.039
GO:0005576	EHMN	extracellular region	5	24	0.031
GO:0009605	EHNT	response to external stimulus	9	42	0.003

Table S2. (Continued)

GO term	Ontology	Description	NO. DE in list	NO. in reference	P-value
GO:0006820	EMPT	anion transport	6	39	0.050
GO:0009267	ET	cellular response to starvation	3	11	0.043
GO:0006935	HNT	chemotaxis	6	7	0.000
GO:0042330	HNT	taxis	6	7	0.000
GO:0098561	HNT	methyl accepting chemotaxis protein complex	3	5	0.004
GO:0040012	MT	regulation of locomotion	2	3	0.020
GO:1902021	MT	regulation of bacterial-type flagellum-dependent cell motility	2	3	0.020
GO:2000145	MT	regulation of cell motility	2	3	0.020
GO:0051270	MT	regulation of cellular component movement	2	3	0.020
GO:0009425	N	bacterial-type flagellum basal body	10	10	0.000
GO:0044461	N	bacterial-type flagellum part	15	15	0.000
GO:0071978	N	bacterial-type flagellum-dependent swarming motility	10	10	0.000
GO:0009288	N	bacterial-type flagellum	16	18	0.000
GO:0044463	N	cell projection part	15	16	0.000
GO:0042995	N	cell projection	16	20	0.000
GO:0009424	N	bacterial-type flagellum hook	7	7	0.000
GO:0043228	N	non-membrane-bounded organelle	16	92	0.000
GO:0044422	N	organelle part	15	87	0.000
GO:0043226	N	organelle	16	111	0.002
GO:0120100	N	bacterial-type flagellum motor	2	2	0.004
GO:0120101	N	bacterial-type flagellum stator complex	2	2	0.004
GO:0007165	NT	signal transduction	3	7	0.012
GO:0023052	NT	signaling	3	7	0.012
GO:0031399	NT	regulation of protein modification process	2	3	0.019
GO:0031401	NT	positive regulation of protein modification process	2	3	0.019
GO:1901873	NT	regulation of post-translational protein modification	2	3	0.019
GO:1901875	NT	positive regulation of post-translational protein modification	2	3	0.019
GO:0010921	P	regulation of phosphatase activity	3	3	0.000
GO:0006817	P	phosphate ion transport	3	4	0.001
GO:0015698	P	inorganic anion transport	3	8	0.014
GO:0035435	P	phosphate ion transmembrane transport	2	3	0.016
GO:0098661	P	inorganic anion transmembrane transport	2	5	0.043
GO:0035303	PT	regulation of dephosphorylation	4	4	0.000
GO:0019220	PT	regulation of phosphate metabolic process	4	10	0.004
GO:0051174	PT	regulation of phosphorus metabolic process	4	10	0.004
GO:0004673	T	protein histidine kinase activity	2	3	0.019
GO:0018106	T	peptidyl-histidine phosphorylation	2	3	0.019
GO:0018202	T	peptidyl-histidine modification	2	3	0.019
GO:0000160	T	phosphorelay signal transduction system	2	3	0.019
GO:0016775	T	phosphotransferase activity, nitrogenous group as acceptor	2	3	0.019
GO:0023014	T	signal transduction by protein phosphorylation	2	3	0.019
GO:0035556	T	intracellular signal transduction	2	3	0.019

Table S3. Output of gene set enrichment analysis (GSEA) performed for the down-regulated genes of *Paraburkholderia graminis* colonizing the roots of Coronado, a cultivar of Broccoli, seedlings. GSEA was performed using Goseq using $P < 0.05$.

GO term	Ontology	Description	NO. DE in list	NO. in reference	P-value
GO:0010447	C	response to acidic pH	1	2	0.026
GO:0034357	C	photosynthetic membrane	1	1	0.013
GO:0036294	C	cellular response to decreased oxygen levels	1	1	0.013
GO:0071453	C	cellular response to oxygen levels	1	1	0.013
GO:0071456	C	cellular response to hypoxia	1	1	0.013
GO:0010034	C	response to acetate	1	1	0.013
GO:0070542	C	response to fatty acid	1	1	0.013
GO:0033993	C	response to lipid	1	2	0.026
GO:0075141	C	maintenance of symbiont tolerance to host environment	1	1	0.013
GO:0009579	C	thylakoid	1	1	0.013
GO:0042651	C	thylakoid membrane	1	1	0.013
GO:0044436	C	thylakoid part	1	1	0.013
GO:0003995	C	acyl-CoA dehydrogenase activity	1	1	0.013
GO:0008470	C	isovaleryl-CoA dehydrogenase activity	1	1	0.013
GO:0004451	C	isocitrate lyase activity	1	1	0.013
GO:0006102	C	isocitrate metabolic process	1	1	0.013
GO:0035375	C	zymogen binding	1	1	0.013
GO:0046421	C	methylisocitrate lyase activity	1	1	0.013
GO:0006097	C	glyoxylate cycle	1	3	0.038
GO:0005515	CDOP	protein binding	7	198	0.019
GO:0042802	CDOP	identical protein binding	6	169	0.032
GO:0006950	CLO	response to stress	6	157	0.028
GO:0009405	CO	pathogenesis	2	10	0.008
GO:0010033	CO	response to organic substance	3	17	0.003
GO:0005576	CO	extracellular region	2	24	0.048
GO:0044419	COP	interspecies interaction between organisms	4	34	0.002
GO:0044403	COP	symbiont process	4	30	0.001
GO:0051704	COP	multi-organism process	4	37	0.002
GO:0046820	EH	4-amino-4-deoxychorismate synthase activity	1	1	0.013
GO:0003910	L	DNA ligase (ATP) activity	1	1	0.013
GO:0003909	L	DNA ligase activity	1	2	0.025
GO:0006266	L	DNA ligation	1	2	0.025
GO:0051103	L	DNA ligation involved in DNA repair	1	2	0.025
GO:0006271	L	DNA strand elongation involved in DNA replication	1	2	0.027
GO:0006273	L	lagging strand elongation	1	2	0.027
GO:0022616	L	DNA strand elongation	1	2	0.027
GO:0016886	L	ligase activity, forming phosphoric ester bonds	1	3	0.042
GO:0016465	O	chaperonin ATPase complex	2	6	0.006
GO:0051084	O	'de novo' posttranslational protein folding	2	10	0.012
GO:0006458	O	'de novo' protein folding	2	11	0.014
GO:0009408	O	response to heat	3	36	0.020
GO:0009266	O	response to temperature stimulus	3	44	0.033
GO:0033644	O	host cell membrane	1	3	0.038
GO:0033647	O	host intracellular organelle	1	3	0.038
GO:0033648	O	host intracellular membrane-bounded organelle	1	3	0.038
GO:0044174	O	host cell endosome	1	3	0.038
GO:0044175	O	host cell endosome membrane	1	3	0.038
GO:0051082	O	unfolded protein binding	2	13	0.021
GO:0061077	O	chaperone-mediated protein folding	2	18	0.033
GO:0031249	O	denatured protein binding	1	1	0.013
GO:0051085	O	chaperone cofactor-dependent protein refolding	2	10	0.012
GO:0006986	O	response to unfolded protein	2	6	0.006
GO:0035966	O	response to topologically incorrect protein	2	7	0.007
GO:0044406	O	adhesion of symbiont to host	1	3	0.038

Table S3. (Continued)

GO term	Ontology	Description	NO. DE in list	NO. in reference	P-value
GO:0044650	O	adhesion of symbiont to host cell	1	3	0.038
GO:0046812	O	host cell surface binding	1	3	0.038
GO:0052047	O	interaction with other organism via secreted substance involved in symbiotic interaction	1	3	0.038
GO:0052212	O	modification of morphology or physiology of other organism via secreted substance involved in symbiotic interaction	1	3	0.038
GO:0101031	O	chaperone complex	2	6	0.006
GO:1990220	O	GroEL-GroES complex	2	6	0.006
GO:0019058	O	viral life cycle	2	7	0.007
GO:0019068	O	virion assembly	2	7	0.007
GO:0016032	O	viral process	2	10	0.014
GO:0022610	O	biological adhesion	1	3	0.038
GO:0044218	O	other organism cell membrane	1	3	0.038
GO:0044279	O	other organism membrane	1	3	0.038
GO:1901222	O	regulation of NIK/NF-kappaB signaling	1	3	0.038
GO:1901224	O	positive regulation of NIK/NF-kappaB signaling	1	3	0.038
GO:2000535	O	regulation of entry of bacterium into host cell	1	3	0.038
GO:0006878	P	cellular copper ion homeostasis	1	1	0.016
GO:0055070	P	copper ion homeostasis	1	1	0.016
GO:0046688	P	response to copper ion	1	2	0.042
GO:0030973	P	molybdate ion binding	1	1	0.015
GO:0015208	S	guanine transmembrane transporter activity	1	1	0.013
GO:0015854	S	guanine transport	1	1	0.013
GO:0098710	S	guanine import across plasma membrane	1	1	0.013
GO:1903716	S	guanine transmembrane transport	1	1	0.013
GO:0072530	S	purine-containing compound transmembrane transport	1	1	0.013
GO:0015205	S	nucleobase transmembrane transporter activity	1	2	0.026
GO:0015851	S	nucleobase transport	1	2	0.026
GO:0005345	S	purine nucleobase transmembrane transporter activity	1	1	0.013
GO:0006863	S	purine nucleobase transport	1	1	0.013
GO:1904823	S	purine nucleobase transmembrane transport	1	1	0.013
GO:0035344	S	hypoxanthine transport	1	1	0.013

Table S4. Output of gene set enrichment analysis (GSEA) performed for the up-regulated genes of *Paraburkholderia graminis* colonizing the roots of Malibu, a cultivar of Broccoli, seedlings. GSEA was performed using Goseq using $P < 0.05$.

GO term	Ontology	Description	NO. DE in list	NO. in reference	P-value
GO:0015002	C	heme-copper terminal oxidase activity	2	3	0.018
GO:0033177	C	proton-transporting two-sector ATPase complex, proton-transporting domain	2	3	0.014
GO:0045263	C	proton-transporting ATP synthase complex, coupling factor F(o)	2	3	0.014
GO:0045264	C	plasma membrane proton-transporting ATP synthase complex, coupling factor F(o)	2	3	0.014
GO:0009055	C	electron transfer activity	5	19	0.013
GO:0022900	C	electron transport chain	6	30	0.025
GO:1902600	C	proton transmembrane transport	4	18	0.048
GO:0042126	C	nitrate metabolic process	2	2	0.006
GO:2001057	C	reactive nitrogen species metabolic process	2	4	0.034
GO:0070469	C	respiratory chain	3	8	0.020
GO:0070470	C	plasma membrane respiratory chain	3	8	0.020
GO:0098803	C	respiratory chain complex	3	8	0.020
GO:0022904	C	respiratory electron transport chain	4	18	0.047
GO:0045333	C	cellular respiration	7	38	0.027
GO:0009060	C	aerobic respiration	5	22	0.029
GO:0000104	C	succinate dehydrogenase activity	3	8	0.018
GO:0051538	C	3 iron, 4 sulfur cluster binding	2	4	0.032
GO:0005623	CDEFHIJK-MNOPSTV	cell	79	905	0.037
GO:0044464		cell part	79	905	0.037
GO:0005575		cellular_component	80	926	0.048
GO:0016020	CDEFHM-NOPSTV	membrane	46	376	0.000
GO:0005886	CDEFHN-OPSTV	plasma membrane	44	336	0.000
GO:0051179	CDEFMNP-TU	localization	32	156	0.000
GO:0044459	CDEFNP	plasma membrane part	17	107	0.003
GO:0031226	CDEFNP	intrinsic component of plasma membrane	12	79	0.020
GO:0044425	CDEFNPT	membrane part	18	134	0.015
GO:0031224	CDEFNPT	intrinsic component of membrane	15	110	0.024
GO:0071944	CDEGHM-NPQST	cell periphery	46	385	0.000
GO:1902494	CEFJP	catalytic complex	11	62	0.009
GO:0016021	CEFNPT	integral component of membrane	14	98	0.021
GO:0005887	CEFNPT	integral component of plasma membrane	11	75	0.034
GO:0006811	CEPT	ion transport	11	63	0.007
GO:1990204	CF	oxidoreductase complex	6	16	0.001
GO:0040011	CHMNT	locomotion	22	26	0.000
GO:0044780	CN	bacterial-type flagellum assembly	4	5	0.000
GO:0044781	CN	bacterial-type flagellum organization	4	5	0.000
GO:0030030	CN	cell projection organization	4	8	0.003
GO:0030031	CN	cell projection assembly	4	8	0.003
GO:0001539	CNM	cilium or flagellum-dependent cell motility	16	19	0.000
GO:0071973	CNM	bacterial-type flagellum-dependent cell motility	16	19	0.000
GO:0097588	CNM	archaeal or bacterial-type flagellum-dependent cell motility	16	19	0.000
GO:0006928	CNM	movement of cell or subcellular component	16	20	0.000
GO:0048870	CNM	cell motility	16	20	0.000
GO:0051674	CNM	localization of cell	16	20	0.000
GO:0098660	CP	inorganic ion transmembrane transport	6	26	0.014
GO:0034220	CP	ion transmembrane transport	9	52	0.017
GO:0098797	CP	plasma membrane protein complex	7	25	0.002
GO:0098796	CP	membrane protein complex	8	41	0.012
GO:0051782	DK	negative regulation of cell division	2	5	0.046
GO:0009605	EHNT	response to external stimulus	9	42	0.005

Table S4. (Continued)

GO term	Ontology	Description	NO. DE in list	NO. in reference	P-value
GO:0007154	ENT	cell communication	6	30	0.030
GO:0006820	EPT	anion transport	7	39	0.024
GO:0098561	HNT	methyl accepting chemotaxis protein complex	3	5	0.005
GO:0006935	HNT	chemotaxis	6	7	0.000
GO:0042330	HNT	taxis	6	7	0.000
GO:0051270	MT	regulation of cellular component movement	2	3	0.021
GO:0040012	MT	regulation of locomotion	2	3	0.021
GO:1902021	MT	regulation of bacterial-type flagellum-dependent cell motility	2	3	0.021
GO:2000145	MT	regulation of cell motility	2	3	0.021
GO:0043228	N	non-membrane-bounded organelle	16	92	0.001
GO:0009425	N	bacterial-type flagellum basal body	10	10	0.000
GO:0044461	N	bacterial-type flagellum part	15	15	0.000
GO:0071978	N	bacterial-type flagellum-dependent swarming motility	10	10	0.000
GO:0009288	N	bacterial-type flagellum	16	18	0.000
GO:0044463	N	cell projection part	15	16	0.000
GO:0042995	N	cell projection	16	20	0.000
GO:0009424	N	bacterial-type flagellum hook	7	7	0.000
GO:0120100	N	bacterial-type flagellum motor	2	2	0.005
GO:0120101	N	bacterial-type flagellum stator complex	2	2	0.005
GO:0044422	N	organelle part	15	87	0.001
GO:0043226	N	organelle	16	111	0.006
GO:0031399	NT	regulation of protein modification process	2	3	0.021
GO:0031401	NT	positive regulation of protein modification process	2	3	0.021
GO:1901873	NT	regulation of post-translational protein modification	2	3	0.021
GO:1901875	NT	positive regulation of post-translational protein modification	2	3	0.021
GO:0007165	NT	signal transduction	4	7	0.001
GO:0023052	NT	signaling	4	7	0.001
GO:0055052	P	ATP-binding cassette (ABC) transporter complex, substrate-binding subunit-containing	2	3	0.015
GO:0043190	P	ATP-binding cassette (ABC) transporter complex	2	5	0.046
GO:0015698	P	inorganic anion transport	3	8	0.018
GO:0098661	P	inorganic anion transmembrane transport	2	5	0.050
GO:0010921	P	regulation of phosphatase activity	3	3	0.000
GO:0006817	P	phosphate ion transport	3	4	0.002
GO:0015169	P	glycerol-3-phosphate transmembrane transporter activity	2	3	0.015
GO:0015605	P	organophosphate ester transmembrane transporter activity	2	3	0.015
GO:0035435	P	phosphate ion transmembrane transport	2	3	0.018
GO:0015794	P	glycerol-3-phosphate transmembrane transport	2	4	0.031
GO:0044110	PS	growth involved in symbiotic interaction	3	6	0.007
GO:0044116	PS	growth of symbiont involved in interaction with host	3	6	0.007
GO:0044117	PS	growth of symbiont in host	3	6	0.007
GO:0019220	PST	regulation of phosphate metabolic process	5	10	0.000
GO:0051174	PST	regulation of phosphorus metabolic process	5	10	0.000
GO:0035303	PT	regulation of dephosphorylation	4	4	0.000
GO:0046777	ST	protein autophosphorylation	4	7	0.001
GO:0006468	ST	protein phosphorylation	4	10	0.006
GO:0004673	T	protein histidine kinase activity	3	3	0.001
GO:0018202	T	peptidyl-histidine modification	3	3	0.001
GO:0023014	T	signal transduction by protein phosphorylation	3	3	0.001
GO:0000160	T	phosphorelay signal transduction system	3	3	0.001
GO:0016775	T	phosphotransferase activity, nitrogenous group as acceptor	3	3	0.001
GO:0018106	T	peptidyl-histidine phosphorylation	3	3	0.001
GO:0000155	T	phosphorelay sensor kinase activity	2	2	0.006
GO:0035556	T	intracellular signal transduction	3	3	0.001
GO:0004672	T	protein kinase activity	3	6	0.011

Table S5. Output of gene set enrichment analysis (GSEA) performed for the down-regulated genes of *Paraburkholderia graminis* colonizing the roots of Malibu, a cultivar of Broccoli, seedlings. GSEA was performed using Goseq using $P < 0.05$.

GO term	Ontology	Description	NO. DE in list	NO. in reference	P-value
GO:0035375	C	zymogen binding	1	1	0.016
GO:0075141	C	maintenance of symbiont tolerance to host environment	1	1	0.016
GO:0010447	C	response to acidic pH	1	2	0.032
GO:0051701	C	interaction with host	2	14	0.028
GO:0036455	C	iron-sulfur transferase activity	1	1	0.030
GO:0004451	C	isocitrate lyase activity	1	1	0.016
GO:0006102	C	isocitrate metabolic process	1	1	0.016
GO:0034357	C	photosynthetic membrane	1	1	0.016
GO:0001897	C	cytolysis by symbiont of host cells	1	3	0.048
GO:0019835	C	cytolysis	1	3	0.048
GO:0019836	C	hemolysis by symbiont of host erythrocytes	1	3	0.048
GO:0044179	C	hemolysis in other organism	1	3	0.048
GO:0051715	C	cytolysis in other organism	1	3	0.048
GO:0051801	C	cytolysis in other organism involved in symbiotic interaction	1	3	0.048
GO:0052331	C	hemolysis in other organism involved in symbiotic interaction	1	3	0.048
GO:0071456	C	cellular response to hypoxia	1	1	0.016
GO:0009579	C	thylakoid	1	1	0.016
GO:0042651	C	thylakoid membrane	1	1	0.016
GO:0044436	C	thylakoid part	1	1	0.016
GO:0006212	C	uracil catabolic process	1	2	0.038
GO:0019860	C	uracil metabolic process	1	2	0.038
GO:0003995	C	acyl-CoA dehydrogenase activity	1	1	0.015
GO:0008470	C	isovaleryl-CoA dehydrogenase activity	1	1	0.015
GO:0010034	C	response to acetate	1	1	0.016
GO:0036294	C	cellular response to decreased oxygen levels	1	1	0.016
GO:0046421	C	methylisocitrate lyase activity	1	1	0.016
GO:0070542	C	response to fatty acid	1	1	0.016
GO:0071453	C	cellular response to oxygen levels	1	1	0.016
GO:0033993	C	response to lipid	1	2	0.031
GO:0003868	C	4-hydroxyphenylpyruvate dioxygenase activity	1	2	0.032
GO:0006097	C	glyoxylate cycle	1	3	0.046
GO:0006572	C	tyrosine catabolic process	1	3	0.047
GO:0016782	C	transferase activity, transferring sulfur-containing groups	2	9	0.011
GO:0005488	CEJKLOPS	binding	15	513	0.041
GO:0043167	CEJOPS	ion binding	10	264	0.013
GO:0016226	CES	iron-sulfur cluster assembly	3	6	0.001
GO:0008198	CJS	ferrous iron binding	3	9	0.001
GO:0005506	CJS	iron ion binding	3	15	0.004
GO:0005515	CKOP	protein binding	9	198	0.006
GO:0042802	CKOP	identical protein binding	8	169	0.009
GO:1903506	CKST	regulation of nucleic acid-templated transcription	4	67	0.049
GO:2001141	CKST	regulation of RNA biosynthetic process	4	67	0.049
GO:0010033	CO	response to organic substance	3	17	0.005
GO:0009628	CO	response to abiotic stimulus	5	94	0.032
GO:0009405	CO	pathogenesis	2	10	0.012
GO:0006950	CO	response to stress	7	157	0.026
GO:0035821	CO	modification of morphology or physiology of other organism	2	8	0.007
GO:0051817	CO	modification of morphology or physiology of other organism involved in symbiotic interaction	2	8	0.007
GO:0044764	CO	multi-organism cellular process	2	7	0.005
GO:0044403	COP	symbiont process	5	30	0.000
GO:0044419	COP	interspecies interaction between organisms	5	34	0.000
GO:0051704	COP	multi-organism process	5	37	0.001
GO:0097428	CS	protein maturation by iron-sulfur cluster transfer	2	5	0.007
GO:0051537	CS	2 iron, 2 sulfur cluster binding	2	10	0.034

Table S5. (Continued)

GO term	Ontology	Description	NO. DE in list	NO. in reference	P-value
GO:0051604	CS	protein maturation	2	13	0.039
GO:0006790	CS	sulfur compound metabolic process	3	44	0.050
GO:0031163	CS	metallo-sulfur cluster assembly	3	6	0.001
GO:0009000	E	selenocysteine lyase activity	1	1	0.016
GO:0031071	E	cysteine desulfurase activity	1	1	0.016
GO:0008713	EGP	ADP-heptose-lipopolysaccharide heptosyltransferase activity	1	2	0.031
GO:0015530	EGP	shikimate transmembrane transporter activity	1	1	0.016
GO:0015733	EGP	shikimate transmembrane transport	1	1	0.016
GO:0015850	EGP	organic hydroxy compound transport	1	1	0.016
GO:1901618	EGP	organic hydroxy compound transmembrane transporter activity	1	1	0.016
GO:0046820	EH	4-amino-4-deoxychorismate synthase activity	1	1	0.015
GO:0008483	EH	transaminase activity	2	16	0.025
GO:0016769	EH	transferase activity, transferring nitrogenous groups	2	18	0.032
GO:0008920	EPG	lipopolysaccharide heptosyltransferase activity	1	2	0.031
GO:0008463	J	formylmethionine deformylase activity	1	1	0.026
GO:0018206	J	peptidyl-methionine modification	1	2	0.050
GO:0042586	J	peptide deformylase activity	1	2	0.050
GO:0043686	J	co-translational protein modification	1	2	0.050
GO:0101031	O	chaperone complex	2	6	0.009
GO:0016465	O	chaperonin ATPase complex	2	6	0.009
GO:0051084	O	'de novo' posttranslational protein folding	2	10	0.018
GO:0006458	O	'de novo' protein folding	2	11	0.021
GO:0009408	O	response to heat	4	36	0.005
GO:0009266	O	response to temperature stimulus	4	44	0.011
GO:0033644	O	host cell membrane	1	3	0.046
GO:0033647	O	host intracellular organelle	1	3	0.046
GO:0033648	O	host intracellular membrane-bounded organelle	1	3	0.046
GO:0044174	O	host cell endosome	1	3	0.046
GO:0044175	O	host cell endosome membrane	1	3	0.046
GO:0046812	O	host cell surface binding	1	3	0.046
GO:0044406	O	adhesion of symbiont to host	1	3	0.046
GO:0044650	O	adhesion of symbiont to host cell	1	3	0.046
GO:0052047	O	interaction with other organism via secreted substance involved in symbiotic interaction	1	3	0.046
GO:0052212	O	modification of morphology or physiology of other organism via secreted substance involved in symbiotic interaction	1	3	0.046
GO:2000535	O	regulation of entry of bacterium into host cell	1	3	0.046
GO:0031249	O	denatured protein binding	1	1	0.015
GO:0051082	O	unfolded protein binding	3	13	0.002
GO:0006986	O	response to unfolded protein	2	6	0.009
GO:0006457	O	protein folding	3	23	0.009
GO:0051085	O	chaperone cofactor-dependent protein refolding	2	10	0.018
GO:1990220	O	GroEL-GroES complex	2	6	0.009
GO:0019058	O	viral life cycle	2	7	0.011
GO:0019068	O	virion assembly	2	7	0.011
GO:0035966	O	response to topologically incorrect protein	2	7	0.011
GO:0016032	O	viral process	2	10	0.022
GO:0000774	O	adenyl-nucleotide exchange factor activity	1	1	0.023
GO:0009986	O	cell surface	2	16	0.032
GO:0022610	O	biological adhesion	1	3	0.046
GO:0044218	O	other organism cell membrane	1	3	0.046
GO:0044279	O	other organism membrane	1	3	0.046
GO:1901222	O	regulation of NIK/NF-kappaB signaling	1	3	0.046
GO:1901224	O	positive regulation of NIK/NF-kappaB signaling	1	3	0.046
GO:0061077	O	chaperone-mediated protein folding	2	18	0.049
GO:0030973	P	molybdate ion binding	1	1	0.018
GO:0140104	S	molecular carrier activity	2	6	0.012

Table S5. (Continued)

GO term	Ontology	Description	NO. DE in list	NO. in reference	P-value
GO:0046484		oxazole or thiazole metabolic process	1	1	0.016
GO:0097163		sulfur carrier activity	1	1	0.016
GO:0018131		oxazole or thiazole biosynthetic process	1	1	0.016
GO:0004123		cystathionine gamma-lyase activity	1	2	0.031
GO:0031119		tRNA pseudouridine synthesis	1	2	0.033

Chapter 7

General discussion

General discussion

Plant growth-promoting rhizobacteria (PGPR) are bacteria that colonize roots of specific or several plant species and promote plant growth directly or indirectly by suppressing pests or diseases. In recent years, advances in mass spectrometry and chemo-informatics are contributing immensely to our understanding of the impact of rhizobacteria on the chemistry, providing a mechanistic understanding of growth promoting and disease suppression but also new opportunities to explore and exploit rhizobacteria as a new platform to produce high value natural plant products (HVNP) (Etalo *et al.*, 2018). To date, the majority of studies on rhizobacteria-mediated reprogramming of plant chemistry are descriptive in nature and provide limited insights into the biological relevance of the changes induced by the rhizobacteria in the plant metabolome and if or how these changes affect host phenotype. Particularly most information on rhizobacteria-induced changes in common and specific metabolic pathways that are central to plant growth and defense is either preliminary or non-existent. When it comes to the rhizobacteria side, if and how the intrinsic or altered metabolic state of the host influences rhizobacterial traits that are directly or indirectly affecting host fitness is still an undiscovered island. On the technological side, the majority of past and present studies employed targeted metabolite profiling and those that used untargeted metabolomics are often bound to either profiling of primary metabolites or focused on a specific subset of secondary metabolites. To address these knowledge gaps and to advance our understanding of the chemical continuum between rhizobacteria and their host, my thesis focused on investigating the impact of three bacteria genera comprising five bacterial species (*Pseudomonas fluorescens* SS101, *Microbacterium*, and *Paraburkholderia graminis*, *P. hospita*, and *P. terricola*) on different phenotypes and on the shoot metabolome of three plant species (*Arabidopsis thaliana*, *Artemisia annua*, *Brassica oleracea* var. *italica*).

The **aims of my thesis** were to i) identify common and specific changes in the plant metabolome induced by different rhizobacterial species ii) link rhizobacteria-induced changes in plant chemistry to other plant phenotypes, iii) identify rhizobacterial genes, pathways and traits associated with changes in plant chemistry and plant phenotypes. Although the results of the experiments conducted in my thesis do not provide all the answers to the above-mentioned questions, it does give new insights into the diverse effects of rhizobacteria on the host metabolome and the potential impact of the metabolome changes on host fitness. Furthermore, with the magnitude of data generated during the course of my PhD study more questions were generated than answered. Here, I will discuss the major findings as well as the limitations of my study and provide future directions to investigate the chemical continuum between rhizobacteria and plants.

1. Are plants the sole masters of their metabolic regulation?

Plants synthesize a vast array of secondary metabolites. Several metabolites from wild or cultivated plant have shown pharmaceutical activities either as metabolite itself or as a

scaffold to synthesize pharmaceutically improved drugs candidates (Oksman-Caldentey & Inzé, 2004; Etalo *et al.*, 2018). Because of this, a great deal of efforts has been invested in identifying factors that influence the biosynthesis, metabolic fluxes, transport and storage of plant metabolites with medicinal and nutritional value for human and animals as well as metabolites contributing to plant tolerance against (a)biotic stress factors. Earlier studies focused more on the impact of external environmental conditions such as light, drought, temperature and edaphic factors on primary and secondary plant metabolism (Gautier *et al.*, 2008; Griesser *et al.*, 2015; Yang *et al.*, 2018). Recently the impact of rhizobacteria and other plant-associated microbes, collectively referred to as the plant microbiome, on metabolism of their host is gaining significant attraction (Etalo *et al.*, 2018; Korenblum & Aharoni, 2019). Particular interest also emerged for metabolites that were initially thought to be of plant origin but now appear to be either exclusively or in part synthesized by the microbes that live on or in the host plant tissue (Kusari *et al.*, 2011; Kusari *et al.*, 2014; Ludwig-Muller, 2015). Such evidences of a microbial footprint on the host metabolome not only signifies the importance of microbes in plant metabolism but also poses questions on the long-held assumption that portrays plants as the sole masters of their metabolism.

To have a broader understanding of the specific impact of rhizobacteria on the host metabolism, we performed non-targeted metabolomics in **Chapters 3**, **4**, and **5** and revealed that different rhizobacteria-plants combinations can significantly (18-74%) perturb the relative abundance or presence/absence of the host metabolome when compared to non-bacterized plants. For example, in **Chapter 3**, root tip inoculation of Arabidopsis with *Pseudomonas fluorescens* SS101, *Microbacterium* EC8, or *Paraburkholderia graminis* significantly altered 64% of secondary metabolites in the shoot in comparison with non-treated control. Interestingly, in **Chapter 4** root tip inoculation of two Broccoli cultivars Coronado and Malibu with three different *Paraburkholderia* species led to 49% and 74% alteration of their shoot metabolome, respectively. These results strongly suggest that rhizobacteria have substantial effect on their host metabolome and that the magnitude of alteration of the host metabolome is highly dependent on the interacting partners. Beyond their overarching impact on the metabolome, we also showed that rhizobacteria can modulate specific metabolic pathways of their host. In **Chapters 3** and **4,** we showed that the phenylpropanoid pathways is the prime target of rhizobacteria and its induction is associated with enhanced plant defense against bacterial pathogens. Similarly, I showed in **Chapter 4** that rhizobacteria influence both sugar generation and utilization of their host and the combined effect showed an association with plant growth. Results shown in my thesis and by other researchers magnifies the enormous impact of rhizobacteria on their host metabolism, growth and defense and force us to re-think both the mechanisms underlying the regulation of the metabolic pathways. On the other side, results in **Chapter 6** showed that plants also have big impact on rhizobacteria transcriptome landscape with significant variation between different plant cultivars. Perhaps this way of looking at the partnership between plants and rhizobacteria could help to redefine the question of who is the driver of the association. Altogether, mechanisms governing the

partnership between plants and rhizobacteria are still largely elusive as microbe-host plant interaction is the product of over 450 million years of co-evolution (Zhalnina *et al.*, 2018).

2. Metabolic signatures of plant growth, defense and their trade-off

A recent study on closely related strains within the *Pseudomonas fluorescens* species complex tied the transition between pathogenic and commensal bacterial life style in Arabidopsis to particular genetic loci such as lipopeptide/quorum island whose presence is essential to pathogenicity in the bacterium (Melnyk *et al.*, 2019). Contrary to that, both phenotype- and metabolome-based assessment of the host plants in our "blind date experiment" involving Arabidopsis, Artemisia, and Broccoli as hosts and *Pseudomonas fluorescens* SS101 (*Pf* SS101), *Microbacterium* (MB) and *Paraburkholderia graminis* (*Pbg*) as interacting rhizobacteria revealed that none of the rhizobacterial genera promoted plant growth of all plant species (**Chapter 3**). While *Pf* SS101 enhanced biomass of Arabidopsis and Artemisia, it reduced biomass of Broccoli when compared to the non-treated control. Likewise, *Pbg* root inoculation enhanced growth of Artemisia and Broccoli but showed detrimental effects on Arabidopsis growth. The shoot metabolome profiles of Broccoli treated with *Pf* SS101 and Arabidopsis treated with *Pbg* were characterized by the accumulation of defensive and stress-related phenolic metabolites such as anthocyanin. Moreover, *Paraburkholderia terricola* exhibited Broccoli cultivar dependent growth promotion (**Chapter 4**). These results strongly suggest that the impact of rhizobacteria on plant growth and health is not only linked to specific bacterial determinants but also to the genetic background of the interacting plant. During the course of my study, we used the metabolic signature of several rhizobacteria-plant interaction to understand metabolic networks governing growth, defense and the potential trade-off between these processes. Trade-off between growth and defense is a widely accepted concept and arises from resource limitation and differential allocation of resources for defense, growth and development (Herms & Mattson, 1992; Pieterse *et al.*, 2012; Lozano-Durán & Zipfel, 2015). Plant metabolites can be structurally categorized into five major groups, i.e. polyketides, isoprenoids (e.g. terpenoids), alkaloids, phenylpropanoids and flavonoids (Oksman-Caldentey & Inzé, 2004). Among others, metabolites that belong to phenylpropanoid pathways such as hydroxycinnamates and flavonoids represent the largest group of plant secondary metabolites, existing ubiquitously across the plant kingdom and playing important roles as chemical weapons against biotic stresses (Treutter, 2005; Korkina, 2007; War *et al.*, 2012). In **Chapters 3**, **4** and **5,** we showed that accumulation of metabolites belonging to the phenylpropanoid pathway, in particular hydroxycinnamates and flavonoids, was associated with ineffective partnerships between the plants and rhizobacteria tested, i.e. partnerships that had an adverse effect on specific phenotypes such as plant growth. The accumulation of defensive compounds such as hydroxycinnamates and flavonoids particularly the flavonol subclass could potentially affect plant growth through several ways. High abundance of flavonoids particularly the flavonol subclass may impact auxin transport (Besseau *et al.*, 2007), auxin biosynthesis and its conjugation/degradation

(Kuhn *et al.*, 2016). Additionally, the higher accumulation of phenylpropanoids and other carbon and energy-costly secondary metabolites in the ineffective partnerships could pose resource limitation to plant growth-related processes and lead to an adverse effect on plant growth. For example, the metabolic cost for pro-anthocyanidins and lignin is similar to that of biosynthesis of protein and phenylalanine, the major precursor for these metabolite classes and other phenylpropanoids and the metabolically most expensive amino acid (after tryptophan) to synthesize (Hemingway *et al.*, 1989; Seigler, 1998). Other metabolites such as indolic glucosinolates induced by rhizobacteria treatment in Broccoli also could compete for tryptophan and other intermediates of the tryptophan-dependent auxin biosynthesis and concomitantly affect plant growth (Malka & Cheng, 2017). In **Chapter 4**, plants treated with *Paraburkholderia* species (*Pbg* and *Pbh*) showed substantial accumulation of various secondary metabolites via phenylpropanoid biosynthesis and surprisingly showed also enhanced growth. The primary metabolite profile of these plants revealed high accumulation of soluble sugars such as fructose (>280-fold increase relative to untreated control). Fructose is the primary substrate for fructose-6-phospate, a key substrate for the biosynthesis of both phosphoenolpyruvate (PEP) and erythrose-4-phosphate. These two intermediates are channeled into the shikimate pathway that bridges carbohydrate metabolism to biosynthesis of aromatic primary and secondary metabolites (Herrmann & Weaver, 1999). The shikimate pathway provides all the important precursors for the biosynthesis of phenylpropanoids including hydroxycinnamates, flavonoids, stilbenoids, coumarins and lignins which were significantly accumulated in Broccoli plants treated with *Paraburkholderia* species. These results suggest that rhizobacteria enable plants to sustain enhanced growth while producing numerous defensive secondary metabolites by enhancing both sugar generation and utilization to fuel both growth and defense. To our best knowledge, this is the first comprehensive study that employed combined primary and secondary metabolomics techniques to understand rhizobacteria-mediated changes in global metabolism of plants, linking metabolic flux from primary metabolites (soluble sugar and amino acid) to specific secondary metabolites that potentially function as chemical weapon against pathogen infection.

3. Tilting plant metabolism towards high value natural plant products

Recent studies on microbe-mediate phytochemical alteration have predominantly focused on medicinal plants as they are shown to be an attractive source for pharmaceutically important bioactive secondary metabolites (**Chapter 2**). Some good examples are PGPR-mediated induction of artemisinin and dihydroartemisinin, antimalarial agents in Artemisia ((Arora *et al.*, 2016), **Chapter 3**), and of morphine in Poppy (Pandey, Shiv S *et al.*, 2016). Similar attempts were also employed to improve pharmaceutically important secondary metabolites in crops. For instance, inoculations of *Glycine max* with single or consortia of various rhizobacteria strains belonging to *Arthrobacter, Azotobacter, Bacillus, Chryseobacterium, Curtobacterium, Pseudomonas, Stenotrophomonas,* and *Streptomyces,* induced the level of isoflavonoids and phytoestrogen agents with cancer chemo-prevention ability (Birt *et al.*,

2001; Ramos-Solano *et al.*, 2010; Algar *et al.*, 2012; Algar *et al.*, 2013; Chamam *et al.*, 2013; Kiprovski *et al.*, 2016). Furthermore, similar studies reported modulating effects of plant-associated microbes on the metabolome of *Oryza sativa* (Mishra *et al.*, 2006; Chamam *et al.*, 2013; Chamam *et al.*, 2015), *Zea mays* (Walker *et al.*, 2011; Walker *et al.*, 2012; Couillerot *et al.*, 2013; Planchamp *et al.*, 2015; Rozier *et al.*, 2016) and *Mentha piperita* (Santoro *et al.*, 2011; del Rosario Cappellari *et al.*, 2015; Santoro *et al.*, 2015). Likewise, our result indicated that different rhizobacteria alter the host metabolome both in effective or ineffective partnerships. Both kinds of partnership can be employed to tilt the host metabolism towards nutritionally and/or pharmaceutically important high value natural plant compounds (HVPC). To empirically demonstrate the bioactivity of metabolites that were altered by rhizobacteria in plants, I subjected extracts from the shoots of plants treated on roots with (or not) rhizobacteria to a series of non-receptor-mediated CALUX bioassays to test if bacteria inoculation enhanced biological activities plant materials on various human health promoting traces. Among others, shoot extracts of *Pbg*-inoculated Broccoli cultivar Malibu demonstrated higher anti-oxidative capacity in Nrf2 basis CALUX assay when compared to the non-treated control samples (**Box**). Interestingly, in **Chapter 4** *Pbg* inoculation of cultivar Malibu led to the induction of plant metabolites belonging to different subclass of phenylpropanoid pathway such as flavonoids, hydroxycinnamates and stilbenoids that have displayed, in other studies, various bioactivities against multiple diseases and disorders (Nijveldt *et al.*, 2001; Erlund, 2004; Leopoldini *et al.*, 2011; Gülcin, 2012). Collectively these results suggest that these enhanced phenolic compounds may play a key role as anti-oxidants. Activity-guided fractionation and purification will be further strategy to shed light on these bioactive metabolites. Considering that each rhizobacteria-host plant combination differently modulates plant chemistry (**Chapters 3**, **4**, and **5**), detailed understanding of the underlying primary and secondary metabolic pathways and their interconnection will be instrumental to fine-tune the most appropriate plant and rhizobacterial species association for selected bioactivities.

4. Microbial traits affecting plant chemistry and vice-versa

While a growing number of studies is steadily reporting the effects of bacterial strains on plant chemistry (**Chapter 2**), bacterial traits that trigger specific changes in the plant metabolome remain largely unknown. In this thesis, we unraveled some bacterial traits influencing host plant chemistry changes. First, root colonization ability of rhizobacteria seemed to play an essential role, as in nature successful bacterial colonization is generally the first step to establish a beneficial interaction with the host (Lugtenberg *et al.*, 2001; Bhattacharyya & Jha, 2012). For example, in **Chapter 3**, I showed that *Microbacterium* (*MB*) did not efficiently colonize Artemisia roots and showed no significant impact on the host metabolome. Also for *Paraburkholderia* we showed that temporal changes in the rhizosphere population densities coincided with the magnitude of their impact on the host primary and secondary metabolome (**Chapter 4**). Genome-wide analysis of plant growth-promoting *Pseudomonas*

Box

CALUX bioassays

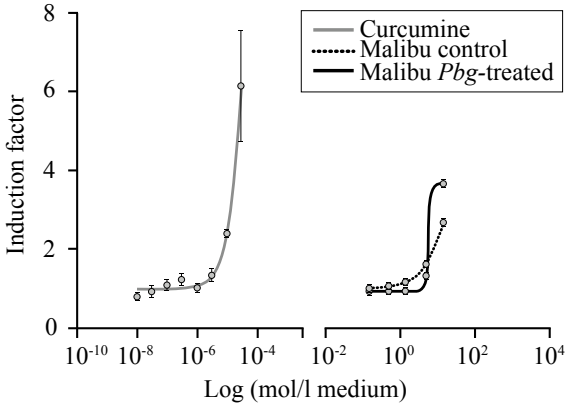

Fig 1. Results of Nrf2 CALUX assay. The dose-response curves of the tested samples are given, including curcumine, the reference compound.

Freshly frozen plant tissue materials (300 mg) were extracted with 900 ul of 97% ethanol for 30 minutes under sonication. Next, the samples were dried by speed vacuuming and were re-dissolved in 200 ul of DMSO. Serial dilution at different concentrations were prepared. Nrf1 cells were seeded in 96-wells plates and pre-incubated for 24 hours. Following pre-incubation, CALUX cells were exposed for 24 hours to the serial dilutions in triplicate (1% DMSO) and then lysed to measure luciferase activities. Thereafter, the Nrf2 CALUX activity in both control and *Pbg*-treated Broccoli cultivar Malibu samples were comparable. The Nrf2 CALUX (van der Linden *et al.*, 2014) measures activity of the Nrf2 transcription factor that trigger expression of genes involved in detoxification and the anti-oxidant stress response (Ma, 2013). As shown in **Fig 1**, *Paraburkholderia graminis* (*Pbg*) treated Broccoli shoot sample (Malibu) exhibited higher luciferase activity when compared to control, indicating *Pbg* induced anti-oxidative capacity in Broccoli sample.

I would like to acknowledge the expert input of Dr. Harrie Besselink, Dr. Tjalf de Boer and Prof. Bram Brouwer at BioDetection Systems (BDS, Science Park 406 1098 XH Amsterdam) for the CALUX bioassays.

fluorescens strain SS101 (*Pf* SS101) combined with site-directed mutagenesis and genetic complementation recently revealed that sulfur assimilation plays an important role in growth promotion and induced systemic resistance of the model plant Arabidopsis (Cheng *et al.*, 2017). In **Chapter 5** of my thesis, we showed that bacterial sulfur assimilation affects both sulfur containing and non-sulfur containing metabolites in two Broccoli cultivars. Furthermore, in **Chapter 5** comparative metabolomics analysis of Arabidopsis plants treated with *Pf* SS101and its *cysH* mutant showed that sulfur assimilation in *Pf* SS101 affects side chain elongation of the aliphatic glucosinolates. Plants treated with the mutant showed an accumulation of short and medium chain aliphatic glucosinolates, whereas in plants treated

with wildtype *Pf* SS101 the long chain aliphatic glucosinolates were more abundant.

Plant-microbe interactions alter gene expression profiles of both interacting organisms. Thus, transcriptome analysis is often preferred as generic tool to unravel genes and pathways that govern the interaction. In Arabidopsis, for instance, several strains of *Pseudomonas fluorescens* were shown to alter the expression of several genes related to auxin biosynthesis and transport, sulfur assimilation and disease resistance (Wang *et al.*, 2005; Cheng *et al.*, 2017). Microbes can also alter the expression of plant genes even without direct contact through a blend of their volatile organic compounds (VOCs). Recently, exposure of Arabidopsis to *Microbacterium* EC8 VOCs was shown to alter the expression of genes involved in the assimilation and transport of sulfate and nitrate (Cordovez *et al.*, 2018). However, relatively less attention has been given on the impact of the host on the gene expression profile of the associated rhizobacteria. In **Chapter 6**, we showed that the gene expression profile of *Pbg* on synthetic media and on plant roots is significantly different. Our analysis showed that genes corresponding to flagella assembly and chemotaxis, energy metabolism, phosphate and nitrate metabolism and transport were significantly overexpressed in *Pbg*-plant interactions when compared to *Pbg* grown only on the synthetic media. These group of genes were upregulated and significantly enriched when *Pbg* interacts with both Broccoli cultivars and can be considered as a general response representing establishment of an association with the host. Our result is in line with previous study that showed maize exudate induced *Bacillus amyloliquefaciens* genes involved in nutrient utilization, bacterial chemotaxis and motility (Fan *et al.*, 2012). The induction of genes associated with energy metabolism and nutrient mobilization in *Pbg* suggests the establishment of symbiotic relationship between the plant and rhizobacteria, with the rhizobacteria contributing to nutrient acquisition and the host providing carbon sources for the energy production of the rhizobacteria. Furthermore, the results showed a number of genes expressed in *Pbg* in a Broccoli cultivar specific manner. Among those, ABC transporters were significantly enriched when *Pbg* interacted with cultivar Malibu. To further unravel the molecular interplay, site-directed mutagenesis, heterologous expression or overexpression of these specific genes is needed to identify the effects these specific mutations on plant chemistry and plant phenotypes.

5. A milestone in future breeding strategy and obstacle in field trial

In the past century, crop improvement strategies gave greater emphasis to yield, nutritional quality, disease resistance, or abiotic stress tolerance. In this context, breeding practices have emphasized more on enhancing plant intrinsic genetic characteristic to influence a desired phenotype. This approach has proven to be an effective strategy and was the corner stone of the green revolution. Currently we are facing huge challenges to meet the global food demand. Furthermore, an increasing awareness of the impact of agricultural practices on biodiversity and our environment is putting a great deal of pressure on agricultural production systems towards more sustainable practices (Wei & Jousset, 2017). Findings of my thesis

demonstrate that the use of beneficial rhizobacteria can be a novel and more generic means to complement conventional agricultural practices. Microbiome-assisted agriculture can be considered as a "taking care of microbe to take care of plant" approach. Recent studies empirically support the impact microbes can have on plant phenotype and chemistry. For example, a recent study by Carrión (Carrión *et al.*, 2019) demonstrated that invasion of the root system by the soil-borne fungus *Rhizoctonia solani* enriched for Chitinophagaceae and Flavobacteriaceae inside the roots which in turn suppressed the disease development via enhancing enzymatic activities associated with fungal cell-wall degradation as well as other secondary metabolites encoded by a novel NRPS-PKS gene cluster. Similarly, *Pseudomonas simiae* WCS417 induced root exudation of scopoletin, an iron-mobilizing coumarin with selective antimicrobial activity, suppressing the growth of fungal root pathogens but supporting root colonization by beneficial *Pseudomonas* strains (Stringlis, Ioannis A *et al.*, 2018). Thus, in future plant breeding programs, identifying plant characteristics that promote the recruitment and activities of beneficial microbes can be highly instrumental for developing sustainable agricultural practices. Furthermore, the "microbial-Gene Positioning System (m-GPS)" concept that we proposed in **Chapter 2** also can have an important contribution. The first principle resides on the identification of plant metabolic pathways that are altered by rhizobacteria and linked to plant phenotypes such as yield, quality or stress tolerance. For example, in my thesis, soluble sugars such as fructose, phenylpropanoids and glucosinolates were highly influenced by rhizobacteria treatment in plants and they are crucial for plant productivity, quality (nutritional, medicinal and flavor) and stress tolerance. The next step is to identify which part of the pathway is highly impacted by the rhizobacteria treatment. This will provide us with essential information on the rate-limiting steps in the biosynthesis of a given metabolite. For example, if we consider the glucosinolate pathway, the subclass aliphatic glucosinolate was impacted greatly by rhizobacteria treatment. Previous studies on the transcriptome profile of Arabidopsis treated with *Pf* SS101 and its *CysH* mutant showed that sulfur assimilation by the bacteria affects the chain elongation steps in aliphatic glucosinolate biosynthesis and key genes in the chain elongation steps such as MAM1 and MAM3 were significantly upregulated in *Pf* SS101 treated plants. Interestingly, in **Chapter 5** comparative metabolome analysis of Arabidopsis plant treated with *Pf* SS101 and its *cysH* mutant confirmed that long chain glucosinolate indeed accumulated in plants treated with *Pf* SS101 while short and medium chain glucosinolate were more abundant in plants treated with the mutant. Based on the expression profile of genes and the corresponding metabolites, the most influential genes in the biosynthesis pathway such as MAM1 and MAM3 can be targeted for improvement by conventional breeding or the current gene editing technologies. Furthermore, this conceptual framework allows screening for bacterial traits involved in the phenotypic and metabolome alteration in plants by using integrated ~omic technologies i.e. metagenomics, transcriptomics, and metabolomics combined with site-directed mutagenesis for functional analysis of potential bacterial traits identified by the omics analyses. The *cysH* gene from *Pf* SS101 is a good example and screening of allelic variants/orthologues across

several rhizobacteria species and strains of a given species can be performed to identify the best performing allelic variants(s) involved in the alteration of sulfur-containing metabolites of the host. Similar approaches can be followed for other groups of plant metabolites that are altered by rhizobacteria and have influence on yield, quality or stress tolerance of crops.

While *in vitro* screening allows to identify specific rhizobacteria that enhance plant performance, getting reproducible and consistent results under field settings is the major hurdle. This phenomenon is mainly due to unsuccessful root colonization of introduced strains (Kloepper, J *et al.*, 1980; Bhattacharyya & Jha, 2012). To facilitate efficient root colonization of selected rhizobacteria in field experiments, several applications such as drenching seed and seedlings, or continuous treatments have been carried out. However, such methods are not always successful. In our soil experiment, continuous application of *Pbg* broth (50 ml per application, 3 times in three weeks) displayed induction of shoot biomass of Broccoli and Arabidopsis in early development stage when compared to untreated control but the effect faded in time (data not shown). This might be due to the 'buffering' effects of the existing root and soil-associated microbes on the proliferation and activity of the introduced rhizobacteria. Therefore, exploration of proper field application and most importantly understanding of the interaction of introduced microbes with the existing soil and root associated microbial community is vital for the success of introduced rhizobacteria. Another approach could be steering of the existing microbial community in agricultural system towards desired groups of microbes that provide specific functions to the plant using probiotic approach or by 'pre-biotics' that alter the physico-chemical properties of the soil to favor the growth or activity of desired groups within the plant microbiome. Another innovative approach is to introduce beneficial bacteria into seeds. The introduction of endophyte bacteria *Paraburkholderia phytofirmans* PsJN into maize progeny seeds by spraying flower with this bacteria is one of the success stories and was shown to significantly increase yield (Mitter *et al.*, 2017).

Concluding remarks

The research presented in my thesis demonstrated that, apart from visible phenotypic changes, rhizobacteria also modulate the levels of a substantial number of plant secondary metabolites in a rhizobacteria-specific and even cultivar-specific manner. Our findings further demonstrated that rhizobacteria-mediated changes in the plant metabolome arise from both effective and ineffective partnership between plants and rhizobacteria. Changes in metabolism of the plant by rhizobacteria showed an association with plant growth and defense. Although it is widely accepted that plant defense has an adverse effect on growth, some rhizobacteria can induce plant defense and induces growth at the same time. Integrating the data from primary and secondary metabolome analyses of plants treated with rhizobacteria showed that rhizobacteria enhance the generation and utilization of soluble sugars in the host to fuel both defense and growth. Therefore, effective partnerships can enhance the production of nutritionally and pharmaceutically important plant metabolites and at the same time

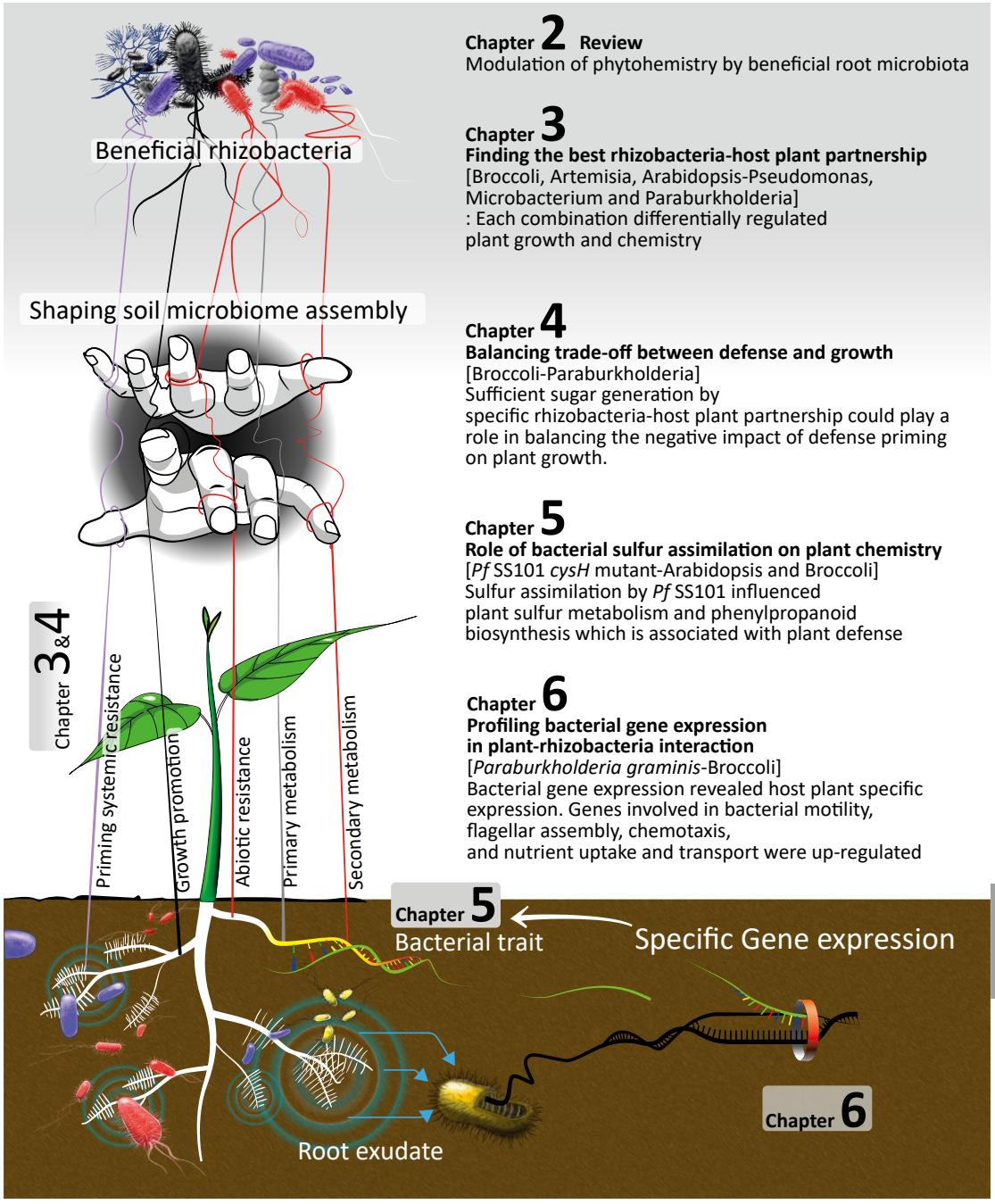

Fig 2. Summary of the main finding of the thesis.

enhance plant biomass. The combined effect could maximize the amount of plant metabolite recovered per unit of plant biomass and will make rhizobacteria-mediated host metabolome reprogramming an attractive approach to enhance the production of high value natural plant products. In conclusion, the results of this thesis exemplify that the fundamental basis of many if not all biological interactions are chemical in nature. The contribution of my work to the advancement of the field is not only tied to a number of answers that my thesis provides about rhizobacteria-host interaction but also to a number of testable hypotheses it has generated during the course of this study. So far, understood only a minute portion of the interaction between plant and rhizobacteria was resolved and the larger portion of the interaction is still a “black box” that awaits to be unlocked.

References

A
Abdel-Wahab M, El-Mahdy MA, Abd-Ellah MF, Helal G, Khalifa F, Hamada F. 2003. Influence of p-coumaric acid on doxorubicin-induced oxidative stress in rat's heart. *Pharmacological Research* **48**(5): 461-465.

Adler J, Hazelbauer GL, Dahl MM. 1973. Chemotaxis toward sugars in *Escherichia coli*. *Journal of Bacteriology* **115**(3): 824-847.

Afek U, Sztejnberg A. 1988. Accumulation of scoparone, a phytoalexin associated with resistance of Citrus to *Phytophthora citrophthora*. *Phytopathology* **78**(12): 1678-1682.

Ahmed E, Holmström SJ. 2014. Siderophores in environmental research: roles and applications. *Microbial Biotechnology* **7**(3): 196-208.

Akram W, Anjum T, Ali B. 2016. Phenylacetic acid is ISR determinant produced by *Bacillus fortis* IAGS162, which involves extensive re-modulation in metabolomics of tomato to protect against *Fusarium wilt*. *Frontiers in Plant Science* **7**: 498.

Algar E, Gutierrez-Mañero FJ, Bonilla A, Lucas JA, Radzki W, Ramos-Solano B. 2012. *Pseudomonas fluorescens* N21. 4 metabolites enhance secondary metabolism isoflavones in soybean (*Glycine max*) calli cultures. *Journal of Agricultural and Food Chemistry* **60**(44): 11080-11087.

Algar E, Gutierrez-Mañero FJ, Garcia-Villaraco A, García-Seco D, Lucas JA, Ramos-Solano B. 2014. The role of isoflavone metabolism in plant protection depends on the rhizobacterial MAMP that triggers systemic resistance against *Xanthomonas axonopodis* pv. *glycines* in *Glycine max* (L.) Merr. cv. Osumi. *Plant Physiology and Biochemistry* **82**: 9-16.

Algar E, Ramos-Solano B, García-Villaraco A, Sierra MDS, Gómez MSM, Gutiérrez-Mañero FJ. 2013. Bacterial bioeffectors modify bioactive profile and increase isoflavone content in soybean sprouts (*Glycine max* var Osumi). *Plant Foods for Human Nutrition* **68**(3): 299-305.

Ali A, Shah L, Rahman S, Riaz MW, Yahya M, Xu YJ, Liu F, Si W, Jiang H, Cheng B. 2018. Plant defense mechanism and current understanding of salicylic acid and NPRs in activating SAR. *Physiological and Molecular Plant Pathology* **104**: 15-22.

Antunes-Ricardo M, Moreno-García BE, Gutiérrez-Uribe JA, Aráiz-Hernández D, Alvarez MM, Serna-Saldivar SO. 2014. Induction of apoptosis in colon cancer cells treated with isorhamnetin glycosides from *Opuntia ficus-indica* pads. *Plant Foods for Human Nutrition* **69**(4): 331-336.

Aronesty E 2011. ea-utils: Command-line tools for processing biological sequencing data: Durham, NC.

Arora M, Saxena P, Choudhary DK, Abdin MZ, Varma A. 2016. Dual symbiosis between *Piriformospora indica* and *Azotobacter chroococcum* enhances the artemisinin content in *Artemisia annua* L. *World Journal of Microbiology and Biotechnology* **32**(2): 19.

Arrigoni O, De Tullio MC. 2002. Ascorbic acid: much more than just an antioxidant. *Biochimica et Biophysica Acta (BBA)-General Subjects* **1569**(1-3): 1-9.

Aziz M, Nadipalli RK, Xie X, Sun Y, Surowiec K, Zhang J-L, Paré PW. 2016. Augmenting sulfur metabolism and herbivore defense in *Arabidopsis* by bacterial volatile signaling. *Frontiers in Plant Science* **7**(458).

B
Bais HP, Weir TL, Perry LG, Gilroy S, Vivanco JM. 2006. The role of root exudates in rhizosphere interactions with plants and other organisms. *Annual Review of Plant Biology* **57**: 233-266.

Bak S, Tax FE, Feldmann KA, Galbraith DW, Feyereisen R. 2001. CYP83B1, a cytochrome P450 at the metabolic branch paint in auxin and indole glucosinolate biosynthesis in Arabidopsis. *Plant Cell* **13**(1): 101-111.

Bakker PA, Pieterse CM, Van Loon L. 2007. Induced systemic resistance by fluorescent *Pseudomonas* spp. *Phytopathology* **97**(2): 239-243.

Balachandran C, Duraipandiyan V, Al-Dhabi NA, Balakrishna K, Kalia NP, Rajput VS, Khan IA, Ignacimuthu S. 2012. Antimicrobial and antimycobacterial activities of methyl caffeate isolated from *Solanum torvum* Swartz. Fruit. *Indian Journal of Microbiology* **52**(4): 676-681.

Baldani VL, Baldani JI, Döbereiner J. 1983. Effects of *Azospirillum* inoculation on root infection and nitrogen incorporation in wheat. *Canadian Journal of Microbiology* **29**(8): 924-929.

Baliña LM, Graupe K. 1991. The treatment of melasma 20% azelaic acid versus 4% hydroquinone cream. *International Journal of Dermatology* **30**(12): 893-895.

Banchio E, Bogino PC, Santoro M, Torres L, Zygadlo J, Giordano W. 2010. Systemic induction of monoterpene biosynthesis in *Origanum* x *majoricum* by soil bacteria. *Journal of Agricultural and Food Chemistry* **58**(1): 650-654.

Barillari J, Canistro D, Paolini M, Ferroni F, Pedulli GF, Iori R, Valgimigli L. 2005. Direct antioxidant activity of purified glucoerucin, the dietary secondary metabolite contained in rocket (*Eruca sativa* Mill.) seeds and sprouts. *Journal of Agricultural and Food Chemistry* **53**(7): 2475-2482.

Barriuso J, Ramos Solano B, Fray RG, Cámara M, Hartmann A, Gutiérrez Mañero FJ. 2008. Transgenic tomato plants alter quorum sensing in plant growth-promoting rhizobacteria. *Plant Biotechnology Journal* **6**(5): 442-452.

Bashan Y, Holguin G, De-Bashan LE. 2004. *Azospirillum*-plant relationships: physiological, molecular, agricultural, and environmental advances (1997-2003). *Canadian Journal of Microbiology* **50**(8): 521-577.

Bauer A, Brönstrup M. 2014. Industrial natural product chemistry for drug discovery and development. *Natural Product Reports* **31**(1): 35-60.

Bednarek P, Piślewska-Bednarek M, Svatoš A, Schneider B, Doubský J, Mansurova M, Humphry M, Consonni C, Panstruga R, Sanchez-Vallet A. 2009. A glucosinolate metabolism pathway in living plant cells mediates broad-spectrum antifungal defense. *Science* **323**(5910): 101-106.

Beekwilder J, Van Leeuwen W, Van Dam NM, Bertossi M, Grandi V, Mizzi L, Soloviev M, Szabados L, Molthoff JW, Schipper B. 2008. The impact of the absence of aliphatic glucosinolates on insect herbivory in Arabidopsis. *PloS One* **3**(4): e2068.

Bennett RN, Wallsgrove RM. 1994. Secondary metabolites in plant defence mechanisms. *New Phytologist* **127**(4): 617-633.

Bentley SD, Chater KF, Cerdeño-Tárraga A-M, Challis GL, Thomson N, James KD, Harris DE, Quail MA, Kieser H, Harper D. 2002. Complete genome sequence of the model actinomycete *Streptomyces coelicolor* A3 (2). *Nature* **417**(6885): 141.

Bergelson J, Purrington CB. 1996. Surveying patterns in the cost of resistance in plants. *American Naturalist* **148**(3): 536-558.

Besseau S, Hoffmann L, Geoffroy P, Lapierre C, Pollet B, Legrand M. 2007. Flavonoid accumulation in *Arabidopsis* repressed in lignin synthesis affects auxin transport and plant growth. *Plant Cell* **19**(1): 148-162.

Bharti N, Pandey SS, Barnawal D, Patel VK, Kalra A. 2016. Plant growth promoting rhizobacteria *Dietzia natronolimnaea* modulates the expression of stress responsive genes providing protection of wheat from salinity stress. *Scientific Reports* **6**: 34768.

Bhattacharyya PN, Jha DK. 2012. Plant growth-promoting rhizobacteria (PGPR): emergence in agriculture. *World Journal of Microbiology and Biotechnology* **28**(4): 1327-1350.

Bindea G, Mlecnik B, Hackl H, Charoentong P, Tosolini M, Kirilovsky A, Fridman W-H, Pagès F, Trajanoski Z, Galon J. 2009. ClueGO: a Cytoscape plug-in to decipher functionally grouped gene ontology and pathway annotation networks. *Bioinformatics* **25**(8): 1091-1093.

Birt DF, Hendrich S, Wang W. 2001. Dietary agents in cancer prevention: flavonoids and isoflavonoids. *Pharmacology & Therapeutics* **90**(2-3): 157-177.

Boller T, Felix G. 2009. A renaissance of elicitors: perception of microbe-associated molecular patterns and danger signals by pattern-recognition receptors. *Annual Review of Plant Biology* **60**: 379-406.

Boulogne I, Petit P, Ozier-Lafontaine H, Desfontaines L, Loranger-Merciris G. 2012. Insecticidal and antifungal chemicals produced by plants: a review. *Environmental Chemistry Letters* **10**(4): 325-347.

Bourgaud F, Gravot A, Milesi S, Gontier E. 2001. Production of plant secondary metabolites: a historical perspective. *Plant Science* **161**(5): 839-851.

Bouwmeester HJ, Matusova R, Sun ZK, Beale MH. 2003. Secondary metabolite signalling in host-parasitic plant interactions. *Current Opinion in Plant Biology* **6**(4): 358-364.

Brittenham G. 1994. New advances in iron metabolism, iron deficiency, and iron overload. *Current Opinion in Plant Biology* **1**(2): 101-106.

Brotman Y, Lisec J, Meret M, Chet I, Willmitzer L, Viterbo A. 2012. Transcript and metabolite analysis of the *Trichoderma*-induced systemic resistance response to *Pseudomonas syringae* in *Arabidopsis thaliana*. *Microbiology-Sgm* **158**: 139-146.

Brown DE, Rashotte AM, Murphy AS, Normanly J, Tague BW, Peer WA, Taiz L, Muday GK. 2001. Flavonoids act as negative regulators of auxin transport in vivo in Arabidopsis. *Plant Physiology* **126**(2): 524-535.

Brusamarello-Santos LC, Gilard F, Brulé L, Quilleré I, Gourion B, Ratet P, Maltempi de Souza E, Lea PJ, Hirel B. 2017. Metabolic profiling of two maize (*Zea mays* L.) inbred lines inoculated with the nitrogen fixing plant-interacting bacteria *Herbaspirillum seropedicae* and *Azospirillum brasilense*. *PLoS One* **12**(3): 1-19.

Buer CS, Kordbacheh F, Truong TT, Hocart CH, Djordjevic MA. 2013. Alteration of flavonoid accumulation patterns in transparent testa mutants disturbs auxin transport, gravity responses, and imparts long-term effects on root and shoot architecture. *Planta* **238**(1): 171-189.

Burdman S, Jurkevitch E, Okon Y. 2000. Recent advances in the use of plant growth promoting rhizobacteria (PGPR) in agriculture. *Microbial Interactions in Agriculture and Forestry (Volume II)*: 229-250.

C

Calvo P, Nelson L, Kloepper JW. 2014. Agricultural uses of plant biostimulants. *Plant and Soil* **383**(1-2): 3-41.

Campos-Soriano L, García-Martínez J, Segundo BS. 2012. The arbuscular mycorrhizal symbiosis promotes the

systemic induction of regulatory defence-related genes in rice leaves and confers resistance to pathogen infection. *Molecular Plant Pathology* **13**(6): 579-592.

Carreno-Quintero N, Acharjee A, Maliepaard C, Bachem CW, Mumm R, Bouwmeester H, Visser RG, Keurentjes JJ. 2012. Untargeted metabolic quantitative trait loci analyses reveal a relationship between primary metabolism and potato tuber quality. *Plant Physiology* **158**(3): 1306-1318.

Carrión VJ, Cordovez V, Tyc O, Etalo DW, de Bruijn I, de Jager VC, Medema MH, Eberl L, Raaijmakers JM. 2018. Involvement of Burkholderiaceae and sulfurous volatiles in disease-suppressive soils. *The ISME Journal* **12**(9): 2307-2321.

Carrión VJ, Perez-Jaramillo J, Cordovez V, Tracanna V, De Hollander M, Ruiz-Buck D, Mendes LW, van Ijcken WF, Gomez-Exposito R, Elsayed SS. 2019. Pathogen-induced activation of disease-suppressive functions in the endophytic root microbiome. *Science* **366**(6465): 606-612.

Cartieaux F, Contesto C, Gallou A, Desbrosses G, Kopka J, Taconnat L, Renou J-P, Touraine B. 2008. Simultaneous interaction of *Arabidopsis thaliana* with *Bradyrhizobium* sp. strain ORS278 and *Pseudomonas syringae* pv. *tomato* DC3000 leads to complex transcriptome changes. *Molecular Plant-Microbe Interactions* **21**(2): 244-259.

Cassán F, Vanderleyden J, Spaepen S. 2014. Physiological and agronomical aspects of phytohormone production by model plant-growth-promoting rhizobacteria (PGPR) belonging to the genus *Azospirillum*. *Journal of Plant Growth Regulation* **33**(2): 440-459.

Castanheira N, Dourado A, Kruz S, Alves P, Delgado-Rodríguez A, Pais I, Semedo J, Scotti-Campos P, Sánchez C, Borges N. 2016. Plant growth-promoting *Burkholderia* species isolated from annual ryegrass in Portuguese soils. *Journal of Applied Microbiology* **120**(3): 724-739.

Chamam A, Sanguin H, Bellvert F, Meiffren G, Comte G, Wisniewski-Dyé F, Bertrand C, Prigent-Combaret C. 2013. Plant secondary metabolite profiling evidences strain-dependent effect in the *Azospirillum-Oryza sativa* association. *Phytochemistry* **87**: 65-77.

Chamam A, Wisniewski-Dyé F, Comte G, Bertrand C, Prigent-Combaret C. 2015. Differential responses of *Oryza sativa* secondary metabolism to biotic interactions with cooperative, commensal and phytopathogenic bacteria. *Planta* **242**(6): 1439-1452.

Chen H-H, Zhou H-J, Wang W-Q, Wu G-D. 2004. Antimalarial dihydroartemisinin also inhibits angiogenesis. *Cancer Chemotherapy and Pharmacology* **53**(5): 423-432.

Chen H, Sun B, Pan S, Jiang H, Sun X. 2009. Dihydroartemisinin inhibits growth of pancreatic cancer cells *in vitro* and *in vivo*. *Anti-Cancer Drugs* **20**(2): 131-140.

Chen Q, Espey MG, Krishna MC, Mitchell JB, Corpe CP, Buettner GR, Shacter E, Levine M. 2005. Pharmacologic ascorbic acid concentrations selectively kill cancer cells: action as a pro-drug to deliver hydrogen peroxide to tissues. *Proceedings of the National Academy of Sciences of the United States of America* **102**(38): 13604-13609.

Chen T, Chen H, Wang Y, Zhang J. 2016. *In vitro* and *in vivo* antitumour activities of puerarin 6″-O-xyloside on human lung carcinoma A549 cell line via the induction of the mitochondria-mediated apoptosis pathway. *Pharmaceutical Biology* **54**(9): 1793-1799.

Chen T, Li M, Zhang R, Wang H. 2009. Dihydroartemisinin induces apoptosis and sensitizes human ovarian cancer cells to carboplatin therapy. *Journal of Cellular and Molecular Medicine* **13**(7): 1358-1370.

Chen X-H, Koumoutsi A, Scholz R, Borriss R. 2009. More than anticipated–production of antibiotics and other secondary metabolites by *Bacillus amyloliquefaciens* FZB42. *Journal of Molecular Microbiology and Biotechnology* **16**(1-2): 14-24.

Chen X, Koumoutsi A, Scholz R, Schneider K, Vater J, Süssmuth R, Piel J, Borriss R. 2009. Genome analysis of *Bacillus amyloliquefaciens* FZB42 reveals its potential for biocontrol of plant pathogens. *Journal of Biotechnology* **140**(1-2): 27-37.

Cheng X, Etalo DW, van de Mortel JE, Dekkers E, Nguyen L, Medema MH, Raaijmakers JM. 2017. Genome-wide analysis of bacterial determinants of plant growth promotion and induced systemic resistance by *Pseudomonas fluorescens*. *Environmental Microbiology* **19**(11): 4638-4656.

Chitarra G, Breeuwer P, Nout M, Van Aelst A, Rombouts F, Abee T. 2003. An antifungal compound produced by *Bacillus subtilis* YM 10–20 inhibits germination of *Penicillium roqueforti* conidiospores. *Journal of Applied Microbiology* **94**(2): 159-166.

Cho JY, Nam KH, Kim AR, Park J, Yoo ES, Baik KU, Yu YH, Park MH. 2001. In-vitro and in-vivo immunomodulatory effects of syringin. *Journal of Pharmacy and Pharmacology* **53**(9): 1287-1294.

Choi J, Shin K-M, Park H-J, Jung H-J, Kim HJ, Lee YS, Rew J-H, Lee K-T. 2004. Anti-inflammatory and antinociceptive effects of sinapyl alcohol and its glucoside syringin. *Planta Medica* **70**(11): 1027-1032.

Cis J, Nowak G, Kisiel W. 2006. Antifeedant properties and chemotaxonomic implications of sesquiterpene lactones

and syringin from *Rhaponticum pulchrum*. *Biochemical Systematics and Ecology* **34**(12): 862-867.

Clarkson DT, Hanson JB. 1980. The mineral nutrition of higher plants. *Annual Review of Plant Physiology* **31**(1): 239-298.

Clay NK, Adio AM, Denoux C, Jander G, Ausubel FM. 2009. Glucosinolate metabolites required for an *Arabidopsis* innate immune response. *Science* **323**(5910): 95-101.

Cole BJ, Feltcher ME, Waters RJ, Wetmore KM, Mucyn TS, Ryan EM, Wang G, Ul-Hasan S, McDonald M, Yoshikuni Y. 2017. Genome-wide identification of bacterial plant colonization genes. *PLoS Biology* **15**(9): e2002860.

Compant S, Clément C, Sessitsch A. 2010. Plant growth-promoting bacteria in the rhizo-and endosphere of plants: their role, colonization, mechanisms involved and prospects for utilization. *Soil Biology and Biochemistry* **42**(5): 669-678.

Cordovez V, Dini-Andreote F, Carrión VJ, Raaijmakers JM. 2019. Ecology and evolution of plant microbiomes. *Annual Review of Microbiology* **73**.

Cordovez V, Mommer L, Moisan K, Lucas-Barbosa D, Pierik R, Mumm R, Carrion VJ, Raaijmakers JM. 2017. Plant phenotypic and transcriptional changes induced by volatiles from the fungal root pathogen *Rhizoctonia solani*. *Frontiers in Plant Science* **8**: 1262.

Cordovez V, Schop S, Hordijk K, de Boulois HD, Coppens F, Hanssen I, Raaijmakers JM, Carrion VJ. 2018. Priming of plant growth promotion by volatiles of root-associated *Microbacterium* spp. *Applied and Environmental Microbiology* **84**(22): e01865-01818.

Couillerot O, Ramírez-Trujillo A, Walker V, von Felten A, Jansa J, Maurhofer M, Défago G, Prigent-Combaret C, Comte G, Caballero-Mellado J. 2013. Comparison of prominent *Azospirillum* strains in *Azospirillum–Pseudomonas–Glomus* consortia for promotion of maize growth. *Applied Microbiology and Biotechnology* **97**(10): 4639-4649.

Couto D, Zipfel C. 2016. Regulation of pattern recognition receptor signalling in plants. *Nature Reviews Immunology* **16**(9): 537.

Cragg GM, Newman DJ. 2013. Natural products: a continuing source of novel drug leads. *Biochimica et Biophysica Acta* **1830**(6): 3670-3695.

Cvikrova M, Mala J, Hrubcova M, Eder J. 2006. Soluble and cell wall-bound phenolics and lignin in *Ascocalyx abietina* infected Norway spruces. *Plant Science* **170**(3): 563-570.

D

Daisy BH, Strobel GA, Castillo U, Ezra D, Sears J, Weaver DK, Runyon JB. 2002. Naphthalene, an insect repellent, is produced by *Muscodor vitigenus*, a novel endophytic fungus. *Microbiology-Sgm* **148**: 3737-3741.

Dardanelli MS, Manyani H, González-Barroso S, Rodríguez-Carvajal MA, Gil-Serrano AM, Espuny MR, López-Baena FJ, Bellogín RA, Megías M, Ollero FJ. 2010. Effect of the presence of the plant growth promoting rhizobacterium (PGPR) *Chryseobacterium balustinum* Aur9 and salt stress in the pattern of flavonoids exuded by soybean roots. *Plant and Soil* **328**(1-2): 483-493.

De Freitas J, Banerjee M, Germida J. 1997. Phosphate-solubilizing rhizobacteria enhance the growth and yield but not phosphorus uptake of canola (*Brassica napus* L.). *Biology and Fertility of Soils* **24**(4): 358-364.

De Meyer G, Höfte M. 1997. Salicylic acid produced by the rhizobacterium *Pseudomonas aeruginosa* 7NSK2 induces resistance to leaf infection by *Botrytis cinerea* on bean. *Phytopathology* **87**(6): 588-593.

de Souza JT, de Boer M, de Waard P, van Beek TA, Raaijmakers JM. 2003. Biochemical, genetic, and zoosporicidal properties of cyclic lipopeptide surfactants produced by *Pseudomonas fluorescens*. *Applied and Environmental Microbiology* **69**(12): 7161-7172.

De Vleesschauwer D, Höfte M 2009. Chapter 6 Rhizobacteria-Induced Systemic Resistance. *Advances in Botanical Research*: Academic Press, 223-281.

De Vos RC, Moco S, Lommen A, Keurentjes JJ, Bino RJ, Hall RD. 2007. Untargeted large-scale plant metabolomics using liquid chromatography coupled to mass spectrometry. *Nature Protocols* **2**(4): 778-791.

de Weert S, Kuiper I, Lagendijk EL, Lamers GE, Lugtenberg BJ. 2004. Role of chemotaxis toward fusaric acid in colonization of hyphae of *Fusarium oxysporum* f. sp. *radicis-lycopersici* by *Pseudomonas fluorescens* WCS365. *Molecular Plant-Microbe Interactions* **17**(11): 1185-1191.

de Weert S, Vermeiren H, Mulders IH, Kuiper I, Hendrickx N, Bloemberg GV, Vanderleyden J, De Mot R, Lugtenberg BJ. 2002. Flagella-driven chemotaxis towards exudate components is an important trait for tomato root colonization by *Pseudomonas fluorescens*. *Molecular Plant-Microbe Interactions* **15**(11): 1173-1180.

Del Giudice L, Massardo DR, Pontieri P, Bertea CM, Mombello D, Carata E, Tredici SM, Tala A, Mucciarelli M, Groudeva VI, et al. 2008. The microbial community of Vetiver root and its involvement into essential

oil biogenesis. *Environmental Microbiology* **10**(10): 2824-2841.

del Rosario Cappellari L, Santoro MV, Reinoso H, Travaglia C, Giordano W, Banchio E. 2015. Anatomical, morphological, and phytochemical effects of inoculation with plant growth-promoting rhizobacteria on peppermint (*Mentha piperita*). *Journal of Chemical Ecology* **41**(2): 149-158.

Delaney TP, Uknes S, Vernooij B, Friedrich L, Weymann K, Negrotto D, Gaffney T, Gut-Rella M, Kessmann H, Ward E. 1994. A central role of salicylic acid in plant disease resistance. *Science* **266**(5188): 1247-1250.

DeMoss J, Hsu P. 1991. NarK enhances nitrate uptake and nitrite excretion in *Escherichia coli*. *Journal of Bacteriology* **173**(11): 3303-3310.

Deschner EE, Ruperto J, Wong G, Newmark HL. 1991. Quercetin and rutin as inhibitors of azoxymethanol-induced colonic neoplasia. *Carcinogenesis* **12**(7): 1193-1196.

Dimkpa C, Weinand T, Asch F. 2009. Plant–rhizobacteria interactions alleviate abiotic stress conditions. *Plant, Cell & Environment* **32**(12): 1682-1694.

Dixon R, Kahn D. 2004. Genetic regulation of biological nitrogen fixation. *Nature Reviews Microbiology* **2**(8): 621-631.

Dixon RA, Achnine L, Kota P, Liu CJ, Reddy MSS, Wang LJ. 2002. The phenylpropanoid pathway and plant defence - a genomics perspective. *Molecular Plant Pathology* **3**(5): 371-390.

Dodd I, Zinovkina N, Safronova V, Belimov A. 2010. Rhizobacterial mediation of plant hormone status. *Annals of Applied Biology* **157**(3): 361-379.

Dondorp AM, Nosten F, Yi P, Das D, Phyo AP, Tarning J, Lwin KM, Ariey F, Hanpithakpong W, Lee SJ. 2009. Artemisinin resistance in *Plasmodium falciparum* malaria. *New England Journal of Medicine* **361**(5): 455-467.

Drogue B, Sanguin H, Chamam A, Mozar M, Llauro C, Panaud O, Prigent-Combaret C, Picault N, Wisniewski-Dyé F. 2014. Plant root transcriptome profiling reveals a strain-dependent response during *Azospirillum*-rice cooperation. *Frontiers in Plant Science* **5**: 607.

Dupont PY, Eaton CJ, Wargent JJ, Fechtner S, Solomon P, Schmid J, Day RC, Scott B, Cox MP. 2015. Fungal endophyte infection of ryegrass reprograms host metabolism and alters development. *New Phytologist* **208**(4): 1227-1240.

Durrant WE, Dong X. 2004. Systemic acquired resistance. *Annual Review of Phytopathology* **42**: 185-209.

El-Gendy MMAA, Al-Zahrani HAA, El-Bondkly AMA. 2016. Genome shuffling of mangrove endophytic *Aspergillus luchuensis* MERV10 for Improving the cholesterol-lowering agent lovastatin under solid state fermentation. *Mycobiology* **44**(3): 171-179.

E

Erlund I. 2004. Review of the flavonoids quercetin, hesperetin, and naringenin. Dietary sources, bioactivities, bioavailability, and epidemiology. *Nutrition Research* **24**(10): 851-874.

Ermis U, Weis J, Schulz JB. 2013. PML in a patient treated with fumaric acid. *New England Journal of Medicine* **368**(17): 1657-1658.

Etalo DW, Jeon J-S, Raaijmakers JM. 2018. Modulation of plant chemistry by beneficial root microbiota. *Natural Product Reports* **35**(5): 398-409.

Etesami H, Alikhani HA, Hosseini HM 2015. Indole-3-acetic acid and 1-aminocyclopropane-1-carboxylate deaminase: bacterial traits required in rhizosphere, rhizoplane and/or endophytic competence by beneficial bacteria. *Bacterial Metabolites in Sustainable Agroecosystem*: Springer, 183-258.

F

Fan B, Carvalhais LC, Becker A, Fedoseyenko D, von Wirén N, Borriss R. 2012. Transcriptomic profiling of *Bacillus amyloliquefaciens* FZB42 in response to maize root exudates. *BMC Microbiology* **12**(1): 116.

Fang S-H, Rao YK, Tzeng Y-M. 2005. Inhibitory effects of flavonol glycosides from *Cinnamomum osmophloeum* on inflammatory mediators in LPS/IFN-γ-activated murine macrophages. *Bioorganic & Medicinal Chemistry* **13**(7): 2381-2388.

Fatima S, Anjum T. 2017. Identification of a potential ISR determinant from *Pseudomonas aeruginosa* PM12 against Fusarium wilt in tomato. *Frontiers in Plant Science* **8**: 848.

Fernie AR, Carrari F, Sweetlove LJ. 2004. Respiratory metabolism: glycolysis, the TCA cycle and mitochondrial electron transport. *Current Opinion in Plant Biology* **7**(3): 254-261.

Fiorentino A, Ricci A, D'Abrosca B, Golino A, Izzo A, Pascarella MT, Piccolella S, Esposito A. 2009. Kaempferol glycosides from *Lobularia maritima* and their potential role in plant interactions. *Chemistry & Biodiversity* **6**(2): 204-217.

Foyer CH 2017. Ascorbic acid. *Antioxidants in Higher Plants*: CRC press, 39-66.

Fraga CG, Motchnik PA, Shigenaga MK, Helbock HJ, Jacob RA, Ames BN. 1991. Ascorbic acid protects against endogenous oxidative DNA damage in human sperm. *Proceedings of the National Academy of Sciences of the United States of America* **88**(24): 11003-11006.

Fu Y, Yin ZH, Yin CY. 2017. Biotransformation of ginsenoside Rb1 to ginsenoside Rg3 by endophytic bacterium *Burkholderia* sp GE 17-7 isolated from *Panax ginseng*. *Journal of Applied Microbiology* **122**(6): 1579-1585.

Fu ZQ, Dong X. 2013. Systemic acquired resistance: turning local infection into global defense. *Annual Review of Plant Biology* **64**: 839-863.

Furuhashi T, Fragner L, Furuhashi K, Valledor L, Sun XL, Weckwerth W. 2012. Metabolite changes with induction of *Cuscuta haustorium* and translocation from host plants. *Journal of Plant Interactions* **7**(1): 84-98.

G

Gao Y, Liu Q, Zang P, Li X, Ji Q, He Z, Zhao Y, Yang H, Zhao X, Zhang L. 2015. An endophytic bacterium isolated from *Panax ginseng* CA Meyer enhances growth, reduces morbidity, and stimulates ginsenoside biosynthesis. *Phytochemistry Letters* **11**: 132-138.

García de Salamone IE, Hynes RK, Nelson LM. 2001. Cytokinin production by plant growth promoting rhizobacteria and selected mutants. *Canadian Journal of Microbiology* **47**(5): 404-411.

Gautier H, Diakou-Verdin V, Bénard C, Reich M, Buret M, Bourgaud F, Poëssel JL, Caris-Veyrat C, Génard M. 2008. How does tomato quality (sugar, acid, and nutritional quality) vary with ripening stage, temperature, and irradiance? *Journal of Agricultural and Food Chemistry* **56**(4): 1241-1250.

Geu-Flores F, Moldrup ME, Bottcher C, Olsen CE, Scheel D, Halkier BA. 2011. Cytosolic *γ*-glutamyl peptidases process glutathione conjugates in the biosynthesis of glucosinolates and camalexin in *Arabidopsis*. *Plant Cell* **23**(6): 2456-2469.

Ghorbanpour M, Hatami M, Kariman K, Abbaszadeh Dahaji P. 2016. Phytochemical variations and enhanced efficiency of antioxidant and antimicrobial ingredients in *Salvia officinalis* as inoculated with different rhizobacteria. *Chemistry & Biodiversity* **13**(3): 319-330.

Glawischnig E. 2007. Camalexin. *Phytochemistry* **68**(4): 401-406.

Glick BR. 2014. Bacteria with ACC deaminase can promote plant growth and help to feed the world. *Microbiological Research* **169**(1): 30-39.

Goswami D, Thakker JN, Dhandhukia PC. 2016. Portraying mechanics of plant growth promoting rhizobacteria (PGPR): A review. *Cogent Food & Agriculture* **2**(1): 1127500.

Grabherr MG, Haas BJ, Yassour M, Levin JZ, Thompson DA, Amit I, Adiconis X, Fan L, Raychowdhury R, Zeng Q. 2011. Trinity: reconstructing a full-length transcriptome without a genome from RNA-Seq data. *Nature Biotechnology* **29**(7): 644.

Gray E, Smith D. 2005. Intracellular and extracellular PGPR: commonalities and distinctions in the plant–bacterium signaling processes. *Soil Biology and Biochemistry* **37**(3): 395-412.

Griesser M, Weingart G, Schoedl-Hummel K, Neumann N, Becker M, Varmuza K, Liebner F, Schuhmacher R, Forneck A. 2015. Severe drought stress is affecting selected primary metabolites, polyphenols, and volatile metabolites in grapevine leaves (*Vitis vinifera* cv. Pinot noir). *Plant Physiology and Biochemistry* **88**: 17-26.

Gross H, Loper JE. 2009. Genomics of secondary metabolite production by *Pseudomonas* spp. *Natural Product Reports* **26**(11): 1408-1446.

Gülcin I. 2012. Antioxidant activity of food constituents: an overview. *Archives of Toxicology* **86**(3): 345-391.

Gülçin İ. 2006. Antioxidant activity of caffeic acid (3, 4-dihydroxycinnamic acid). *Toxicology* **217**(2-3): 213-220.

Guardia T, Rotelli AE, Juarez AO, Pelzer LE. 2001. Anti-inflammatory properties of plant flavonoids. Effects of rutin, quercetin and hesperidin on adjuvant arthritis in rat. *Il Farmaco* **56**(9): 683-687.

Gunatilaka AAL. 2006. Natural products from plant-associated microorganisms: Distribution, structural diversity, bioactivity, and implications of their occurrence. *Journal of Natural Products* **69**(3): 509-526.

Gupta S, Kaul S, Singh B, Vishwakarma RA, Dhar MK. 2016. Production of gentisyl alcohol from *Phoma herbarum* endophytic in *Curcuma longa* L. and its antagonistic activity towards leaf spot pathogen *Colletotrichum gloeosporioides*. *Applied Biochemistry and Biotechnology* **180**(6): 1093-1109.

Gutiérrez-Mañero FJ, Ramos-Solano B, Probanza An, Mehouachi J, R. Tadeo F, Talon M. 2001. The plant-growth-promoting rhizobacteria *Bacillus pumilus* and *Bacillus licheniformis* produce high amounts of physiologically active gibberellins. *Physiologia Plantarum* **111**(2): 206-211.

H

Haack M, Löwinger M, Lippmann D, Kipp A, Pagnotta E, Iori R, Monien BH, Glatt H, Brauer MN, Wessjohann LA. 2010. Breakdown products of neoglucobrassicin inhibit activation of Nrf2 target genes mediated by myrosinase-derived glucoraphanin hydrolysis products. *Biological Chemistry* **391**(11): 1281-1293.

Haas D, Défago G. 2005. Biological control of soil-borne pathogens by fluorescent pseudomonads. *Nature Reviews Microbiology* **3**(4): 307-319.

Hagemeier J, Schneider B, Oldham NJ, Hahlbrock K. 2001. Accumulation of soluble and wall-bound indolic

metabolites in *Arabidopsis thaliana* leaves infected with Virulent or avirulent *Pseudomonas syringae* pathovar tomato strains. *Proceedings of the National Academy of Sciences of the United States of America* **98**(2): 753-758.

Hahlbrock K, Bednarek P, Ciolkowski I, Hamberger B, Heise A, Liedgens H, Logemann E, Nurnberger T, Schmelzer E, Somssich IE, et al. 2003. Non-self recognition, transcriptional reprogramming, and secondary metabolite accumulation during plant/pathogen interactions. *Proceedings of the National Academy of Sciences of the United States of America* **100**: 14569-14576.

Haichar FZ, Marol C, Berge O, Rangel-Castro JI, Prosser JI, Balesdent J, Heulin T, Achouak W. 2008. Plant host habitat and root exudates shape soil bacterial community structure. *The ISME Journal* **2**(12): 1221-1230.

Han H-S, Lee K. 2006. Effect of co-inoculation with phosphate and potassium solubilizing bacteria on mineral uptake and growth of pepper and cucumber. *Plant Soil and Environment* **52**(3): 130.

Han SH, Lee SJ, Moon JH, Park KH, Yang KY, Cho BH, Kim KY, Kim YW, Lee MC, Anderson AJ. 2006. GacS-dependent production of 2R, 3R-butanediol by *Pseudomonas chlororaphis* O6 is a major determinant for eliciting systemic resistance against *Erwinia carotovora* but not against *Pseudomonas syringae* pv. *tabaci* in tobacco. *Molecular Plant-Microbe Interactions* **19**(8): 924-930.

Hardoim PR, van Overbeek LS, Berg G, Pirttila AM, Compant S, Campisano A, Doring M, Sessitsch A. 2015. The hidden world within plants: ecological and evolutionary considerations for defining functioning of microbial endophytes. *Microbiology and Molecular Biology Reviews* **79**(3): 293-320.

Hartmann H, Trumbore S. 2016. Understanding the roles of nonstructural carbohydrates in forest trees - from what we can measure to what we want to know. *New Phytologist* **211**(2): 386-403.

Hartmann T. 2007. From waste products to ecochemicals: fifty years research of plant secondary metabolism. *Phytochemistry* **68**(22-24): 2831-2846.

Hederstedt L, Rutberg L. 1981. Succinate dehydrogenase--a comparative review. *Microbiological Reviews* **45**(4): 542.

Heinig U, Scholz S, Jennewein S. 2013. Getting to the bottom of Taxol biosynthesis by fungi. *Fungal Divers* **60**(1): 161-170.

Hemingway RW, Karchesy JJ, Branham SJ. 1989. *Chemistry and significance of condensed tannins*. New York: Plenum Press.

Herms DA, Mattson WJ. 1992. The dilemma of plants: to grow or defend. *The Quarterly Review of Biology* **67**(3): 283-335.

Herrmann KM, Weaver LM. 1999. The shikimate pathway. *Annual Review of Plant Physiology and Plant Molecular Biology* **50**: 473-503.

Hilal M, Parrado MF, Rosa M, Gallardo M, Orce L, Massa EM, Gonzalez JA, Prado FE. 2004. Epidermal lignin deposition in quinoa cotyledons in response to UV-B radiation. *Photochemistry and Photobiology* **79**(2): 205-210.

Hiltpold I, Turlings TC. 2008. Belowground chemical signaling in maize: when simplicity rhymes with efficiency. *Journal of Chemical Ecology* **34**(5): 628-635.

Hiradate S, Yoshida S, Sugie H, Yada H, Fujii Y. 2002. Mulberry anthracnose antagonists (iturins) produced by *Bacillus amyloliquefaciens* RC-2. *Phytochemistry* **61**(6): 693-698.

Hoffman MT, Arnold AE. 2010. Diverse bacteria inhabit living hyphae of phylogenetically diverse fungal endophytes. *Applied and Environmental Microbiology* **76**(12): 4063-4075.

Honma M, Shimomura T. 1978. Metabolism of 1-aminocyclopropane-1-carboxylic acid. *Agricultural and Biological Chemistry* **42**(10): 1825-1831.

Hu C, Kitts DD. 2004. Luteolin and luteolin-7-O-glucoside from dandelion flower suppress iNOS and COX-2 in RAW264. 7 cells. *Molecular and Cellular Biochemistry* **265**(1-2): 107-113.

Hu LF, Robert CAM, Cadot S, Zhang X, Ye M, Li BB, Manzo D, Chervet N, Steinger T, van der Heijden MGA, et al. 2018. Root exudate metabolites drive plant-soil feedbacks on growth and defense by shaping the rhizosphere microbiota. *Nature Communications* **9**(1): 2738.

Huang AC, Jiang T, Liu Y-X, Bai Y-C, Reed J, Qu B, Goossens A, Nützmann H-W, Bai Y, Osbourn A. 2019. A specialized metabolic network selectively modulates *Arabidopsis* root microbiota. *Science* **364**(6440): eaau6389.

Huang J, Agus DB, Winfree CJ, Kiss S, Mack WJ, McTaggart RA, Choudhri TF, Kim LJ, Mocco J, Pinsky DJ. 2001. Dehydroascorbic acid, a blood–brain barrier transportable form of vitamin C, mediates potent cerebroprotection in experimental stroke. *Proceedings of the National Academy of Sciences of the United States of America* **98**(20): 11720-11724.

Huang M-T, Smart RC, Wong C-Q, Conney AH. 1988. Inhibitory effect of curcumin, chlorogenic acid, caffeic

acid, and ferulic acid on tumor promotion in mouse skin by 12-O-tetradecanoylphorbol-13-acetate. *Cancer Research* **48**(21): 5941-5946.

Huang S, Zhang J, Tao Z, Lei L, Yu Y, Huang L. 2014. Enzymatic conversion from pyridoxal to pyridoxine caused by microorganisms within tobacco phyllosphere. *Plant Physiol Biochem* **85**: 9-13.

Huang WY, Cai YZ, Hyde KD, Corke H, Sun M. 2008. Biodiversity of endophytic fungi associated with 29 traditional Chinese medicinal plants. *Fungal Diversity* **33**(1560-2745): 61-75.

Huot B, Yao J, Montgomery BL, He SY. 2014. Growth–defense tradeoffs in plants: a balancing act to optimize fitness. *Molecular Plant* **7**(8): 1267-1287.

Hyun SK, Jung YJ, Chung HY, Jung HA, Choi JS. 2006. Isorhamnetin glycosides with free radical and ONOO− scavenging activities from the stamens of *Nelumbo nucifera*. *Archives of Pharmacal Research* **29**(4): 287.

I

Idris EE, Iglesias DJ, Talon M, Borriss R. 2007. Tryptophan-dependent production of indole-3-acetic acid (IAA) affects level of plant growth promotion by *Bacillus amyloliquefaciens* FZB42. *Molecular Plant-Microbe Interactions* **20**(6): 619-626.

Islam MT, Lee BR, Das PR, La VH, Jung HI, Kim TH. 2018. Characterization of *p*-Coumaric acid-induced soluble and cell wall-bound phenolic metabolites in relation to disease resistance to *Xanthomonas campestris* pv. *campestris* in Chinese cabbage. *Plant Physiology and Biochemistry* **125**: 172-177.

J

Jacobs M, Rubery PH. 1988. Naturally occurring auxin transport regulators. *Science* **241**(4863): 346-349.

Jha CK, Saraf M. 2015. Plant growth promoting rhizobacteria (PGPR): a review. *Journal of Agricultural Research and Development* **5**(2): 108-119.

Ji W, Leng X, Jin Z, Li H. 2019. Plant growth promoting bacteria increases biomass, effective constituent, and modifies rhizosphere bacterial communities of *Panax ginseng*. *Acta Agriculturae Scandinavica, Section B-Soil & Plant Science* **69**(2): 135-146.

Jishma P, Hussain N, Chellappan R, Rajendran R, Mathew J, Radhakrishnan E. 2017. Strain-specific variation in plant growth promoting volatile organic compounds production by five different *Pseudomonas* spp. as confirmed by response of *Vigna radiata* seedlings. *Journal of Applied Microbiology* **123**(1): 204-216.

John P. 1991. How plant molecular biologists revealed a surprising relationship between two enzymes, which took an enzyme out of a membrane where it was not located, and put it into the soluble phase where it could be studied. *Plant Molecular Biology Reporter* **9**(3): 192-194.

Joo G-J, Kim Y-M, Kim J-T, Rhee I-K, Kim J-H, Lee I-J. 2005. Gibberellins-producing rhizobacteria increase endogenous gibberellins content and promote growth of red peppers. *Journal of Microbiology* **43**(6): 510-515.

K

Karakida F, Ikeya Y, Tsunakawa M, Yamaguchi T, Ikarashi Y, Takeda S, Aburada M. 2007. Cerebral protective and cognition-improving effects of sinapic acid in rodents. *Biological and Pharmaceutical Bulletin* **30**(3): 514-519.

Kawashima K, Miyako D, Ishino Y, Makino T, Saito K-i, Kano Y. 2004. Anti-stress effects of 3, 4, 5-trimethoxycinnamic acid, an active constituent of roots of *Polygala tenuifolia* (Onji). *Biological and Pharmaceutical Bulletin* **27**(8): 1317-1319.

Kim HJ, Nam HS, Anderson AJ, Yang KY, Cho BH, Kim YC. 2007. Mutation in the edd gene encoding the 6-phosphogluconate dehydratase of *Pseudomonas chlororaphis* O6 impairs root colonization and is correlated with reduced induction of systemic resistance. *Letters in Applied Microbiology* **44**(1): 56-61.

Kim S-J, Ishii G. 2006. Glucosinolate profiles in the seeds, leaves and roots of rocket salad (*Eruca sativa* Mill.) and anti-oxidative activities of intact plant powder and purified 4-methoxyglucobrassicin. *Soil Science and Plant Nutrition* **52**(3): 394-400.

Kim TY, Jang JY, Jeon SJ, Lee HW, Bae CH, Yeo JH, Lee HB, Kim IS, Park HW, Kim JC. 2016. Nematicidal activity of kojic acid produced by *Aspergillus oryzae* against *Meloidogyne incognita*. *Journal of Microbiology and Biotechnology* **26**(8): 1383-1391.

Kimura Y, Sumiyoshi M. 2015. Antitumor and antimetastatic actions of dihydroxycoumarins (esculetin or fraxetin) through the inhibition of M2 macrophage differentiation in tumor-associated macrophages and/or G1 arrest in tumor cells. *European Journal of Pharmacology* **746**: 115-125.

Kiprovski B, Malenčić Đ, Đurić S, Bursać M, Cvejić J, Sikora V. 2016. Isoflavone content and antioxidant activity of soybean inoculated with plant-growth promoting rhizobacteria. *Journal of the Serbian Chemical Society* **81**(11): 1239-1249.

Kloepper J, Schroth M, Miller T. 1980. Effects of rhizosphere colonization by plant growth-promoting rhizobacteria on potato plant development and yield. *Phytopathology* **70**(11): 1078-1082.

Kloepper JW 1978. Plant growth-promoting rhizobacteria on radishes. *Proc. of the 4th Internet. Conf. on Plant Pathogenic Bacter, Station de Pathologie Vegetale et Phytobacteriologie, INRA, Angers, France, 1978*. 879-882.

Kloepper JW, Leong J, Teintze M, Schroth MN. 1980. Enhanced plant growth by siderophores produced by plant growth-promoting rhizobacteria. *Nature* **286**(5776): 885.

Kobayashi DY, Reedy RM, Bick J, Oudemans PV. 2002. Characterization of a chitinase gene from *Stenotrophomonas maltophilia* strain 34S1 and its involvement in biological control. *Applied and Environmental Microbiology* **68**(3): 1047-1054.

Kobriger KM, Hagedorn DJ. 1983. Determination of bean root-rot potential in vegetable production fields of wisconsins central sands. *Plant Disease* **67**(2): 177-178.

Kondo Y, Takano F, Hojo H. 1994. Suppression of chemically and immunologically induced hepatic injuries by gentiopicroside in mice. *Planta Medica* **60**(05): 414-416.

Koo H-J, Lim K-H, Jung H-J, Park E-H. 2006. Anti-inflammatory evaluation of gardenia extract, geniposide and genipin. *Journal of Ethnopharmacology* **103**(3): 496-500.

Korenblum E, Aharoni A. 2019. Phytobiome metabolism: beneficial soil microbes steer crop plants' secondary metabolism. *Pest Management Science* **75**(9): 2378-2384.

Korkina L. 2007. Phenylpropanoids as naturally occurring antioxidants: from plant defense to human health. *Cellular and Molecular Biology* **53**(1): 15-25.

Köster J, Rahmann S. 2012. Snakemake—a scalable bioinformatics workflow engine. *Bioinformatics* **28**(19): 2520-2522.

Kpomblekou-a K, Tabatabai M. 1994. Effect of organic acids on release of phosphorus from phosphate rocks1. *Soil Science* **158**(6): 442-453.

Kudoyarova GR, Vysotskaya LB, Arkhipova TN, Kuzmina LY, Galimsyanova NF, Sidorova LV, Gabbasova IM, Melentiev AI, Veselov SY. 2017. Effect of auxin producing and phosphate solubilizing bacteria on mobility of soil phosphorus, growth rate, and P acquisition by wheat plants. *Acta Physiologiae Plantarum* **39**(11): 253.

Kuhn BM, Errafi S, Bucher R, Dobrev P, Geisler M, Bigler L, Zažímalová E, Ringli C. 2016. 7-Rhamnosylated flavonols modulate homeostasis of the plant hormone auxin and affect plant development. *Journal of Biological Chemistry* **291**(10): 5385-5395.

Kuhn BM, Geisler M, Bigler L, Ringli C. 2011. Flavonols accumulate asymmetrically and affect auxin transport in Arabidopsis. *Plant Physiology* **156**(2): 585-595.

Kusari S, Lamshoft M, Kusari P, Gottfried S, Zuhlke S, Louven K, Hentschel U, Kayser O, Spiteller M. 2014. Endophytes are hidden producers of maytansine in putterlickia roots. *Journal of Natural Products* **77**(12): 2577-2584.

Kusari S, Zuhlke S, Spiteller M. 2011. Effect of artificial reconstitution of the interaction between the plant *Camptotheca acuminata* and the fungal endophyte *Fusarium solani* on camptothecin biosynthesis. *Journal of Natural Products* **74**(4): 764-775.

Kwak Y-S, Bonsall RF, Okubara PA, Paulitz TC, Thomashow LS, Weller DM. 2012. Factors impacting the activity of 2, 4-diacetylphloroglucinol-producing *Pseudomonas fluorescens* against take-all of wheat. *Soil Biology and Biochemistry* **54**: 48-56.

L

L. C. van Loon, P. A. H. M. Bakker a, Pieterse CMJ. 1998. Systemic resistance induced by rhizobacteria. *Annual Review of Phytopathology* **36**(1): 453-483.

Lakshmanan V, Castaneda R, Rudrappa T, Bais HP. 2013. Root transcriptome analysis of *Arabidopsis thaliana* exposed to beneficial *Bacillus subtilis* FB17 rhizobacteria revealed genes for bacterial recruitment and plant defense independent of malate efflux. *Planta* **238**(4): 657-668.

Lambers H, Mougel C, Jaillard B, Hinsinger P. 2009. Plant-microbe-soil interactions in the rhizosphere: an evolutionary perspective. *Plant and Soil* **321**(1): 83-115.

Langmead B, Salzberg SL. 2012. Fast gapped-read alignment with Bowtie 2. *Nature Methods* **9**(4): 357.

Lavania M, Chauhan PS, Chauhan S, Singh HB, Nautiyal CS. 2006. Induction of plant defense enzymes and phenolics by treatment with plant growth–promoting rhizobacteria *Serratia marcescens* NBRI1213. *Current Microbiology* **52**(5): 363-368.

Ledger T, Rojas S, Timmermann T, Pinedo I, Poupin MJ, Garrido T, Richter P, Tamayo J, Donoso R. 2016. Volatile-mediated effects predominate in *Paraburkholderia phytofirmans* growth promotion and salt stress tolerance of *Arabidopsis thaliana*. *Frontiers in Microbiology* **7**: 1838.

Lee JC, Lobkovsky E, Pliam NB, Strobel G, Clardy J. 1995. Subglutinols A and B: Immunosuppressive compounds from the endophytic fungus *Fusarium subglutinans*. *The Journal of Organic Chemistry* **60**(22): 7076-7077.

Lee S-K, Mo S, Suh J-W. 2012. An ABC transporter complex containing S-adenosylmethionine (SAM)-induced ATP-binding protein is involved in antibiotics production and SAM signaling in *Streptomyces coelicolor* M145. *Biotechnology Letters* **34**(10): 1907-1914.

Leeman M, Vanpelt JA, Denouden FM, Heinsbroek M, Bakker PAHM, Schippers B. 1995. Induction of systemic resistance against fusarium wilt of radish by lipopolysaccharides of *Pseudomonas fluorescens*. *Phytopathology* **85**(9): 1021-1027.

Leopoldini M, Russo N, Toscano M. 2011. The molecular basis of working mechanism of natural polyphenolic antioxidants. *Food Chemistry* **125**(2): 288-306.

Levy A, Gonzalez IS, Mittelviefhaus M, Clingenpeel S, Paredes SH, Miao J, Wang K, Devescovi G, Stillman K, Monteiro F. 2018. Genomic features of bacterial adaptation to plants. *Nature Genetics* **50**(1): 138-150.

Li EW, Jiang LH, Guo LD, Zhang H, Che YS. 2008. Pestalachlorides A-C, antifungal metabolites from the plant endophytic fungus *Pestalotiopsis adusta*. *Bioorganic & Medicinal Chemistry* **16**(17): 7894-7899.

Li H, Chen B, Pang G, Chen J, Xie J, Huang H. 2016. Anti-osteoporotic activity of puerarin 6″-O-xyloside on ovariectomized mice and its potential mechanism. *Pharmaceutical Biology* **54**(1): 111-117.

Li J, Zhao G-Z, Varma A, Qin S, Xiong Z, Huang H-Y, Zhu W-Y, Zhao L-X, Xu L-H, Zhang S. 2012. An endophytic *Pseudonocardia* species induces the production of artemisinin in *Artemisia annua*. *PLoS One* **7**(12): e51410.

Li ZJ, Liu M, Dawuti G, Dou Q, Ma Y, Liu HG, Aibai S. 2017. Antifungal activity of gallic acid *in vitro* and *in vivo*. *Phytotherapy Research* **31**(7): 1039-1045.

Lim J-H, Kim S-D. 2013. Induction of drought stress resistance by multi-functional PGPR *Bacillus licheniformis* K11 in pepper. *The Plant Pathology Journal* **29**(2): 201.

Lisec J, Schauer N, Kopka J, Willmitzer L, Fernie AR. 2006. Gas chromatography mass spectrometry–based metabolite profiling in plants. *Nature Protocols* **1**(1): 387.

Liu X-L, Zhang L, Fu X-L, Chen K, Qian B-C. 2001. Effect of scopoletin on PC3 cell proliferation and apoptosis. *Acta Pharmacologica Sinica* **22**(10): 929-933.

Lloyd JC, Zakhleniuk OV. 2004. Responses of primary and secondary metabolism to sugar accumulation revealed by microarray expression analysis of the *Arabidopsis* mutant, *pho3*. *Journal of Experimental Botany* **55**(400): 1221-1230.

Lodewyckx C, Vangronsveld J, Porteous F, Moore ER, Taghavi S, Mezgeay M, der Lelie Dv. 2002. Endophytic bacteria and their potential applications. *Critical Reviews in Plant Sciences* **21**(6): 583-606.

Lommen A. 2009. MetAlign: interface-driven, versatile metabolomics tool for hyphenated full-scan mass spectrometry data preprocessing. *Analytical Chemistry* **81**(8): 3079-3086.

Lopez-Fernandez S, Compant S, Vrhovsek U, Bianchedi PL, Sessitsch A, Pertot I, Campisano A. 2016. Grapevine colonization by endophytic bacteria shifts secondary metabolism and suggests activation of defense pathways. *Plant Soil* **405**(1-2): 177-177.

Lopez-Gonzalez JS, Prado-Garcia H, Aguilar-Cazares D, Molina-Guarneros JA, Morales-Fuentes J, Mandoki JJ. 2004. Apoptosis and cell cycle disturbances induced by coumarin and 7-hydroxycoumarin on human lung carcinoma cell lines. *Lung Cancer* **43**(3): 275-283.

Lou Z, Wang H, Rao S, Sun J, Ma C, Li J. 2012. *p*-Coumaric acid kills bacteria through dual damage mechanisms. *Food Control* **25**(2): 550-554.

Lozano-Durán R, Zipfel C. 2015. Trade-off between growth and immunity: role of brassinosteroids. *Trends in Plant Science* **20**(1): 12-19.

Ludwig-Muller J. 2015. Plants and endophytes: equal partners in secondary metabolite production? *Biotechnology Letters* **37**(7): 1325-1334.

Lugtenberg B, Kamilova F. 2009. Plant-growth-promoting rhizobacteria. *Annual Review of Microbiology* **63**: 541-556.

Lugtenberg BJ, Dekkers L, Bloemberg GV. 2001. Molecular determinants of rhizosphere colonization by *Pseudomonas*. *Annual Review of Phytopathology* **39**(1): 461-490.

Lundberg DS, Teixeira PJPL. 2018. Root-exuded coumarin shapes the root microbiome. *Proceedings of the National Academy of Sciences of the United States of America* **115**(22): 5629-5631.

Ma Q. 2013. Role of nrf2 in oxidative stress and toxicity. *Annual Review of Pharmacology and Toxicology* **53**: 401-426.

Mabrouk Y, Simier P, Arfaoui A, Sifi B, Delavault P, Zourgui L, Belhadj O. 2007. Induction of phenolic compounds in pea (*Pisum sativum* L.) inoculated by *Rhizobium leguminosarum* and infected with *Orobanche crenata*. *Journal of Phytopathology* **155**(11-12): 728-734.

Macho AP, Zipfel C. 2015. Targeting of plant pattern recognition receptor-triggered immunity by bacterial type-III secretion system effectors. *Current Opinion in Microbiology* **23**: 14-22.

Maddox CE, Laur LM, Tian L. 2010. Antibacterial activity of phenolic compounds against the phytopathogen *Xylella fastidiosa*. *Current Microbiology* **60**(1): 53-58.

Madloo P, Lema M, Francisco M, Soengas P. 2019. Role of major glucosinolates in the defense of kale against

Sclerotinia sclerotiorum and *Xanthomonas campestris* pv. *campestris*. *Phytopathology* **109**(7): 1246-1256.

Malka SK, Cheng YF. 2017. Possible interactions between the biosynthetic pathways of indole glucosinolate and auxin. *Frontiers in Plant Science* **8**.

Manici LM, Lazzeri L, Baruzzi G, Leoni O, Galletti S, Palmieri S. 2000. Suppressive activity of some glucosinolate enzyme degradation products on *Pythium irregulare* and *Rhizoctonia solani* in sterile soil. *Pest Management Science* **56**(10): 921-926.

Manici LM, Leoni O, Lazzeri L, Galletti S, Palmieri S. 1999. Fungitoxic activity of four thio-functionalised glucosinolate enzyme-derived products on ten soil-borne pathogens. *Pesticide Science* **55**(4): 486-488.

Manzoor M, Abbasi MK, Sultan T. 2017. Isolation of phosphate solubilizing bacteria from maize rhizosphere and their potential for rock phosphate solubilization–mineralization and plant growth promotion. *Geomicrobiology Journal* **34**(1): 81-95.

Mark GL, Dow JM, Kiely PD, Higgins H, Haynes J, Baysse C, Abbas A, Foley T, Franks A, Morrissey J. 2005. Transcriptome profiling of bacterial responses to root exudates identifies genes involved in microbe-plant interactions. *Proceedings of the National Academy of Sciences* **102**(48): 17454-17459.

Martín-Aragón S, Benedí JM, Villar AM. 1997. Modifications on antioxidant capacity and lipid peroxidation in mice under fraxetin treatment. *Journal of Pharmacy and Pharmacology* **49**(1): 49-52.

Martinez-Medina A, Flors V, Heil M, Mauch-Mani B, Pieterse CMJ, Pozo MJ, Ton J, van Dam NM, Conrath U. 2016. Recognizing plant defense priming. *Trends in Plant Science* **21**(10): 818-822.

Masalha J, Kosegarten H, Elmaci Ö, Mengel K. 2000. The central role of microbial activity for iron acquisition in maize and sunflower. *Biology and Fertility of Soils* **30**(5-6): 433-439.

Matusheski NV, Jeffery EH. 2001. Comparison of the bioactivity of two glucoraphanin hydrolysis products found in broccoli, sulforaphane and sulforaphane nitrile. *Journal of Agricultural and Food Chemistry* **49**(12): 5743-5749.

Mazzola M, De Bruijn I, Cohen MF, Raaijmakers JM. 2009. Protozoan-induced regulation of cyclic lipopeptide biosynthesis is an effective predation defense mechanism for *Pseudomonas fluorescens*. *Applied and Environmental Microbiology* **75**(21): 6804-6811.

McCarthy DJ, Chen Y, Smyth GK. 2012. Differential expression analysis of multifactor RNA-Seq experiments with respect to biological variation. *Nucleic Acids Research* **40**(10): 4288-4297.

McNeil MB, Clulow JS, Wilf NM, Salmond GP, Fineran PC. 2012. SdhE is a conserved protein required for flavinylation of succinate dehydrogenase in bacteria. *Journal of Biological Chemistry* **287**(22): 18418-18428.

Meister A. 1995. Glutathione biosynthesis and its inhibition. *Methods Enzymol* **252**: 26-30.

Meldau DG, Meldau S, Hoang LH, Underberg S, Wünsche H, Baldwin IT. 2013. Dimethyl disulfide produced by the naturally associated bacterium *Bacillus* sp B55 promotes *Nicotiana attenuata* growth by enhancing sulfur nutrition. *Plant Cell* **25**(7): 2731-2747.

Melnyk RA, Hossain SS, Haney CH. 2019. Convergent gain and loss of genomic islands drive lifestyle changes in plant-associated *Pseudomonas*. *Molecular Plant-Microbe Interactions* **32**(10): 241-241.

Mendes R, Garbeva P, Raaijmakers JM. 2013. The rhizosphere microbiome: significance of plant beneficial, plant pathogenic, and human pathogenic microorganisms. *FEMS Microbiology Reviews* **37**(5): 634-663.

Mendes R, Kruijt M, De Bruijn I, Dekkers E, van der Voort M, Schneider JH, Piceno YM, DeSantis TZ, Andersen GL, Bakker PA. 2011. Deciphering the rhizosphere microbiome for disease-suppressive bacteria. *Science* **332**(6033): 1097-1100.

Meziane H, Van Der Sluis I, Van Loon LC, Höfte M, Bakker PA. 2005. Determinants of *Pseudomonas putida* WCS358 involved in inducing systemic resistance in plants. *Molecular Plant Pathology* **6**(2): 177-185.

Miedes E, Vanholme R, Boerjan W, Molina A. 2014. The role of the secondary cell wall in plant resistance to pathogens. *Frontiers in Plant Science* **5**: 358.

Miller G, Huang IJ, Welkie G, Pushnik J 1995. Function of iron in plants with special emphasis on chloroplasts and photosynthetic activity. *Iron Nutrition in Soils and Plants*: Springer, 19-28.

Ming Q, Su C, Zheng C, Jia M, Zhang Q, Zhang H, Rahman K, Han T, Qin L. 2013. Elicitors from the endophytic fungus *Trichoderma atroviride* promote *Salvia miltiorrhiza* hairy root growth and tanshinone biosynthesis. *Journal of Experimental Botany* **64**(18): 5687-5694.

Mishra RP, Singh RK, Jaiswal HK, Kumar V, Maurya S. 2006. *Rhizobium*-mediated induction of phenolics and plant growth promotion in rice (*Oryza sativa* L.). *Current Microbiology* **52**(5): 383-389.

Mitter B, Pfaffenbichler N, Flavell R, Compant S, Antonielli L, Petric A, Berninger T, Naveed M, Sheibani-Tezerji R, von Maltzahn G. 2017. A new approach to modify plant microbiomes and traits by introducing beneficial bacteria at flowering into progeny seeds. *Frontiers in Microbiology* **8**: 11.

Molina-Jiménez MaF, Sánchez-Reus MaI, Andres D, Cascales Ma, Benedi J. 2004. Neuroprotective effect of fraxetin and myricetin against rotenone-induced apoptosis in neuroblastoma cells. *Brain Research* **1009**(1-2): 9-16.

Monteiro L, Mariano RdLR, Souto-Maior AM. 2005. Antagonism of *Bacillus* spp. against *Xanthomonas campestris* pv. *campestris*. *Brazilian Archives of Biology and Technology* **48**(1): 23-29.

Moyne AL, Shelby R, Cleveland T, Tuzun S. 2001. Bacillomycin D: an iturin with antifungal activity against *Aspergillus flavus*. *Journal of Applied Microbiology* **90**(4): 622-629.

Murali R, Srinivasan S, Ashokkumar N. 2013. Antihyperglycemic effect of fraxetin on hepatic key enzymes of carbohydrate metabolism in streptozotocin-induced diabetic rats. *Biochimie* **95**(10): 1848-1854.

Murphy A, Peer WA, Taiz L. 2000. Regulation of auxin transport by aminopeptidases and endogenous flavonoids. *Planta* **211**(3): 315-324.

N

Naguib AE-MM, El-Baz FK, Salama ZA, Hanaa HAEB, Ali HF, Gaafar AA. 2012. Enhancement of phenolics, flavonoids and glucosinolates of Broccoli (*Brassica olaracea*, var. *Italica*) as antioxidants in response to organic and bio-organic fertilizers. *Journal of the Saudi Society of Agricultural Sciences* **11**(2): 135-142.

Nakazawa T, Yasuda T, Ueda J, Ohsawa K. 2003. Antidepressant-like effects of apigenin and 2, 4, 5-trimethoxycinnamic acid from *Perilla frutescens* in the forced swimming test. *Biological and Pharmaceutical Bulletin* **26**(4): 474-480.

Nam HS, Anderson AJ, Yang KY, Cho BH, Kim YC. 2006. The *dctA* gene of *Pseudomonas chlororaphis* O6 is under RpoN control and is required for effective root colonization and induction of systemic resistance. *FEMS Microbiology Letters* **256**(1): 98-104.

Natarajan K, Singh S, Burke TR, Grunberger D, Aggarwal BB. 1996. Caffeic acid phenethyl ester is a potent and specific inhibitor of activation of nuclear transcription factor NF-kappa B. *Proceedings of the National Academy of Sciences of the United States of America* **93**(17): 9090-9095.

Nazir R, Warmink JA, Boersma H, Van Elsas JD. 2009. Mechanisms that promote bacterial fitness in fungal-affected soil microhabitats. *FEMS Microbiology Ecology* **71**(2): 169-185.

Neilands JB. 1995. Siderophores - structure and function of microbial iron transport compounds. *The Journal of Biological Chemistry* **270**(45): 26723-26726.

Newman DJ, Cragg GM. 2015. Endophytic and epiphytic microbes as "sources" of bioactive agents. *Frontiers in Chemistry* **3**.

Nguyen DM, Seo DJ, Lee HB, Kim IS, Kim KY, Park RD, Jung WJ. 2013. Antifungal activity of gallic acid purified from *Terminalia nigrovenulosa* bark against *Fusarium solani*. *Microbial Pathogenesis* **56**: 8-15.

Nijveldt RJ, Van Nood E, Van Hoorn DE, Boelens PG, Van Norren K, Van Leeuwen PA. 2001. Flavonoids: a review of probable mechanisms of action and potential applications. *The American Journal of Clinical Nutrition* **74**(4): 418-425.

Niu H-S, Liu I-M, Cheng J-T, Lin C-L, Hsu F-L. 2008. Hypoglycemic effect of syringin from *Eleutherococcus senticosus* in streptozotocin-induced diabetic rats. *Planta Medica* **74**(02): 109-113.

O

Ockels FS, Eyles A, McPherson BA, Wood DL, Bonello P. 2007. Phenolic chemistry of coast live oak response to *Phytophthora ramorum* infection. *Journal of Chemical Ecology* **33**(9): 1721-1732.

Oh S, Warnasooriya SN, Montgomery BL. 2014. Mesophyll-localized phytochromes gate stress- and light-inducible anthocyanin accumulation in *Arabidopsis thaliana*. *Plant Signaling & Behavior* **9**(1): e28013.

Okmen B, Etalo DW, Joosten MHAJ, Bouwmeester HJ, de Vos RCH, Collemare J, de Wit PJGM. 2013. Detoxification of α-tomatine by *Cladosporium fulvum* is required for full virulence on tomato. *New Phytologist* **198**(4): 1203-1214.

Okon Y, Bloemberg GV, Lugtenberg BJ. 1998. Biotechnology of biofertilization and phytostimulation. *Agricultural Biotechnology* **327**: 349.

Oksman-Caldentey K-M, Inzé D. 2004. Plant cell factories in the post-genomic era: new ways to produce designer secondary metabolites. *Trends in Plant Science* **9**(9): 433-440.

Olanrewaju OS, Glick BR, Babalola OO. 2017. Mechanisms of action of plant growth promoting bacteria. *World Journal of Microbiology and Biotechnology* **33**(11): 197.

Ongena M, Duby F, Jourdan E, Beaudry T, Jadin V, Dommes J, Thonart P. 2005. *Bacillus subtilis* M4 decreases plant susceptibility towards fungal pathogens by increasing host resistance associated with differential gene expression. *Applied Microbiology and Biotechnology* **67**(5): 692-698.

Ongena M, Jourdan E, Adam A, Paquot M, Brans A, Joris B, Arpigny JL, Thonart P. 2007. Surfactin and fengycin lipopeptides of *Bacillus subtilis* as elicitors of induced systemic resistance in plants. *Environmental Microbiology* **9**(4): 1084-1090.

Ongena M, Jourdan E, Schafer M, Kech C, Budzikiewicz H, Luxen A, Thonart P. 2005. Isolation of an n-alkylated benzylamine derivative from *Pseudomonas putida* BTP1 as elicitor of induced systemic

resistance in bean. *Molecular Plant-Microbe Interactions* **18**(6): 562-569.

Ordal GW, Villani DP, Rosendahl MS. 1979. Chemotaxis towards sugars by *Bacillus subtilis*. *Journal of General Microbiology* **115**(Nov): 167-172.

Ostlind DA, Felcetto T, Misura A, Ondeyka J, Smith S, Goetz M, Shoop W, Mickle W. 1997. Discovery of a novel indole diterpene insecticide using first instars of *Lucilia sericata*. *Medical and Veterinary Entomology* **11**(4): 407-408.

Ostonen I, Lõhmus K, Helmisaari H-S, Truu J, Meel S. 2007. Fine root morphological adaptations in Scots pine, Norway spruce and silver birch along a latitudinal gradient in boreal forests. *Tree Physiology* **27**(11): 1627-1634.

P

Panda S, Kar A. 2006. Evaluation of the antithyroid, antioxidative and antihyperglycemic activity of scopoletin from *Aegle marmelos* leaves in hyperthyroid rats. *Phytotherapy Research* **20**(12): 1103-1105.

Pandey SS, Singh S, Babu CSV, Shanker K, Srivastava NK, Shukla AK, Kalra A. 2016. Fungal endophytes of *Catharanthus roseus* enhance vindoline content by modulating structural and regulatory genes related to terpenoid indole alkaloid biosynthesis. *Scientific Reports* **6**: 1-14.

Pandey SS, Singh S, Babu CV, Shanker K, Srivastava N, Kalra A. 2016. Endophytes of opium poppy differentially modulate host plant productivity and genes for the biosynthetic pathway of benzylisoquinoline alkaloids. *Planta* **243**(5): 1097-1114.

Panke-Buisse K, Poole AC, Goodrich JK, Ley RE, Kao-Kniffin J. 2015. Selection on soil microbiomes reveals reproducible impacts on plant function. *The ISME Journal* **9**(4): 980-989.

Park M-H, Arasu MV, Park N-Y, Choi Y-J, Lee S-W, Al-Dhabi NA, Kim JB, Kim S-J. 2013. Variation of glucoraphanin and glucobrassicin: anticancer components in *Brassica* during processing. *Food Science and Technology* **33**(4): 624-631.

Park Y-S, Dutta S, Ann M, Raaijmakers JM, Park K. 2015. Promotion of plant growth by *Pseudomonas fluorescens* strain SS101 via novel volatile organic compounds. *Biochemical and Biophysical Research Communications* **461**(2): 361-365.

Pérez-Jaramillo JE, Carrión VJ, de Hollander M, Raaijmakers JM. 2018. The wild side of plant microbiomes. *Microbiome* **6**(1): 143.

Pérez-Jaramillo JE, Mendes R, Raaijmakers JM. 2016. Impact of plant domestication on rhizosphere microbiome assembly and functions. *Plant Molecular Biology* **90**(6): 635-644.

Philippot L, Raaijmakers JM, Lemanceau P, Van Der Putten WH. 2013. Going back to the roots: the microbial ecology of the rhizosphere. *Nature Reviews Microbiology* **11**(11): 789.

Pieterse CM, Van der Does D, Zamioudis C, Leon-Reyes A, Van Wees SC. 2012. Hormonal modulation of plant immunity. *Annual Review of Cell and Developmental Biology* **28**: 489-521.

Pieterse CM, Van Pelt JA, Van Wees SC, Ton J, Léon-Kloosterziel KM, Keurentjes JJ, Verhagen BW, Knoester M, Van der Sluis I, Bakker PA. 2001. Rhizobacteria-mediated induced systemic resistance: triggering, signalling and expression. *European Journal of Plant Pathology* **107**(1): 51-61.

Pieterse CM, Zamioudis C, Berendsen RL, Weller DM, Van Wees SC, Bakker PA. 2014. Induced systemic resistance by beneficial microbes. *Annual Review of Phytopathology* **52**: 347-375.

Pineda A, Zheng S-J, van Loon JJA, Pieterse CMJ, Dicke M. 2010. Helping plants to deal with insects: the role of beneficial soil-borne microbes. *Trends in Plant Science* **15**(9): 507-514.

Planchamp C, Glauser G, Mauch-Mani B. 2015. Root inoculation with *Pseudomonas putida* KT2440 induces transcriptional and metabolic changes and systemic resistance in maize plants. *Frontiers in Plant Science* **5**: 719.

Pongprayoon U, Baeckström P, Jacobsson U, Lindström M, Bohlin L. 1992. Antispasmodic activity of β-damascenone and *E*-phytol isolated from *Ipomoea pes-caprae*. *Planta Medica* **58**(01): 19-21.

Poupin MJ, Timmermann T, Vega A, Zuñiga A, González B. 2013. Effects of the plant growth-promoting bacterium *Burkholderia phytofirmans* PsJN throughout the life cycle of *Arabidopsis thaliana*. *PLoS One* **8**(7).

Prasad CV, Mohan SS, Banerji A, Gopalakrishnapillai A. 2009. Kaempferitrin inhibits GLUT4 translocation and glucose uptake in 3T3-L1 adipocytes. *Biochemical and Biophysical Research Communications* **380**(1): 39-43.

R

Raaijmakers JM, De Bruijn I, de Kock MJ. 2006. Cyclic lipopeptide production by plant-associated *Pseudomonas* spp.: diversity, activity, biosynthesis, and regulation. *Molecular Plant-Microbe Interactions* **19**(7): 699-710.

Raaijmakers JM, De Bruijn I, Nybroe O, Ongena M. 2010. Natural functions of lipopeptides from *Bacillus* and *Pseudomonas*: more than surfactants and antibiotics. *FEMS Microbiology Reviews* **34**(6): 1037-1062.

Raaijmakers JM, Mazzola M. 2012. Diversity and natural functions of antibiotics produced by beneficial and plant

pathogenic bacteria. *Annual Review of Phytopathology* **50**: 403-424.

Raaijmakers JM, Mazzola M. 2016. Soil immune responses soil microbiomes may be harnessed for plant health. *Science* **352**(6292): 1392-1393.

Raaijmakers JM, Paulitz TC, Steinberg C, Alabouvette C, Moënne-Loccoz Y. 2009. The rhizosphere: a playground and battlefield for soilborne pathogens and beneficial microorganisms. *Plant and Soil* **321**(1-2): 341-361.

Raaijmakers JM, Weller DM. 1998. Natural plant protection by 2, 4-diacetylphloroglucinol-producing *Pseudomonas* spp. in take-all decline soils. *Molecular Plant-Microbe Interactions* **11**(2): 144-152.

Radzki W, Mañero FG, Algar E, García JL, García-Villaraco A, Solano BR. 2013. Bacterial siderophores efficiently provide iron to iron-starved tomato plants in hydroponics culture. *Antonie Van Leeuwenhoek* **104**(3): 321-330.

Rahman M, Sabir AA, Mukta JA, Khan MMA, Mohi-Ud-Din M, Miah MG, Rahman M, Islam MT. 2018. Plant probiotic bacteria *Bacillus* and *Paraburkholderia* improve growth, yield and content of antioxidants in strawberry fruit. *Scientific Reports* **8**(1): 2504.

Rajkumar M, Ae N, Prasad MNV, Freitas H. 2010. Potential of siderophore-producing bacteria for improving heavy metal phytoextraction. *Trends in Biotechnology* **28**(3): 142-149.

Ramos-Solano B, Algar E, Garcia-Villaraco A, Garcia-Cristobal J, Lucas Garcia JA, Gutierrez-Mañero FJ. 2010. Biotic elicitation of isoflavone metabolism with plant growth promoting rhizobacteria in early stages of development in *Glycine max* var. Osumi. *Journal of Agricultural and Food Chemistry* **58**(3): 1484-1492.

Rando RR, Bangerter F. 1977. The in vivo inhibition of GABA-transaminase by gabaculine. *Biochemical and Biophysical Research Communications* **76**(4): 1276-1281.

Rashid M, Kim H-J, Yeom S-I, Yu H-A, Manir M, Moon S-S, Kang YJ, Chung YR. 2018. *Bacillus velezensis* YC7010 enhances plant defenses against brown planthopper through transcriptomic and metabolic changes in rice. *Frontiers in Plant Science* **9**: 1904.

Rattan RS. 2010. Mechanism of action of insecticidal secondary metabolites of plant origin. *Crop Protection* **29**(9): 913-920.

Raupach GS, Liu L, Murphy JF, Tuzun S, Kloepper JW. 1996. Induced systemic resistance in cucumber and tomato against cucumber mosaic cucumovirus using plant growth-promoting rhizobacteria (PGPR). *Plant Disease* **80**(8): 891-894.

Ray T, Pandey SS, Pandey A, Srivastava M, Shanker K, Kalra A. 2019. Endophytic consortium with diverse gene-regulating capabilities of benzylisoquinoline alkaloids biosynthetic pathway can enhance endogenous morphine biosynthesis in *Papaver somniferum*. *Frontiers in Microbiology* **10**: 925.

Razis AFA, Bagatta M, De Nicola GR, Iori R, Ioannides C. 2011. Up-regulation of cytochrome P450 and phase II enzyme systems in rat precision-cut rat lung slices by the intact glucosinolates, glucoraphanin and glucoerucin. *Lung Cancer* **71**(3): 298-305.

Reimers PJ, Leach JE. 1991. Race-specific resistance to *Xanthomonas oryzae* pv. *oryzae* conferred by bacterial blight resistance gene Xa-10 in rice (*Oryza sativa*) involves accumulation of a lignin-like substance in host tissues. *Physiological and Molecular Plant Pathology* **38**(1): 39-55.

Reinhold-Hurek B, Bunger W, Burbano CS, Sabale M, Hurek T. 2015. Roots shaping their microbiome: global hotspots for microbial activity. *Annual Review of Phytopathology* **53**: 403-424.

Ridder L, van der Hooft JJJ, Verhoeven S, de Vos RCH, Bino RJ, Vervoort J. 2013. Automatic chemical structure annotation of an LC–MSn based metabolic profile from green tea. *Analytical Chemistry* **85**(12): 6033-6040.

Robinson MD, McCarthy DJ, Smyth GK. 2010. edgeR: a Bioconductor package for differential expression analysis of digital gene expression data. *Bioinformatics* **26**(1): 139-140.

Rodrigues EP, Rodrigues LS, de Oliveira ALM, Baldani VLD, dos Santos Teixeira KR, Urquiaga S, Reis VM. 2008. *Azospirillum amazonense* inoculation: effects on growth, yield and N2 fixation of rice (*Oryza sativa* L.). *Plant and Soil* **302**(1-2): 249-261.

Rodríguez H, Fraga R. 1999. Phosphate solubilizing bacteria and their role in plant growth promotion. *Biotechnology Advances* **17**(4-5): 319-339.

Rohwer F, Seguritan V, Azam F, Knowlton N. 2002. Diversity and distribution of coral-associated bacteria. *Marine Ecology Progress Series* **243**: 1-10.

Rojas-Solís D, Zetter-Salmón E, Contreras-Pérez M, del Carmen Rocha-Granados M, Macías-Rodríguez L, Santoyo G. 2018. *Pseudomonas stutzeri* E25 and *Stenotrophomonas maltophilia* CR71 endophytes produce antifungal volatile organic compounds and exhibit additive plant growth-promoting effects. *Biocatalysis and Agricultural Biotechnology* **13**: 46-52.

Rolland F, Baena-Gonzalez E, Sheen J. 2006. Sugar sensing and signaling in plants: conserved and novel mechanisms. *Annual Review of Plant Biology* **57**: 675-709.

Romero D, de Vicente A, Rakotoaly RH, Dufour SE, Veening J-W, Arrebola E, Cazorla FM, Kuipers OP, Paquot M, Pérez-García A. 2007. The iturin and fengycin families of lipopeptides are key factors in antagonism of *Bacillus subtilis* toward *Podosphaera fusca*. *Molecular Plant-Microbe Interactions* **20**(4): 430-440.

Romero MR, Efferth T, Serrano MA, Castano B, Macias RI, Briz O, Marin JJ. 2005. Effect of artemisinin/artesunate as inhibitors of hepatitis B virus production in an "in vitro" replicative system. *Antiviral Research* **68**(2): 75-83.

Rosenberg E, Zilber-Rosenberg I. 2016. Microbes drive evolution of animals and plants: the hologenome concept. *mBio* **7**(2): e01395-01315.

Rowan DD. 1993. Lolitrems, peramine and paxilline: mycotoxins of the ryegrass/endophyte interaction. *Agriculture, Ecosystems & Environment* **44**(1-4): 103-122.

Rozier C, Erban A, Hamzaoui J, Prigent-Combaret C, Comte G, Kopka J, Czarnes S, Legendre L. 2016. Xylem sap metabolite profile changes during phytostimulation of maize by the plant growth-promoting rhizobacterium, *Azospirillum lipoferum* CRT1. *Metabolomics* **6**: 2153-0769.

Rudrappa T, Czymmek KJ, Pare PW, Bais HP. 2008. Root-secreted malic acid recruits beneficial soil bacteria. *Plant Physiology* **148**(3): 1547-1556.

Ryffel F, Helfrich EJN, Kiefer P, Peyriga L, Portais J-C, Piel J, Vorholt JA. 2016. Metabolic footprint of epiphytic bacteria on *Arabidopsis thaliana* leaves. *The ISME Journal* **10**(3): 632-643.

Ryu C-M, Farag MA, Hu C-H, Reddy MS, Kloepper JW, Paré PW. 2004. Bacterial volatiles induce systemic resistance in Arabidopsis. *Plant Physiol* **134**(3): 1017-1026.

Ryu C-M, Farag MA, Hu C-H, Reddy MS, Wei H-X, Paré PW, Kloepper JW. 2003. Bacterial volatiles promote growth in Arabidopsis. *Proceedings of the National Academy of Sciences* **100**(8): 4927-4932.

S

Santana M, Ionescu MS, Vertes A, Longin R, Kunst F, Danchin A, Glaser P. 1994. *Bacillus subtilis* F0F1 ATPase: DNA sequence of the *atp* operon and characterization of *atp* mutants. *Journal of Bacteriology* **176**(22): 6802-6811.

Santoro M, Cappellari LdR, Giordano W, Banchio E. 2015. Plant growth-promoting effects of native *Pseudomonas* strains on *Mentha piperita* (peppermint): an in vitro study. *Plant Biology* **17**(6): 1218-1226.

Santoro MV, Zygadlo J, Giordano W, Banchio E. 2011. Volatile organic compounds from rhizobacteria increase biosynthesis of essential oils and growth parameters in peppermint (*Mentha piperita*). *Plant Physiology and Biochemistry* **49**(10): 1177-1182.

Sarma BK, Singh DP, Mehta S, Singh HB, Singh UP. 2002. Plant growth-promoting rhizobacteria-elicited alterations in phenolic profile of chickpea (*Cicer arietinum*) infected by *Sclerotium rolfsii*. *Journal of Phytopathology* **150**(4-5): 277-282.

Sarma BK, Singh UP. 2003. Ferulic acid may prevent infection of *Cicer arietinum* by *Sclerotium rolfsii*. *World Journal of Microbiology & Biotechnology* **19**(2): 123-127.

Sato Y, Itagaki S, Kurokawa T, Ogura J, Kobayashi M, Hirano T, Sugawara M, Iseki K. 2011. *In vitro* and *in vivo* antioxidant properties of chlorogenic acid and caffeic acid. *International Journal of Dermatology* **403**(1-2): 136-138.

Sawana A, Adeolu M, Gupta RS. 2014. Molecular signatures and phylogenomic analysis of the genus *Burkholderia*: proposal for division of this genus into the emended genus *Burkholderia* containing pathogenic organisms and a new genus *Paraburkholderia* gen. nov. harboring environmental species. *Frontiers in Genetics* **5**: 429.

Sayyed RZ, Chincholkar SB, Reddy MS, Gangurde NS, Patel PR 2013. Siderophore producing PGPR for crop nutrition and phytopathogen suppression. In: Maheshwari DK ed. *Bacteria in Agrobiology: Disease Management*. Berlin, Heidelberg: Springer Berlin Heidelberg, 449-471.

Scherling C, Ulrich K, Ewald D, Weckwerth W. 2009. A metabolic signature of the beneficial interaction of the endophyte *Paenibacillus* sp. isolate and in vitro-grown poplar plants revealed by metabolomics. *Molecular Plant-Microbe Interactions* **22**(8): 1032-1037.

Schlatter D, Kinkel L, Thomashow L, Weller D, Paulitz T. 2017. Disease suppressive soils: new insights from the soil microbiome. *Phytopathology* **107**(11): 1284-1297.

Schmidt R, Cordovez V, De Boer W, Raaijmakers J, Garbeva P. 2015. Volatile affairs in microbial interactions. *The ISME Journal* **9**(11): 2329.

Schouten A. 2016. Mechanisms involved in nematode control by endophytic fungi. *Annual Review of Phytopathology* **54**: 121-142.

Schulz-Bohm K. 2018. *The ecological role of volatile mediated interactions belowground.* Wageningen:

Wageningen University.
Schulz-Bohm K, Gerards S, Hundscheid M, Melenhorst J, de Boer W, Garbeva P. 2018. Calling from distance: attraction of soil bacteria by plant root volatiles. *The ISME Journal* **12**(5): 1252.
Schwartz RE, Smith SK, Onishi JC, Meinz M, Kurtz M, Giacobbe RA, Wilson KE, Liesch J, Zink D, Horn W, et al. 2000. Isolation and structural determination of enfumafungin, a triterpene glycoside antifungal agent that is a specific inhibitor of glucan synthesis. *Journal of the American Chemical Society* **122**(20): 4882-4886.
Schwarz M, Kopcke B, Weber RWS, Sterner O, Anke H. 2004. 3-Hydroxypropionic acid as a nematicidal principle in endophytic fungi. *Phytochemistry* **65**(15): 2239-2245.
Schweiger R, Baier MC, Persicke M, Müller C. 2014. High specificity in plant leaf metabolic responses to arbuscular mycorrhiza. *Nature Communications* **5**: 3886.
Seigler DS. 1998. *Plant secondary metabolism*. Boston: Kluwer Academic.
Selle K, Barrangou R. 2015. Harnessing CRISPR-Cas systems for bacterial genome editing. *Trends in Microbiology* **23**(4): 225-232.
Sharifi R, Ryu C-M. 2018. Sniffing bacterial volatile compounds for healthier plants. *Current Opinion in Plant Biology* **44**: 88-97.
Sharma A, Johri BN. 2003. Combat of iron-deprivation through a plant growth promoting fluorescent *Pseudomonas* strain GRP3A in mung bean (*Vigna radiata* L. Wilzeck). *Microbiological Research* **158**(1): 77-81.
Shidore T, Dinse T, Ohrlein J, Becker A, Reinhold-Hurek B. 2012. Transcriptomic analysis of responses to exudates reveal genes required for rhizosphere competence of the endophyte *Azoarcus* sp. strain BH72. *Environmental Microbiology* **14**(10): 2775-2787.
Shukla ST, Habbu PV, Kulkarni VH, Jagadish KS, Pandey AR, Sutariya VN. 2014. Endophytic microbes: A novel source for biologically/pharmacologically active secondary metabolites. *Asian Journal of Pharmacology and Toxicology* **2**(3): 1-16.
Siddiqui I, Shaukat S. 2002. Resistance against the damping-off fungus *Rhizoctonia solani* systemically induced by the plant-growth-promoting rhizobacteria *Pseudomonas aeruginosa* (IE-6S+) and *P. fluorescens* (CHA0). *Journal of Phytopathology* **150**(8-9): 500-506.
Singh B, Kaur T, Kaur S, Manhas RK, Kaur A. 2016. Insecticidal potential of an endophytic *Cladosporium velox* against *Spodoptera litura* mediated through inhibition of alpha glycosidases. *Pesticide Biochemistry and Physiology* **131**: 46-52.
Singh M, Kumar A, Singh R, Pandey KD. 2017. Endophytic bacteria: a new source of bioactive compounds. *3 Biotech* **7**.
Singh NP, Lai H. 2001. Selective toxicity of dihydroartemisinin and holotransferrin toward human breast cancer cells. *Life Sciences* **70**(1): 49-56.
Singh NP, Lai HC. 2004. Artemisinin induces apoptosis in human cancer cells. *Anticancer Research* **24**(4): 2277-2280.
Smirnoff N. 2018. Ascorbic acid metabolism and functions: a comparison of plants and mammals. *Free Radical Biology and Medicine* **122**: 116-129.
Spaepen S, Vanderleyden J, Remans R. 2007. Indole-3-acetic acid in microbial and microorganism-plant signaling. *FEMS Microbiology Reviews* **31**(4): 425-448.
Staniek A, Woerdenbag HJ, Kayser O. 2008. Endophytes: exploiting biodiversity for the improvement of natural product-based drug discovery. *Journal of Plant Interactions* **3**(2): 75-93.
Stierle A, Strobel G, Stierle D. 1993. Taxol and taxane production by *Taxomyces andreanae*, an endophytic fungus of Pacific yew. *Science* **260**(5105): 214-216.
Stringlis IA, Yu K, Feussner K, de Jonge R, Van Bentum S, Van Verk MC, Berendsen RL, Bakker PA, Feussner I, Pieterse CM. 2018. MYB72-dependent coumarin exudation shapes root microbiome assembly to promote plant health. *Proceedings of the National Academy of Sciences of the United States of America* **115**(22): E5213-E5222.
Stringlis IA, Zhang H, Pieterse CMJ, Bolton MD, de Jonge R. 2018. Microbial small molecules - weapons of plant subversion. *Natural Product Reports* **35**(5): 410-433.
Strobel GA, Hess WM. 1997. Glucosylation of the peptide leucinostatin A, produced by an endophytic fungus of European yew, may protect the host from leucinostatin toxicity. *Chemistry & Biology* **4**(7): 529-536.
Sumayo M, Hahm M-S, Ghim S-Y. 2013. Determinants of plant growth-promoting *Ochrobactrum lupini* KUDC1013 Involved in induction of systemic resistance against *Pectobacterium carotovorum* subsp. *carotovorum* in Tobacco Leaves. *The Plant Pathology Journal* **29**(2): 174-181.
Suzuki Y, Kondo K, Ikeda Y, Umemura K. 2001. Antithrombotic effect of geniposide and genipin in the mouse thrombosis model. *Planta Medica* **67**(09): 807-810.

T
Tabassum B, Khan A, Tariq M, Ramzan M, Khan MSI, Shahid N, Aaliya K. 2017. Bottlenecks in commercialisation and future prospects of PGPR. *Applied Soil Ecology* **121**: 102-117.

Tanaka A, Tapper BA, Popay A, Parker EJ, Scott B. 2005. A symbiosis expressed non-ribosomal peptide synthetase from a mutualistic fungal endophyte of perennial ryegrass confers protection to the symbiotum from insect herbivory. *Molecular Microbiology* **57**(4): 1036-1050.

Tang Y-W. 2014. *Molecular medical microbiology*: Academic press.

Textor S, Bartram S, Kroymann J, Falk KL, Hick A, Pickett JA, Gershenzon J. 2004. Biosynthesis of methionine-derived glucosinolates in Arabidopsis thaliana: recombinant expression and characterization of methylthioalkylmalate synthase, the condensing enzyme of the chain-elongation cycle. *Planta* **218**(6): 1026-1035.

Textor S, de Kraker JW, Hause B, Gershenzon J, Tokuhisa JG. 2007. MAM3 catalyzes the formation of all aliphatic glucosinolate chain lengths in arabidopsis. *Plant Physiology* **144**(1): 60-71.

Tian Y, Arnand S, Buisson D, Kunz C, Hachette F, Dupont J, Nay B, Prado S. 2014. The fungal leaf endophyte *Paraconiothyrium variabile* specifically metabolizes the host-plant metabolome for its own benefit. *Phytochemistry* **108**: 95-101.

Tikunov Y, Laptenok S, Hall R, Bovy A, De Vos R. 2012. MSClust: a tool for unsupervised mass spectra extraction of chromatography-mass spectrometry ion-wise aligned data. *Metabolomics* **8**(4): 714-718.

Timmermann T, Armijo G, Donoso R, Seguel A, Holuigue L, González B. 2017. *Paraburkholderia phytofirmans* PsJN protects *Arabidopsis thaliana* against a virulent strain of *Pseudomonas syringae* through the activation of induced resistance. *Molecular Plant-Microbe Interactions* **30**(3): 215-230.

Tiwari R, Awasthi A, Mall M, Shukla AK, Srinivas KVNS, Syamasundar KV, Kalra A. 2013. Bacterial endophyte-mediated enhancement of *in planta* content of key terpenoid indole alkaloids and growth parameters of *Catharanthus roseus*. *Industrial Crops and Products* **43**: 306-310.

Toure Y, Ongena M, Jacques P, Guiro A, Thonart P. 2004. Role of lipopeptides produced by *Bacillus subtilis* GA1 in the reduction of grey mould disease caused by *Botrytis cinerea* on apple. *Journal of Applied Microbiology* **96**(5): 1151-1160.

Treutter D. 2005. Significance of flavonoids in plant resistance and enhancement of their biosynthesis. *Plant Biology* **7**(06): 581-591.

U
Uma Sankari J. DS, and Sekar C. 2011. Dual effect of *Azospirillum* xxopolysaccharides (EPS) on the enhancement of plant growth and biocontrol of blast (*Pyricularia oryzae*) disease in upland rice (var. ASD-19) *Journal of Phytology* **3**(10): 16-19.

Urdangarin C, Regente M, Jorrin J, De La Canal L. 1999. Sunflower coumarin phytoalexins inhibit the growth of the virulent pathogen *Sclerotinia sclerotiorum*. *Journal of Phytopathology* **147**(7-8): 441-443.

V
Valenzuela-Soto JH, Estrada-Hernández MG, Ibarra-Laclette E, Délano-Frier JP. 2010. Inoculation of tomato plants (*Solanum lycopersicum*) with growth-promoting *Bacillus subtilis* retards whitefly *Bemisia tabaci* development. *Planta* **231**(2): 397.

van Dam NM, Baldwin IT. 1998. Costs of jasmonate-induced responses in plants competing for limited resources. *Ecology Letters* **1**(1): 30-33.

van de Mortel JE, de Vos RC, Dekkers E, Pineda A, Guillod L, Bouwmeester K, van Loon JJ, Dicke M, Raaijmakers JM. 2012. Metabolic and transcriptomic changes induced in Arabidopsis by the rhizobacterium *Pseudomonas fluorescens* SS101. *Plant Physiology* **160**(4): 2173-2188.

Van der Ent S, Van Wees SCM, Pieterse CMJ. 2009. Jasmonate signaling in plant interactions with resistance-inducing beneficial microbes. *Phytochemistry* **70**(13): 1581-1588.

van der Linden SC, von Bergh AR, van Vught-Lussenburg BM, Jonker LR, Teunis M, Krul CA, van der Burg B. 2014. Development of a panel of high-throughput reporter-gene assays to detect genotoxicity and oxidative stress. *Genetic Toxicology and Environmental Mutagenesis* **760**: 23-32.

Van Loon LC. 2007. Plant responses to plant growth-promoting rhizobacteria. *European Journal of Plant Pathology* **119**(3): 243-254.

Van Peer R, Niemann GJ, Schippers B. 1991. Induced resistance and phytoalexin accumulation in biological control of Fusarium wilt of carnation by *Pseudomonas* sp. strain WCS417r. *Phytopathology* **81**(7): 728-734.

Van Wees SC, Luijendijk M, Smoorenburg I, Van Loon LC, Pieterse CM. 1999. Rhizobacteria-mediated induced systemic resistance (ISR) in *Arabidopsis* is not associated with a direct effect on expression of known defense-related genes but stimulates the expression of the jasmonate-inducible gene Atvsp upon challenge. *Plant Molecular Biology* **41**(4): 537-549.

Vansuyt G, Robin A, Briat J-F, Curie C, Lemanceau P. 2007. Iron acquisition from Fe-pyoverdine by *Arabidopsis thaliana*. *Molecular Plant-Microbe Interactions* **20**(4): 441-447.

Velázquez-Becerra C, Macías-Rodríguez LI, López-Bucio J, Altamirano-Hernández J, Flores-Cortez I, Valencia-Cantero E. 2011. A volatile organic compound analysis from *Arthrobacter agilis* identifies dimethylhexadecylamine, an amino-containing lipid modulating bacterial growth and *Medicago sativa* morphogenesis in vitro. *Plant and Soil* **339**(1-2): 329-340.

Verhagen BW, Glazebrook J, Zhu T, Chang H-S, Van Loon L, Pieterse CM. 2004. The transcriptome of rhizobacteria-induced systemic resistance in *Arabidopsis*. *Molecular Plant-Microbe Interactions* **17**(8): 895-908.

Vessey JK. 2003. Plant growth promoting rhizobacteria as biofertilizers. *Plant and Soil* **255**(2): 571-586.

Vieira RF, Paula Júnior TJ, Carneiro JES, Teixeira H, Queiroz TFN. 2012. Management of white mold in type III common bean with plant spacing and fungicide. *Tropical Plant Pathology* **37**: 91-101.

von Meyenburg K, Jørgensen BB, Nielsen J, Hansen FG. 1982. Promoters of the *atp* operon coding for the membrane-bound ATP synthase of *Escherichia coli* mapped by Tn *10* insertion mutations. *Molecular and General Genetics* **188**(2): 240-248.

Vurukonda SSKP, Vardharajula S, Shrivastava M, SkZ A. 2016. Enhancement of drought stress tolerance in crops by plant growth promoting rhizobacteria. *Microbiological Research* **184**: 13-24.

W

Wagner AE, Rimbach G. 2009. Ascorbigen: chemistry, occurrence, and biologic properties. *Clinics in Dermatology* **27**(2): 217-224.

Walker V, Bertrand C, Bellvert F, Moënne-Loccoz Y, Bally R, Comte G. 2011. Host plant secondary metabolite profiling shows a complex, strain-dependent response of maize to plant growth-promoting rhizobacteria of the genus *Azospirillum*. *New Phytologist* **189**(2): 494-506.

Walker V, Couillerot O, Von Felten A, Bellvert F, Jansa J, Maurhofer M, Bally R, Moënne-Loccoz Y, Comte G. 2012. Variation of Secondary Metabolite Levels in maize seedling roots induced by inoculation with *Azospirillum*, *Pseudomonas* and *Glomus* consortium under field conditions. *Plant Soil* **356**(1): 151-163.

Walsh UF, Morrissey JP, O'Gara F. 2001. *Pseudomonas* for biocontrol of phytopathogens: from functional genomics to commercial exploitation. *Current Opinion in Biotechnology* **12**(3): 289-295.

Wang F, Wu L, Li L, Chen S. 2014. Monotropein exerts protective effects against IL-1β-induced apoptosis and catabolic responses on osteoarthritis chondrocytes. *International Immunopharmacology* **23**(2): 575-580.

Wang J, Liu J, Chen H, Yao J. 2007. Characterization of *Fusarium graminearum* inhibitory lipopeptide from *Bacillus subtilis* IB. *Applied Microbiology and Biotechnology* **76**(4): 889-894.

Wang XN, Radwan MM, Tarawneh AH, Gao JT, Wedge DE, Rosa LH, Cutler HG, Cutler SJ. 2013. Antifungal activity against plant pathogens of metabolites from the endophytic fungus *Cladosporium cladosporioides*. *Journal of Agricultural and Food Chemistry* **61**(19): 4551-4555.

Wang Y, Ohara Y, Nakayashiki H, Tosa Y, Mayama S. 2005. Microarray analysis of the gene expression profile induced by the endophytic plant growth-promoting rhizobacteria, *Pseudomonas fluorescens* FPT9601-T5 in *Arabidopsis*. *Molecular Plant-Microbe Interactions* **18**(5): 385-396.

War AR, Paulraj MG, Ahmad T, Buhroo AA, Hussain B, Ignacimuthu S, Sharma HC. 2012. Mechanisms of plant defense against insect herbivores. *Plant Signaling & Behavior* **7**(10): 1306-1320.

Weckwerth W, Wenzel K, Fiehn O. 2004. Process for the integrated extraction, identification and quantification of metabolites, proteins and RNA to reveal their co-regulation in biochemical networks. *Proteomics* **4**(1): 78-83.

Wehrens R, Hageman JA, van Eeuwijk F, Kooke R, Flood PJ, Wijnker E, Keurentjes JJ, Lommen A, van Eekelen HD, Hall RD. 2016. Improved batch correction in untargeted MS-based metabolomics. *Metabolomics* **12**(5): 88.

Wei Z, Jousset A. 2017. Plant breeding goes microbial. *Trends in Plant Science* **22**(7): 555-558.

Weller DM, Landa B, Mavrodi O, Schroeder K, De La Fuente L, Bankhead SB, Molar RA, Bonsall R, Mavrodi D, Thomashow L. 2007. Role of 2, 4-diacetylphloroglucinol-producing fluorescent *Pseudomonas* spp. in the defense of plant roots. *Plant Biology* **9**(01): 4-20.

Weller DM, van Pelt JA, Mavrodi DV, Pieterse CMJ, Bakker PAHM, van Loon LC. 2004. Induced systemic resistance (ISR) in Arabidopsis against *Pseudomonas syringae* pv. *tomato* by 2,4-diacetylphloroglucinol (DAPG)-producing *Pseudomonas fluorescens*. *Phytopathology* **94**(6): 108-109.

Wenke K, Kopka J, Schwachtje J, van Dongen J, Piechulla B. 2019. Volatiles of rhizobacteria *Serratia* and *Stenotrophomonas* alter growth and metabolite composition of *Arabidopsis thaliana*. *Plant Biology* **21**: 109-119.

Weston DJ, Pelletier DA, Morrell-Falvey JL, Tschaplinski TJ, Jawdy SS, Lu T-Y, Allen SM, Melton SJ, Martin MZ, Schadt CW, et al. 2012. *Pseudomonas fluorescens* induces strain-dependent and strain-independent host plant responses in defense networks, primary metabolism, photosynthesis, and fitness. *Molecular Plant-Microbe Interactions* **25**(6): 765-778.

Whang WK, Park HS, Ham I, Oh M, Namkoong H, Kim HK, Hwang DW, Hur SY, Kim TE, Park YG. 2005. Natural compounds, fraxin and chemicals structurally related to fraxin protect cells from oxidative stress. *Experimental & Molecular Medicine* **37**(5): 436.

Wicklow DT, Roth S, Deyrup ST, Gloer JB. 2005. A protective endophyte of maize: *Acremonium zeae* antibiotics inhibitory to *Aspergillus flavus* and *Fusarium verticillioides*. *Mycological Research* **109**: 610-618.

Widmer TL, Laurent N. 2006. Plant extracts containing caffeic acid and rosmarinic acid inhibit zoospore germination of *Phytophthora* spp. pathogenic to *Theobroma cacao*. *European Journal of Plant Pathology* **115**(4): 377–388.

Wightman F, Lighty DL. 1982. Identification of phenylacetic acid as a natural auxin in the shoots of higher plants. *Physiologia Plantarum* **55**(1): 17-24.

Wink M. 2010. *Biochemistry of plant secondary metabolism, second edition*: Wiley Online Library.

Wu S-y, Wang G-f, Liu Z-q, Rao J-j, Lü L, Xu W, Wu S-g, Zhang J-j. 2009. Effect of geniposide, a hypoglycemic glucoside, on hepatic regulating enzymes in diabetic mice induced by a high-fat diet and streptozotocin. *Acta Pharmacologica Sinica* **30**(2): 202.

X

Xie S, Wu H, Chen L, Zang H, Xie Y, Gao X. 2015. Transcriptome profiling of *Bacillus subtilis* OKB105 in response to rice seedlings. *BMC Microbiology* **15**(1): 21.

Xie Y, Yang W, Tang F, Chen X, Ren L. 2015. Antibacterial activities of flavonoids: structure-activity relationship and mechanism. *Current Medicinal Chemistry* **22**(1): 132-149.

Y

Yang J, Guo J, Yuan J. 2008. In vitro antioxidant properties of rutin. *LWT-Food Science and Technology* **41**(6): 1060-1066.

Yang J, Kloepper JW, Ryu C-M. 2009. Rhizosphere bacteria help plants tolerate abiotic stress. *Trends in Plant Science* **14**(1): 1-4.

Yang L, Wen KS, Ruan X, Zhao YX, Wei F, Wang Q. 2018. Response of plant secondary metabolites to environmental factors. *Molecules* **23**(4).

Yang SY, Park MR, Kim IS, Kim YC, Yang JW, Ryu C-M. 2011. 2-Aminobenzoic acid of *Bacillus* sp. BS107 as an ISR determinant against *Pectobacterium carotovorum* subsp. *carotovotrum* SCC1 in tobacco. *European Journal of Plant Pathology* **129**(3): 371-378.

Yang X, Guo S, Zhang L, Shao H. 2003. Select of producing podophyllotoxin endophytic fungi from podophyllin plant. *Natural Product Research and Development* **15**(5): 419-422.

Yasuda M, Isawa T, Shinozaki S, Minamisawa K, Nakashita H. 2009. Effects of colonization of a bacterial endophyte, *Azospirillum* sp B510, on disease resistance in rice. *Bioscience, Biotechnology, and Biochemistry* **73**(12): 2595-2599.

Yoon BH, Jung JW, Lee J-J, Cho Y-W, Jang C-G, Jin C, Oh TH, Ryu JH. 2007. Anxiolytic-like effects of sinapic acid in mice. *Life Sciences* **81**(3): 234-240.

Young MD, Wakefield MJ, Smyth GK, Oshlack A. 2010. Gene ontology analysis for RNA-seq: accounting for selection bias. *Genome Biology* **11**(2): R14.

Yousuf B, Gul K, Wani AA, Singh P. 2016. Health benefits of anthocyanins and their encapsulation for potential use in food systems: a review. *Critical Reviews in Food Science and Nutrition* **56**(13): 2223-2230.

Yu G, Sinclair J, Hartman GL, Bertagnolli B. 2002. Production of iturin A by *Bacillus amyloliquefaciens* suppressing *Rhizoctonia solani*. *Soil Biology and Biochemistry* **34**(7): 955-963.

Yu K, Liu Y, Tichelaar R, Savant N, Lagendijk E, van Kuijk SJ, Stringlis IA, van Dijken AJ, Pieterse CM, Bakker PA. 2019. Rhizosphere-associated *Pseudomonas* suppress local root immune responses by gluconic acid-mediated lowering of environmental pH. *Current Biology* **29**(22): 3913-3920. e3914.

Yu L, Chen C, Wang L-F, Kuang X, Liu K, Zhang H, Du J-R. 2013. Neuroprotective effect of kaempferol glycosides against brain injury and neuroinflammation by inhibiting the activation of NF-κB and STAT3 in transient focal stroke. *PloS One* **8**(2): e55839.

Yuan J, Li B, Zhang N, Waseem R, Shen Q, Huang Q. 2012. Production of bacillomycin-and macrolactin-type antibiotics by *Bacillus amyloliquefaciens* NJN-6 for suppressing soilborne plant pathogens. *Journal of Agricultural and Food Chemistry* **60**(12): 2976-2981.

Yun K-J, Koh D-J, Kim S-H, Park SJ, Ryu JH, Kim D-G, Lee J-Y, Lee K-T. 2008. Anti-inflammatory effects of sinapic acid through the suppression of inducible nitric oxide synthase, cyclooxygase-2, and proinflammatory cytokines expressions via nuclear factor-κB inactivation. *Journal of Agricultural and Food Chemistry* **56**(21): 10265-10272.

Z

Zang L-Y, Cosma G, Gardner H, Shi X, Castranova V, Vallyathan V. 2000. Effect of antioxidant protection by *p*-coumaric acid on low-density lipoprotein cholesterol oxidation. *American Journal of Physiology-Cell Physiology* **279**(4): C954-C960.

Zang Y, Zhang L, Igarashi K, Yu C. 2015. The anti-obesity and anti-diabetic effects of kaempferol glycosides from

unripe soybean leaves in high-fat-diet mice. *Food & Function* **6**(3): 834-841.

Zebelo S, Song Y, Kloepper JW, Fadamiro H. 2016. Rhizobacteria activates (+)-*δ*-cadinene synthase genes and induces systemic resistance in cotton against beet armyworm (*Spodoptera exigua*). *Plant, Cell & Environment* **39**(4): 935-943.

Zhalnina K, Louie KB, Hao Z, Mansoori N, da Rocha UN, Shi S, Cho H, Karaoz U, Loqué D, Bowen BP. 2018. Dynamic root exudate chemistry and microbial substrate preferences drive patterns in rhizosphere microbial community assembly. *Nature Microbiology* **3**(4): 470.

Zhang A, Sun H, Dou S, Sun W, Wu X, Wang P, Wang X. 2013. Metabolomics study on the hepatoprotective effect of scoparone using ultra-performance liquid chromatography/electrospray ionization quadruple time-of-flight mass spectrometry. *Analyst* **138**(1): 353-361.

Zhang B, Salituro G, Szalkowski D, Li ZH, Zhang Y, Royo I, Vilella D, Diez MT, Pelaez F, Ruby C, et al. 1999. Discovery of a small molecule insulin mimetic with antidiabetic activity in mice. *Science* **284**(5416): 974-977.

Zhang H, Kim M-S, Krishnamachari V, Payton P, Sun Y, Grimson M, Farag MA, Ryu C-M, Allen R, Melo IS. 2007. Rhizobacterial volatile emissions regulate auxin homeostasis and cell expansion in *Arabidopsis*. *Planta* **226**(4): 839.

Zhang H, Sun Y, Xie X, Kim MS, Dowd SE, Paré PW. 2009. A soil bacterium regulates plant acquisition of iron via deficiency-inducible mechanisms. *The Plant Journal* **58**(4): 568-577.

Zhang XL, Wang BB, Mo JS. 2018. Puerarin 6"-O-xyloside possesses significant antitumor activities on colon cancer through inducing apoptosis. *Oncology Letters* **16**(5): 5557-5564.

Zhang Z, Zhang Q, Yang H, Liu W, Zhang N, Qin L, Xin H. 2016. Monotropein isolated from the roots of *Morinda officinalis* increases osteoblastic bone formation and prevents bone loss in ovariectomized mice. *Fitoterapia* **110**: 166-172.

Zhao K, Penttinen P, Zhang X, Ao X, Liu M, Yu X, Chen Q. 2014. Maize rhizosphere in Sichuan, China, hosts plant growth promoting *Burkholderia cepacia* with phosphate solubilizing and antifungal abilities. *Microbiological Research* **169**(1): 76-82.

Zhi-lin Y, Chuan-chao D, Lian-qing C. 2007. Regulation and accumulation of secondary metabolites in plant-fungus symbiotic system. *African Journal of Biotechnology* **6**(11): 1266-1271.

Zhou H, Tao N, Jia L. 2014. Antifungal activity of citral, octanal and α-terpineol against *Geotrichum citri-aurantii*. *Food Control* **37**: 277-283.

Zhu C-Y, Loft S. 2003. Effect of chemopreventive compounds from *Brassica* vegetables on NAD (P) H: quinone reductase and induction of DNA strand breaks in murine hepa1c1c7 cells. *Food and Chemical Toxicology* **41**(4): 455-462.

Zhu D, Wang J, Zeng Q, Zhang Z, Yan R. 2010. A novel endophytic Huperzine A-producing fungus, *Shiraia* sp. Slf14, isolated from *Huperzia serrata*. *Applied Microbiology and Biotechnology* **109**(4): 1469-1478.

Zhu XY, Lin HM, Chen X, Xie J, Wang P. 2011. Mechanochemical-assisted extraction and antioxidant activities of kaempferol glycosides from *Camellia oleifera* Abel. meal. *Journal of Agricultural and Food Chemistry* **59**(8): 3986-3993.

Summary
Samenvatting
요약

Summary

Plants and microbes have a history of coevolution that extends over 450 million years. The rhizosphere encompasses a few millimeters of soil layer surrounding and influenced by plant roots. This zone is rich in organic compounds released by roots and is a hot spot for microbial activity and plant-microbe interactions. Plant-microbe interactions in the rhizosphere can have a positive, negative or neutral influence on plant fitness. The rhizosphere bacteria with beneficial effects on plant growth and health are also referred to as plant growth-promoting rhizobacteria (PGPR). Recent studies also revealed that PGPR can alter plant chemistry which in turn can lead to effective or ineffective partnerships. Hence, understanding the chemical continuum between plants and microbes during their interaction could provide us with new tools to modulate plant growth, defense and the level of high value natural plant products (HVNP). The **overall aim of this thesis** was to investigate the impact of rhizobacteria on plant metabolism and how these changes are associated with plant growth and plant defense. Factorial combinations of different plant species, including *Arabidopsis thaliana* (model plant), *Brassica oleracea* var. italica (crop) and *Artemisia annua* (medicinal plant), and phylogenetically distinct rhizobacterial species, including *Pseudomonas fluorescens* SS101 (*Pf* SS101), *Microbacterium* and three *Paraburkholderia* species, were used as study model systems in this thesis. Untargeted metabolomics was used to assess the impact of these rhizobacteria on the shoot chemistry of the host plant species. Transcriptome profiling was employed to assess the impact of the host on the gene expression in the rhizobacteria.

A series of *in vitro* bioassays revealed specific phenotypic and chemotypic responses of the host plants to rhizobacterial colonization. For example, *P. fluorescens* (*Pf* SS101) established an effective partnership with Arabidopsis and Artemisia while in Broccoli it led to significant reduction in shoot biomass. Similarly, *P. graminis* (*Pbg*) exhibited an effective partnership with Artemisia and Broccoli while its partnership with Arabidopsis was characterized by stunted growth with concomitant accumulation of stress-related metabolites in the leaves. Untargeted metabolomics demonstrated that under ineffective partnerships i.e. *Pf* SS101-Broccoli and *Pbg*-Arabidopsis, secondary metabolites downstream of the phenylpropanoid pathway, such as flavonoids, anthocyanin and stilbenoids, showed a sharp increase. These classes of metabolites were either suppressed or showed no change in effective partnerships. Particularly, flavonoid accumulation was associated with retarded plant growth most likely by interfering with auxin transport, distribution and turnover. This study revealed that root treatment of different plant species with rhizobacteria altered 18-78% of the detected plant secondary metabolites in the shoot. Fueling such carbon skeleton and energy demanding or competing plant responses without compromising plant growth requires a robust metabolic regulation. The combined primary and secondary metabolite analysis revealed that rhizobacterial treatment boosted the production of soluble sugars in the plant shoot, potentially enabling the plant to accommodate the high demand for energy and carbon required for enhanced growth and secondary metabolite production. Fructose was the

central target of rhizobacteria in the plant shoot. Rhizobacteria-treated plants showed more than 280-fold increase in fructose abundance when compared to control plants. Fructose is the primary substrate for fructose-6-phosphate, a key substrate for the biosynthesis of phosphoenolpyruvate and erythros-4-phosphate. These two intermediates are the pillars of energy and secondary metabolism. Furthermore, fructose is one of the potent chemotaxis agent for bacteria. By targeting such multipurpose metabolite, rhizobacteria could potentially alter multiple processes in plants to establish an effective partnership. *Paraburkholderia* species were also able to induce a systemic resistance response (ISR) in Broccoli against the bacterial leaf pathogen *Xanthomonas campestris*. The causal relationship between the induced defense response and the induced metabolites remains to be resolved.

Beyond their impact on plant growth and defense, rhizobacteria treatment also showed their effectiveness in boosting the indigenous level of a number of metabolites with nutritional, health promoting and pharmaceutical importance. For instance, *Pbg*-Artemisia significantly upregulated the abundance of dihydroartemisinin, an antimalarial agent, whereas *Pbg* and *Pf* SS101 boosted several indolic glucosinolates, cancer chemo preventive agents in Broccoli. Considering the greater impact of rhizobacteria on the host phenotype and chemotype, we also assessed the impact of a known bacterial trait on plant phenotype and chemistry. Previous studies that employed genome-wide analysis of *Pf* SS101 followed by mutagenesis and genetic complementation revealed that sulfur assimilation attested by *cysH* gene, plays an important role in the induction of growth and defense in Arabidopsis. Our current study revealed that the *cysH* mutation in *Pf* SS101 affected the chain elongation step of aliphatic glucosinolate biosynthesis in Arabidopsis whereas in Broccoli, the *cysH* mutation led to an accumulation of indolic glucosinolates and flavonoids. These results indicated that sulfur assimilation in *Pf* SS101 modulates shoot metabolism in a plant species specific manner. In the "blind date experiment" that aimed at finding the right partnership between different rhizobacteria and host plants, *Pbg*-Broccoli exhibited an effective partnership that led to significant increase in shoot biomass and changes in shoot metabolome. To shed light on the bacterial traits that are altered by the host during their interaction, genome wide transcriptome analysis was carried out on *Pbg* grown in the presence and absence of the host. Among the differently expressed genes (DEGs) in *Pbg*, genes involved in flagellar assembly, chemotaxis, and motility together with nutrient uptake and (an)ion transporter were upregulated in the presence of the host. Future studies that examine the role of plant root exudates in the modulation of rhizobacteria gene expression will be instrumental in our quest for understanding architecture of the chemical continuum between plants and their rhizosphere microbiome.

Integrating *in vitro* assay, plant phenotyping and plant chemotyping by state-of-the-art technologies, this thesis provided new insights into the strong influence rhizobacteria and plants have on each other. The findings of this thesis can potentially feed into the theory that asserts plant and their microbiome as multipartite entities potentially co-evolving as a holobiont. Plant breeding strategies and agricultural practices that gear towards steering the

composition and function of plant microbiomes in such a way to influence plant phenotypic and chemical traits will be the next frontier in agriculture and will have a profound contribution for the next green revolution.

Samenvatting

De co-evolutie tussen planten en microörganismen gaat meer dan 450 miljoen jaren terug. De rhizosfeer omvat slechts een paar millimeter grond nauw geassocieerd met en beïnvloed door plantenwortels. Het is rijk in organische stoffen die door de wortels uitgescheiden worden en is daardoor een hotspot voor microbiële activiteit en plant-microbe interacties. Deze interacties kunnen positieve, neutrale of negatieve effecten hebben op plant fitness. Rhizosfeerbacteriën met een positief effect op plantengroei en plantgezondheid worden ook wel aangeduid als 'plant growth-promoting rhizobacteria (PGPR)'. Recente studies toonden aan dat PGPR ook de chemie van planten kunnen veranderen, hetgeen kan leiden tot effectieve of ineffectieve partnerschappen tussen de microben en de plant. Een beter begrip van de chemie in deze partnerschappen zou daardoor nieuwe mogelijkheden kunnen bieden om plantengroei en afweer te sturen alsook de productie van waardevolle plant metabolieten. Het **doel van dit proefschrift** was om de impact van rhizosfeerbacteriën op plant metabolisme te onderzoeken en hoe veranderingen in dit metabolisme gekoppeld zijn aan plantengroei en afweer.

Diverse combinaties van plantensoorten, waaronder *Arabidopsis thaliana* (modelplant), *Brassica oleracea* var. *italica* (gewas) en *Artemisia annua* (medicinale plant), en fylogenetisch verschillende rhizobacteriële soorten, waaronder *Pseudomonas fluorescens* SS101 (*Pf* SS101), *Microbacterium* en drie *Paraburkholderia*-soorten, werden in dit proefschrift gebruikt als studiemodelsystemen. Metabolomics werd gebruikt om de impact van deze rhizobacteriën op de chemie van de waardplanten te bestuderen. Transcriptoom analyse werd gebruikt om de impact van de waardplant op de genexpressie in de rhizobacteriën te onderzoeken. Een reeks biotoetsen onthulden specifieke fenotypische en chemotypische reacties van de waardplanten op rhizobacteriële kolonisatie. Zo zette *P. fluorescens* (*Pf* SS101) een effectief partnerschap op met Arabidopsis en Artemisia, terwijl het in Broccoli leidde tot een aanzienlijke vermindering van de scheutbiomassa. Evenzo vertoonde *P. graminis* (*Pbg*) een effectief partnerschap met Artemisia en Broccoli, terwijl het partnerschap met Arabidopsis werd gekenmerkt door groeiachterstand en gelijktijdige accumulatie van stress-gerelateerde metabolieten in de bladeren. Metabolomics toonde vervolgens aan dat bij ineffectieve partnerschappen, d.w.z. *Pf* SS101-Broccoli en *Pbg*-Arabidopsis, secundaire metabolieten volgend op de phenylpropanoïde route, zoals flavonoïden, anthocyanine en stilbenoïden, verhoogd aanwezig waren in de scheut. Deze klassen van metabolieten werden onderdrukt of lieten geen verandering zien in effectieve partnerschappen tussen de rhizobacteriën en de waardplanten. In het bijzonder was accumulatie van flavonoïden geassocieerd met verminderde plantengroei, hoogstwaarschijnlijk door het transport, de distributie en/of de omzetting van auxine te verstoren. Deze studie toonde tevens aan dat wortelbehandeling van verschillende plantensoorten met rhizobacteriën 18-78% van de gedetecteerde secundaire metabolieten van planten in de scheut van de planten veranderde. Het voeden van deze energie-eisende reacties van planten op rhizobacteriën zonder de plantengroei in gevaar te brengen, vereist een verfijnde metabole regulatie.

Uit de gecombineerde analyse van primaire en secundaire metabolieten bleek dat behandeling van planten met rhizobacteriën de productie van oplosbare suikers in de scheut van de plant verhoogde, waarmee de plant mogelijk in staat was om te voldoen aan de hoge vraag naar energie en koolstof die nodig is voor groei en de productie van secundaire metabolieten. Fructose bleek een centraal 'doelwit' van rhizobacteriën in de plant. Planten behandeld met rhizobacteriën vertoonden een meer dan 280-voudige toename in fructose in vergelijking met niet behandelde planten. Fructose is het primaire substraat voor fructose-6-fosfaat, een belangrijk substraat voor de biosynthese van fosfo-enolpyruvaat en erytro-4-fosfaat. Deze twee tussenproducten zijn de pijlers van energie en secundair metabolisme. Bovendien kan fructose een rol spelen bij chemotaxis door bacteriën. Door zich te richten op een dergelijke multifunctionele metaboliet, kunnen rhizobacteriën mogelijk meerdere processen in planten veranderen om een effectief partnerschap tot stand te brengen. *Paraburkholderia*-soorten waren ook in staat om in Broccoli een systemische resistentie-respons (ISR) op te wekken tegen het bacteriële bladpathogeen *Xanthomonas campestris*. Het causale verband tussen de geïnduceerde afweerreactie en de geïnduceerde metabolieten moet nog verder worden onderzocht.

Naast hun impact op de groei en afweer van planten, toonde de behandeling met rhizobacteriën ook hun doeltreffendheid bij het stimuleren van de concentraties van een aantal metabolieten met voedings-, gezondheidsbevorderende en farmaceutische betekenis. Zo reguleerde *Pbg*-Artemisia de overvloed aan dihydro-artemisinine, een antimalaria-middel, aanzienlijk, terwijl *Pbg* en *Pf* SS101 verschillende indolische glucosinolaten, kankerchemo-preventieve middelen in Broccoli, stimuleerden. Gezien de grotere impact van rhizobacteriën op het fenotype en chemotype van de waardplant, hebben we ook de impact van een bekende bacteriële eigenschap op het fenotype en de chemie van planten bestudeerd. Eerdere studies die gebruik maakten van genoom-brede analyse van *Pf* SS101 gevolgd door mutagenese en genetische complementatie, toonden aan dat assimilatie van zwavel gereguleerd door het *cysH*-gen, een belangrijke rol speelt bij de inductie van groei en afweer in Arabidopsis. Onze huidige studie toonde aan dat de *cysH*-mutatie in *Pf* SS101 de ketenverlenging van de alifatische glucosinolaten in Arabidopsis beïnvloedde, terwijl bij Broccoli de *cysH*-mutatie leidde tot een accumulatie van indolische glucosinolaten en flavonoïden. Deze resultaten gaven aan dat zwavelassimilatie in *Pf* SS101 het metabolisme van de scheut op een plantensoort-specifieke manier moduleert.

In het "blind date experiment" dat gericht was op het vinden van het juiste partnerschap tussen verschillende rhizobacteriën en waardplanten, vertoonde *Pbg*-Broccoli een effectief partnerschap dat leidde tot een significante toename van scheutbiomassa en veranderingen in het metaboloom. Om licht te werpen op de bacteriële eigenschappen die door de gastheer tijdens hun interactie werden geactiveerd of onderdrukt, werd een genoom-brede transcriptoom-analyse uitgevoerd op *Pbg* die was gekweekt in aan- en afwezigheid van de waardplant. Onder de verschillend tot expressie gebrachte genen (DEG's) in *Pbg*, waren

genen die betrokken zijn bij flagellaire assemblage, chemotaxis en beweeglijkheid alsook genen geassocieerd met opname van voedingsstoffen en (een) ionentransporter. Toekomstige studies naar de rol van exudaten van plantenwortels in de modulatie van genexpressie van rhizobacteriën zullen nodig zijn voor een beter begrip van de architectuur van het chemische continuüm tussen planten en hun microbioom.

Dit proefschrift integreerde biotoetsen, fenotypering en chemotypering van planten door middel van de allernieuwste technologieën en leverde nieuwe inzichten op ten aanzien van de invloed die rhizobacteriën en planten op elkaar hebben. De bevindingen in dit proefschrift kunnen bijdragen aan de theorie die plant en hun microbioom ziet als multi-partiete entiteiten die samen evolueren als holobiont. Plantenveredelingsstrategieën en landbouwpraktijken die erop gericht zijn de samenstelling en functie van plantenmicrobiomen zodanig te sturen dat ze fenotypische en chemische eigenschappen van planten beïnvloeden, zullen de volgende uitdaging worden en een diepgaande bijdrage kunnen leveren aan de volgende groene revolutie.

요약

식물과 미생물은 4억 5천만 년이 넘는 공진화(Coevolution)의 역사를 가지고 있다. 근권(Rhizosphere)은 식물의 뿌리 부근에서 뿌리의 영향을 받는 수 mm의 토양층을 지칭한다. 이 구역은 뿌리에 의해 방출된 풍부한 유기 화합물로 인한 미생물 활동 및 식물-미생물 상호작용이 활발하게 일어나는 구역 중 하나이다. 근권에서 일어나는 식물-미생물 상호 작용은 식물의 상태에 긍정적, 부정적 또는 중립적 영향을 미칠 수 있다. 이중 식물 성장 및 건강에 유익한 영향을 미치는 근권세균(Rhizobacteria)은 식물성장촉진근권세균(Plant growth promoting rhizobacteria: PGPR)으로 지칭된다. 더 나아가 최근 연구에 의하면 PGPR은 식물 속 화학물질을 변화시킬 수 있고 이 화학변화는 때론 식물-미생물간 협력/비협력적 상호관계의 원인이나 결과로 이어지기도 한다는 것이 밝혀졌다. 따라서 식물과 미생물이 상호 작용하는 동안 화학변화의 이해를 통한 식물 성장, 방어 및 고부가가치 천연물(High value natural product: HVNP) 의 생산수단이 될 새로운 도구를 개발할 수 있을 것이다.

이 논문의 최종 목표는 근권세균이 식물의 대사(Metabolism)에 어떠한 영향을 미치고 이러한 대사체의 변화가 식물 성장 및 방어에 어떻게 관련되는가이다. 본논문에서 식물-미생물 상호작용 연구에 사용된 식물은 애기장대 *Arabidopsis thaliana*(표본식물), 브로콜리 *Brassica oleracea* var. italica(작물), 그리고 개똥쑥 *Artemisia annua*(약용식물)이고, 상호작용 상대인 근권세균으로는 계통발생적으로 상이한 3속 5종의 근권세균, *Pseudomonas fluorescens* SS101 (*Pf* SS101), *Microbacterium* (MB) 및 *Paraburkholderia* spp. (*Pbg, Pbh, Pbt*)이 사용되었다. 근권세균이 기주식물의 지상부 천연물질 변화에 미치는 영향은 비표적 대사체학(Untargeted metabolomics) 연구기법을 통해 분석하였으며, 미생물 전사체 프로파일링(Transcriptome profiling)을 통해 기주식물과 근권세균의 상호작용이 미생물의 유전자 발현에 미치는 영향을 분석하였다.

일련의 기내실험(*in vitro* bioassay)은 근권세균의 식물 뿌리정착이 기주식물의 특정 표현형 및 화학형을 끌어낸다는 것을 보여주었다. 예를 들어, *P. fluorescens* (*Pf* SS101)는 애기장대와 개똥쑥의 성장을 촉진 시키지만, 브로콜리의 지상부 성장은 유의적으로 줄이는 것을 확인했다. 유사하게, *P. graminis* (*Pbg*)는 개똥쑥과 브로콜리의 성장에 효과를 보였던 반면 애기장대와의 상생은 좋지 않아 잎 내부에 스트레스와 관련된 대사체의 축적과 함께 성장을 저해함을 확인했다. 비표적 대사체 분석은 *Pf* SS101-브로콜리 및 *Pbg*-애기장대와 같이 비효과적 조합에서 phenylpropanoid pathway의 하위 경로에 있는 flavonoids, anthocyanin 그리고 stilbenoids 등의 이차 대사산물(Secondary metabolites)이 급격하게 증가함을 보여주었다. 식물-근권세균의 효과적인 조합에서는 이러한 대사 산물의 변화가 없거나 억제되었음을 확인하였다. 특히, flavonoids의 축적은 auxin의 수송, 분포 및 전환을 방해함으로써 식물의 성장지연에 관련이 깊다.

본 연구는 식물-근권세균의 각 조합에 따라 기주식물에 지상부의 검출 가능한 물질 중 근권세균 미처리구 대비 18~78%의 이차 대산물이 정량적으로 변한다는 것을 밝혔다. 기주식물의 반응에 있어 식물의 성장을 저해하지 않으면서도 많은 에너지를 필요로 하는 탄소 골격을 지속적으로 공급하기 위해서는 강력한 대사조절이 필요하다. 일차 대사산물(Primary metabolites)과 이차대 사산물의 통합 분석을 통해 기주식물 뿌리에 대한 근권세균의 처리가 식물 지상부의 가용성당(Soluble sugar)의 생산을 증가시켜, 식물이 성장 및 이차 대사산물 생산을 향상시키는데 필요한 높은 에너지 및 탄소에 대한 수요를 수용할 수 있게 함을 증명했다.

근권 세균의 주된 목표중 하나는 식물내의 과당(Fructose) 대사에 있다. 비처리구와 비교했을 때, 근권세균이 처리 된 처리구의 과당 함량은 280배 증가했다. 과당은 phosphoenolpyruvate와 erythros-4-phosphate 생합성의 주요 기질이고, 이 두 중간 물질은 에너지 및 이차대사의 중심축이다. 또한, 과당은 박테리아에 대한 강력한 주화성 (Chemotaxis) 물질 중 하나이다. 이에, 근권세균이 이처럼 다양한 역할을 하는 대사 산물에 집중함에따라, 식물 내 일련의 과정에 변화를 주어 효과적 식물-미생물 상호관계를 구축하는 것으로 짐작된다.

한편 근권세균중 *Paraburkholderia* 종들은 브로콜리의 전신유도저항성(Induced systemic resistance: ISR)을 일으켜 세균성 잎 병원균인 *Xanthomonas campestris*에 대한 저항성을 유도하였다. 다만 유도저항 반응과 근권세균에 의해 변화된 대사체의 관계는 여전히 해결되어야 할 과제로 남아있다.

근권세균이 식물의 생장 및 방어에 미치는 영향 이외에도 영양, 건강증진 및 약학적으로 중요한 여러 고유대사체의 함량을 높이는 데 효과가 있음을 확인했다. 예를 들어, *Pbg*가 처리된 개똥쑥에서는 단위 무게당 항말라리 성분인 dihydroartemisinin의 양이 획기적으로 증가하는 것을 확인했고, *Pbg*와 *Pf* SS101는 브로콜리의 화학적 암 예방물질인 여러종의 indole glucosinolate 함량을 증가시켰다.

본 연구에서는 근권세균의 어떠한 특성이 변화를 촉진시키는지 알아보기 위해 기존에 알려져 있는 세균의 특성을 이용해 세균내 황 대사가(Sulphur-metabolism) 식물의 표현형 및 화학형에 미치는 영향을 알아보았다. *Pf* SS101의 전체 유전자 분석, 돌연변이생성 및 돌연변이 유전자 재도입을 포함한 선행 연구에서 *Pf* SS101의 황 동화(Sulphur assimilation)와 관련된 *cysH* 유전자가 애기장대의 생장과 방어작용에 중요한 역할을 하는 것을 밝혔다. 본고에서는 *Pf* SS101의 *cysH* 돌연변이가 애기장대 내 aliphatic glucosinolate의 지방족 가지(aliphatic chain)의 생합성에 영향을 미치고, 브로콜리의 경우 indole glucosinolate와 flavonoid의 함량을 증가시키는 역할을 하는 것으로 분석되었다. 이로써 *Pf* SS101의 황 대사에 의한 기주식물 내 대사산물 함량 변화는 식물의 종 특이성이라는 결과에 닿는다.

한편 근권세균과 기주식물간의 효과적인 상생을 찾기 위한 "blind date 실험" 에서, *Pbg*-브로콜리 조합이 지상부의 생육 및 대사체의 변화를 효과적으로 일으키는 것을 확인했다. 근

권세균-식물의 상호작용 중 세균의 특성을 밝히기 위한 연구의 일환으로, 기주식물인 브로콜리가 자라고 있는 배지와 없는 배지에서 자란 *Pbg* 균주의 전체 전자체 분석(Genome-wide transcriptome analysis)을 시도했다. *Pbg* 내 여러가지 차별발현 유전자 (Differently expressed genes: DEGs)를 봤을 때, 브로콜리 뿌리에 정착해 영향을 받고 있는 *Pbg*의 경우 편모의 조립 (Flagellar assembly), 주화성 및 운동 (Motility)과 관련된 유전자와 영양분의 흡수 (Nutrient uptake) 및 이온수송 ((an)Ion transporter)과 관련된 유전자의 발현이 훨씬 높은 것으로 분석됐다. 앞으로 식물과 근권미생물 생태계 사이의 화학적 연속체의 구조를 이해하기 위해서는, 근권세균의 유전자 발현에 영향을 주는 브로콜리의 식물뿌리 삼출액 (Root exudates)에 대한 연구가 후속되어야 할 것이다.

최신기술을 통한 기내실험, 식물 표현형 및 화학형을 포괄하는 연구를 통해, 본 논문은 근권세균과 식물이 서로에게 미치는 강력한 영향에 대한 새로운 통찰을 제공하고자 했다. 본연구의 결과는 식물과 미생물군집이 여러 부분으로 나뉜 독립체로서 공진화한 전생물체(Holobiont)라는 이론을 뒷받침한다. 앞으로 식물육종 전략 및 농업 관행은 식물의 표현형 및 화학적 특성에 영향을 미치는 미생물의 구성 및 기능을 향상시키는 쪽으로 발전할 것이고, 이는 다가오는 녹색혁명에 크게 기여할 것이다.

About the author and publications

About the author

Je-Seung Jeon was born on 25th of February 1984 in PyeongChang-gun, Republic of Korea. Growing up on a family farm in a rural area, he dreamed about being a farmer, and hence joined the Department of Applied Plant Science at Gangneung National University. During his bachelor degree, he fulfilled a military service for two years at the GOP (general outpost) where South Korea borders North Korea. After being discharged from the military in 2005, he realized the reality of becoming a farmer, and decided instead to continue his studies in the plant sciences. In line with this decision, in 2007 he started an internship program at the Gangneung Institute of Natural Products at the Korean Institute of Science and Technology (KIST), and this led to the start a Master program at the KIST and Gangneung-wonju National University in 2009. Here, he majored in natural product chemistry discovering new and known antioxidative phytochemicals in medicinal plants under the supervision of Dr. Byung-Hun Um, Dr. Chul Young Kim and Prof. Dr. Hakgi Kim. In 2012, he moved to Prof. Dr. Chul Young Kim's Pharmacognosy lab at the college of pharmacy at Hanyang University and worked as a researcher developing a massive isolation method of medicinal compounds from various herbal plants using liquid-liquid based platform including centrifugal partition chromatography (CPC). In 2014, he was awarded with a Korean government scholarship program supporting a PhD fellowship, which gave him an opportunity to study abroad. In 2015, he relocated to the Netherlands and started his doctoral research under the supervision of Prof. Dr. Jos Raaijmakers and Dr. Desalegn Etalo in the Microbial Ecology department at the Netherlands Institute of Ecology. Here, he focused on unearthing the modulation of phytochemicals by microbe-plant interaction and its mechanism together with bacterial traits that affect physio chemical properties of hosting plants. Apart from his experimental expertise, he has also developed in scientific infographic technique, contributing scheme figures for several grant applications and journal cover pages.

The findings of this research project are described in the present thesis. After his PhD, Je-Seung would like to continue his research in Academia, digging into the mystery of microbe-plant interaction and developing its field application.

List of publications

Je-Seung Jeon, Desalegn W. Etalo, Natalia Carreno-Quintero, Ric De Vos, and Jos M. Raaijmakers "Effects of sulfur assimilation in *Pseudomonas fluorescens* SS101 on growth, defense and metabolome of *Brassica* species" **(Chapter 5, submitted)**

Je-Seung Jeon, Natalia Carreno-Quintero, Ric De Vos, Jos M. Raaijmakers and Desalegn W. Etalo "Impact of root-associated beneficial *Paraburkholderia* species on primary and secondary metabolism of *Brassica oleracea*" **(Chapter 4, submitted)**

Je-Seung Jeon, Natalia Carreno-Quintero, Ric De Vos, Jos M. Raaijmakers and Desalegn W. Etalo "The metabolic signature of rhizobacteria-induced growth promotion in different plant species" **(Chapter 3, submitted)**

Desalegn W Etalo*, **Je-Seung Jeon***, Jos M Raaijmakers. "Modulation of plant chemistry by beneficial root microbiota", Nat Prod Rep. **(2018)** * shared first authors

Sung Hum Yeon*, **Je-Seung Jeon*,** Key An Um, Chul Young Kim, Young-Joon Ahn, "Large-scale purification of unstable, water-soluble secologanic acid using centrifugal partition chromatography", *Phytochem Anal*. **(2018)** * shared first authors

Ahmed Shah Syed, **Je-Seung Jeon**, Chul Young Kim "A new diacetylated flavonol triglycoside from the aerial parts of Actinidia polygama", Nat. Prod. Res. **(2017)**

Je-Seung Jeon, Byung-Hun Um, Chul Young Kim, "A New Geranyl Phenylpropanoid from Heracleum moellendorffii Leaves", *Chem. Nat. Compd.* **(2017)**

Je-Seung Jeon, Chae Lee Park, Ahmed Shah Syed, Young-Mi Kim, Il Je Cho, Chul Young Kim, "Preparative separation of sesamin and sesamolin from defatted sesame meal via centrifugal partition chromatography with consecutive sample injection", *J. Chromatogr. B*. **(2016)**

Je-Seung Jeon, Jeeyoung Kim, Soyoung Park, Chongsuk Ryou and Chul Young Kim, "Preparative purification of plasmin activity stimulating phenolic derivatives from *Gastrodia elata* using centrifugal partition chromatography", *Biomed. Chromatogr*. **(2015)**

Je-Seung Jeon, Ji Hoon Kim, Chae Lee Park, Chul Young Kim, "Preparative Isolation of Polar Antioxidant Constituents from *Abies Koreana* using Centrifugal Partition Chromatography Guided by DPPH$^{\bullet}$-HPLC experiment", *J. Liq. Chromatogr. Relat. Technol.* **(2015)**

Je-Seung Jeon, Suk Woo Kang, Byung-Hun Um, Chul Young Kim, "Preparative Isolation of Antioxidant Flavonoids from Small Black Soybeans by Centrifugal Partition Chromatography and Sequential Solid-phase Extraction", *Sep. Sci. Technol.* **(2014)**

Suk Woo Kang, Kyungsu Kang, Mi Ae Kim, Na Ra Jeon, Sang Min Kim, **Je-Seung Jeon**, Chu Won Nho, Byung-Hun Um, "Phytoestrogenic activity of *Aceriphyllum rossii* and rapid identification of phytoestrogens by LC–NMR/MS and bioassay-guided isolation", *Eur Food Res Technol*. **(2014)**

Ya Fang Shang, Sarangerel Oidovsambuu, **Je-Seung Jeon**, Chu Won Nho, Byung-Hun Um, "Chalcones from the flowers of *Coreopsis lanceolata* and their *in vitro* anti-oxidative activity", *Planta Med*. **(2013)**

Je-Seung Jeon, Chul Young Kim, "Preparative separation and purification of flavonoids and stilbenoids from *Parthenocissus tricuspidata* stems by dual-mode centrifugal partition chromatography", *Sep. Purif. Technol.* **(2013)**

Kiwon Jung, **Je-Seung Jeon**, Mi-Jeong Ahn, Chul Young Kim, Jinwoong Kim, "Preparative Isolation and Purification of Flavonoids from *Pterocarpus Saltalinus* using Centrifugal Partition Chromatography", *J. Liq. Chromatogr. Relat. Technol.* **(2012)**

Sang Min Kim, **Je-Seung Jeon**, Suk-Woo Kang, Woo-Ri Kim, Ki-Deok Lee, Byung-Hun Um, "Composition Analysis and Antioxidant Activity of Ojuk (*Phyllostachys nigra* Munro) Leaf Tea and Shoot Tea", *J. Appl. Biol. Chem.* **(2012)**

Sang Min Kim, Suk Woo Kang, **Je-Seung Jeon**, Yu-Jin Jung, Woo-Ri Kim, Chul Young Kim, Byung-Hun Um, "Determination of major phlorotannins in *Eisenia bicyclis* using hydrophilic interaction chromatography: seasonal variation and extraction characteristics", *Food Chem.* **(2012)**

Sang Min Kim, **Je-Seung Jeon**, Suk Woo Kang, Yu-Jin Jung, Lin Na Ly, and Byung-Hun Um, "Content of Antioxidative Caffeoylquinic Acid Derivatives in Field-Grown *Ligularia fischeri* (Ledeb.) Turcz and Responses to Sunlight", *J. Agric. Food Chem*. **(2012)**

Sang Min Kim, Suk-Woo Kang, **Je-Seung Jeon** and Byung-Hun Um, "A comparison of Pycnogenol® and bark extracts from *Pinus thunbergii* and *Pinus densiflora*: Extractability, antioxidant activity and proanthocyanidin composition", *J. Med. Plants Res.* **(2012)**

Je-Seung Jeon, Sang-Min Kim, Hee Ju Lee, Byung Hun Um, Hak Ki Kim, Chul Young Kim, "Preparative Isolation and Purification of Prenylated Isoflavonoids from *Cudrania Tricuspidata* Fruits using Centrifugal Partition Chromatography", *J. Liq. Chromatogr. Relat. Technol.* **(2011)**

Sang Min Kim, Kyungsu Kang, **Je-Seung Jeon**, Eun Hye Jho, Chul Young Kim, Chu Won Nho, Byung-Hun Um, "Isolation of phlorotannins from *Eisenia bicyclis* and their hepatoprotective effect against oxidative stress induced by tert-butyl hyperoxide", *Appl. Biochem. Biotechnol.* **(2011)**

Je-Seung Jeon, Hak Gi Kim, Byung Hun Um, Chul Young Kim, "Rapid Detection of Antioxidant Flavonoids in Azalea (*Rhododendron mucronulatum*) Flowers using On-line HPLC-ABTS^{+} System and Preparative Isolation of Three Flavonoids by Centrifugal Partition Chromatography", *Sep. Sci. Technol.* **(2011)**

Golam Mezbah Uddin, Hee Ju Lee, **Je-Seung Jeon**, Donghwa Chung, and Chul Young Kim, "Isolation of Prenylated Isoflavonoids from *Cudrania tricuspidata* Fruits that Inhibit A2E Photooxidation", *Natural Product Science* **(2011)**

Sang Min Kim, Suk Woo Kang, **Je-Seung Jeon**, Yu-Jin Jung, Chul Young Kim, Cheol Ho Pan, Byung-Hun Um, "Rapid identification and evaluation of antioxidant compounds from extracts of *Petasites japonicus* by hyphenated-HPLC technigues", *Biomed. Chromatogr.* **(2011)**

Amir Husni, **Je-Seung Jeon**, Byung-Hun Um, Nam Soo Han and Donghwa Chung, "Tyrosinase inhibition by water and ethanol extracts of a Far Eastern sea cucumber, *Stichopus japonicas*", *J. Sci. Food Agric.* **(2011)**

The research described in this thesis was performed at the Department of Microbial Ecology of the Netherlands Institute of Ecology (NIOO-KNAW) in Wageningen. The doctoral research was financially supported by NIOO and National institute for international education (NIIED), the Korean government scholarship program.

This is NIOO-thesis number 177

Cover and layout by Je-Seung

Printed by GVO drukkers & vormgevers B.V. ||www.gvo.nl